NOVEL EVAPORATIVE COOLING SYSTEMS

FOR BUILDING APPLICATIONS

By

MU'AZU MUSA
B.Eng, M.Eng &United Nations University Renewable Energy Training and Research Cert.

Thesis submitted to the University of Nottingham, UK for the degree of Doctor of Philosophy

May 2008

Table of Contents

Abstract

The technology and applications of evaporative cooling to provide human comfort in buildings is not new and has been used in different places based on different methods and materials. Conventional CFCs and HCFCs based air conditioning and refrigeration systems overshadowed the application of evaporative cooling for buildings despite their ozone layer depletion. Evaporative cooling using porous ceramic evaporators were experimentally investigated. Encouraging results in terms of temperature reduction and cooling effectiveness were reported. In this work thermoelectric unit was integrated in to the evaporative cooling system containing porous ceramic evaporators. The warm inlet air cooled in the porous ceramics' evaporative cooling chamber was passed over the hot-side fins of the thermoelectric cooling device to act as a better heat sink. This increases the coefficient of performance (COP) and is a measure of reducing high humidity associated with direct evaporative cooling applications. Also the power supplies to the thermoelectric unit as well as the exhaust fan were varied. Typical test results showed that the cold side temperature of thermoelectric unit was $5^{o}C$ lower and the hot side was $10^{o}C$ lower, respectively when operated on the wet and dry porous ceramics evaporative cooling chamber. The overall system performance is discussed and presented in this thesis.

Direct evaporative cooling is often associated with the rise in relative humidity which may result in uncomfortable feeling due to unwanted increase in moisture. Indirect evaporative cooling offers a solution but still requires improvements in the effectiveness. There is also need for using cheap and readily available materials for the construction, requiring simple fabrication

technology without very complex engineering infrastructure. Most widely used common fibrous materials have very limited capillary effect. They cannot draw-up water high enough to moisten the length required for effective heat transfer if the cooler is to be kept vertical. So a periodic water spray system with an automatic control is required for running the cooler which adds to the power consumption, rise in operation costs as well as construction and operational difficulties. As a compromise using horizontal arrangement was considered. Use of pump for supplying water required to moisten the evaporative cooling surface was eliminated. The system was constructed and tested under varying temperature, relative humidity and air flow rates. Results showed significant temperature reduction accompanied with acceptable increase in relative humidity. Temperature drop of 6-10^{o}C between the inlet and outlet temperatures of the product or supply air was recorded. Increase in relative humidity of the supply air was 6 - 10% less than the working air. Application of this novel system was demonstrated in the parasol self-cooling arrangement. The fibre tube evaporative cooler has the potential of cooling a building space to the acceptable comfort limits.

The application of porous ceramics for building space cooling, integrating the system to be used as a heat sink and the use of horizontal fibre tubes for evaporative cooling are all novel ideas in this field of research. Other novel features also include the ability to minimise energy consumption by eliminating common methods of continuous water circulation. However, still more needs to be done to make the systems very attractive.

Acknowledgement

I firstly would like to express my sincere thanks to ALLAH the God for His up to date supports and sustenance prior to and during the undertaking of this programme.

I am very grateful to my supervisor Professor S. B. Riffat and my co-supervisor Dr. X. Zhao for their unlimited supports, encouragement and patience during the entire period of my study.

I am also very grateful to The School of the Built Environment, The University of Nottingham for the tuition fee discount offered to my sponsors for my programme. I wish to thank my organisation The Sokoto Energy Research Centre, Usmanu Danfodiyo University Sokoto for the study fellowship and partial supports for living expenses during my studies.

Many thanks to Elfatih Ibrahim, Dr. Guoquan Qiu, Dr. Li Shao Professor Brian Dr.S.Omer, Dr.Xiaoli Ma, Dr.Nasir, Dr.Rabah, Dr.JieZhu, Dr.Mark Gillot Dr.Wanqi, Professor Brian Ford for their material supports and advices in the area of this research. Many thanks to Mr. L.U Kangiwa and Mr.T.Suleman of SERC for the photographs of our local pots and some drawings, respectively.

I am very grateful to my family members, relatives and friends for various kinds of supports from the beginning of this study to date.

I wish to express my sincere gratitude to Mr. Patrick Hodgkinson and all technical and other staff and students in the school for their helps and un-tiring supports during my studies. I particularly wish to thank Mrs. Zeny Amante-Roberts followed by Mrs. Claire Hardwidge, Ms Lyn Shaw and Mrs. Angela for various forms of assistances during the period of my studies. I am also very grateful to the staff of the International Office and the Students' Registry particularly the kind cooperation of Mrs. Gray for giving me the opportunity to submit my thesis.

I am also very grateful to the staff of the Cripps health Centre and the City Hospital, particularly Dr. A. Connor and Dr. M. Arora as well as my consultant surgeon and physiotherapist for their continuous medical helps.

Finally I wish to acknowledge direct or indirect contributions of any other person or colleague during the pursuit of my studies.

Nomenclature

Symbol	Term	Unit
Chapter 3:		
A	heat transfer surface area	m^2
h	enthalpy	kJ/kg
h_c	convective heat transfer coefficient	W/m^2K
h_{fg}	latent heat of vaporisation of water	2.45×10^6 J/kg
m_v`	evaporative mass flux	$kg/s.m^2$
P	pressure	Pa
P_v	partial pressure of water vapour	Pa
P_{vs}	saturation pressure of water vapor at T_{db},	Pa
P_{wb}	saturation pressure of water vapor at T_{wb},	Pa
Q_v	sensible convection heat flux from air/vapour	(W/m^2)
Q_a	heat added by other means or source	(W/m^2)
Q_{rad}	heat added due to radiation	(W/m^2)
Q_e	energy required for the evaporation	(W/m^2)
T_s	temperature at the surface	^oC
T_∞	temperature at the free stream or bulk temperature	^oC
ω_s	surface specific humidity/ humidity ratio	kg(vapour)/kg(dry air)
ω_∞	free stream specific humidity/humidity ratio	kg(vapour)/kg(dry air)
ρ_w	density of water	kg/m^3
R_a	gas constant,	J/kg K
T	temperature	K
T_{db}	dry bulb temperature	K
T_{dp}	dew point temperature	K
T_{wb}	wet bulb temperature	K
v	specific volume, m^3/kg	
m_c	rate of water evaporation or water consumption	kg/s
v	wind velocity or air flow	(m/s)
P_w-saturated vapour pressure for wet or water body surface		(N/m^2)
P_a – saturated vapour pressure ambient air surface		(N/m^2)

a	effective surface area per unit volume	$m^2.m^{-3}$
Cp	specific heat at constant pressure	$J.kg^{-1}K^{-1}$
g	gravitational acceleration	$m.s^{-2}$
h	heat transfer coefficient	$W.m^{-2}K^{-1}$
h_D	mass transfer coefficient	$kg.m^{-2}s^{-1}$
h_w	film heat transfer coefficient	$W.m^{-2}K^{-1}$
i	enthalpy	J kg-1
k	thermal conductivity	$W.m^{-1}K^{-1}$
Le	Lewis number	
Le_f	Lewis factor	
m	mass flow rate	kgs^{-1}
NTU	number of transfer units	
Re	Reynolds number	dimensionless
k	thickness	m
T	Temperature	^oC
U	overall heat transfer coefficient	$Wm^{-2}K^{-1}$
v	velocity	ms^{-1}
w	humidity ratio	kg water(kg dry air)$^{-1}$

Q_v	Air/vapour sensible convection heat flux	W/m^2
Q_a	Heat added	W/m^2
Q_e	Energy for evaporation	W/m^2
A	Heat transfer surface area	m^2
h_c	Convective heat transfer coefficient	W/m^2K
Pr	Prandtl number	dimensionless
T_s	Temperature at the surface	^oC
T_∞	Temperature at the free stream	^oC
h_m	Convective mass transfer coefficient	m/s
ρ_w	Density of water	kg/m^3
ρ_a	Density of air	kg/m^3
dm_v	Evaporative mass flux	$kg/s.m^2$
h_{fg}	Latent heat of vaporisation	J/kgK

h_s	Specific enthalpy of air close to the surface	kJ/kg
h_∞.	Free stream specific enthalpy of air	kJ/kg
C_{pa}	Constant pressure specific heat capacity of the air	$W/m^{-2}K$
C_{pv}	Constant pressure specific heat capacity of the vapour	$W/m^{-2}K$
Le	Lewis number [dimensionless]	
T_{am}	Arithmetic mean temperature of the thermal boundary	K
E	Effectiveness	%
A_{duct}	Duct area	m^2
V	Air velocity	m/s
Cp	Specific heat capacity	Wm^{-2} K
T_{in}	Inlet temperature	K
T_{out}	Outlet temperature	K
A_{ce}	Ceramic evaporators surface area	m^2

Greek Symbols

η	efficiency	
μ	dynamic viscosity	$kg.m^{-1}.s^{-1}$
υ	kinematic viscosity	$m^2.s^{-1}$
ρ	density	$[kg.m^{-3}]$

Subscripts

c	convective or convection
db	dry bulb
f	film or fouling
i	inlet or inside
m	moist
o	outlet
p	process fluid (dry side air or plate)
v	vapour
w	water (recirculating)
wb	wet bulb

Abbreviations:

AS adiabatic saturation (spray chamber)

DEC direct evaporative cooler

IEC indirect evaporative cooler

RIEC regenerative indirect evaporative cooler

Dimensionless Numbers

Le - Lewis number, $k/(\rho C_p D)$ or Sc/Pr, or α /D

Pr – Prandtl number, $C_p\mu/k$

Re - Reynolds number, $\rho uL/ \mu$

Subscripts

a air

i inlet

m mass transfer or mean

o outlet

s saturation

w water

Chapter 5:

$Q_{cooling}$	the cooling energy produced by the system	W/m^2
Q_{input}	the electrical energy input to the thermoelectric cell	W
R_T	thermal resistance	$^oC/Watt$
Ts	heat sink surface temperature	^oC
Ta	heat sink air temperature	^oC
Q	heat input to heat sink	Watts

Chapter 6:

A_{in}	Cross sectional area at inlet	m^2
C_p	The specific heat of the air	kJ/kg-K
$d_{B\text{-}wet}$	Humidity ratio of wet channel exhaust air	$kg_{water\text{-}vapour}/kg_{dry\text{-}air}$
$d_{B\text{-}in}$	Humidity ratio of at inlet	$kg_{water\text{-}vapour}/kg_{dry\text{-}air}$
E_{dp}	Effectiveness based on dew- point temperature	%

E_{wb}	Effectiveness based on wet - bulb temperature	%
h_{Ain}	Supply air inlet enthalpy	kJ/kg
h_{Aout}	Supply air outlet enthalpy	kJ/kg
h_{Bin}	Working air inlet enthalpy	kJ/kg
h_{Bout}	Working air out let enthalpy	kJ/kg
m^*	Mass flow rate of the air	m^3/s
m^*_A	Supply air mass flow rate	m^3/s
m^*_B	Working air mass flow rate	m^3/s
Q_o	Cooling capacity	Watts
Q_{wf}	Water consumption of the fibre	g/s
$T=T_{db}$	Dry bulb temperature	^oC
T_{dp}	Dew point temperature	^oC
T_{wb}	Wet bulb the temperature	^oC
v	Air flow velocity	m/s
ρ_{in}	Density of the air at inlet	kg/m^3

Subscripts

in	Inlet state of the system
out	Outlet state of the system

List of Figures

Chapter 1: **Page**

Chapter 2

Chapter 3

Chapter 4

Chapter 5

Chapter 6

List of Tables

CHAPTER 1

1.1 Background

World energy consumption pattern showed that fossil fuels including oil, coal and gas are being consumed significantly higher than the environmentally friendly renewable energy sources as shown in Figure 1-1. This will result in increased CO_2 emission to the environment and subsequent climate change.

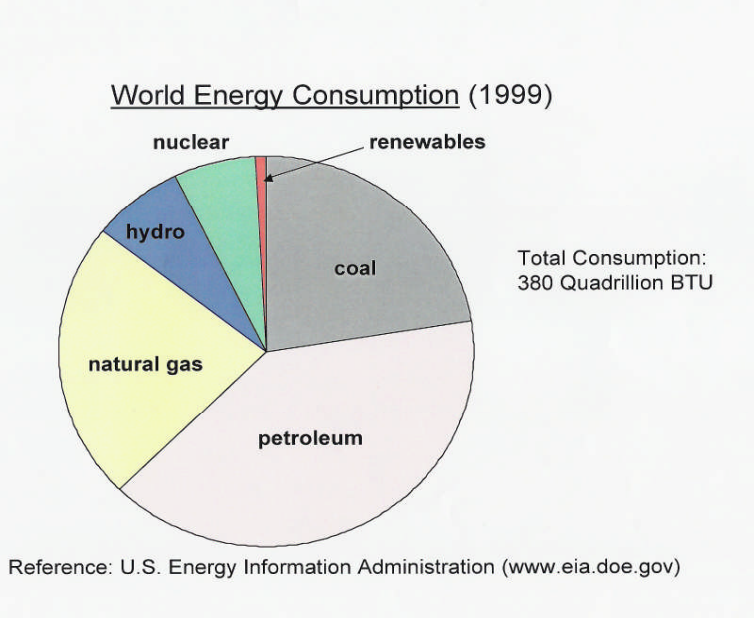

Figure 1.1 Graphical representation of the world energy consumption

Similarly the historical and projected share of primary world energy consumption represented in Figure 1-2(a) indicated continuous dominance on oil, gas and coal (International Energy Outlook, 2000). However, renewable energies which represent very small amount of the world energy consumption are receiving attention because of the falling trend in their costs as shown in Figure 1.2b and are also friendlier to the environment (TCS, 2007). Therefore in 1992 at the Environment and Development (UNCED, 1992) conference in Rio de Janeiro the European Union committed itself to stabilising and then reducing carbon dioxide (CO_2) and CFCs emissions into the environment.

Majority of the energy consumption in building for cooling or heating is derived from fossil fuels. It is therefore very vital to provide a less energy intensive system for space cooling which will replace or minimise dependency on the conventional vapour compression air conditioning systems.

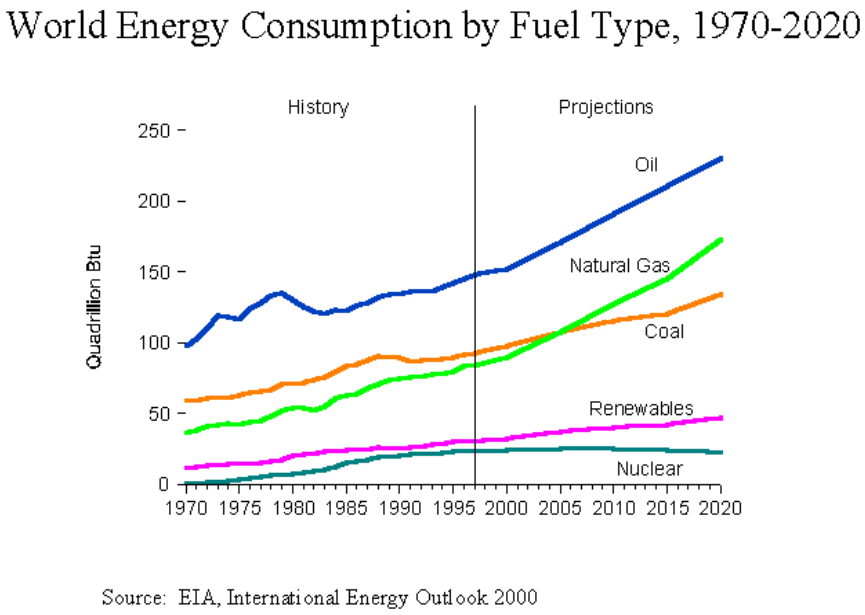

Figure1.2a World energy consumption pattern based on history and projections

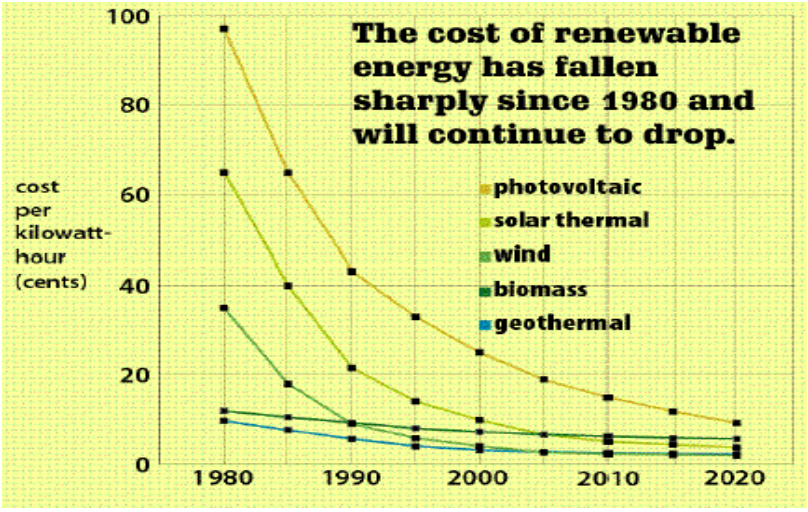

Figure 1.2b Falling trend of renewable energy costs

Usually buildings in hot climates are continuously heated by the sun and dry winds during the day time as shown in Figure 1.3. Therefore the wall mass acts as a heat storage medium emitting heat to the interior making the entire space warm and uncomfortable up to late evening periods. Evaporative cooling is one method of simulating natural cooling effects commonly experienced at or near seas and lakes during warm periods of the day (Figure 1.4) and the same technique have long been realised to be used for the cooling of buildings. The evaporative cooling system can be integrated with a heat transfer unit such as thermo electrics or heat pipes to make the application of the system more flexible for either cooling with humidification or cooling without humidification. It can also be used as a heat sink to other cooling devices such as thermoelectric system.

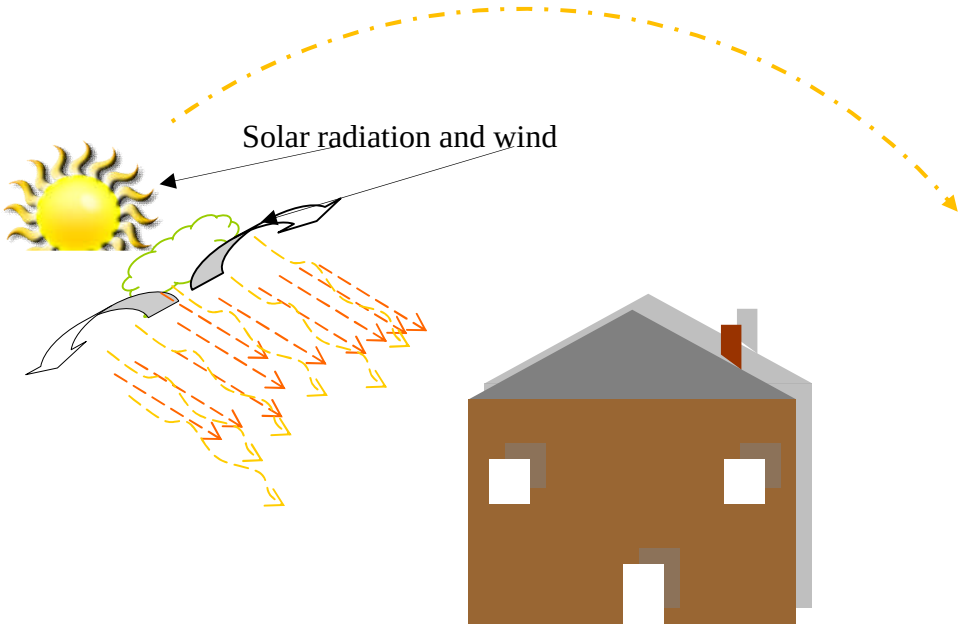

Figure 1.3 Building exposed to solar radiation and dry winds

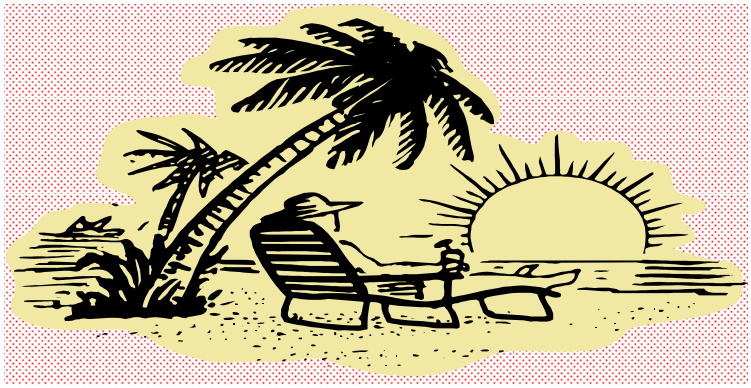

Figure 1.4 Enjoying natural evaporative cooling effects around the sea

As thermoelectric device operates on direct current (D.C.) power supply solar photovoltaic (Khattab et-al, 2006) can be exploited to power the evaporative cooling system integrated with thermoelectric. Although a lot of researches have been carried out there is still need to exploit other ideas to a full scale operation and actual building space cooling application.

This research will deal with several novel evaporative cooling methods and their applications to provide comfortable cooling for building space. It will involve mathematical modelling and experimental investigation of the above mentioned evaporative cooling methods. These are novel evaporative cooling systems using porous ceramics and the porous ceramics-cum-thermoelectric cooling system. Then paper fibre horizontal tubes evaporative cooling system was developed. The proposed systems can be interchanged to be suitable for cooling with humidification or cooling without humidification.

1.2 Aims and Objectives of the Research

- To investigate the performance of some evaporative cooling systems and their potentials for use in building cooling applications.
- Use of locally available materials and safe recyclable items.

- To avoid the current use of recirculation pump in order to save energy and minimise running maintenance.
- To integrate the porous ceramic system with thermoelectric (TE) cooler and investigate its performance as a heat sink in order to improve the coefficient of performance (COP) of the TE.
- To develop and evaluate the performance of horizontal tubes evaporative cooling system using tissue paper.
- Identify several types of the evaporative cooling systems suitable for use in building including:-
  - Theoretical investigation.
  - Experimental investigation.
  - Comparison between theoretical and experimental results.

1.3 Description of the Research

This research is based on the evaporative cooling where hot dry air can be passed through evaporative pad, get cooled and then be blown to a building space as illustrated in Figure 1.5. Simple evaporative cooling process provides cooling effect by adiabatic evaporation of water. The process can be demonstrated on a psychrometric chart as shown in Figure 1.6. In this example air at 30^{o}C dry-bulb temperature and 20% RH passed through an evaporative cooling media making its state to change to a dry-bulb temperature of 18^{o}C and 79% RH. That is lowering the temperature but increasing the relative humidity (RH).

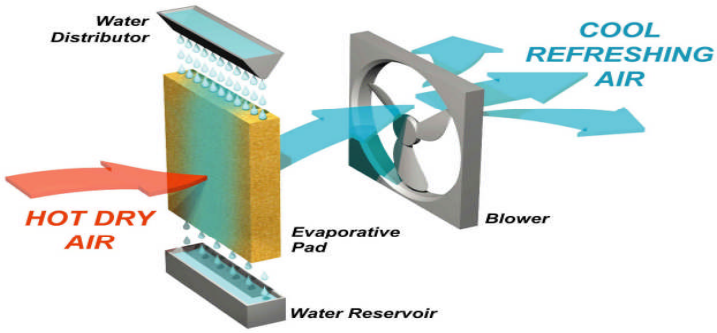

Figure 1.5a Basic evaporative cooling processes

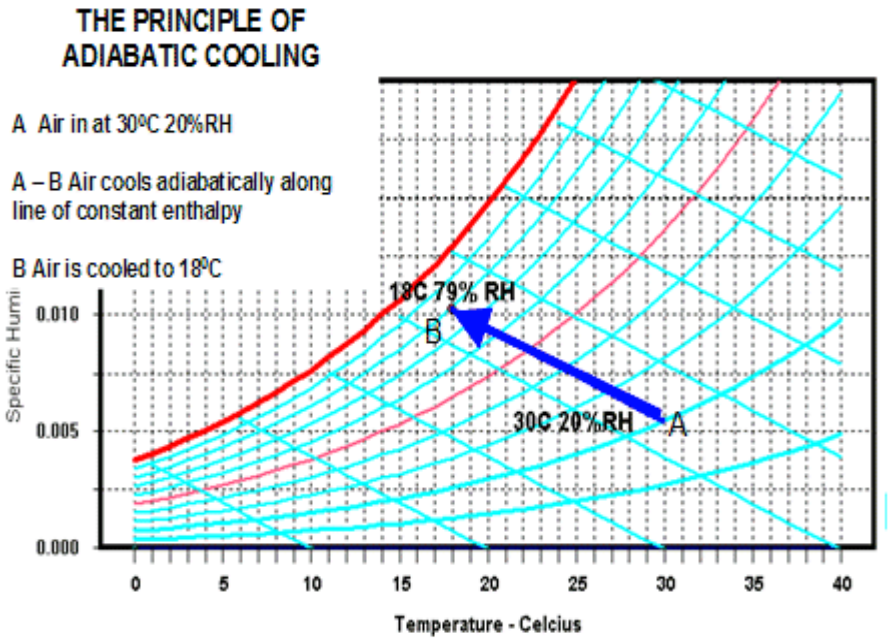

Figure 1.5b Basic evaporative cooling processes on psychrometric chart (Source: www.ecocooling.co.uk/psychr.html)

In this research several novel evaporative cooling devices suitable for building cooling have been identified. These consist of direct evaporative cooling using porous ceramics; porous ceramics integrated with thermoelectric cooler and also indirect cellulose fibre (paper) tubes novel evaporative cooling systems. This chapter briefly outlines these novel evaporative cooling systems, the reasons for undertaking the research and the relevance to potential users.

1.3.1 Direct evaporative cooling using porous ceramics

Basically in this type of evaporative cooling system, dry outside air is blown over water-saturated medium made of porous ceramics and cooled by evaporation. The method introduces moisture to the air until the air stream is close to saturation. So the air temperature falls while its moisture contents increases. As a result energy contained in the exit remains unchanged and its wet bulb temperature kept the same. For this research hollow rectangular containers made of porous ceramics were used as the water saturated medium. The units were produced at a firing temperature of 1130^{o}C (Ibrahim et al, 2003). To utilise the cooling effects in a room of a building, the ceramic evaporators filled with water must be located on an air flow path from outside to inside. The location can be at different parts of the building. In this research the location shown in Figure 1.6 was adopted to allow air to flow over a wider surface area of the ceramics.

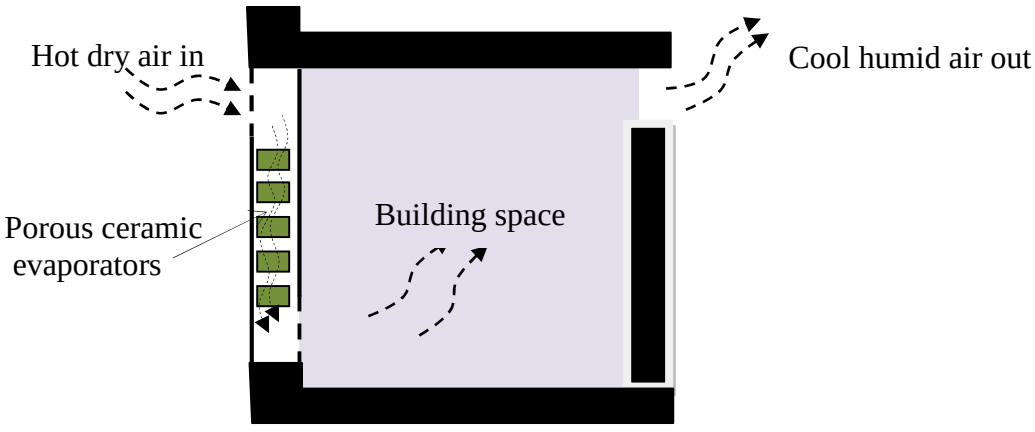

Figure 1.6 Air flow from ambient to the building through the wall integrated ceramic evaporators

Using porous ceramic evaporators for direct evaporative cooling eliminates the requirements for high pressure water circulation. The evaporators can be made out of clay which is locally available in many places. The maintenance associated with water spray nozzles in some direct evaporative cooling systems such as cooling towers is also eliminated. However the system requires a large surface area in order to achieve significant cooling effect. This can be solved depending on how the system is arranged and fitted in to the building constructions.

Two different types of arrangement were investigated in this research. The "hanging system" and the "stacking". In the former evaporators were supported on metallic frames while the latter system consists of units stacked on top of each other.

1.3.2 Integration with thermoelectric cooler

One of the novel evaporative cooling systems investigated in this research consists of integrated system with thermoelectric unit. This is an extension of the research on evaporative cooling using porous ceramic evaporators. In this case thermoelectric unit was integrated in to the porous ceramics evaporative cooling system as shown in Figure 1.7. The arrangement consists of a mobile chamber containing porous ceramic evaporators (unit A). An overhead water tank was provided on top of the chamber. In this way water is supplied to the ceramic evaporators through a feed line by gravity. A condensate tank was provided at the bottom for periodic monitoring of the condensate level. A thermo electric cooling unit (B) was modified and then attached to the chamber to make up the entire integrated system. It was attached so that the hot fins

receive cool air from the outlet of the evaporative cooling chamber while the cooling effect from the cold side of the thermoelectric is channelled to a building space (C). Part D is the power supply terminal for the thermoelectric unit. The completed system was instrumented and monitored in an environmental chamber.

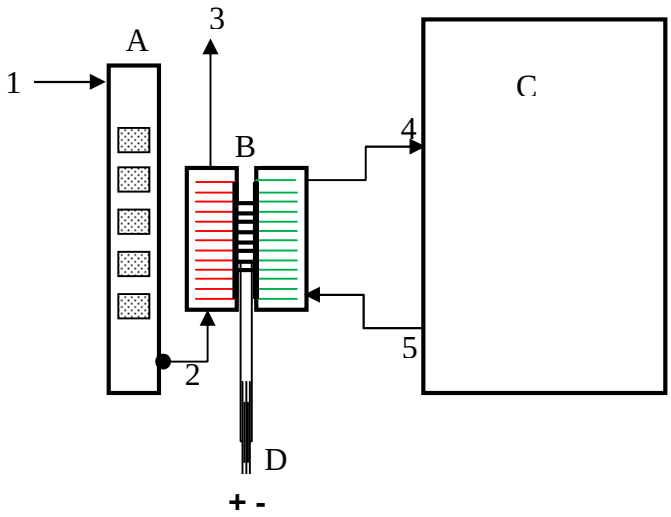

A-evaporative cooling unit
B-thermoelectric unit
C-space to be cooled
D-power supply to thermoelectric unit
1-inlet to ceramics cooling chamber, 2-outlet from ceramics chamber and inlet to thermoelectric heat sink, 3-exshaust from TE heat sink, 4-cooled air from TE cooler, 5-return air to TE cooler.

Figure 1.7 Ceramics evaporative cooler integrated with thermoelectric cooling unit

1.3.3 Novel horizontal cellulose fibre – tubes evaporative cooler

This system consists of arrangement of concentric tubes made out of paper or tissue fibre. The inner tube consists of porous pipe covered with a fibrous material which becomes wet by absorbing water from the supply tank. The outer surface of the wet fibrous material is entirely covered with an

impermeable paper membrane which was attached with the help of a thermal adhesive for better heat transfer. It was then assembled axially in an outer tube as schematically shown in Figure1.8a. The working air flows over the inner tube containing moistened tissue surface. Evaporative cooling takes effect directly and the air is discharged at a high relative humidity.

The supply air simultaneously flows over the outer surface of the impermeable paper heat exchanger which is thermally glued to the moistened tissue paper.

Dry cool air is therefore supplied to the space. This system falls under indirect evaporative cooling system. The heat and mass transfer process taking place across the system boundaries that are applicable to this system are illustrated in Figure 1.8b and the psychrometric representation shown in Figure 1.8c (Zhao, 2007). The product air flows through the dry channel and loses heat across the wall. Therefore its temperature reduces from inlet at P1 to outlet at P2 with little increase in absolute humidity. However, in the wet channel the absolute humidity (moisture content) of the working air increases from W1 to W2 as it absorbs the heat from the wet channel to effect evaporation process.

Simple construction technology, use of safe recycled materials and renewable energy such as solar to provide the small power to run the system are among the motivating factors that influenced this development. One unique feature of this is the horizontal water supply arrangement which enables the entire length of the fibre to be moistened without the use of a pump. Based on these, two systems were developed and investigated for building cooling applications.

Following the results of the window prototype, improvements were recommended. The system was then modified for application on roof tops. Its performance was investigated after installing on the roof of a parasol. It was

provided with a central duct through which the warm ambient air that has been cooled is transferred to the underneath of the parasol for the comfort of the users. The entire system was well instrumented with temperature and relative humidity sensors.

Experiments were conducted under different temperature, relative humidity and air flow rate values in order to analyse the system performance.

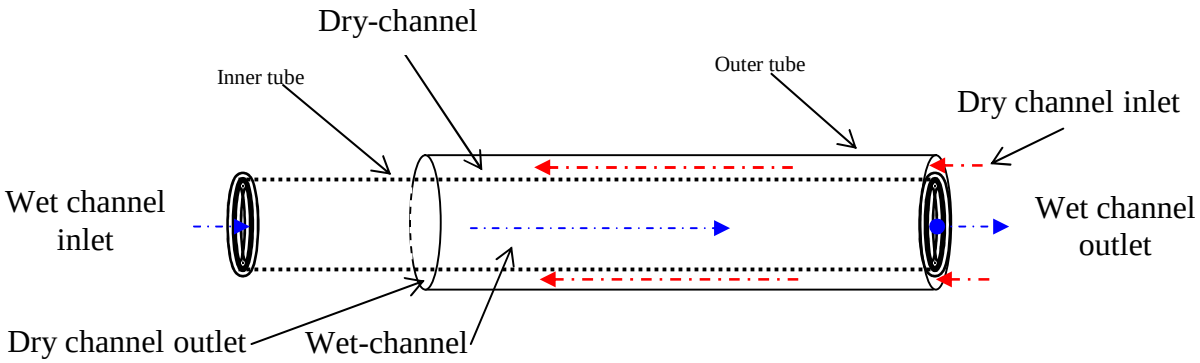

Figure 1.8a Air flow channels of the concentric tubes evaporative cooling

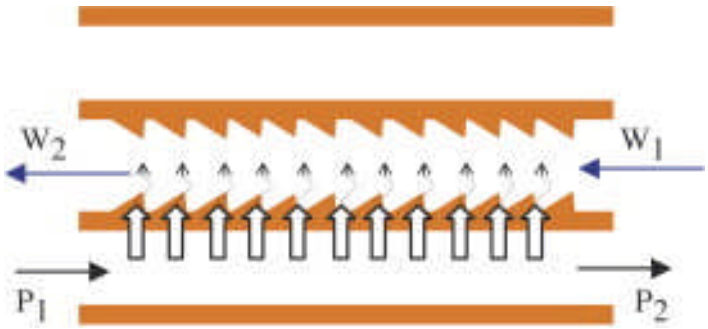

Figure 1.8b Heat and mass (moisture) transfer in an indirect evaporative cooling system applicable to the concentric-tubes evaporative cooler

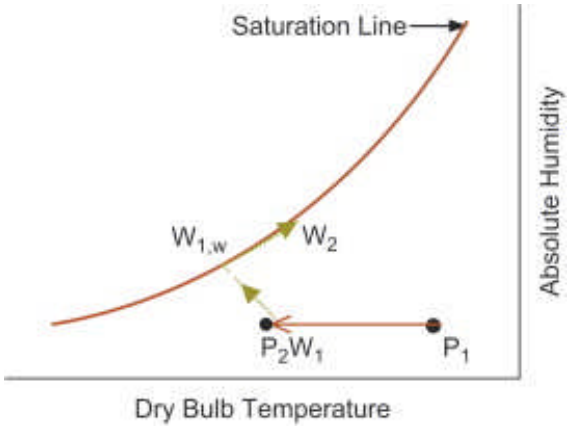

Figure 1.8c Psychrometric diagram representing heat and mass (moisture) transfer in an indirect evaporative cooling system

1.4 Novelty of the research and beneficiaries

1.4.1 Novel features.

The innovative features in the proposed research consist of the following:

- Use of porous ceramic evaporators for cooling of building space and eliminating the use of a pump to circulate water.
- Development of an integrated system with thermoelectric cooler to demonstrate the use of evaporative cooled air as a heat sink.
- Introduction of horizontal tubes arrangement for evaporative cooling without use of a pump.

Also because of low energy requirement for running the system renewable energy in the form of solar photovoltaic can be utilised.

Application of the proposed research results will substantially reduce the vast amounts of energy consumed in building space cooling.

1.4.2 Prospective beneficiaries of the research

Realising the importance of evaporative cooling made European Union (EU) to embark on funding research projects Bowman et al, (2000) in the technology. These included the application of passive down draught evaporative cooling to non- domestic buildings. Examples of some evaporative cooling techniques

have demonstrated its operation and potential energy savings in Europe and Middle East. Results of the proposed research has potential prospects in a number of countries in EU because the temperature and relative humidity distributions in some of these regions as shown in the climatic maps in Figures 1-3a and 1-3b are favourable for the applications of evaporative cooling. This is because the system has an advantage of cooling with humidification and can also be with dehumidification.

In Africa countries like Nigeria will benefit from the system as the country has hot and dry as well as hot and humid regions (ECOWAS.info2003-2006) as shown in Figure 1-4. Also because of low energy requirement for running the system renewable energy in the form of solar photovoltaic can be utilised to provide small power required to run the air blower or fan. Application of the proposed research results will substantially reduce the vast amounts of energy consumed in building space cooling.

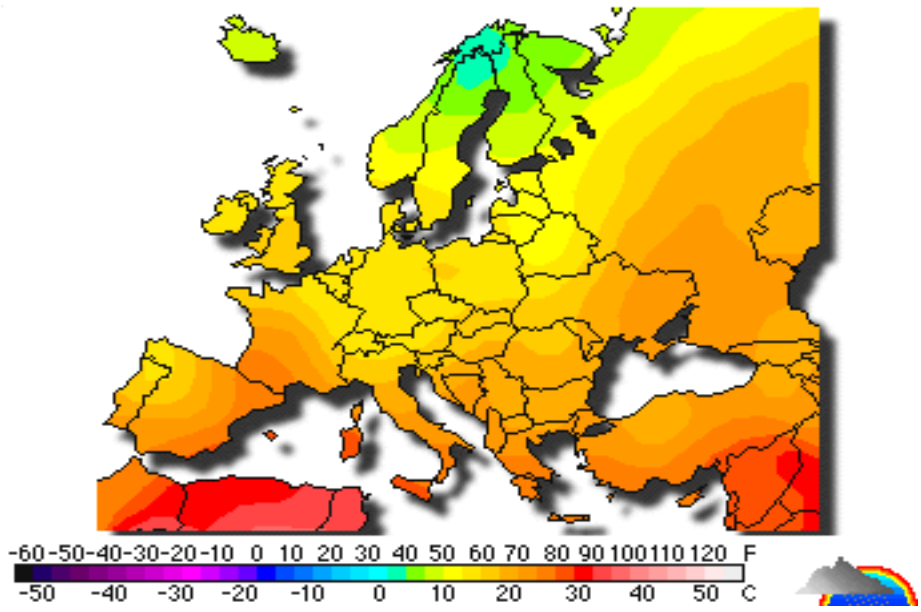

Figure 1.9a EU-Climate map indicating temperature variation

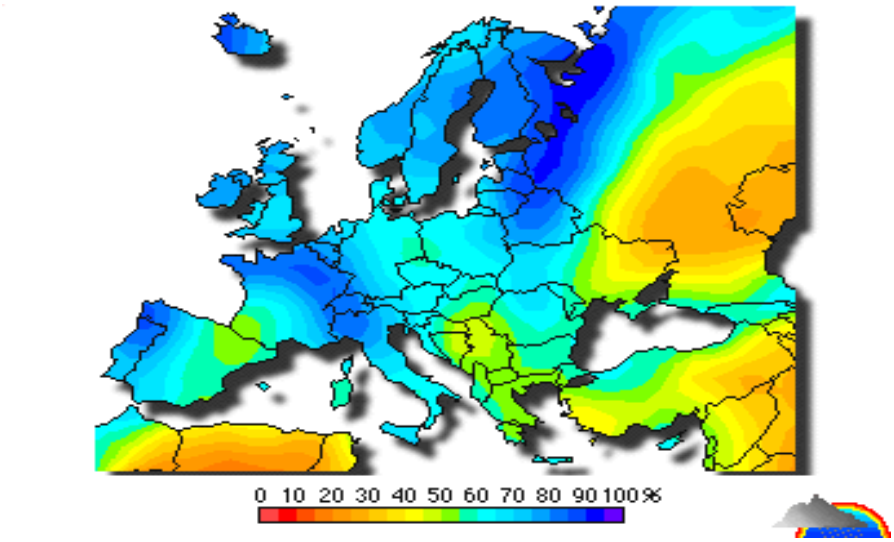

Figure 1.9b EU-Climate map indicating humidity distribution

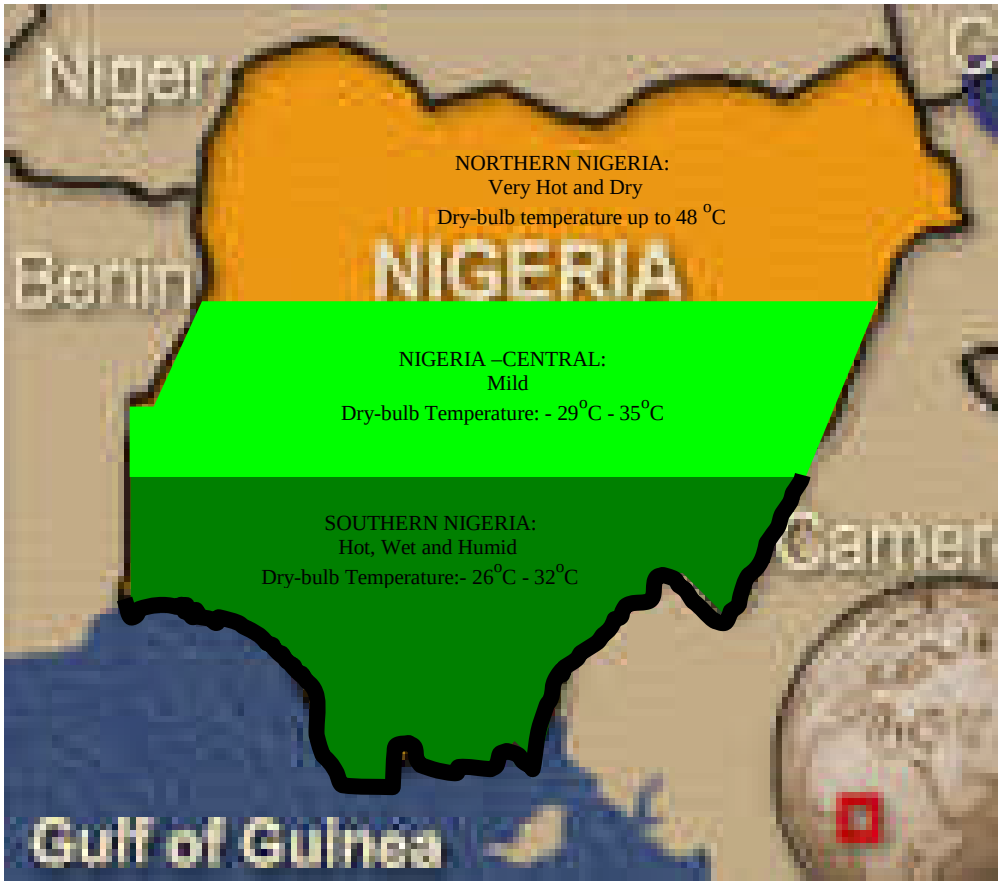

Figure 1.10 Map of Nigeria showing different climates

The research was carried out in different stages and covered a number of tasks as reported in different chapters and sections of this report. A brief outline of these is given below:

Chapter 1 is the general introduction section. It summarises the rational and the research projects involved. Chapter 2 is a review of the developments in the technologies applied to this research work. The areas involved are evaporative cooling including direct, indirect and combined mode or direct / indirect types and also integration with other cooling devices such as thermoelectric and heat pipes. Other evaporative cooling cycles are also reviewed in brief.

Chapters 3 and 4 cover theoretical modelling for direct and indirect types of evaporative cooling respectively. Chapter 5 covered the experimental testing and performance of ceramics-based evaporative cooling on both the supporting frame and stacking configurations of hollow porous ceramic evaporators. Chapter 6 describes the thermoelectric and porous ceramics integrated evaporative cooling system. It covered the development and experimentation as well as the performance analyses based on experimental results. Chapter 7 describes the development and performance of novel cellulose fibre (paper)-tubes evaporative cooler. It covers the reason behind the choice of the horizontal tube arrangement as well the experiments and the performance evaluation of the system. It also describes the application of the paper tubes evaporative cooler on the building roof and demonstrated the application on parasol. In chapter 8 the general conclusions, suggestions for further works and the contribution of the research to knowledge are given.

1.6 Summary

This chapter contains brief introduction on the need for looking in to alternative ways of reducing high dependence on the CFCs based building cooling technologies. It showed the global energy consumptions pattern indicating the dominance of fossil fuels as the main sources of energy for our day to day activities. The chapter gives an outline of the objectives of the project. It also covered brief description of the research and the thesis structure.

CHAPTER 2

Literature Review

2.1 Introduction

This chapter covers literature review from the basics extending to the developments and other investigations in evaporative cooling reported by different researchers. The basic methods or processes of achieving evaporative cooling consisting of misting or drip, cool cells or wetted pads and the forging were discussed in this literature review. In addition to the methods, different types of evaporative cooling are also discussed. These are direct, indirect and combined direct and indirect types. The review also covered use of other materials and configurations for evaporative cooling systems. Integration of the evaporative cooling systems with other cooling devices such as thermoelectric cooler and heat pipes have been covered in this review. Some historical backgrounds where applicable are also discussed to reflect the state of the art in the technological developments of the systems.

Literature review is essential to have an insight into existing knowledge leading to the understanding of the previous works and researches carried out concerning the area keeping in mind the latest state of development. In the process a collection of research materials such as books, journal articles, reports, internet documents etc were used.

2.2. Evaporative Cooling

By definition evaporative cooling is the exchange of sensible heat in air for the latent heat of vaporisation of water droplets on wetted surfaces. It can be used

to cool building air directly by evaporation or indirectly by contact with a surface previously cooled by direct evaporation. Ideally evaporative cooling is adiabatic or constant enthalpy process meaning that sensible heat is extracted from the air (dry-bulb temperature (DBT) is reduced) while an equal amount of latent heat (in the form of water vapour) is added. The enthalpy or total heat remains the same (McGraw-Hills Inc.1993). In simple practical terms evaporative cooling is responsible for the chill one feels when a breeze strikes his skin. The air evaporates the water on the skin by extracting heat from the body. Basically the warmer and dry the air, the more moisture it is able to hold. The amount of water in the air compared to the amount required for it to become saturated is called relative humidity. So if the air contains only half the amount of moisture it can hold when saturated, the relative humidity is 50%. It is a very important parameter that affects evaporative cooling process.

To evaporate water the required heat is absorbed from whatever surface the water comes in contact with. This could be an object, from the air itself or from a wet cooling pad. As heat is removed from an object the temperature of that object or space is decreased. For example, in case of water as it evaporates into vapour it cools both the impinging on saturated air and the remaining water which provided the necessary sensible heat. The amount of heat required to evaporate one gallon (4.547 litres) is about 8700 B.T.U (1 B.T.U = 1055.06 Joules). So it can be seen that through evaporative cooling tremendous amount of heat can be removed from the air having contact with evaporative cooling surface. Typical evaporative air cooler is schematically shown in Figure2.1a and the detailed system components and process shown in Figure 2.1b. It was made with perforated metal box with three side packed with pads of shredded

aspen wood, which could be saturated with water from slotted trough running along their upper edges. With the help of an electrically driven blower air is drawn through the wet pads and discharged into the building space or room. The system is considered hybrid because of the auxiliary energy required to power the blower, but it is a direct method of evaporative cooling. The cooler could reduce the dry bulb temperature of incoming air to within 5^{o}C to 10^{o}C of the outdoor wet bulb temperatures providing very acceptable indoor conditions. Added to that they were reliable, inexpensive and required only a small amount of electricity to operate. Solar energy could therefore be used to run them. As the time passed by, evaporative cooling witnessed series of improvements and the 21st Century technology provides effective, economical environmentally friendly ad healthy cooling.

It can be applied to cool homes, offices, factories, warehouses and many other building areas. Evaporative cooling can be used for space cooling either through direct or indirect methods.

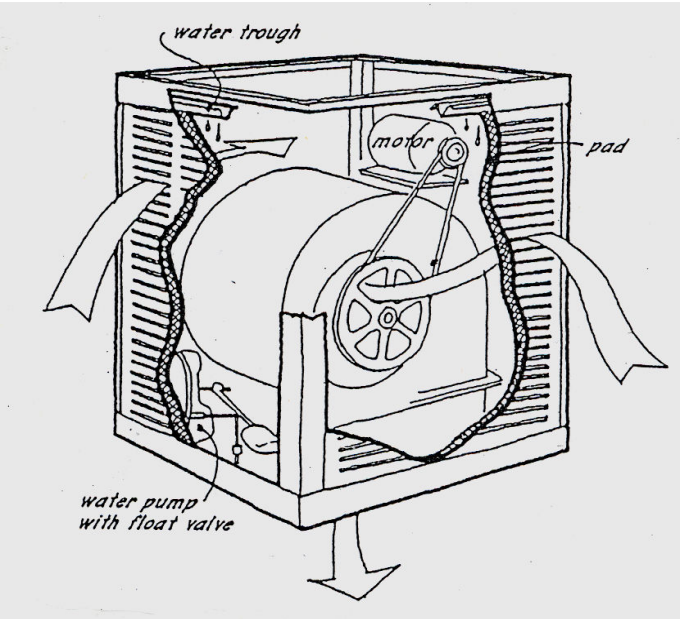

Figure 2.1a Typical direct- type evaporative air cooler

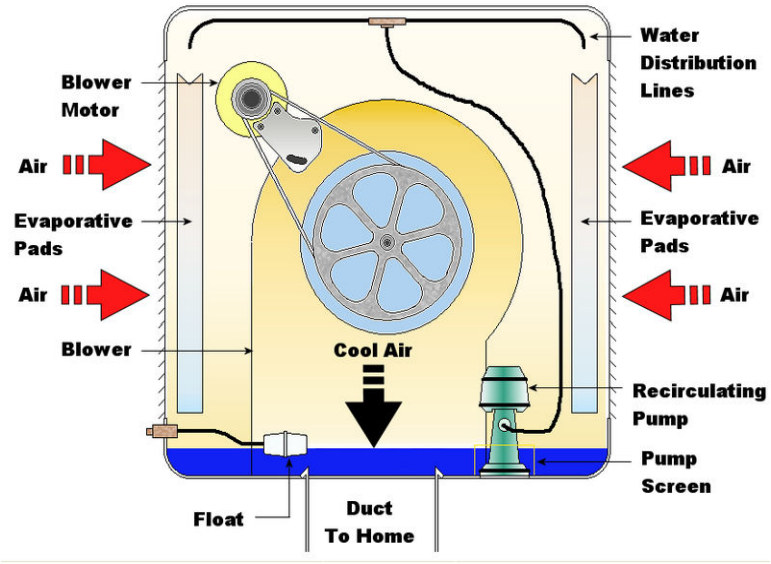

Figure 2.1b Detailed components in direct evaporative cooler (wikimedia.org)

2.3 General Evaporative Cooling Principle

Evaporative cooling is based on the conversion of sensible to latent heat. The two basic principles consist of the direct and indirect as illustrated in psychrometric chart, Figure 2.1c and will be described in details in their is respective sections. The process in which the moisture content of the air is increased falls under direct type of evaporative cooling. Starting at point A on the psychrometric chart, it is shown as a displacement along a constant wet bulb temperature line AB in Figure 2.1c. (Santamouris and Asimakopoulos, 1996). We can have a heat exchanger in which the air or remnant water cooled by direct evaporative cooling is used as a primary circuit and the air to be cooled is circulated in the secondary circuit separated by a boundary with effective heat transfer property. In this case the temperature of the air in the secondary circuit will decrease while its moisture content will remain constant as represented by line AC in Figure 2.1c. This process falls under the *indirect* type of evaporative cooling. However since the temperature of the air falls, its

relative humidity will increase (Qiu and Riffat, 2006) but cannot be as that under the direct evaporative cooling process. Direct and indirect are basically the two main types of evaporative cooling process upon which all others emanate.

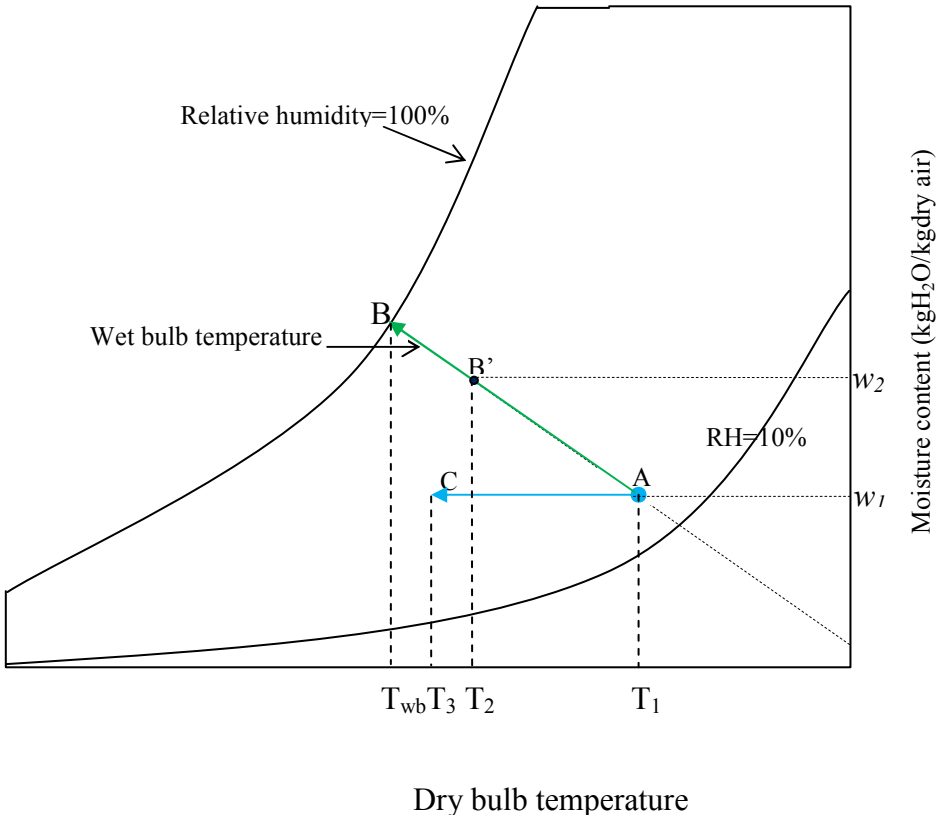

Figure 2.1c Psychrometric representation of direct and indirect evaporative cooling process

2.3.1. Evaporative cooling methods

Basically evaporative cooling can be direct, indirect or combination of direct and indirect. The combination types are also called hybrid or integrated types. There are three main methods of achieving evaporative cooling and the choice of each depends on the type of application required. These include misting or drip systems, cool cells and fogging systems. Each of the systems is briefly explained below and is concerned with the way water can be supplied for evaporation.

(a) Misting or drip method

Drip or misting systems are one of the older evaporative cooling methods around. In this type a low pressure mist or drip is sprayed directly on a body. As moisture evaporates from the surface of the body, heat is absorbed and therefore it becomes cool. This method was commonly used on animals. As water drips sprayed on the animal skin evaporate, heat is absorbed. The animal therefore enjoys cooling.

The method often features use of cooling pads and water drips distribution system as illustrated in Figure.2.2a. Water drips along the distribution pipe and drains down into the pad material. Sump can be provided at the bottom and should be large enough to hold all run-offs when the pump is turned off, (Bucklin et al, 2008).

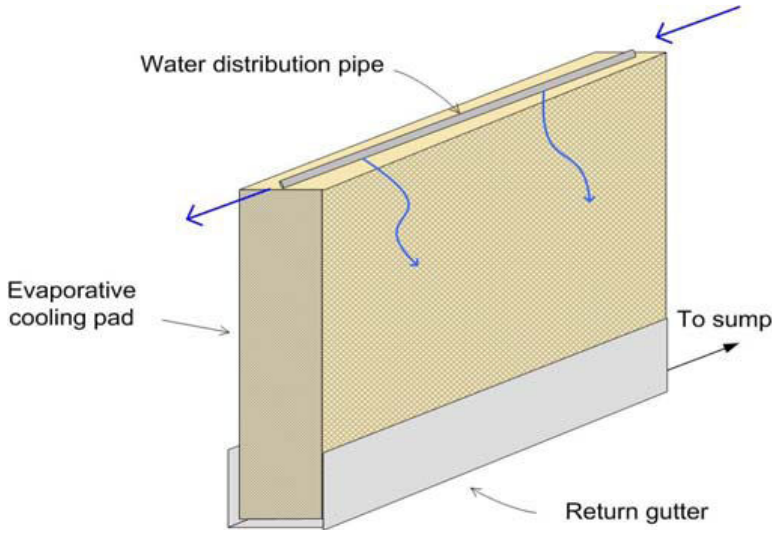

Figure 2.2a Evaporative cooling pad for drip method
(Source: http://edis.ifas.ufl.edu)

Some drip evaporative cooling methods employ loose cooling pads or porous materials. In this case the pad must be confined in a wire mesh to be well supported for the drip water distribution arrangements as illustrated in Figure2.2 (b) and Figure2.2 (c).

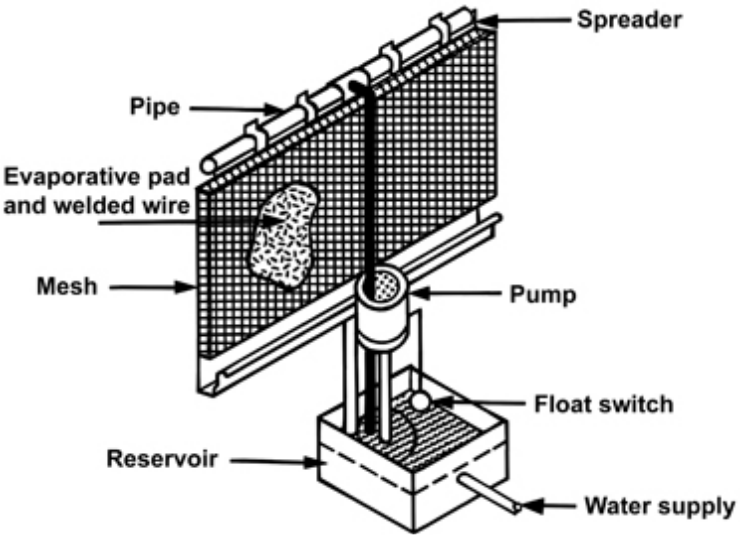

Figure 2.2 (b) Drip system cooling pads secured in a wire-mesh
(Source: http://www.kelleysindia.com/pollutioncontrol.htm)

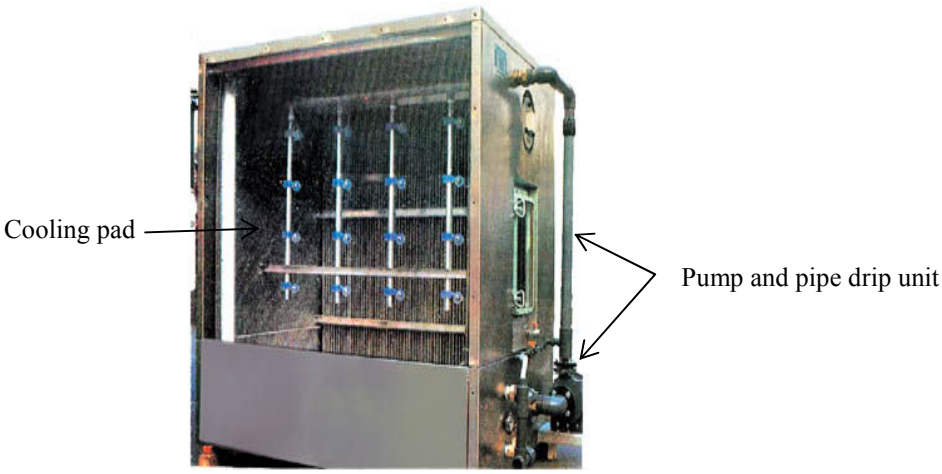

Figure 2.2(c) A cooling pad well secured for water drip
(Source: http://www.kelleysindia.com/pollutioncontrol.htm)

In India (Roy, 1989) drip evaporative cooling method was constructed with simple materials and used for the preservation of fruits and vegetables as shown in Figure 2.3. It consists of a simple low cost cavity wall evaporative cooler constructed from bricks and termed as "Improved Zero-Energy Cool Chamber" in India, (Lisa and Kader, 2003). The sand filled cavity between the walls and the sand were kept saturated with water by simple dripping system as shown. The items to be preserved were loaded in the cooling chamber provided and then covered with a rush mat which was also kept moist. It was reported that this chamber maintained an inside temperature between 15°C and 18°C and a relative humidity of about 95%.

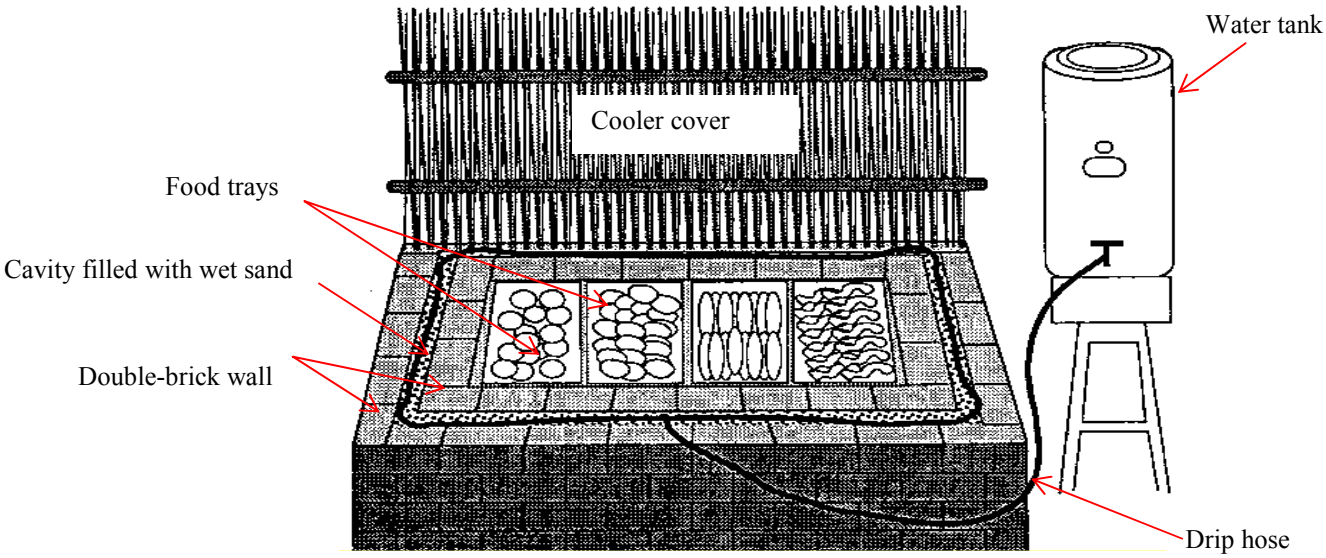

Figure 2.3 Low-cost cavity evaporative cooler based on drip method

Similarly, in Philippines two simple evaporative coolers were developed and used for cooling and storage of vegetables as shown in Figure 2.4, (Acedo, 1997). In the Figure, type (a) cooler stands in a water tank and also has another water tank at the top. The jute sacks evaporation material was kept wet by

dipping their top and bottom edges in to these two tanks. In type (b) the water tank was placed on top of the cooler to supply water through a dipped cloth to the rice hulls filled at the sides to for evaporation process. Produce stored in these coolers has a longer shelf life than those kept at ambient conditions. Tomatoes and peppers lost less weight, had slow ripening rate and could be kept for as long as they typically can be stored under refrigeration (about 3 weeks).

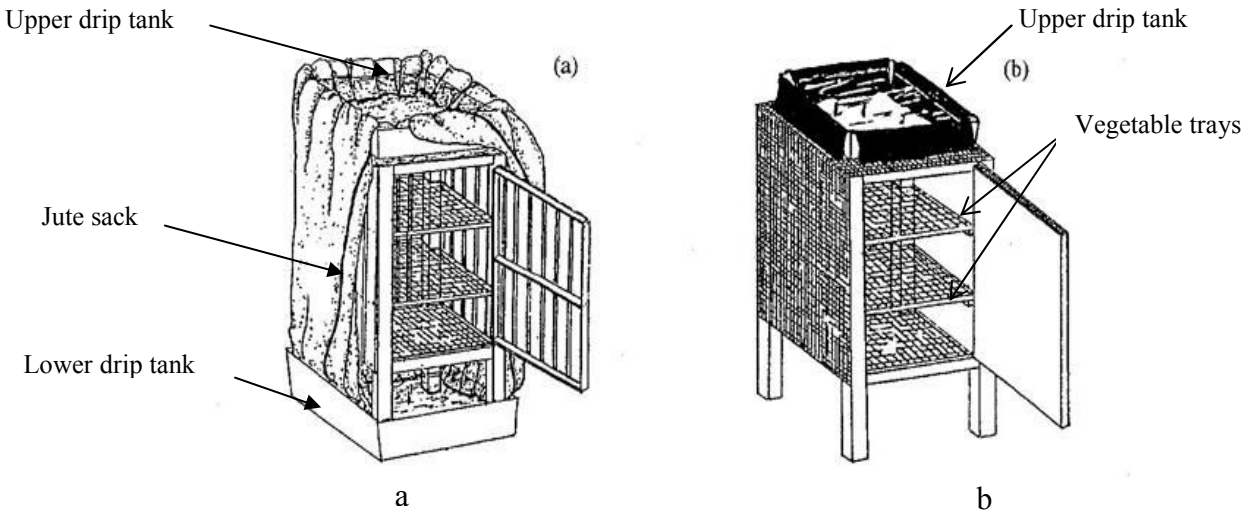

Figure 2.4 Philippines' developed misting evaporative cooler for vegetable storage

Figure 2.5 shows an evaporative cooler equipped with a vortex wind turbine. Chunks of charcoal or straw contained in between chicken wire mesh secured at the sides of the cooler formed the porous surface kept wet by simple drip method. Natural wind turns the turbine causing draught through the wet surface in to the load of produce inside the cooling chamber. With this wind turbine integrated drip cooler, temperatures were reduced to 3^{o}C to 5^{o}C below the ambient air temperature with corresponding relative humidity of about 85%.

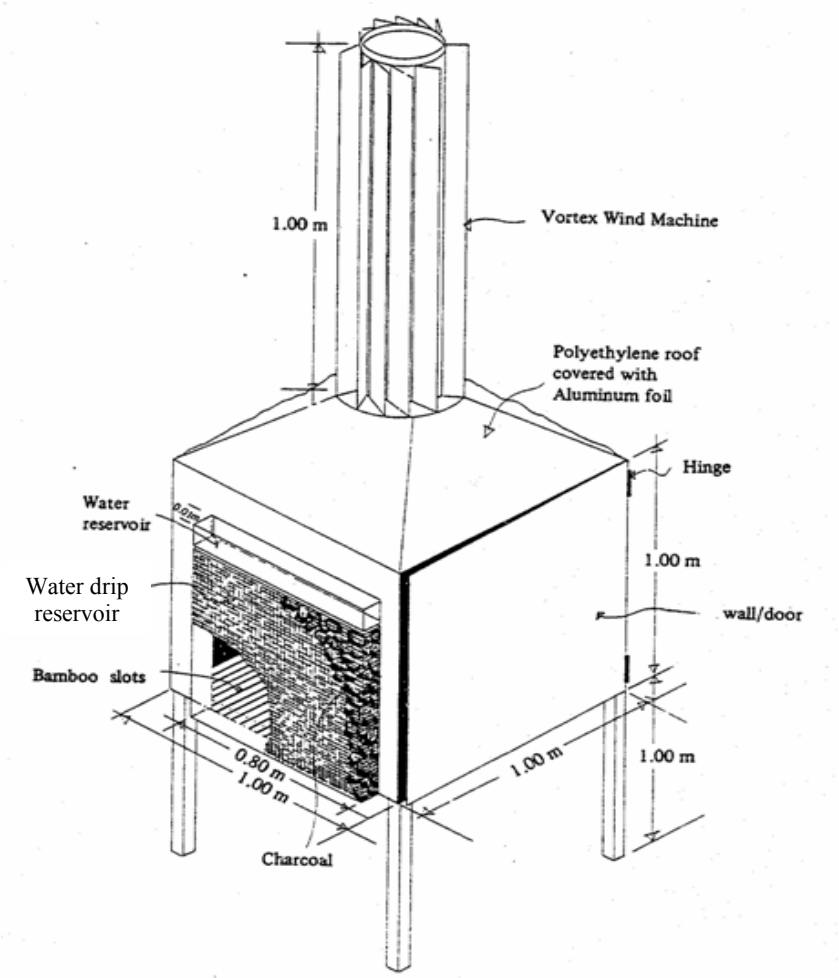

Figure 2.5 Drip-type evaporative cooler equipped with vortex wind turbine

(b) Cool cells or wetted pad

Cool cells are also referred to as wetted pad because in this method water is soaked through a pad made of materials like large paper or felt pack. Cool cell is strategically placed in the inlet opening of the system. The incoming air is driven through the cell as shown in Figure 2.6. As water from the pad evaporates heat is absorbed, causing the incoming air to become cooler. Cool cells work well in conjunction with tunnel ventilation installation. In installing cool cells care must be taken as they can cause air blockage. For this reason adequate or sufficient size of the needed air opening must be considered in selecting material for cool cells or wetted pads.

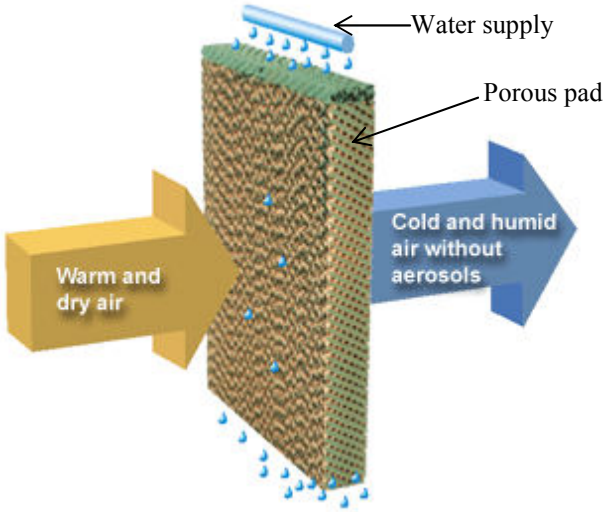

Figure 2.6 Air flow through evaporative cooling pad or cool cell

(A) Cooling pad material

Corrugated cellulose impregnated with wetting agents and rot resistance insoluble salts are the most widely used type of cooling pad material. Under proper maintenance these material should have a life time of ten years and can do an excellent job of cooling air. However, these pads are expensive. Aspen pads which were commonly used in the past are still being used but under certain conditions have a short life. They are also very susceptible to algae infestation that leads to rotting, compaction and subsequently air flow blockage. Therefore to efficiently operate an evaporative cooling system with aspen pads requires frequent and costly replacement of these pads. Other pad materials are also on the market, but none have seen wide acceptance. In choosing a pad material one should *c*ompare costs, life expectancy claims, cooling efficiencies, and probability of maintenance problems before selecting the one that is best for your operation. Since 1960 drip coolers featured excelsior pads made of aspen wood. Also other woods

were tried along with fibre glass and woven paper but were found to have weaknesses that outweighed their advantages. However Aspen pads continue to be sold today because of low cost, limited-benefit cooling option. The photo below shows a sample section of rigid media (A) on the left and aspen pad (B) on the right (Figure2.7).

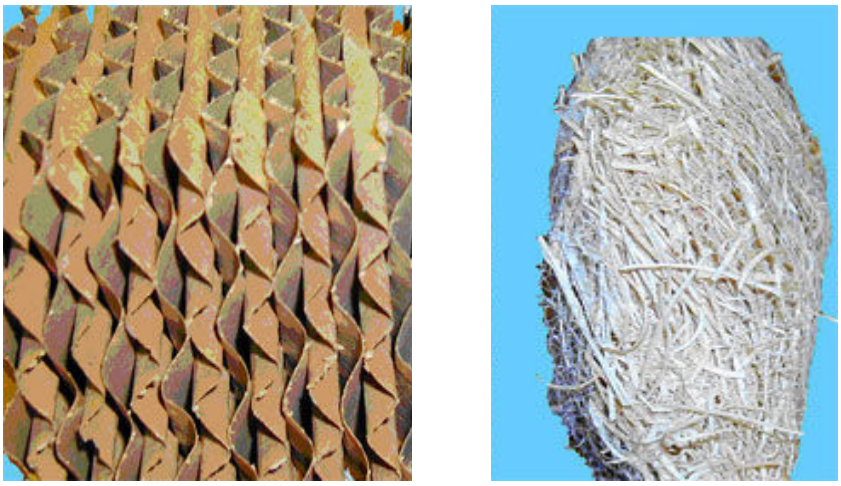

A B

Figure 2.7 Section of a rigid (A) media and aspen pad (B) materials

Several other types of materials can be used in forming a porous pad for evaporative cooling process. Thermal conductivity, water retaining capability (porosity, other factors such as shape formation/holding ability, durability, compatibility to a water-proof coating, contaminations risk as well as cost should be taken in to consideration when selecting the pad materials. Studies showed that porous ceramic could be one of the potential materials for evaporative cooling because of its high capacity force, high thermal conductivity, water-proof, and durability. The TC of porous ceramic depends upon elements contained, the pore size and distribution, the porosity and the manufacturing processes. TC varies from 0.1 to 240W/mK. Generally the TC

decreases with increasing porosity. Also the water retaining capacity (permeability) of the ceramics increases with increasing porosity and pore size. To make porous ceramics one way is to mix ground vermiculite and allophone and heat under temperature range of 600-800^{o}C. Figure 2.8 shows the structure of a porous ceramic made by IKTS, Germany (Fend et al, 2004 and Zhao et al 2007). This structure makes porous ceramics to perform both as moisture retaining and heat exchanging material for use in direct and indirect evaporative cooling applications, (Zhao et al, 2007).

Figure 2.8a An overview of porous ceramics structure

Also performance of some natural porous and non porous materials that can be used to moderate roof surface temperature due to its evaporative cooling effects was investigated. As shown in Figure2.8b these material include silica sand, volcanic ash, siliceous shale and pebbles. Among them siliceous shale of both small and large particle diameter was found to lower the daily average surface temperature by up to 6.8^{o}C and 8.6^{o}C, respectively. Table 2.1 gives the physical properties and pore characteristics of these materials, (Wanphan et al, 2008).

Figure 2.8b Some natural porous and non porous particles that can be used on building roof for evaporative cooling effects (Source:www.elsevier.com/locate/buildenv)

Table 2.1 Physical properties and pore characteristics of porous and non porous particles shown in Figure 2.8b.

Porous materials	Silica sand	Pebbles	Volcanic ash	Siliceous shale
Density (kg/m^3)				
Bulk	1550	2616	1383	868
Particle	2650	2800	1976	2142
Particle porosity (%)	~0	0.1	81.2	60.5
Moisture adsorption ability				
Vapor adsorption (mg/g) (from RH 60–90%)	~0	~0	2.0	242.4
Liquid absorption (%)	~0	~0	79.5	58.7
Average pore diameter (nm)	~0	~0	1.8	9.4
Surface area (m^2/g)	~0	~0	19.1	149.0
Pore volume (cm^3/g)	~0	~0	0.02	0.33

(B) Application of cooling pads

Figure 2.10 shows a conventional evaporative air cooler with a wet pad, a fan and water circulating pump that can be applied for cooling in a building. Air passing through the wet pad can be cooled to within a few degrees of the wet bulb temperature of the ambient air.

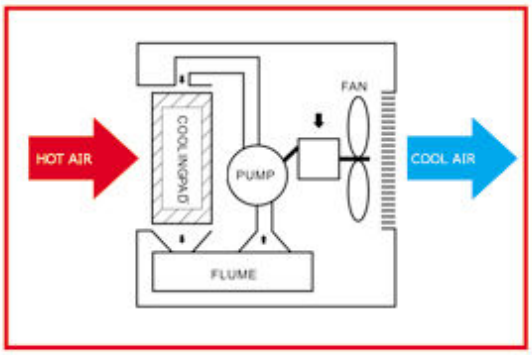

Figure 2.9 Complete evaporative cooling processes with a cooling pad

The application of cooling pad is shown on evaporative cooler that can be installed on a window of a building (Figure 2.10) while multiple cooling pads evaporative coolers installed in a factory building are shown in Figure 2.11.

Figure 2.10 Window unit evaporative cooler with cooling pad

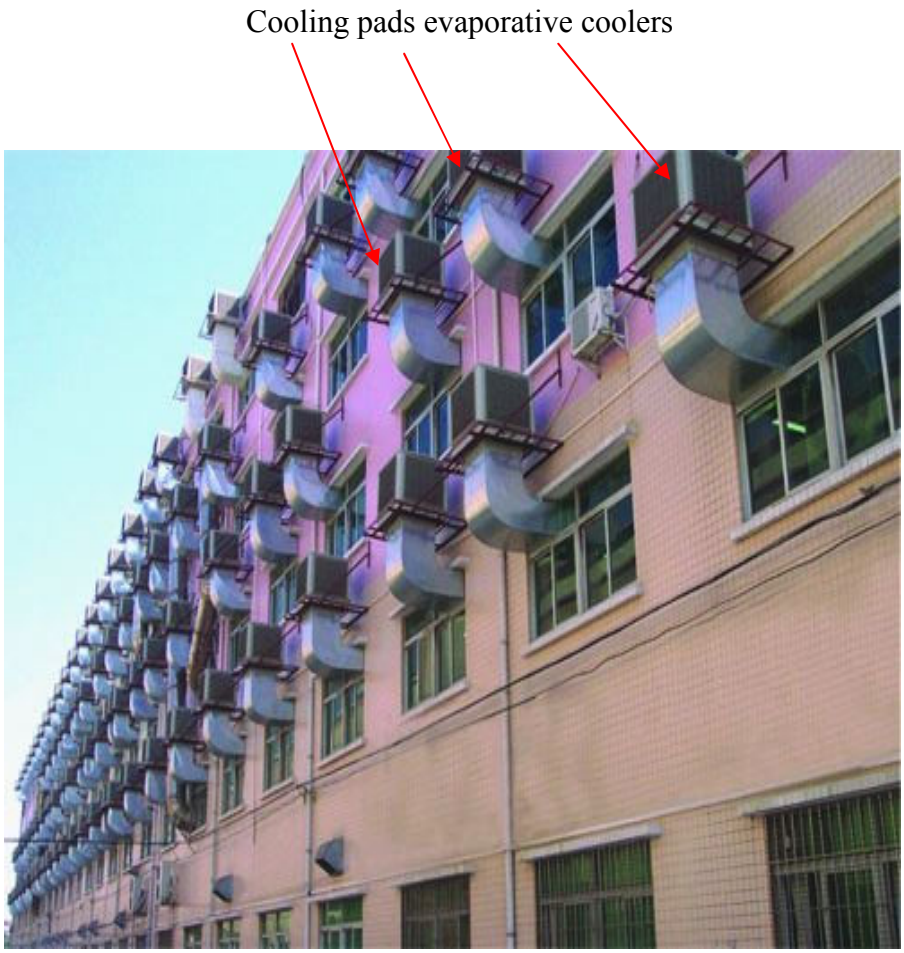

Figure 2.11 Multiple cooling pad evaporative coolers installed on a factory building

Cooling pads can also be used along with wind catchers. Wind catchers were Persian architectural devices used for natural ventilation of buildings by enhancing the air draught through the structure as shown in Figure 2.12(a) (Ghassem et al, 2008) and (b). However, air flow through the wind catcher alone will not be enough to bring the temperature down below ambient because it simply draws in hot air through. Therefore to get colder temperature evaporative cooling pads must be installed before the fresh ambient air intake to the building as shown in Figure 2.13.

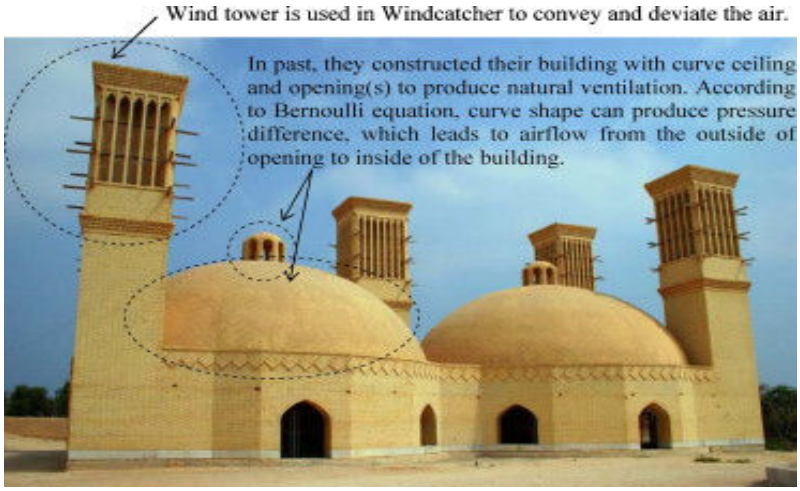

(a)

(b)

Figure 2.12 Persian architecture employing wind catcher to create air draught for natural cooling

The application of evaporative cooling with a cool cell or cooling pad has also been extended to green house systems. As shown in Figure 2.14 an evaporative cooler can be installed at the air inlet to the green house (Sierragreen house, 2008). Figure 2.15 shows an evaporative cooling pad installed along the entire ventilation inlet opening in the wall of the greenhouse. On warm days, the pad is wetted and the incoming air is cooled as it passes through the pad while water evaporates into the incoming air.

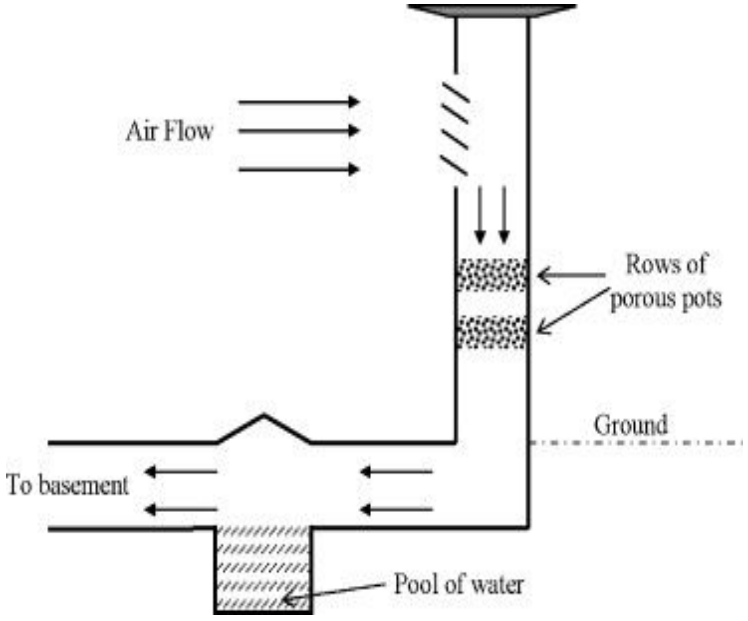

Figure 2.13 Cooling made of porous pots installed along the air flow duct to building basement.

Figure 2.14 Green houses with a pad evaporative cooling unit (GreenConstruction-ww.sierragreenhouse.com/gallery/greenhouse.htm)

The fan-pad evaporative cooling method has been used for experimental study in a cascade greenhouse with inner thermal curtain to see the effect of thermal curtain. It was found that the use of evaporative cooling with a thermal curtain reduces the temperature of greenhouse by 5 °C and 8 °C in the second zone of greenhouse-1 and 2 in comparison to greenhouse without curtain.

Figure 2.15 An evaporative cooling pad installed along the entire ventilation inlet of a large green house.
(http://ecaaser3.ecaa.ntu.edu.tw/weifang/lab551)

Figure 2.16 (a) and (b) respectively show the dimensioned drawings of the full and cross sectional views of wet pad integrated green house used for the experiment, (Shula et al, 2008).

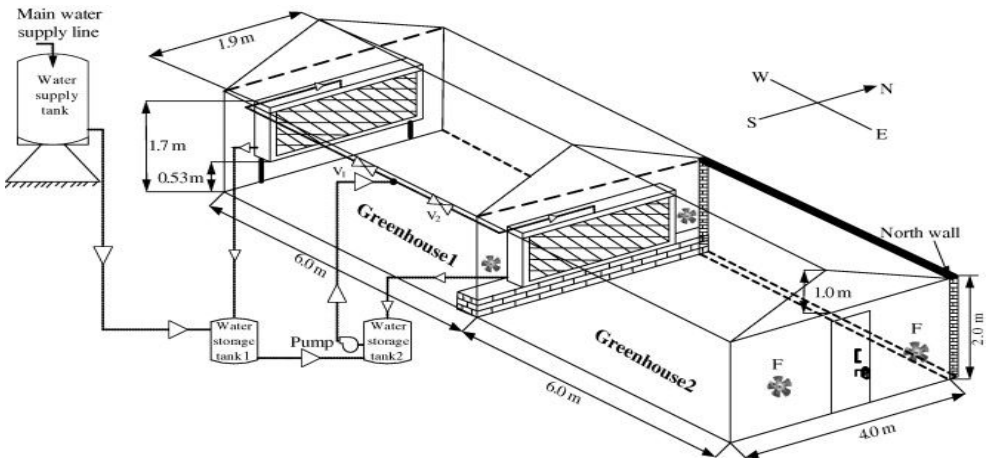

Figure 2.16a Schematic diagram of an even-span cascade green house with evaporative cooling

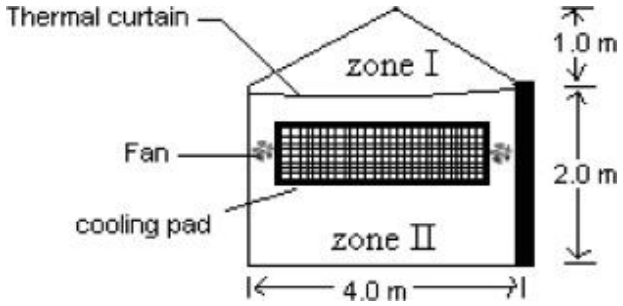

Figure 2.16b Cross-sectional view of greenhouse with curtain and cooling pad

(C) Fogging method

Fogging is a form of misting but in this method water is sprayed via a high-pressure through a fine nozzle and then get atomised as sketched in Figure 2.17 As the water droplets are forced through the nozzle it is transformed into vapour, (Figure 2.18) which absorbs heat from the surroundings. By placing the nozzle beneath the inlet one can direct the spray into the incoming air path, circulation cooler air through the space or room without blocking the air inlet. The systems have mist nozzles or misting rings and a high pressure pump of 800-1000 psi(55.2-69Bar) that can produce and dispense water droplets smaller than10microns (about1/10th the diameter of a human hair) (aqualitywater.com). When this miniscule water droplets hit warm or hot air they flash evaporate. A mist cooling system can reduce the surrounding air temperature by about 2^{o}C. Typical mist evaporative cooling system is shown in Figure 2.19. It consists of misting nozzles integrated in a misting ring attached to a fan-Water pump is also provided. Fogging systems work well with traditional power ventilation systems and in conjunction with tunnel ventilation. Cooling towers fall under this category (WESCOR).

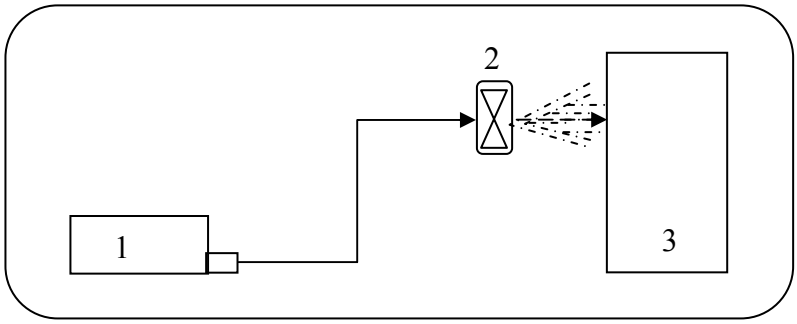

Figure 2.17 Schematic diagram of misting system (1-Water tank and pump unit, 2-air blowing unit, 3-space or object cooled)

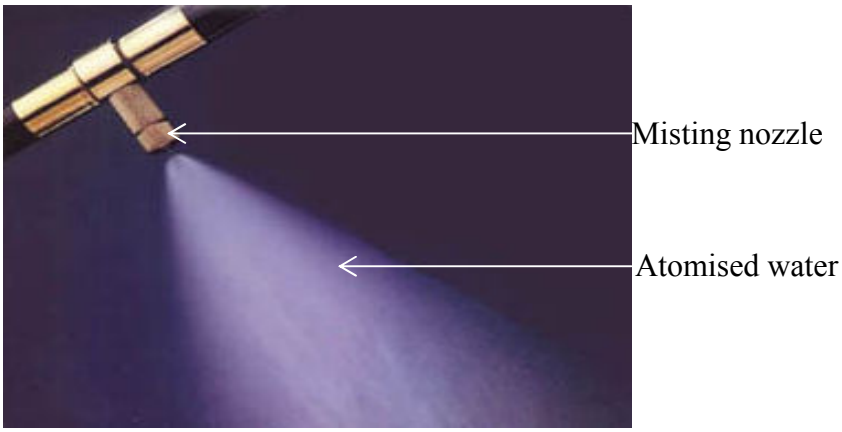

Figure 2.18 Mist system high pressure atomisation nozzles

Figure 2.19 Typical oscillating mobile misting fans integrated with misting ring, water pump and tank (Source: A quality water systems Inc.)

Regardless of the above methods of achieving cooling by evaporation, basically evaporative cooling may be classified into direct and indirect (Ibrahim et al, 2003) and combined indirect/direct each is briefly expressed in the following sections:

2.3.2. Direct evaporative cooling

In this type of evaporative cooling relatively dry outside air is blown through a water-saturated medium (usually cellulose) or porous ceramics where it is cooled by evaporation. As stated in the principle of evaporative cooling, the contact between air and water causes small amount of water to evaporate. Subsequently the latent heat of vaporisation causes simultaneous reduction in the air and water temperatures. Also a smaller amount of sensible heat is exchanged between the two streams. However, the latent heat transfer amounts to 80-95% of the total heat exchanged (El-Dessouky, et al, 2000). The type introduces moisture to the air until the air stream is close to saturation. So the dry bulb or sensible air temperature (DBT) is reduced while the wet bulbs temperature (WBT) stays the same. Direct evaporative cooling raises the relative humidity of the space being cooled. For building applications it will be more effective when there is continuous flow of fresh air from ambient through the evaporative cooler to the building space and then exhausted out through the window as shown in Figure 2.20a.

Figure 2.20(b) shows the direct evaporative cooling process on a psychrometric chart. The fresh ambient air enters the DEC from state 1 and delivered to the building space at state 2’ instead of state 2. The cooling path 1-2’ follows an ideal or adiabatic saturation curve in which the supply air is reduced from the

dry to the wet bulb temperature of the inlet. Point 2' on the curve is the theoretical limit corresponding to 100% of the system cooling efficiency.

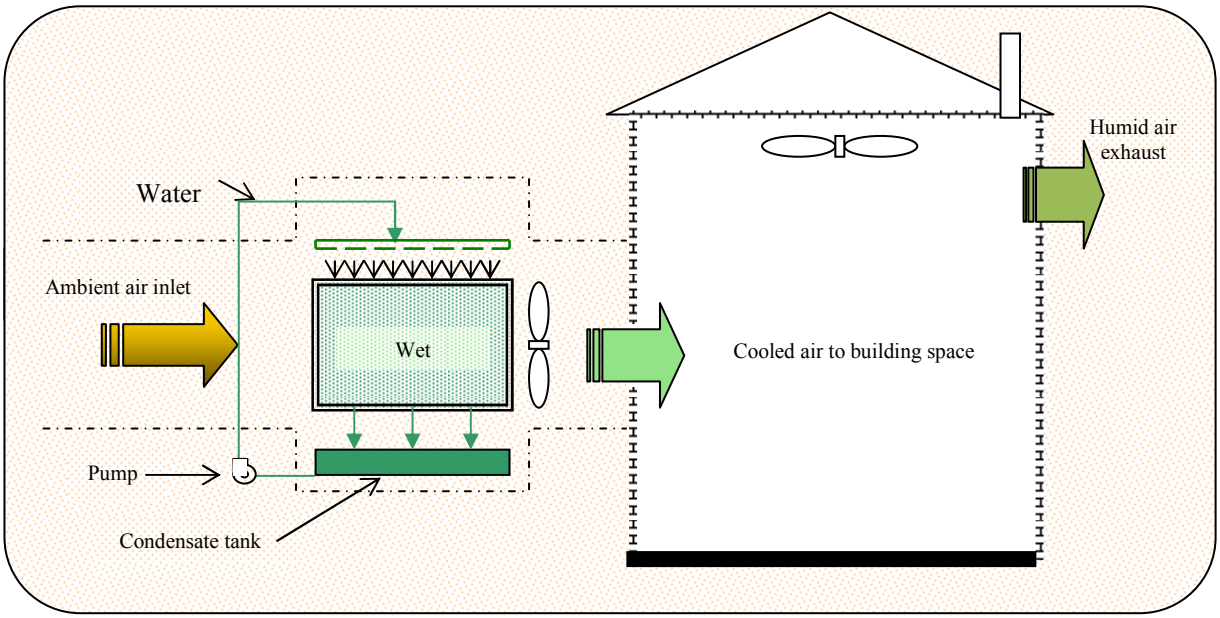

Figure 2.20a Principle of direct evaporative cooling to building space

However, in actual practice because of some defects or other operational factors the real cooling efficiency is limited to lower values between 70-90%. Similarly, the cooling paths are illustrated on a psychrometric chart with typical numerical values of the performance parameters in Figure2.20c, (El-Dessouky et al, 2000).

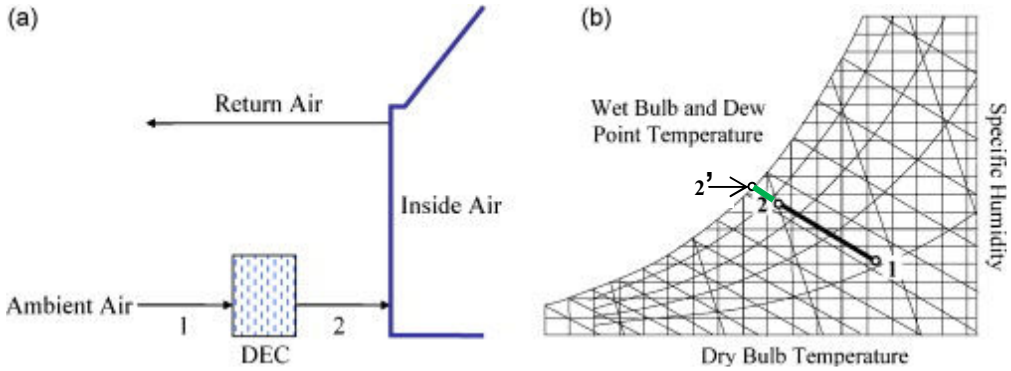

Figure 2.20b Cooling paths for direct evaporative cooler (Path 1-2'corresponds to 100% efficiency and path 1-2 correspond to efficiency of actual operation, 100%).

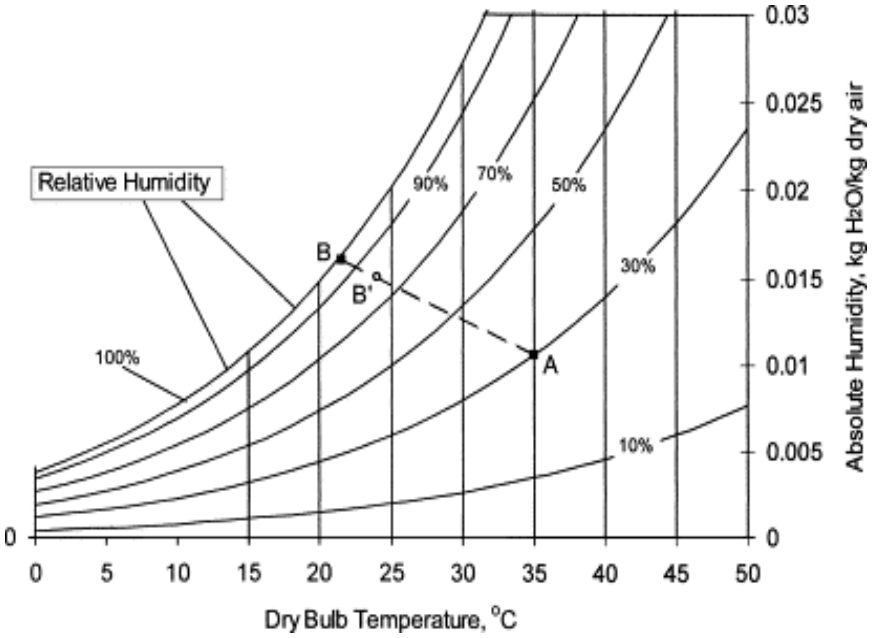

Figure 2.20c Cooling path for direct evaporative cooler (Path AB corresponds to 100% efficiency and path AB′ corresponds to efficiency of actual operation)

2.3.3. Indirect evaporative cooling

In the indirect system cooling is produced without adding moisture to the supply air. Secondary air stream is cooled directly by water and them it goes through heat exchange. The primary air then looses it heat by passing through heat ex. changer. This cooled primary air is circulated by a blower and it does not add moisture to the room. In this case both the dry bulb and wet bulb temperatures are reduced. The secondary air which has high moisture content is then expelled out prevented from entering the building space required to be cooled. This method is schematically shown in Figure2.21a (WESCOR)The cooling path for indirect evaporative cooling is illustrated on a psychrometric chart in Figure 2.21b.

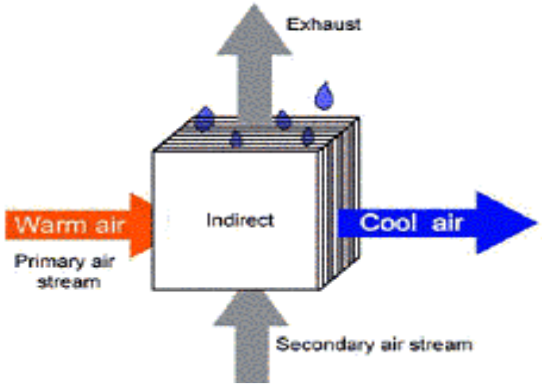

Figure 2.21a Indirect evaporative cooling

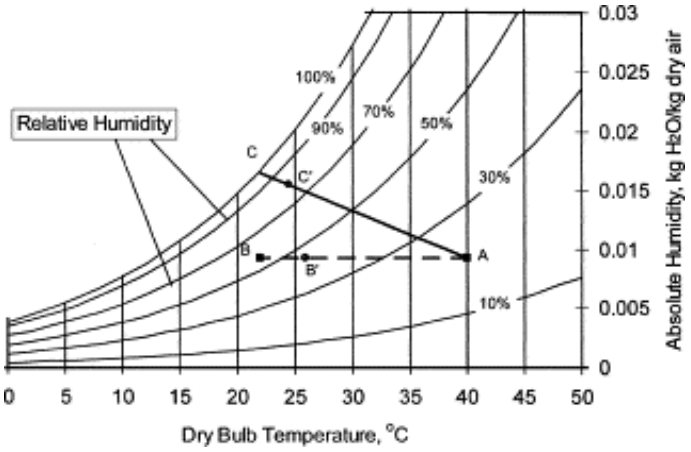

Figure 2.21b Cooling paths for indirect evaporative cooler

From Figure 2.21b above we have: Paths AB and AC correspond to 100% efficiency while paths AB′ and AC′ correspond to an actual operating efficiency, **(**El-Dessouky et al 2004).

In both direct and indirect evaporative cooling modes performance of porous ceramic evaporators for building cooling has been carried out Results obtained showed that using porous ceramic surfaces has demonstrated some potential for possible integration into building for cooling. During the tests as reported a maximum cooling of 224 Wm^{-2} and 48 Wm^{-2} has been measured respectively for the direct and indirect evaporative cooling.

2.3.4. Indirect / Direct evaporative cooling

This is a combination of the direct and indirect system. The primary air is cooled first with indirect method and then cooled further with direct evaporative cooling as illustrated in Figure 2.22a and 2.22b (WESCOR).

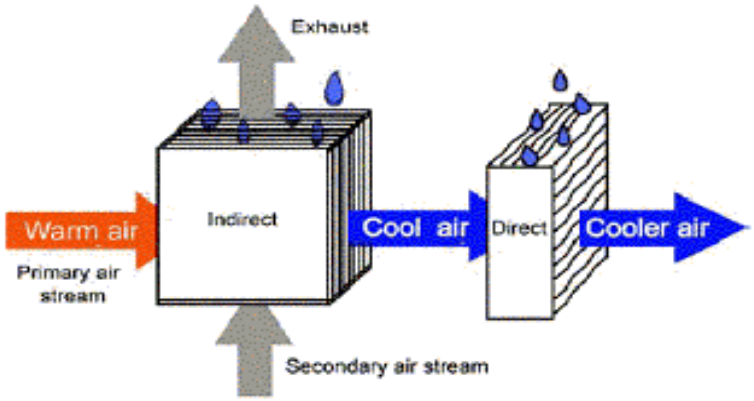

Figure 2.22a Indirect/direct evaporative cooling system

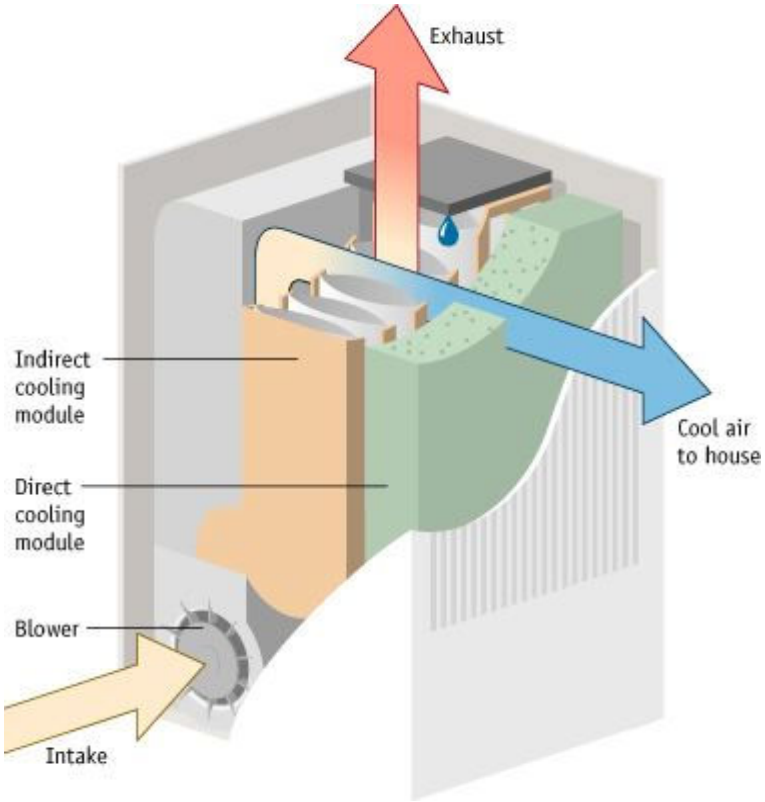

Figure 2.22b Detailed view of the indirect/direct evaporative cooling unit

Figure 2.22c shows the cooling path for combined direct and indirect evaporative cooling process in psychrometric chart (Al-Zeefari et al, 2004).

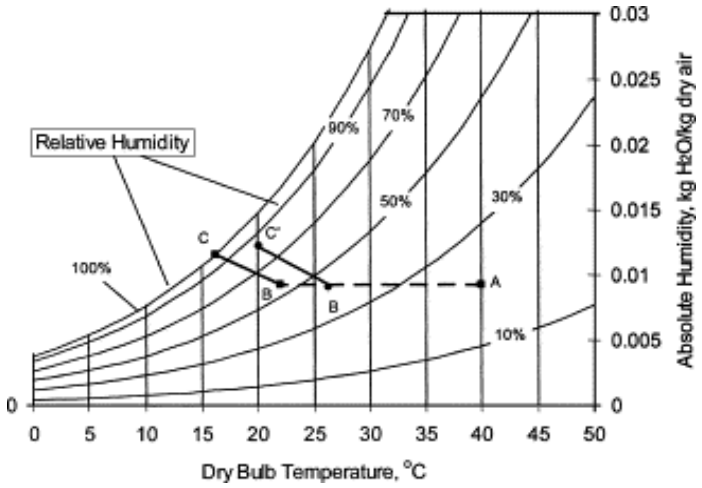

Figure 2.22c Cooling path indirect/direct evaporative cooler on psychrometric chart. (Paths AB and BC correspond to 100% efficiency. Paths AB′ and BC′ correspond to an actual operating efficiency).

2.3.5 Dew point based evaporative cooling

Evaporative cooling has long been recognised as the most efficient ecological and safe method that can be cheaply exploited. The correct dew point level is a key to optimum performance of an evaporative cooling system. Taking advantage of low dew point in evaporative cooling will yield a saving of up to 75%in electrical cost as compared to HVAC conventional cooling equipment. During certain periods in some locations atmospheric air becomes hot and humid. It is therefore vital to condition the air to a comfortable temperature and relative humidity levels of about 25^{o}C and 40%RH respectively (Rao, 2003).

Very high humidity contained in the air can be dehumidified to the desired level by lowering the air temperature below its dew point. This makes the air in turn to be lower than the desired level and should be reheated in order to raise its temperature to the acceptable level. This is the dew point temperature based

evaporative cooling. The cooling unit can be an evaporative cooler while a heat source can be used in the heating unit and a dehumidifier will be included in the system. A novel counter flow indirect evaporative dew point cooling system was numerically investigated (Zhao et al, 2008) as a potential alternative to the conventional mechanical air conditioning system. It was found that for the UK summer design conditions of 28^{o}C dry bulb temperature, 20^{o}C wet bulb temperature and 16^{o}C dew point temperature, and the system can achieve wet-bulb effectiveness of up to 1.3 and dew point effectiveness of up to 0.9. That is 103% and 90% effective in terms of the inlet air's wet bulb temperature and the dew point temperature, respectively. Existing direct evaporative cooling systems are 70-95% effective in terms of the inlet air's wet bulb temperature (Zhao et al., 2008). The investigations revealed that the system is suitable for most regions of EU countries having predominant hot and dry conditions. However, the system is unsuitable for some regions where the air is too humid.

2.3.6 Desiccant based evaporative cooling

A desiccant material is one that absorbs and holds water vapour. The process of absorbing moisture in the desiccant material is classified as absorption or adsorption depending on whether the process goes through a chemical or a physical change, (Amir, 2006). Desiccant based evaporative cooling system utilises desiccant wheel on which adsorptive material like silica gel, activated alumina, lithium chloride, lithium bromide, etc can be deposited. The purpose is to remove relative humidity from the ambient air. That is the dry bulb temperature remains virtually unchanged while the specific humidity decreases

(William et al, 1977). During dehumidification process the dried air becomes hot and must therefore be cooled to a lower dry bulb temperature by rejecting the excess heat. This process can be carried out by using indirect evaporative cooling (IEC). The air can be cooled again by passing it through the direct evaporative cooling (DEC) stage where the air also becomes re-humidified. However, for continues operation the desiccant material must be regenerated. Regeneration can be done by heating in an unsaturated air stream. The material is then cooled so that it will be able to adsorb moisture again for the process to continue. Heat source for the regeneration can be steam or solar assisted (Amir, 2006). In this technique an evaporative cooling process can be either saturated media based or water spray type. For hot and humid climates desiccant based evaporative cooling was thought to be more effective than the other evaporative cooling techniques. A system coupling desiccant dehumidification equipment to evaporative cooler was developed and the influence of some operation parameters that can minimise operating costs have been analysed. Figure2.23 shows the schematic diagram of the system (Carmago et al, 2003).

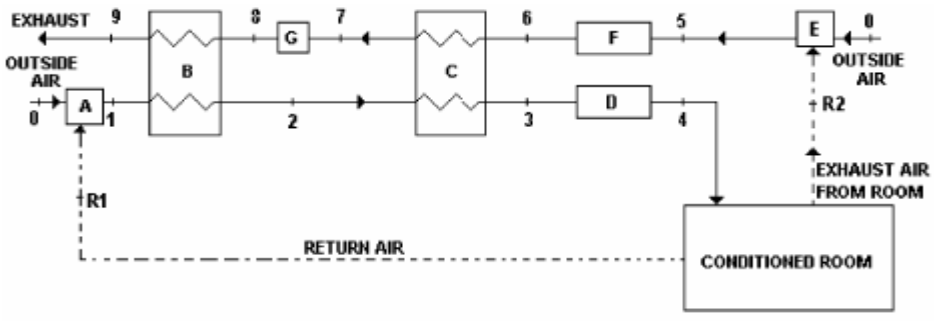

Figure 2.23 Schematic diagram of desiccant dehumidification integrated evaporative cooling system.

[The units in the Figure are: A-mixer and fan of the process air; B-desiccant dehumidifier type rotary wheel; C-energy conservation wheel; D-direct evaporative cooler; E-mixer and fan of the reactivation air; F-direct evaporative cooler; G-source of reactivation energy].

US Patent (No. 5,727,394, 1998) dew point based evaporative cooling relates to a novel combination for moisture removal and cooling process by employing evaporative cooling and desiccation processes through the use of a desiccant wheel as described in some United States patent (Belding et al, 1998). The moisture laden adsorption wheel is regenerated by passing hot air through it to remove the moisture. The resulting moisture free air is divided in to a relatively hot and a relatively cool stream. The hot stream can be passed through the wet side of indirect evaporative cooler and the relatively cool stream through the dry side. This results in the hot stream evaporating water there in and cooling the impervious wall to create cooling effect on the relatively cool stream which will finally be delivered to the building space.

The hot air leaving the desiccant wheel can have a temperature of about 80^{o}C higher than the other portions of the system or ambient. Through the desiccant wheel moisture can be removed from levels of 0.01364 to 0.0054 or lower pounds of water per pound of dry air. The air passed through the indirect evaporative cooler can be cooled and relatively dry having a temperature range of 13^{o}C – 24^{o}C or the process air it can enter the desiccant wheel at 24^{o}C – 43.3^{o}C and leaves at 37.8^{o}C - 82.2^{o}C. The desiccant wheel regeneration is carried out by using reactivation air which is heated from a heater as shown in Figure 2.24. The heat source can therefore be a solar air heater.

To further reduce the temperature of the air coming out of the indirect evaporative cooler (IDEC), a direct evaporative cooler (DEC) may be integrated in to the system. In this case the temperature of the air can be lowered to 10^{o}C – 18.3^{o}C before it is supplied to the room.

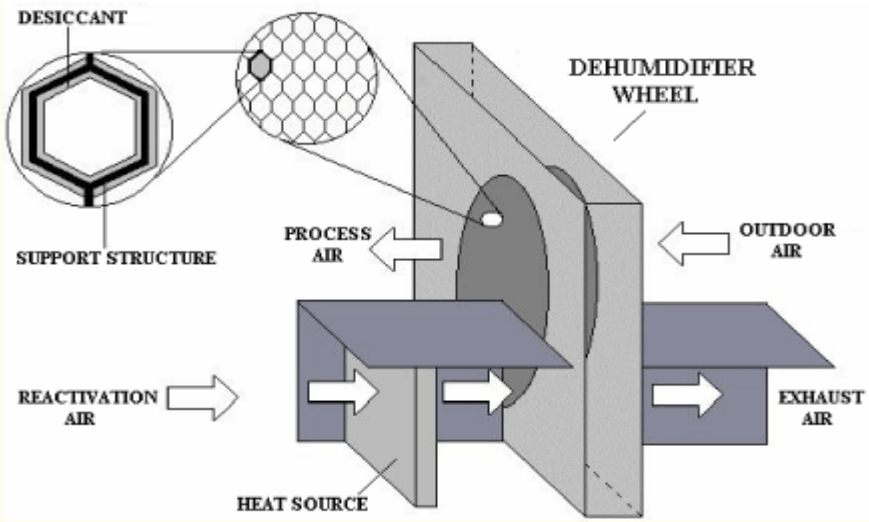

Figure 2.24 Detailed diagram of rotary dehumidifier wheel

2.4 Dehumidification

Dehumidification may sometimes be required to remove the moisture caused by direct evaporative cooling. Hence is briefly discussed in this section though it is not the main subject of this research. Higher humidity associated with direct evaporative cooling can turn out be a source of discomfort and should be controlled. Dehumidification is one of the possibilities of reducing the rising level of humidity from a direct evaporative cooling system. It is the removal of water vapour from room air and can be carried out in three ways. These are dilution with drier air, condensations or desiccant as briefly discussed below:

2.4.1 Ventilative dilution using dry ambient air

As a result of cooking, bathing, perspiration, etc interior air becomes typically moistened than the outside air, provided it is not raining. In this situation dehumidification by diluting the moist interior air with drier outside air is

applied to the design strategy for ventilation cooling. Drier air is therefore injected in to the space to dilute the higher humidity content.

2.4.2. Condensation on passively cooled surfaces

In this type of process latent heat in the form of water vapour is extracted from the air while an equal amount of sensible heat in the form of raised temperature is added. This process is an adiabatic or constant enthalpy dehumidification process (McGraw-Hills Inc.1993).

2.4.3 Desiccant dehumidification

Desiccant is a chemical drying material that removes moisture (latent heat) from the air while raising the temperature (adding sensible heat) that is the enthalpy (total heat) remains unchanged. In desiccant dehumidification the air leaves the desiccant dry and warm. Therefore if desiccants are used to absorb water vapour in warm humid climates, additional sensible cooling is necessary to counter balance the sensible gain that is inherent in the desiccation process. It was stated long ago that while a number of passive desiccant dehumidification systems for buildings have been proposed none have proven practical in operation. Absorption refrigeration falls in hybrid applications of desiccant dehumidification (WESCOR).

General classification and types of desiccants that can be used in dehumidification are given. An isotherm was used to define the capacity of a desiccant to absorb moisture. GAB equation can be used to relate the water activity, α_w and equilibrium content (EMC) of a given dry desiccant (Zhao et al, 2005). It can therefore be used as a guide in a selecting a desiccant to

remove or minimise moisture arising from direct evaporative cooling. However, economic viability of using a desiccant must first be ascertained.

2.5 Developments in evaporative cooling research

Various methods of evaporative cooling covering direct, indirect, combination of direct and indirect as well as incorporating other heat transfer devices have been researched and investigated. This is because of the increasing interests and the significant potential the technology has demonstrated for building cooling applications. (Faleh Al-Sulaiman, 2002) worked on Evaluation of the performance of local fibres in evaporative cooling using date palm fibres, jute and "Luffa" as wetted pads in evaporative cooling. Thermal efficiency, material performance and degradation of cooling efficiency were considered. Results obtained indicated that cooling efficiency was highest for jute at 62.1% compared to 55.1%, 49.9% and 38.9% for "Luffa", commercial pads and date fibres respectively. In terms of material performance tests which comprised of salt deposition and bio-degradation (mould forming) the overall result indicated that "Luffa" has an advantage over commercial fibres. However, if jute surface can be treated to offer higher mould resistance and also maintain uniform distribution after wetting they will be suitable options.

To date not so much work has been reported on the development of small household air conditioning units based on evaporative cooling. (Dai et al, 2002). A cross-flow direct evaporative cooler with wet honeycomb paper as the packing material was investigated. The system was expected to act as both humidifier and evaporative cooler that can create a comfortable indoor environment in arid regions. They presented a mathematical model which was

experimentally validated for theoretical prediction of the system performance. It consists of complicated heat and mass transfer within falling film and air flow. The unit was found to reduce air temperature by 9^{o}C and raise humidity ratio by 50% .The coefficient of water evaporation was presented by (Eames et-al, 1997). Importantly, the developed mathematical model can be applied to other geometries and operating conditions for the optimisation of similar kinds of direct evaporative cooling systems. In designing an indirect evaporative cooling system modelling and simulation is vital to obtain the optimum parameters. Heat and mass transfer model was developed based on the basic principles for evaporative cooling (Alonso et al, 1998). The model was universal that can be used to analyse different indirect evaporative cooling designs and conditions. It can be used for systems energy analyses and product optimisation. Like many engineering applications, in evaporative cooling simultaneous heat and mass transfer between a liquid film and binary mixture are encountered. These processes play very important role in evaporative cooling. Detailed numerical study was performed and results showed that the heat transfer from the gas-liquid interface to the gas stream is predominantly determined by the *latent heat* transfer connected with film evaporation. Also better liquid film was noticed for the system having a higher inlet liquid temperature and a lower liquid flow rate or a higher gas flow Reynolds number (Re), as reported by Wei Mon Yan, (1998) and Lee KT et al, (1997).

In some arid areas 50% of the heating load in building is from roof, therefore (Al-Nimr et al, 2002), studied different passive techniques. These were roof painting with white, thermal insulation underneath the roof, shallow pond with

movable insulation and evaporation using water soaked gunny bags. Results recorded indicated that the fall in air temperature inside the test structure as compared to control were respectively 7 °C, 3°C, 8°C and 10°C. It therefore clearly showed that the performance of evaporative cooling became comparatively increased. However it requires a lot of water which is very scarce in rural arid areas. So an alternative that requires much less water consumption is very much desired. Application of indirect evaporative cooling considering variable load of a typical Iraqi dwelling was reported. The application was evaluated through systematic simulation comparing two arrangements of indirect and direct evaporative cooling systems. Solar and transmission heat gains, interior heat source, cooling load and heat gain were all considered in the program. Results in this case favoured indirect evaporative cooling over direct evaporative cooling because it reduced the process air temperature without increasing its moisture content (Khalid et al, 2000). Therefore for application where high humidity is not desired, indirect evaporative cooling stands to be more favourable. In addition to various achievements made in evaporative cooling, investigation of porous ceramic evaporators for building cooling applications (Ibrahim et al, 2002) under direct as well as indirect types of evaporative cooling was carried out. The prototype porous ceramic evaporators used were classified as low, medium and high porosity evaporators based on firing temperatures of 1110^{o}C, 1130^{o}C and 1170^{o}C respectively.

Experimental results showed that the high porosity ceramic evaporator consistently performed better, more especially with increased water supply head. 6^{o}C - 8^{o}C drops in dry-bulb temperatures, 30% rise in relative humidity

and 224W/m^{-2} maximum cooling was reported. These formed a very good basis for the choice of ceramic evaporators based on porosity considerations. An empirical formulae expressing the force driving evaporation of water from the wetted ceramic surface was found to be [e_s – e] where (e_s – e) is the ambient to saturated vapour pressure difference. Finally the investigation revealed that porous ceramic has demonstrated significant potential for possible integration into building under direct evaporative cooling

(Ibrahim et al, 2003). A lot of materials used as building roofing products are employed for thermal insulation during the cold season to prevent heat dispersion. These products are therefore not suitable for assuring comfort during the warm periods and in warm climates particularly in rooms with higher solar gains, subjected to overheating. As a result conventional air conditioning was heavily used for comfort living. To offer solution to these problems, Manzan and Saro et al (2002), carried out in-depth study of the thermal behaviour of an innovative building component recently introduced to the market so as to exploit the natural phenomenon like water evaporation is unsaturated air. The researchers considered indirect evaporative cooling in which cooling effect is used to remove heat flux from ambient.

2.6 Applications of evaporative cooling

Application of either direct or indirect evaporative cooling techniques depends on whether additional moisture in the supply air to the space is tolerable or not. That is when high humidity is required alongside with cooling or if cooling is desired at a very low relative humidity. In the case of space where high humidity is required the direct system will be more acceptable to the indirect

system. It is on record that a lot has been done in the application of direct and indirect evaporation cooling techniques on buildings. These include the integration of porous ceramic cooling elements in both the direct and indirect systems of evaporative cooling, (Lee KT et al, 1997).

2.7 Thermoelectric

One of the studies conducted in this report involved integrating evaporative cooling system with thermoelectric cooler. An important aspect for large capacity thermoelectric cooling/heating applications is the achievement of a sufficiently high coefficient of performance (COP), (Riffat and Ma,2003).This investigation was therefore aimed at improving the COP by using evaporative cooling from porous ceramics as heat sink hence a review on thermoelectric system is presented in this section.

2.7.1 Thermo electrics-A review of developments

Basically thermoelectric module is a simple solid-state device that converts electrical energy into thermal energy and vice versa. Thermoelectric cooling technology is based on the Peltier principle which defines a temperature change at the junctions between two dissimilar metals when electric current flows through their junctions. A typical thermoelectric module composed of two ceramic substrates that serve as a foundation and electrical insulation for p-type and n-type bismuth telluride thermo elements (semiconductors) which are connected electrically in series and thermally in parallel between the ceramics. A pair of thermo elements is called a thermocouple. More than one pair of thermocouples are usually assembled together to form a thermoelectric module, as shown in Figure 2.25. By passing electric current through the junctions of

the dissimilar materials making up the thermo elements heat is transported from a low temperature to a high temperature region. They can therefore provide either cooling or heating hence can be used either as coolers or heaters depending on requirements. The performance of a thermoelectric device used as a heat pump or refrigerator is affected by the Peltier, Fourier, Joule and Thompson effects. Equations for heat conduction, the maximum rate of heat pumping and the maximum COP, were also derived. Thermoelectric technology is a unique cooling in which the electron gas serves as the working fluid. The device is also noiseless, reliable and environmentally friendly. However their applications in cooling large thermal capacity components or spaces have been limited due to the relatively low COP and high-energy cost. Thermoelectric systems can efficiently work with a PV panel due to the fact that they are low voltage driven devices and can accept PV power supply directly without conversion. These advantages make thermoelectric devices very attractive and worthy of exploitation for building air conditioning applications. Investigation of a thermoelectric refrigeration system using a phase change material integrated with thermal diode (thermosyphons) was conducted. Results indicated that is feasible to use thermosyphons between the PCM and the cold side of thermoelectric cells in order to prevent heat leakage to the PCM in case of power being turned off (Khalid and Mehdi, 2000).

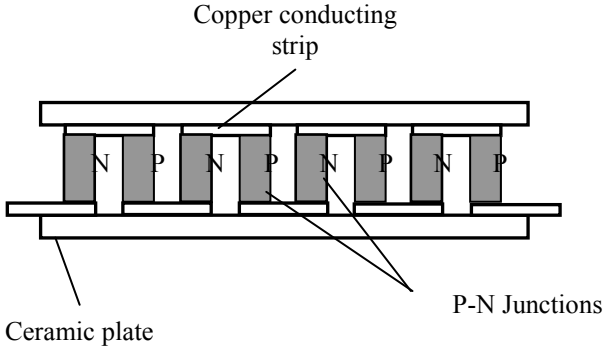

Figure 2.25 Schematic of thermoelectric module

A thermoelectric cooler (TEC) with attached heat sinks centrally positioned at the discharge of a blower and in turn mounted in an enclosure to provide a supply of cooled air to a passenger of a vehicle was reported. In this development a blower/motor assembly produces a steady air flow, a fraction of which is directed over the hot side of the TEC where it removes heat with the aid of efficient heat sink disposed within the air stream. In turn this air is exhausted to the ambient away from the person .The system can be a substitute to a conventional motor vehicle air conditioning system that can provide comfort at very low energy consumption. As reported the invention could be powered by a cigarette lighter of a vehicle and can be mounted to the sun shade of the vehicle for providing cooling air on the person's face or head (Harrington et al, 1996) When combined with a D.C. power source and a means of dissipating the heat from the hot side thermoelectric units are capable of cooling to below ambient temperatures. Therefore unlike conventional air conditioning systems, the physical geometry of TECs requires that flat heat sinks be mated to their active surfaces to increase the heat transfer effective surface area. This fact coupled with lack of working fluid to transfer heat within the system prohibits the use of conventional flow through heat exchangers. This encourages the design of cooling systems in which the air is cooled by contact with cold surfaces in a duct and then circulated through the conditioned space. Equations used to evaluate the performance of the system were given, (Thomas et al, 1997). The studies revealed that location of heat absorbers in a duct having pre-cooled air has effect on the system performance. Use of multi-stage cascades to improve the performance of thermoelectric heat pumps showed that the coefficient of performance of the heat pump decreases

rapidly with increasing temperature difference. Further study therefore investigated the potential improvements in the performance that can be realised by cascading two or more heat pumps in series operation. The findings were that for temperature differences of less than 30^{o}C, the improvement in COP of about 7.3% was too small to justify added cost of cascaded thermo electric heat pump system. Another important observation, (Keith W. Linder, 1997) was that the cooling provided by two identical cascaded modules (at optimised COP) is much less than that provided by a single module of the same size.

A combined thermo electric refrigerator or warmer using no external power for refrigerating/warming method were developed and operated using solar energy. It consists of a plurality of thermocouples connected in series. Owing to temperature difference thermoelectric motive force was generated at both ends of the device which was then amplified to a strong DC voltage. The voltage generated was then supplied to Peltier device to carry out a thermal absorption or a thermal radiation. Therefore the internal temperature of the system was automatically varied to cool the interior of the apparatus when the external temperature becomes higher.

Similarly when the external temperature becomes lower it carries out heating. The system recorded a temperature difference of about 10^{0}C between the internal and external temperatures during either summer or winter season (Kim et al, 1998). A thermoelectric refrigerator having a thermoelectric device and a heat exchanger with evaporating and condensing surfaces reduced the operating temperature across thermoelectric elements and associated components. Technical advantages of this system include an environmentally benign heat transfer system that is energy efficient resulting in to increase in

thermal efficiency of the device (Gilley et al, 1998]). Experimental investigation on novel thermoelectric refrigeration system employing heat pipes and a phase change material showed the potential application of heat pipes and phase change materials for thermoelectric refrigeration system. Initially the system was tested with a conventional heat sink unit (bonded-fins heat sink) on the cold side of the thermoelectric cooler (TEC), and a fan assisted (heat-pipe embedded fins) heat sink unit on the hot side. (Riffat et al, 2002). Performance equations were given for the evaluation of the cooling energy dissipated inside the refrigeration cabinet and the electrical energy input to the thermoelectric cells as well as the coefficient of performance (COP) of the system. Besides improving the performance, in the event of power failure, the system could not withstand losses due to heat leakage through the thermoelectric cells from the hot side to the cold side. Thermoelectric refrigeration system employing phase change material integrated with thermal diode (thermosyphons) was developed as a solution to the above problem (Riffat and Ma, 2003). Thermal diode such as thermosyphons have the advantage that heat transfer takes place in one direction only, that is from the evaporator end to the condenser end. Results reported in this investigation showed that it is feasible to use thermosyphons between the phase changing material (PCM) and the cold side of thermoelectric cells in order to prevent heat leakage to the PCM in the event of the power being turned off. Also the overall system can be operated using renewable energies such as DC from solar photovoltaic (Omer. et al, 2001). These shows that thermoelectric can be integrated with other heat transfer devices for improved performance and reduction in the material failure during operation.

Comprehensive review covering basics and potentials of thermoelectric devices has been presented. It showed that the technology can be used practically in different areas and applications. The application of small capacity thermoelectric coolers are in wide spread while applications of large capacity ones and power generators are limited by their low efficiency. However, concern for the environment to be free of chlorofluorocarbons (CFC_s) and energy costs have revived interests in the use of thermoelectric systems. Efficient, clean energy conversion for high value added applications such as space, defence, etc is needed now and in the future. Thermoelectric devices should be a good choice. (Riffat et al, 2002). Research in to this area is still very much desired. Equations for the maximum rate of heat pumping capacity and the maximum coefficient of performance (COP) (Chen et al, 1997) which can help in analysing the performance of the thermoelectric system have been established. (Yamanashi et-al, 1996) investigated an optimum way to maximise the coefficient of performance (COP) for a thermoelectric cooling system using thermoelectric cooler and heat exchangers at the cold side and hot side.

The consideration was on the importance to design a thermoelectric cooler (TEC) for obtaining the maximum cop of the system.

2.7.2 Heat pipe integration with porous ceramics evaporative cooling

Heat pipe has been used for different applications either separately or integrated with other heat transfer systems. The basic features of a heat pipe are shown in Figure 2.26. In large spectrum of temperature encountered in heat transfer process, heat pipes are used in a wide range of products. These include air conditioning refrigeration, heat exchanger, transistor, etc.

The use of heat pipe with porous ceramic in indirect evaporative cooling has been found to demonstrate some potential for possible integration into building (Jie Zhu et-al, 2004 and Ibrahim et al, 2003). One of the areas of interest in the application of heat pipe technology is in the field of air-conditioning. Activated by temperature difference and therefore consuming no energy it allows the evaporator coil to operate at a lower temperature increasing the moisture removal capability of an air conditioning system. With lower relative humidity, indoor comfort can be achieved. Also the pre-cooling effect of heat pipe allows the use of a small compressor.

Investigation (Cerza et al, 2003) showed that in the satellite or energy conversion industries heat pipes can be used to transfer heat to the thermal sink. Also a conceptual thermo photovoltaic (TPV) energy conversion system utilising flat heat pipes was discussed indicating that flat heat pipes, except for the geometrical shape are similar to cylindrical ones. A study concerning the heating applications of thermal diode was reported (Ochi et al, 1996). However, detailed characterisation of the heat pipe technology based on thermal diode panels for use in building during the cooling season was carried out for the quantification of thermal characteristics for both forward and backward heat transfer operating modes (Armando et al, 2002).

A mathematical model was developed that can be used to predict the performance of evaporative cooling using porous ceramics integrated with heat pipes. It employs thermal resistance phenomena in analysing the heat transfer parameters in the system based on the features shown in Figure2-27 (S.B.Riffat and Jie Zhu, 2004).

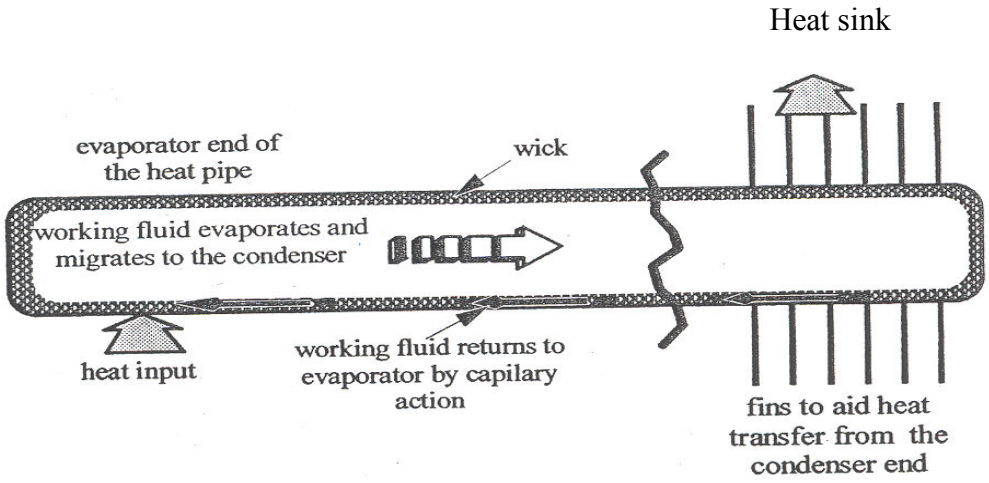

Figure 2.26 A section showing features of a heat pipe

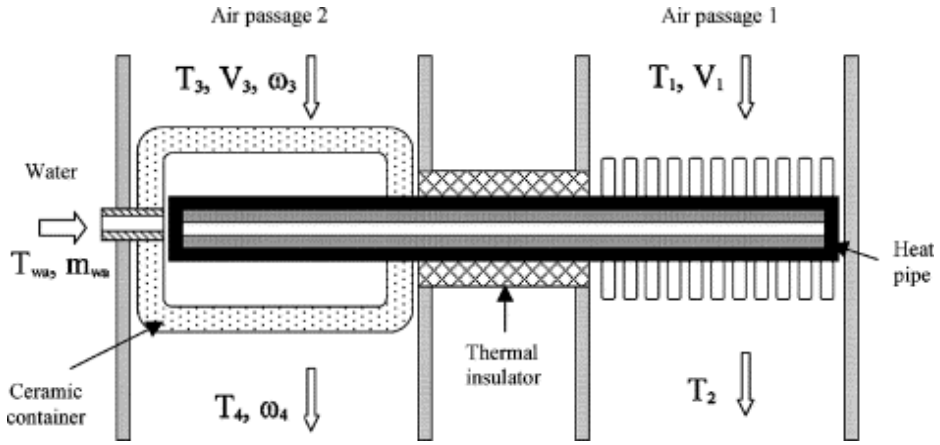

Figure 2.27 Integrated evaporative cooling system using heat pipe and porous ceramic

2.8 Advantages of Evaporative Cooling

The following are some of the advantages of evaporative cooling systems:

2.8.1 Simple to construct and maintain

Figure 2.28 shows the typical diagrams consisting of working elements for conventional refrigerant based air conditioning system. Comparing with complete evaporative cooling process with a cooling pad in shown in Chapter 2 Figure 2.9, it is clear that the evaporative cooling unit is simpler to construct and maintain because the moving parts are less. Similarly the operation pressure of the evaporative cooling system is much lower than the air conditioning system and no complicated piping works.

2.8.2 It reduces environmental pollution, global warming and saves energy

The evaporative cooling system uses water as the working fluid while air conditioning systems (home and auto), rely on the compression and expansion of fluorocarbon refrigerants to produce their cooling effect. The refrigerants include CFCs (chlorofluorocarbons), HCFCs (hydro chlorofluorocarbons) and HFCs (hydro fluorocarbons). These substances can damage the environment if they leak or escape from air conditioners.

CFCs are a major contributor to the thinning of the ozone. HCFCs, while their effect is less drastic than those of CFCs, still contribute to the thinning of the ozone layer. HFCs are not known to damage the ozone layer but are greenhouse gases which cause global warming. The energy requirements for running the compressor and multiple fans in the air conditioning system is much more than the requirement for running a fan and pump or only a fan in evaporative cooling system. [http://www.airconditioning-units.co.uk/motor-vehicle-air-conditioning.html-What is air conditioning].

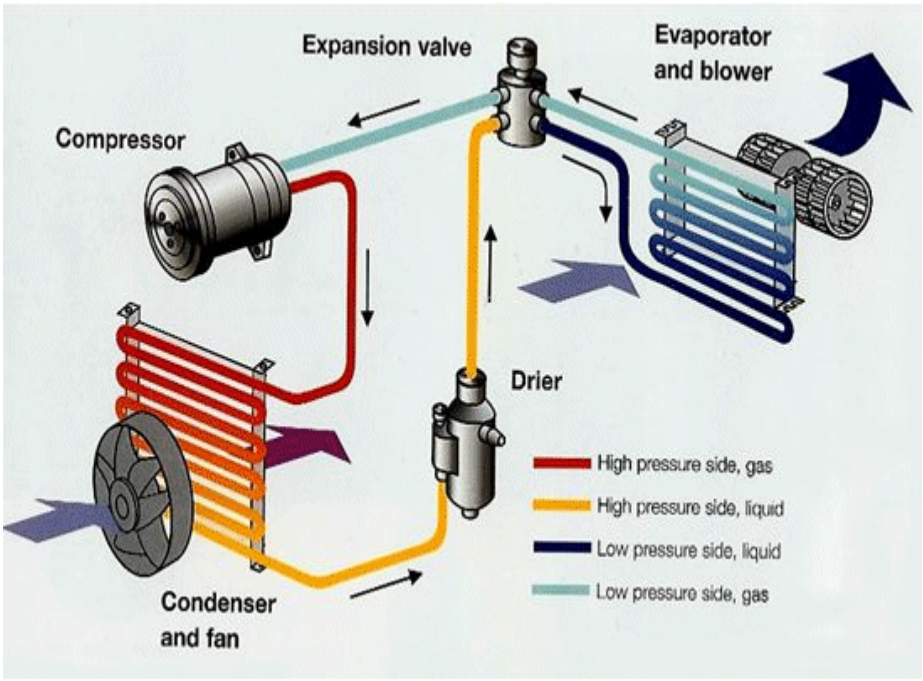

Figure 2.28 Working elements for basic air conditioning system

2.8.3 It lowers actual air temperature and filters the air

Through evaporative cooling hot outside air is passed or circulated over a water soaked media where its heat is extracted for evaporation. In this way the dry bulb temperature (DBT) falls and allows cool air to be delivered in the building space. DBT is the actual temperature as indicated by an ordinary thermometer (Watt et al, 1997) and is simply the layman's idea of temperature. There are other classifications of temperatures consisting of wet bulb and dew point temperatures.

The polluted outside air is filtered as it passes through the water saturated media. The evaporation rate and constantly the cooling effect also depend on the relative humidity of the air. Relative humidity is the measure of how saturated the air is with water vapour. It is the ratio of amount of water vapour

contained in the air to the amount it would be in the same air at saturation condition. In other words (ASHRAE Fundamentals Handbook, 2001) it is the ratio of mole fraction of water vapour in a given moist air sample to the mole fraction in an air sample saturated at the same temperature and pressure. Relative humidity is expressed in percentage.

2.8.4 It reduces effective temperature

Evaporative cooling can reduce effective temperature to generate human comfort. Effective temperature is the resulting temperature people feel on their bodies and it is also influenced by relative humidity, temperature and air movement over the body. As air blows over the skin it increases the rate of moisture evaporation from the skin. The heat required to effect the evaporation comes from the surrounding air and the skin itself. This makes a person to feel cooler while the dry bulb temperature remains the same. During the extreme hot periods such as in April and May in Delhi (India) and for other conditions pertinent to the tropical summer climates (Mullick et al, 2002) evaporative coolers were developed (Sharma et al, 1986) to mitigate discomfort and provide cooling within comfortable effective temperature range in a building.

2.8.5 Provides full fresh air supply

Evaporative cooling raises relative humidity level of the air. Therefore re-circulating the air will increase the humidity to an uncomfortable limit. Always air drawn from evaporative cooling system should be passed to the building space only once. To achieve this exhaust provisions could be made to ensure continuous replacement of the supply air. Therefore it is associated with continuous circulating of fresh air in the building environment.

Generally most evaporative cooling applications require air exchange rate of 25- 35 per hour in order to provide comfort conditions.

2.8.6 Can be portable and standalone renewable energy-operated system

Because of the low power requirement an evaporative cooling system can be a green energy standalone unit operated by solar photovoltaic (PV) panel. Figure 2.29a and Figure 2.29b show an evaporative cooler solar PV retrofit unit studied at the University of Nottingham (Qiu, 2006).The conventional system AC mains power blower was replaced by a DC motor powered by solar panel. The solar panel used was a 30W polycrystalline type (BP Solarex Model SX30M model). It was connected to power the supply air-fan of a TAC-150 evaporative cooler by charging a Sonnenschein A512/10s model battery to run a 12VDC, 12W blower.

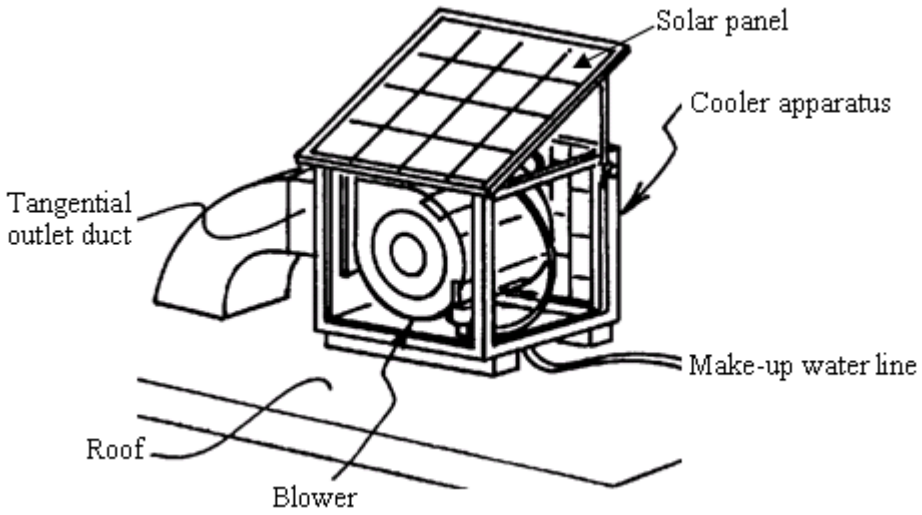

Figure 2.29a Schematic diagram of Retrofit Solar PV operated evaporative cooler (Qiu, 2006)

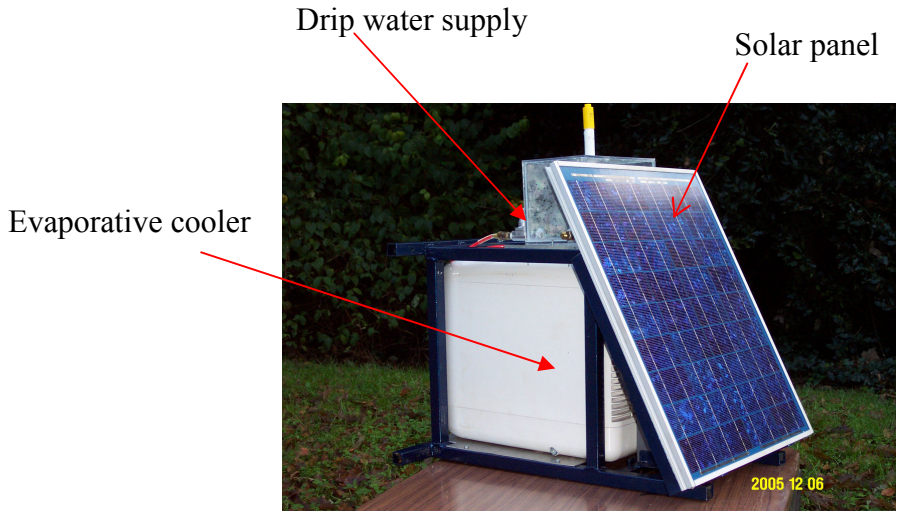

Figure 2.29b Retrofit Solar PV operated evaporative cooler, (Qiu, 2006).

The system operating circuit is shown in Figure 2.29c. It consists of 7Amp ICP charge controller connected between the solar panel and the battery to ensure that the battery is fully charged as well as prevents over charging. This controller is suitable for solar panels ranging from 15W to 105W and has a reliable overcharge protection for 12V batteries.

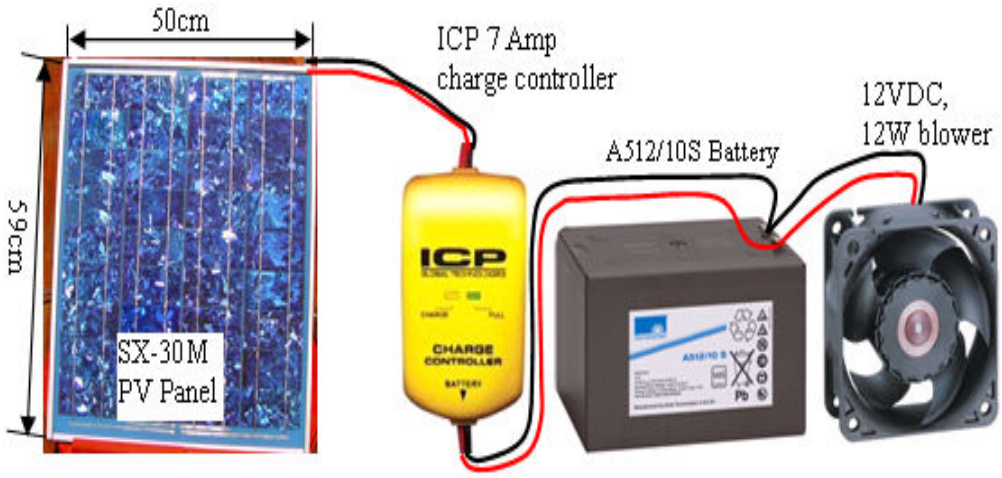

Figure 2.29c The system operating circuit for Retrofit Solar PV operated evaporative cooler, (Qiu, 2006).

A standalone unit can be made by installing the PV solar panel on a pole with a provision for adjustment to capture maximum diurnal solar radiation at different seasons of the year. Both the charge controller and the battery can be installed in a housing provided at the bottom of the pole. The power supply arrangement can then be connected to the evaporative cooler as shown in Figure 2.92d.

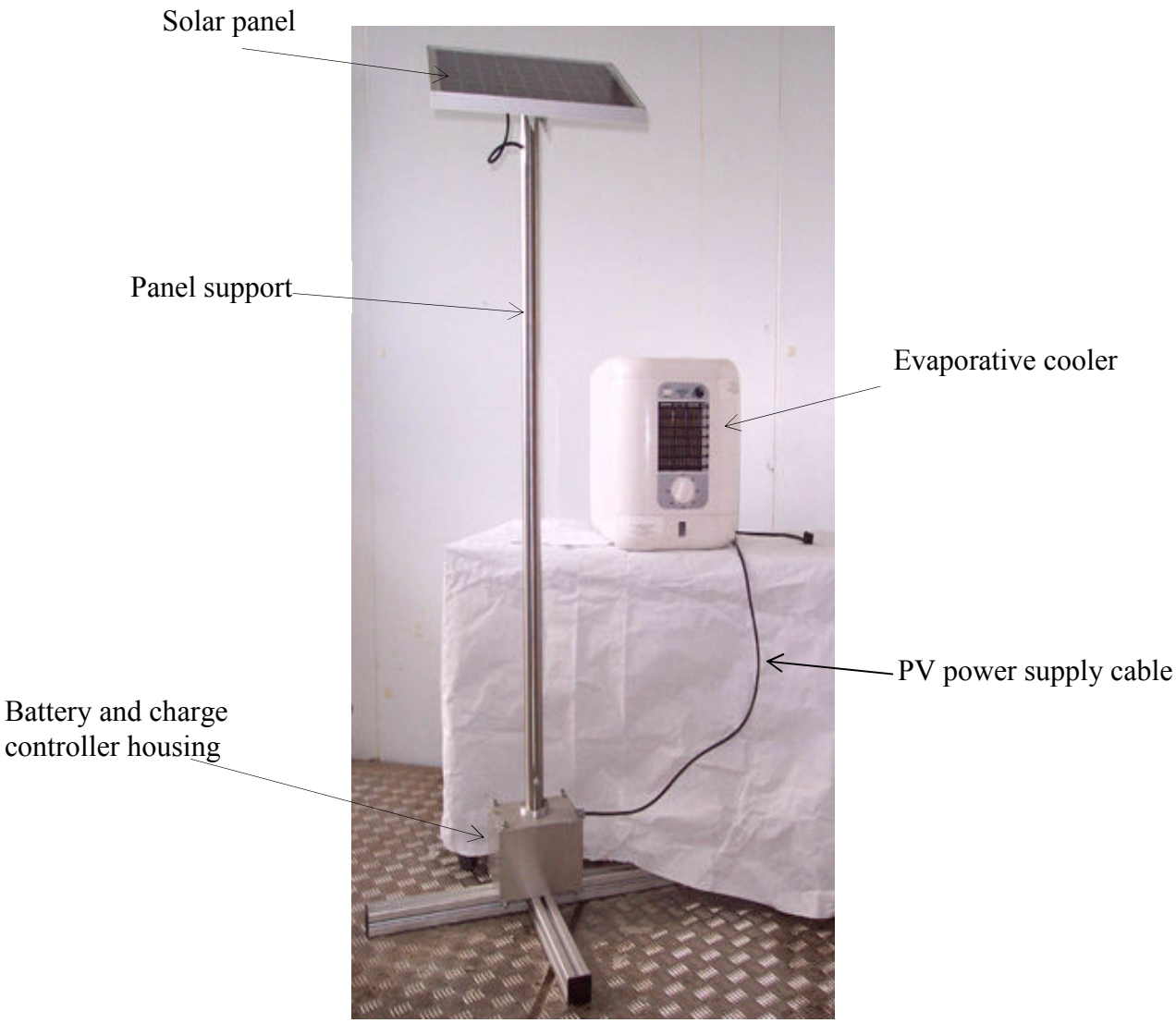

Figure 2.29d Stand-alone Solar PV operated evaporative cooler (Qiu, 2006).

2.9 Disadvantages of Evaporative Cooling

Evaporative cooling has also got some associated disadvantages which can be prevented if the system is properly designed, operated and well maintained. However, the advantages of the system in terms of its benefits in energy savings and the cleaner environment as discussed in section 2.8 provide wider prospects for application in to buildings. Therefore they outweigh the disadvantages. The disadvantages and measures to prevent them are described in the following sections.

2.9.1 Increase in the relative humidity

Some evaporative cooling systems increase the relative humidity level in the building space while building should not have excess moisture. It is very vital to ensure continuous removal of humid air as soon as it is delivered in order to prevent dampness in the building. Fresh air movement across the evaporative cooling media to and out of the building must always be maintained. Ideally the relative humidity level for a home building should be between 30% and 55%. When the level is too much above or below this range then the building space becomes uncomfortable and not healthy enough. Fortunately evaporative cooling system works more effectively when operated along with sufficient ventilation to control the humidity. Figure 2.30 (Residential Energy efficiency Database 1990) shows the optimum relative humidity level required to achieve acceptable building indoor air quality. It also shows associated effects of having less or more than the optimum requirements.

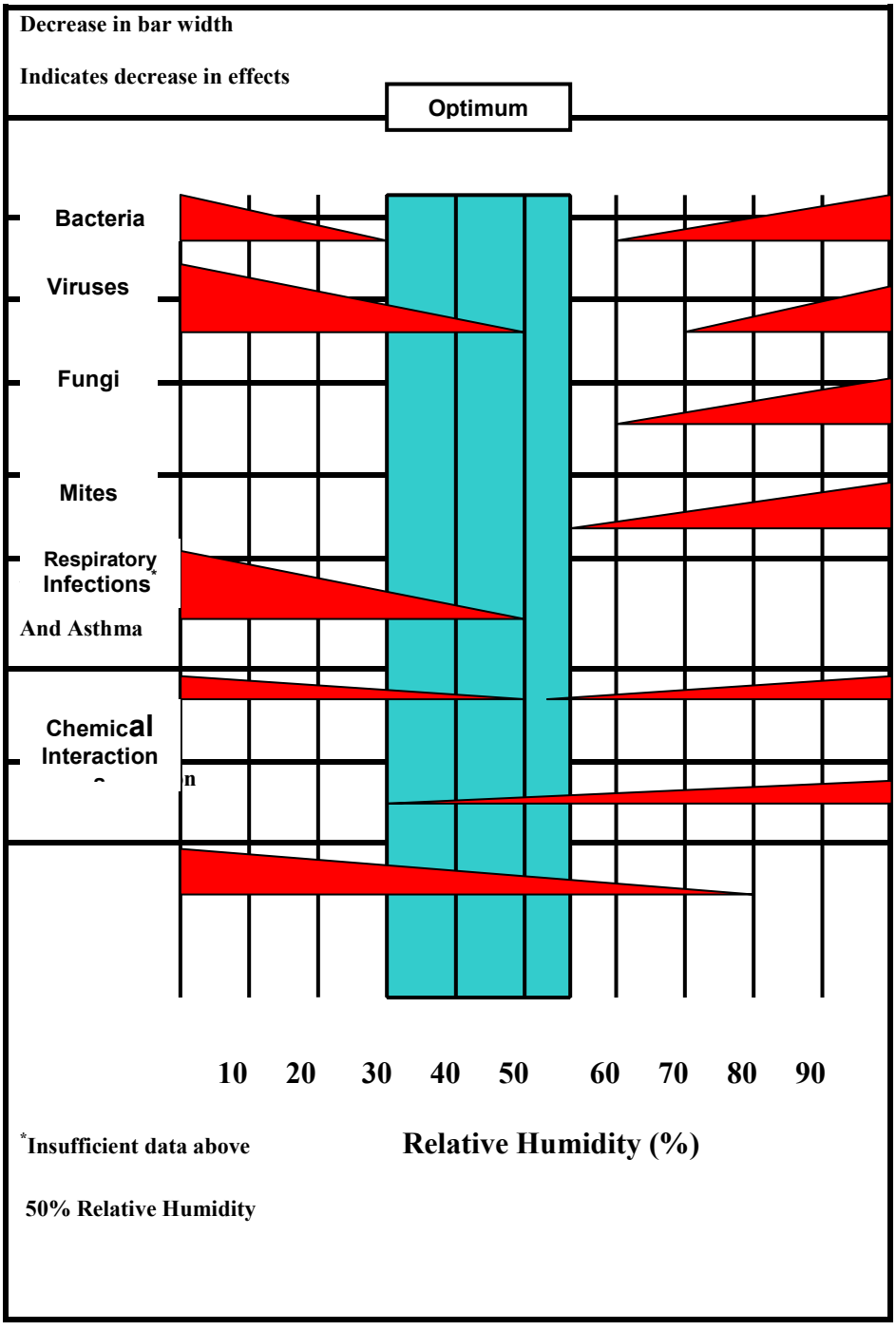

Figure 2.30 Relative humidity and air quality relation.
(Residential Energy efficiency Database 1990, Mark Gillot, 2000)

2 .9.2 Water consumption

Evaporative cooling consumes water which may be very scarce in some areas where its applications is most needed such as in the hot and dry climates. As a remedy the media used should be such that it does not allow excess moisture diffusion in to the air. This can be achieved by careful selection of the porosity of the evaporating media or water retention capability of the evaporation units.

2.9.3 Dust mites effects

House dust mites are microscopic spider like creatures which live in beds, carpets and other soft furnishings. These micro organisms are common source of indoor air pollutants. They are so tiny to be detected by naked eye and yet millions reside in our rooms with maximum concentration on the beddings. Their faeces, skin casts and pieces of dead ones contains substances that triggers asthma attacks, inflammation on the linings of the nose and in some allergic people can cause eczema. Dust mites thrive in a warm humid condition found in modern houses. Since some evaporative cooling systems can raise the relative humidity level it creates conducive breading environment for the dust mites. They do not require direct intake of liquid water for their survival. They get water by absorbing water vapour through their skin. They cannot therefore survive in an environment where the relative humidity is low enough to provide for their water vapour requirements. Laboratory studies show that the optimum conditions for dust mites are a temperature of $25^{O}C$ and relative humidity of 80% (Mc Intyre, 1992). Ideally the population of dust mites can be reduced significantly if the humidity level is below 80% (Howarth and Reid).

Korsgaard (1983) showed that the number of dust mites considerably decreases if the relative humidity is below 45% at room temperature (Gillot, 2000). As a solution to breading of dust mites and other high level moisture caused building problems evaporative cooling system must be always accompanied with effective moisture removal. It can be made indirect to ensure minimum moisture content in the cooling supply air in a situation where provision of moist air exhaust cannot be provided. Figure 2.31 shows a magnified photograph of a typical dust mite.

Figure 2.31 Dust mite photograph

2.10 Ventilation requirements and thermal comfort

Ventilation plays a very vital role in keeping the circulation of fresh ventilation air circulating through the building. It helps replace the harmful carbon dioxide gas that accumulates in the building with fresh air. Provision of fresh air in a building is ideal for comfort, health and good working environment. Unchanged stagnated air can result in the spread of different kinds of illness and discomfort. Effective ventilation can reduce heating and cooling loads in a building. In the application of evaporative cooling for ventilation both the temperature and relative humidity must be maintained within arrange that allows adequate evaporation of sweats due to perspiration from the skin.

2.10.1 Thermal comfort

Thermal comfort is defined as "that condition of mind that expresses satisfaction with the environment" (ASHRAE, 1992). To have thermal comfort means that a person wearing normal amount of clothing feels neither too cold nor too warm depending on the rate of body heat loss. If the rate the body losses heat is too great then the person feels cold and conversely feels warm if the rate of heat loss is too low. A person needs a stable core body temperature of 37.5^{o}C in order to be in good health and comfort. To achieve equilibrium body temperature any heat input to it must be balanced by the corresponding output. Other factors related to the human comfort are the heat gain by the body due to metabolism as well as the additional heat loss due to evaporation of moisture from the lungs and the skin. Food consumed is burnt by the body for it to grow, repair itself and make movements and all the process are more suitable under comfortable environment that can be provided by effective evaporative cooling system. An indication of the metabolic heat output from the body is given in Table 2.2 and graphically represented in Figure2.32 below (Richard Nicholls 2000).

Table 2.2 Body metabolic heat output values

Activity	Metabolic Heat Output (W)
Sedentary	**100**
Active light work	**150**
Very active	**250**

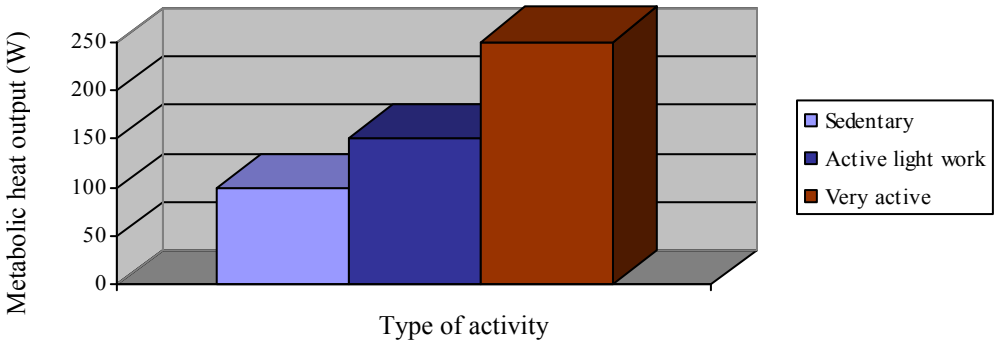

Figure 2.32 Metabolic heat output due to body activity

Also a body encounters heat loss resulting from the evaporation of moisture from the lungs and the skin. In cooling the body latent heat is absorbed and the cooling effect is increased in dry (low humidity) environment. Where relative humidity is very high evaporation is suppressed and the building environment becomes hot, humid and rarely comfortable for the body. Latent heat phenomenon is very crucial for effective evaporative cooling and is described below.

2.10.2 Latent heat

Latent heat plays a very important role in evaporative cooling as it is utilised to vaporise the water mass. It is defined as the heat which flows to or from a material without a change of temperature. The heat will only change the structure or phase of the material, e.g. melting or boiling of pure materials. Example is what takes place from the melting of ice up to the formation of water vapour as illustrated in the Figure 2.33 (Nicholls, 2000).

2.10.3 Effect of clothing

While temperature requirements vary greatly among individuals, clothing also plays an important role in keeping a person comfortable. For clothing a scale is used to represent how much amount of clothing a person is wearing. It is measured in "clothing insulation" abbreviated as "clo" and it reflects the amount of insulation that clothes provide. 1clo represents 0,155m^2k/W of insulation. Typical "clo" values can be 0.5 clo to 0.9clo (0.078 to 0.14m^2k/W) for the summer and winter respectively. ASHRAE gives some examples of "clo" values at acceptable temperature and relative humidity values as shown in table 2.3 (ASHRAE Standard-55, 2004).

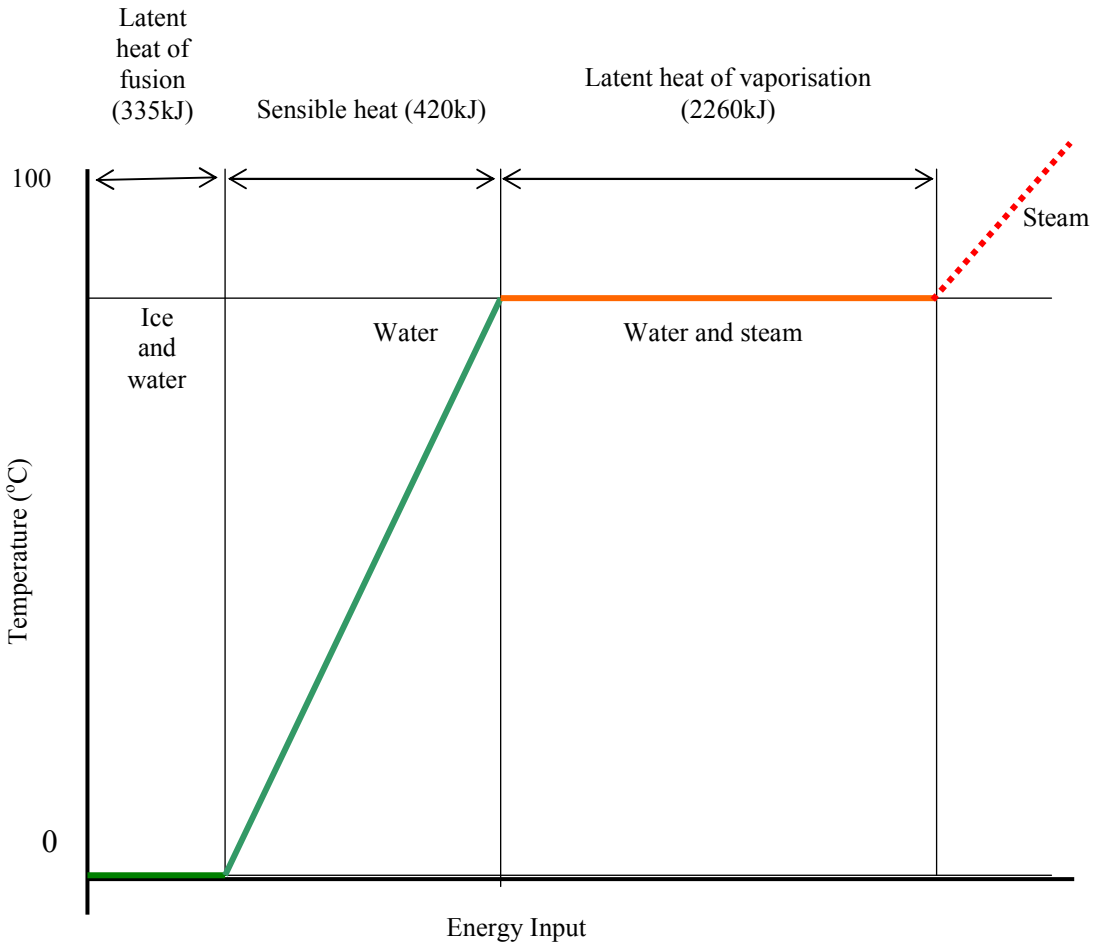

Figure 2.33 Heating of ice to illustrate latent heat

Six variables were used to define comfort zone based on ASHRAE standard-55. These variables are air temperature, air velocity, relative humidity, radiant temperature, occupant's clothing insulation and his activity. In this zone majority of occupants are likely to feel comfortable. Psychrometric chart can also be used to illustrate comfort zone as shown in Figure 2.34. Evaporative cooling system should not provide excessive moisture in the building as it will affect the clothing insulation and subsequently cause discomfort.

Table 2.3 Examples of acceptable operative temperature ranges based on comfort zone diagrams in ASHRAE Standard-55-2004

Conditions	**Acceptable operative temperatures**	
	°C	^{o} F
Summer (clothing insulation = 0.5 clo):		
Relative humidity 30%	24.5 – 28	76 – 82
Relative humidity 60%	23 – 25.5	74 – 78
Winter (clothing insulation = 1.0 clo):		
Relative humidity 30%	20.5 – 25.5	69 – 78
Relative humidity 60%	20 – 24	68 – 75

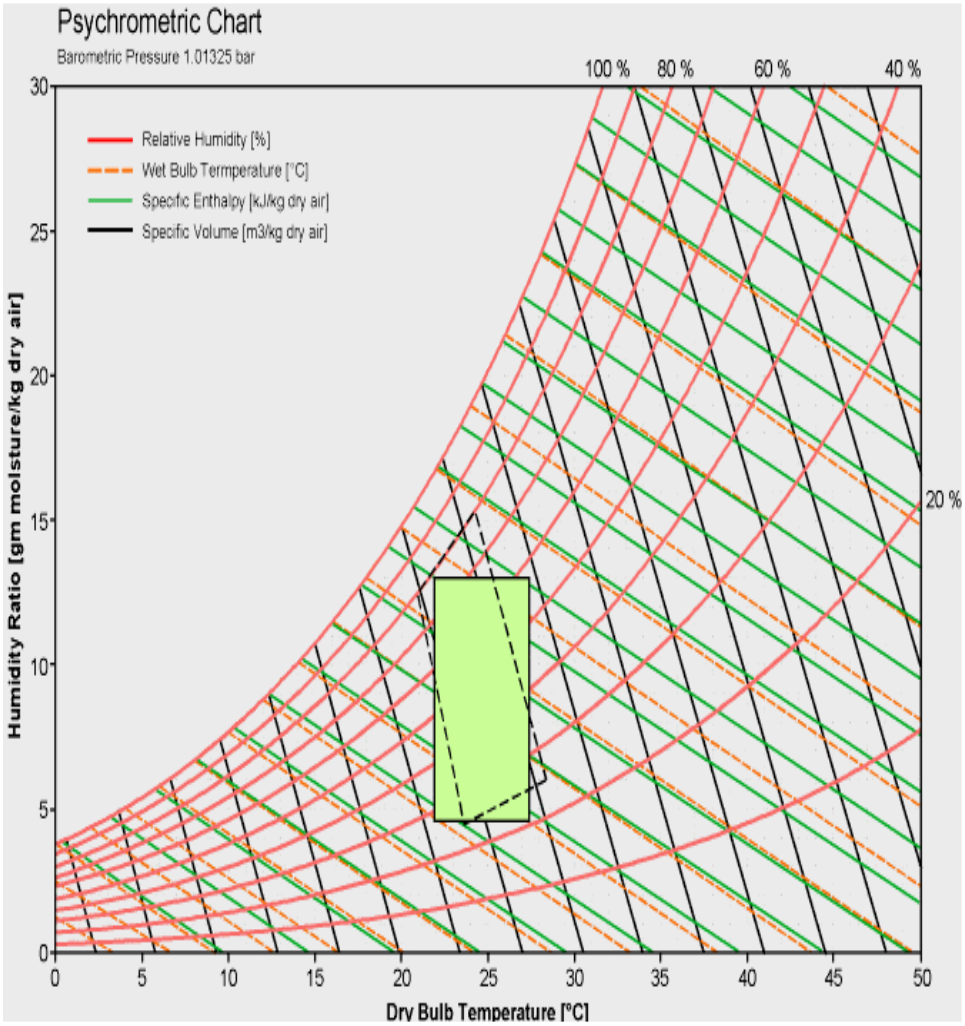

Figure 2.34 Psychrometric chart indicating comfort zone (ASHRAE)

2.11 Potentials for the novel evaporative cooling applications

Current concern for cleaner environment has drawn the attention of scientists to focus attention on the ancient method of using clay jars to be exploited for building space cooling applications. The prospects are enormous from different dry regions to modern cities of the world.

Professor Saffa, University of Nottingham was reported (Evening post, March 14, 2003) to draw attention on huge market for energy free air condition because of the heat generated by office computers and other electronic equipment. Even in places like London there is large number of buildings that need air conditioning throughout the year.

An alternative to conventional methods such as use of porous ceramics therefore has huge prospects. In some parts of the worlds having very hot dry climates peak dry bulb temperatures can reach over 42^{o}C where the wet bulb temperature and relative humidity as low as 19.6^{o}C and 40% respectively. In such areas generally the Dry Bulb/Wet Bulb temperature depression is mostly greater than 15^{o}C (Brian, 2003). Wet-Bulb temperature is always below the value of the dry bulb temperature and the difference termed as DBT/WBT Depression is an indicator of the water content of the air. It is the lowest temperature that will be reached by evaporative cooling.

The DBT/WBT depression is a measure for climatic applicability of evaporative cooling. The greater the depression the greater is the potential for evaporative cooling at a given period of the year as illustrated in the case of passive downdraught evaporative cooling shown below in Figure2.35. In the case of porous ceramics

(Brian and Rosa) demonstrated different ways of achieving cooling effects in a room by locating the wetted ceramics on an air flow passage from outside to the inside.

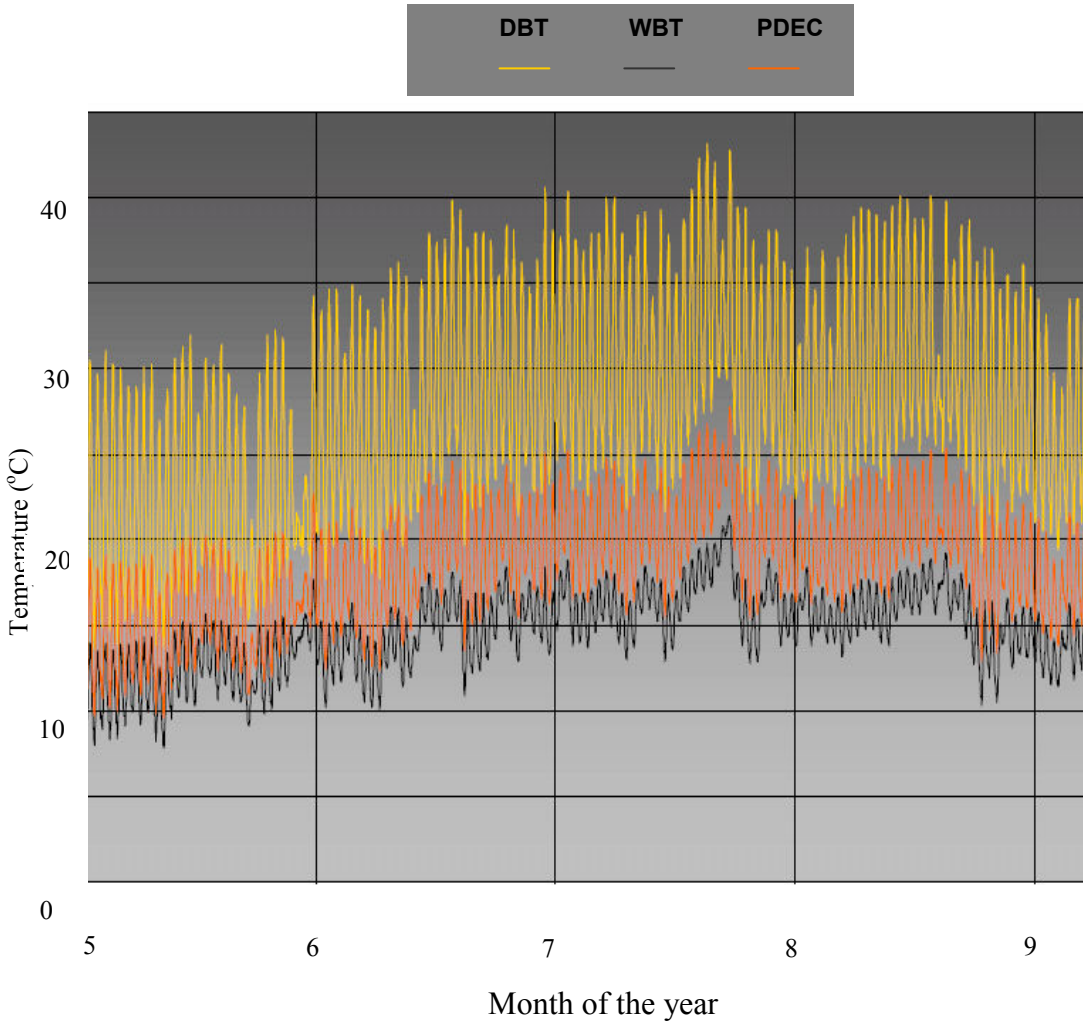

Figure 2.35 Dry and wet bulb temperature and potential for evaporative cooling

2.12 Historical perspective of evaporative cooling

Naturally evaporative air cooling occurs near waterfalls and streams, as well as over lakes and oceans, under dense foliage and on wet surfaces. It also occurs in human skin. It is therefore as old as the creation of man and his environment. The history was categorized as primitive, modern, Eastern and Western judging from the Egyptian water jars of 2500BC manually fanned by slaves to cool water

up to the development of homemade drip coolers of 1935 when they became more popular (Watt et al, 1997).

Historically also the ancient Egyptians hung wet mats in their doors and windows while wind blowing through the mats cooled the air making this to be the first attempt air conditioning. The idea was refined through the centuries. Chronologically; mechanical fans to provide air movement came in the 16th century, cooling towers with fans that blew water-cooled air inside factories in the early19th Century and swamp coolers in the 20th Century. Evaporative cooling have existed in different forms and using different materials for centuries ago. The technologies are increasingly growing worldwide, though they are still underutilised and unknown in many parts of the world. Using porous ceramics stretched in to antiquities and is still the major ways of cooling water and preservation of some perishable agricultural products in some hot and dry climates of the world. Examples include the fired clay porous ceramic jars "Botijos" of Spain and Southern Italy used to provide water for agricultural workers in the fields (Brian and Rosa, 2003). Other areas are Egypt and Sudan, (Ibrahim et al, 2003) Similarly in Nigeria from centuries to the present days locally fired porous clay pots are very popular for cooling water in homes and farms. The most popular shapes are basically spherical differing in the openings at the top. The size of the opening depends on the nature and shapes of the item to be cooled or stored and the size of the ceramic pot as well. Figure2.36a shows the common ones used for cooling water and some soft drinks. The simple evaporative cooling process on these clay pots is illustrated in Figure 2.36b and 2.36c. As warm dry air flows over the wet body of the water filled porous clay pot evaporation takes place on the surface. The air downstream becomes cool

and humidified while the water in the pot becomes cool. The same materials are used for the preservation of some agricultural products such as kola nuts and vegetables as shown in Figure 2.40 (Elkahoji, 2004). However utilisation of the cool air downstream for human comfort in buildings is still very much desired. In vast majority rural areas in Nigeria making of porous clay pots was well mastered in different shapes, sizes and styles as shown in Figure 2.38. Therefore the need for exploitation of the technology to reduce the huge cooling energy requirements and save the environment should be given serious attention.

Figure 2.36a Spherical clay pots for storage and evaporative cooling of water

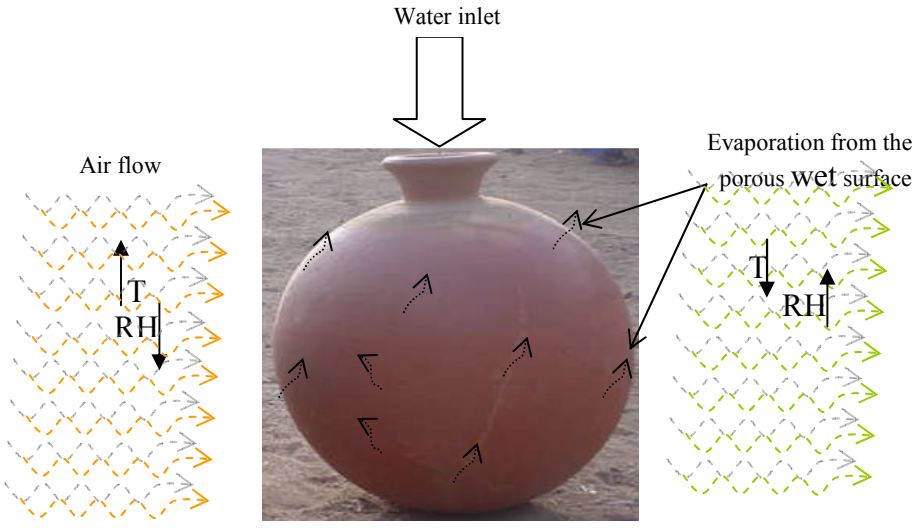

Figure 2.36b Evaporative cooling process on Nigerian porous clay pot

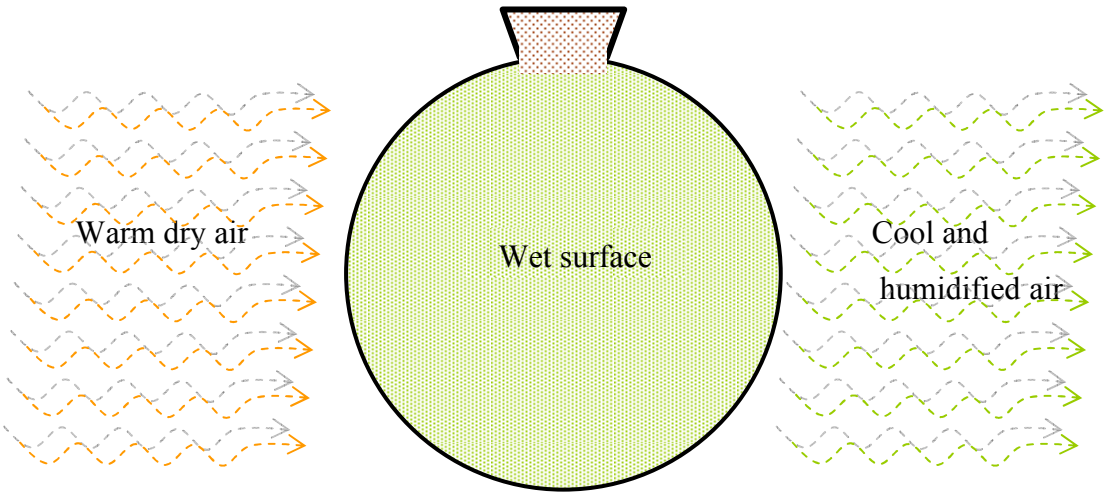

Figure 2.36c Evaporative cooling process on porous clay pot

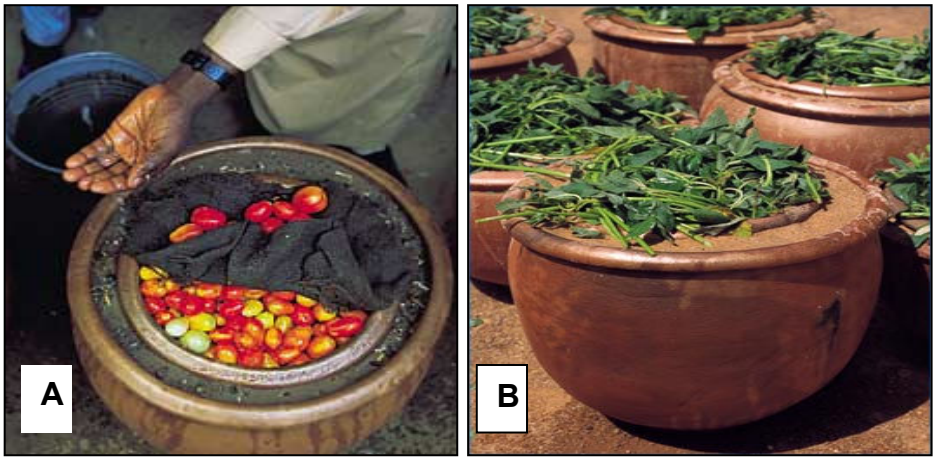

Figure 2.37 Use of traditional clay pots for the preservation of vegetables and fruits by evaporative cooling and constant moisturising, (A -Kola nut, B- Spinach vegetable).

However, the application of these porous ceramic pots for building cooling applications is yet to be exploited. For building applications in dry climates, cooling or comfort is virtually derived from passive cooling considerations. These include provision of windows, planting of trees and construction of heavy walls in buildings. Other means of achieving cool and comfortable building environment is by wind towers and air cooling by evaporation of water where the water can be sufficiently obtained.

Also as reported, the evaporation of water was carried out through porous ceramic pots located within a "wind catcher" to induce cooling and air movement through buildings. Another present day application of porous ceramic is in humidifiers for domestic and non domestic buildings (Brian et al, 2003). However, the use of wetted solid surfaces including porous ceramics was reported to be more water economical than water pond system, (Qiu and Riffat, 2006).

Figure 2.38 Locally manufactured porous clay pots in different styles, shapes and sizes.

2.13 The novel horizontal tubes evaporative cooler

Direct evaporative cooling is often associated with the rise in relative humidity which may sometimes result in making the cooled space rarely comfortable. Indirect evaporative cooling offers a solution but still requires improvements in the effectiveness or performance efficiency. There is also need for using cheap readily available materials for the construction, requiring simple fabrication technology without very complex engineering infrastructure. Preliminary investigations on some commonly available fibrous materials have shown very weak capillary effect. They cannot draw-up water high enough to wet the length required for effective heat transfer if the cooler is to be kept vertical.

So a periodic water spray system with an automatic control is required for running the cooler which adds to the power consumption as well as construction and operation difficulties. As a compromise a novel idea of using horizontal arrangement was considered. Therefore use of pump for supplying water required to moisten the evaporative cooling surface was eliminated. The system was constructed and tested under varying temperature, relative humidity and air flow rates. Results showed significant temperature reduction without unwanted rise in relative humidity.

2.14 Summary

Presented in this chapter is a review of the relevant information on the basics, development and research of some evaporative cooling technologies and their applications on buildings. The use of porous ceramics and integration with other cooling systems consisting of thermoelectric and heat pipes was highlighted. Developments in other concepts such as the dew point evaporative cooling were also reported. The areas discussed in this chapter are all related to this research for understanding of the state of the art in the areas. The history also gives a perspective of what has been done and what needs to be made in order to add to the knowledge in the subject matter. The basics combined with the history provide better understanding of the technical progress necessary for this research. Based on that, the chapter has highlighted the need for novel evaporative cooling systems that takes in to account the advantages and disadvantages of evaporative cooling. These provide potential applications for comfort and healthy environment. The chapter have highlighted all the relevant mechanisms involved.

CHAPTER 3

Review on Theoretical Studies on Evaporative Cooling Systems

3.1 Introduction

This chapter contained literature review on theoretical studies applicable to evaporative cooling for system design and performance evaluations.

In the development and performance evaluation of an evaporative cooling system often modelling is very vital in order to arrive at optimum parameters. These should be based on the theoretical or mathematical relations. It enables theoretical results to be predicted for the optimum system development and performance evaluation. The performance of the system can then be evaluated experimentally in comparison with some theoretical model predictions. Therefore the main areas discussed in this chapter consists of evaporative cooling heat and mass transfer model, model for basic evaporative cooling psychrometric properties, then direct, indirect and combined mode evaporative cooling systems performance models.

3.2 Evaporative Cooling Heat and Mass Transfer Model

Analysis of an evaporative cooling process requires the application of heat and mass transfer analogy. Figure 3.1 shows an outline of water evaporation process from a wetted surface as air flows over it. The energy involved in the phase change from liquid to vapour is the latent heat of vaporization. The liquid molecules near the surface experience collisions that raise their energy above that needed to overcome the surface binding energy or surface tension.

This causes evaporation and the energy required to sustain this evaporation is provided from the internal energy of the liquid resulting in a reduction of the surface temperature. Therefore evaporative cooling involves energy conservation model. It also requires heat and mass transfer process models.

To achieve steady state conditions, the energy transfer from the surrounding air must balance the latent energy demand by the liquid in order to sustain the evaporation. If radiation effects are neglected, the heat transfer process can be due to convection of sensible energy from the air or an external energy source; if the process is not adiabatic. Basic equations for the evaporative cooling process are presented below and refer to the heat exchange process diagram shown in Figure 3.1 (Incropera and DeWitt, 2002).

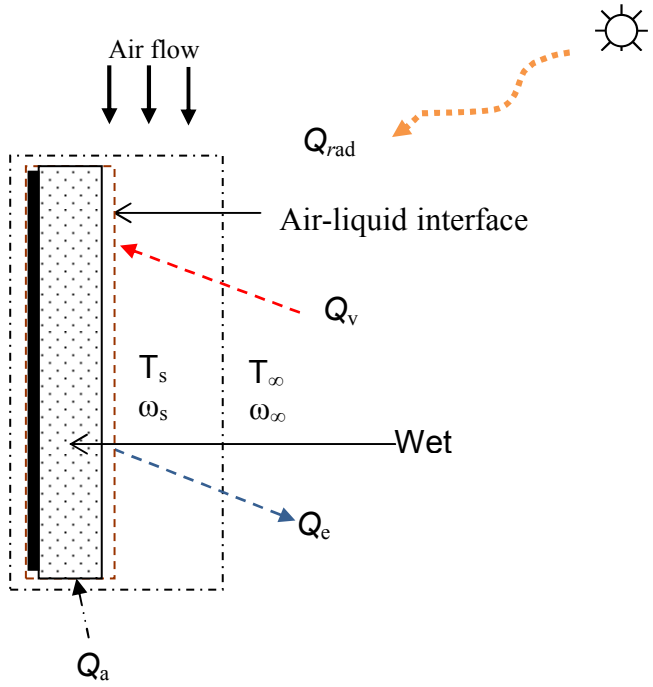

Figure 3.1 Heat exchange process at the vapour – liquid interface of an evaporative cooling system.

The heat transfer components involved across the control volume in the above system model diagram (Figure 3.1) are as follows:

Q_v -sensible convection heat flux from air/vapour, (W/m^2)

Q_a -heat added by other means or source, (W/m^2)

Q_{rad} -heat added due to radiation, (W/m^2)

Q_e -heat required for the evaporation, (W/m^2)

To develop a model for the process the following assumptions are made:

- Kinetic energy gain is negligible.
- Potential energy gain is negligible.
- The process is assumed to be under steady state open system.
- Flow, heat and mass are to be under steady state.
- All thermal properties remains constant within the system

Considering the heat and mass transfer process at the vapour–liquid interface of an evaporative cooling system shown in Figure 3.1. The general energy conservation equation is given by:

$$Q_v + Q_a + Q_{rad} = Q_e \tag{3-1a}$$

That is: $Q_v + Q_a + Q_{rad} - Q_e = 0$ (3-1b)

Under the adiabatic condition, the heat addition term in equation (3-1) disappears because there is no addition of heat from an external source. Also radiant heat exchange between the surface and its surrounding is considered to be negligible. We are therefore left with balance between convection heat

transfer from the vapour and the evaporative heat loss from the wetted surface or liquid. Equation (3-1) reduces to:

$$Q_v = Q_e \tag{3-2}$$

The energy required for evaporation, Q_e can be estimated as the product of evaporative mass flux ($\dot{m}_v$) and latent heat of vaporisation (h_{fg}) as in equation (3-3) given below (Incopera and DeWitt, 2002):

$$Q_e = \dot{m}_v h_{fg} \tag{3-3}$$

Where: $\dot{m}_v$ = - is the evaporative mass flux, (kg/s.m^2)

h_{fg} - is the latent heat of vaporisation, (J/kg)

3.2.1 Convection heat transfer in evaporative cooling

Referring to Figure 3.1, heat transfer will occur if the surface temperature (T_s) is different from the free stream temperature (T_∞) that is $T_s \neq T_\infty$. The resulting local heat flux due to the convection heat transfer is given in the following expression (Incopera et al, 2002)

$$\dot{Q}_v = h_c(T_s - T_\infty) \tag{3-4}$$

In the above equation, h_c is the convective heat transfer coefficient. This sensible convection local or elemental heat flux term in equation (3-2) can be expressed in terms of convective heat transfer coefficient and the temperature difference on the basis of an elemental area (dA) as follows (Carmago et al, 2003):

$$\delta Q_v = h_c dA(T_s - T_\infty) \tag{3-5}$$

As flow conditions vary along the surface both dQ_v and h_c also vary. The total heat transfer rate can therefore be obtained by integrating the local flux expressed in equation (3) over the entire surface area. So we have,

$$Q_v = (T_s - T_\infty) \int_A h_c \, dA \tag{3-6}$$

Alternatively the total heat transfer rate can be expressed in terms of the average convection heat transfer coefficient $\bar{h}$ for the entire surface as follows (Incropera and DeWitt, 2002):

$$Q_v = \overline{h_c} A (T_s - T_\infty) \tag{3-7}$$

Equating expression (3-6) and (3-7) we have:

$$\overline{h_c} A (T_s - T_\infty) = (T_s - T_\infty) \int_A h_c \, dA \tag{3-8}$$

From equation (3-8) the average and local heat transfer convection coefficients are related as in the equation shown below:

$$\bar{h}_c = \frac{1}{A} \int_A h_c \, dA \tag{3-9}$$

The value of convective heat transfer coefficient can be evaluated from the conventional heat transfer relations for flow in cylindrical and rectangular channels.

3.2.2 Convection mass transfer in evaporative cooling

Analogous to heat transfer, if the specific humidity or concentration of the air close to the surface (ω_s) is different from the one at the free stream velocity (ω_∞), that is $\omega_s \neq \omega_\infty$ then evaporative mass transfer will take place.

The total evaporative mass transfer rate on an entire given surface is shown in the following expression (Bergman et al, 2006):

$$\dot{m}_v = \bar{h}_m A\ (\omega_s - \omega_\infty) \tag{3-10}$$

Also elemental rate of mass transfer (dm_v) can be expressed in terms of mass transfer coefficient and difference in specific humidity as (Carmago et al, 2003).

$$dm_v = h_m \rho_w dA(\omega_s - \omega_\infty) \tag{3-11}$$

The average and local mass transfer convection coefficients are related in the integral expression given below:

$$\bar{h}_m = \frac{1}{A}\int_A h_m dA \tag{3-12}$$

The ratio of convective heat transfer coefficient to the mass transfer coefficient is expressed in terms of Lewis number as shown below, (2002 Bergman et al, 2006):

$$\frac{h_c}{h_m} = \frac{k}{D_{AB} Le^n} = \rho C_p Le^{1-n} \tag{3-13}$$

Therefore

$$\frac{h_c}{h_m} = \rho C_p Le^{1-n} \tag{3-14}$$

The above expressions can be used to determine one convection coefficient to be calculated from the knowledge of the other and is also applicable to their respective average values $\bar{h}_c$ and $\bar{h}_m$. The same relation can be used on either turbulent or laminar flow. For most applications the value of "n" can be reasonably assumed as 1/3.

3.3 Basic Evaporative Cooling Psychrometric Properties Models

Regardless of the type of evaporative cooling system, the following mathematical model can be used to evaluate the basic properties required for the performance evaluation of evaporative cooling systems. Figure 3.2a and 3.2b respectively show the process flow diagram and psychrometric representation. These properties consist of specific volume, humidity ratio, pressure, partial pressure of water vapour, saturation pressure of water vapour, enthalpy, dry bulb temperature, wet bulb temperature, dew point temperature, relative humidity and other related parameters. Appendix AI shows psychrometric chart indicating profiles of some of the above mentioned parameters under atmospheric pressure.

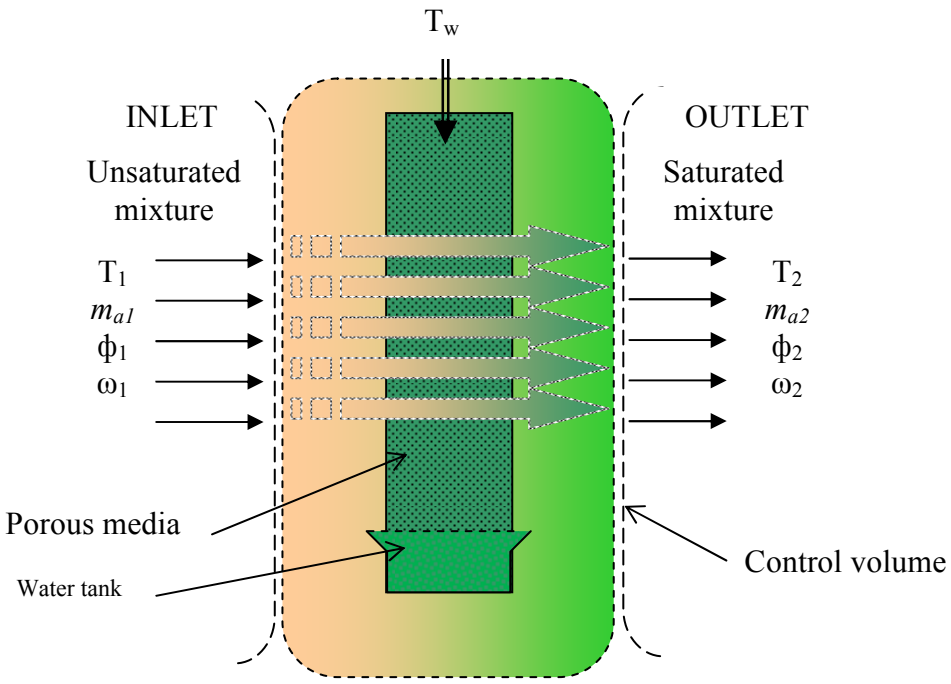

Figure 3.2a Schematic of an evaporative cooling process showing the basic parameters

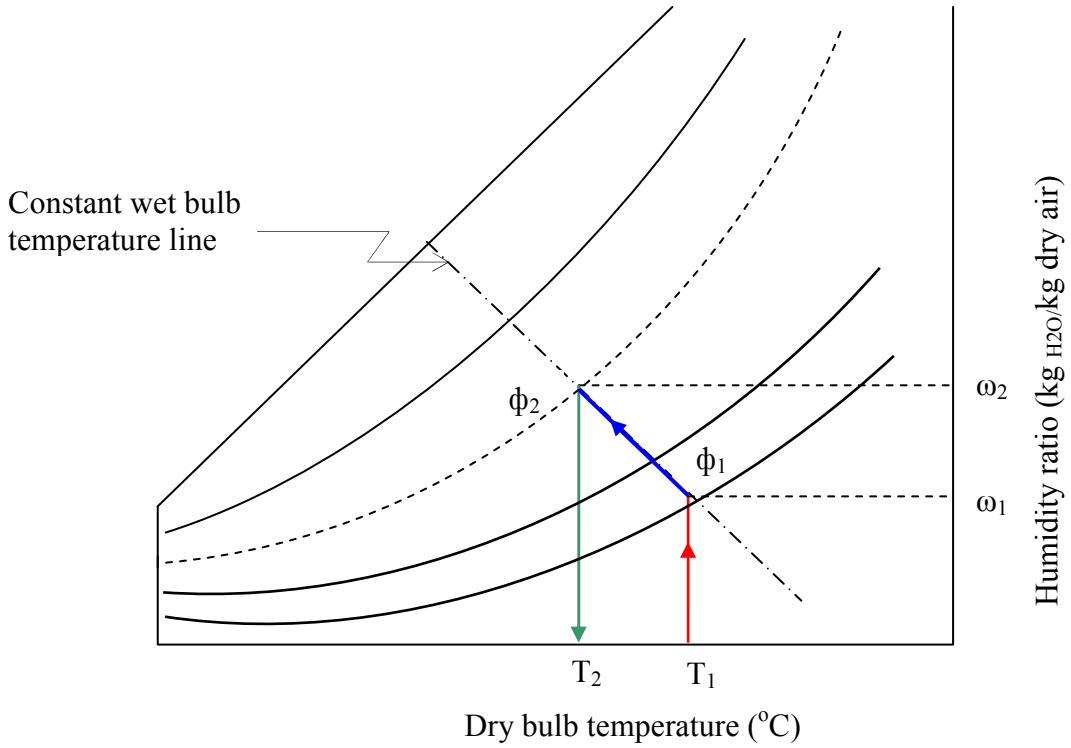

Figure 3.2b Psychrometric chart representation of cooling and humidification involved in direct evaporative cooling process.

3.3.1 Specific volume, specific humidity, relative humidity and specific enthalpy determination models

The psychrometric properties mentioned above are modelled in the following equations (Al-Nimr et al, 2002, CIBSE moist air simulation-website):

- The specific volume can be expressed in terms of dry bulb temperature, absolute and vapour pressure as shown below:

$$v = \frac{R_a T_{db}}{P\text{-}P_v} \qquad (3\text{-}15)$$

Specific humidity can also be expressed in terms of the absolute and vapour pressures as in the equation given below:

$$\omega = 0.622 \frac{P_v}{P - P_v} \tag{3-16}$$

- Relative humidity is given in the following equation:

$$\phi = \frac{\omega(P - P_v)}{0.622 P_{vs}} \tag{3-17}$$

It can also be computed by combining and simplifying equations (3-16) and (3-17) expressed as percentage as follows (CIBSE guide):

$$\phi = \frac{100 P_v}{P_s} \qquad [\%] \tag{3-18}$$

The partial pressure of water vapour can be computed with the following equation.

$$P_v = P_w - \frac{(P - P_w)(T_{db} - T_{wb})}{1532 - 1.3 T_{wb}} \tag{3-19}$$

- The specific enthalpy of the moist air per kilogram of dry air is expressed in terms of the dry bulb temperature and humidity ratio as follows:

$$h = (T_{db} - 273) + \omega[1.86(T_{db} - 273) + 2501.3] \tag{3-20}$$

3.3.2 Vapour pressures, wet and dew point temperatures

Other parameters that can be used in the model are given in the following equations:

- Computing saturation vapour pressure corresponding to a given dry bulb temperature.

$$\mathrm{Ln}\left(\frac{P_{vs}}{2337}\right)=6789\left(\frac{1}{293.15}-\frac{1}{T_{db}}\right)-5.031\ln\left(\frac{T_{db}}{293.15}\right) \quad (3\text{-}21)$$

- Computing vapour pressure corresponding to a given wet bulb temperature

$$\mathrm{Ln}\left(\frac{P_{wb}}{2337}\right)=6789\left(\frac{1}{293.15}-\frac{1}{T_{wb}}\right)-5.031\ln\left(\frac{T_{wb}}{293.15}\right) \quad (3\text{-}22)$$

- The wet bulb and dew point temperatures can be computed using the equations given below respectively (Joudi et al, 2000):

$$T_{wb}=2.265\sqrt{1.97+4.3T_{db}+10^{4}\omega}-14.85 \quad (3\text{-}23)$$

$$T_{dp}=26.13722+16.988833\ln(\phi P_{a})+1.04961[\ln(\phi P_{a})]^{2} \quad (3\text{-}24)$$

3.3.3 Density and specific heat capacities

- The density of the moist air can be computed with the following equation:

$$\rho=\frac{P-0.387\phi P_{s}}{287T}\left[\frac{kg_{moist-air}}{m^{3}}\right] \quad (3\text{-}25)$$

Where

T - is the absolute temperature of the most air [K]

T = t + 273.15 and t = dry bulb temperature [^{o}C]

- The total specific heat capacity of the mixture consists of two different specific heat capacities expressed in the following expression:

$$Cp = Cpa + \omega Cpv \quad [\frac{kJ}{kg_{dryair} K}] \tag{3-26}$$

Where the specific heat capacity of the dry air is given in the following equation:

$$Cp_a = 1.005 + 1.35 \times 10^{-8} (t+30)^2 \quad [\frac{kJ}{kgK}] \tag{3-27a}$$

While the specific heat capacity of the humid air can be computed with the following expression:

$$Cp_v = 1.8684 + 0.0095(\frac{t}{100}) + 0.00373(\frac{t}{100})^2 \quad [\frac{kJ}{kgK}] \tag{3-27b}$$

In both equations temperature t is the dry bulb temperature in ^{O}C.

3.4 Direct Evaporative Cooling System Performance Model

The general working process of direct evaporative cooling system involves water being sprayed on a porous media through which dry air flows as shown in Figure 3.3a. The air will then exit in a cool and humid condition. Figure 3.3b shows the cooling process represented on a psychrometric chart. On the chart process AC corresponds to the ideal process while AB is the actual process.

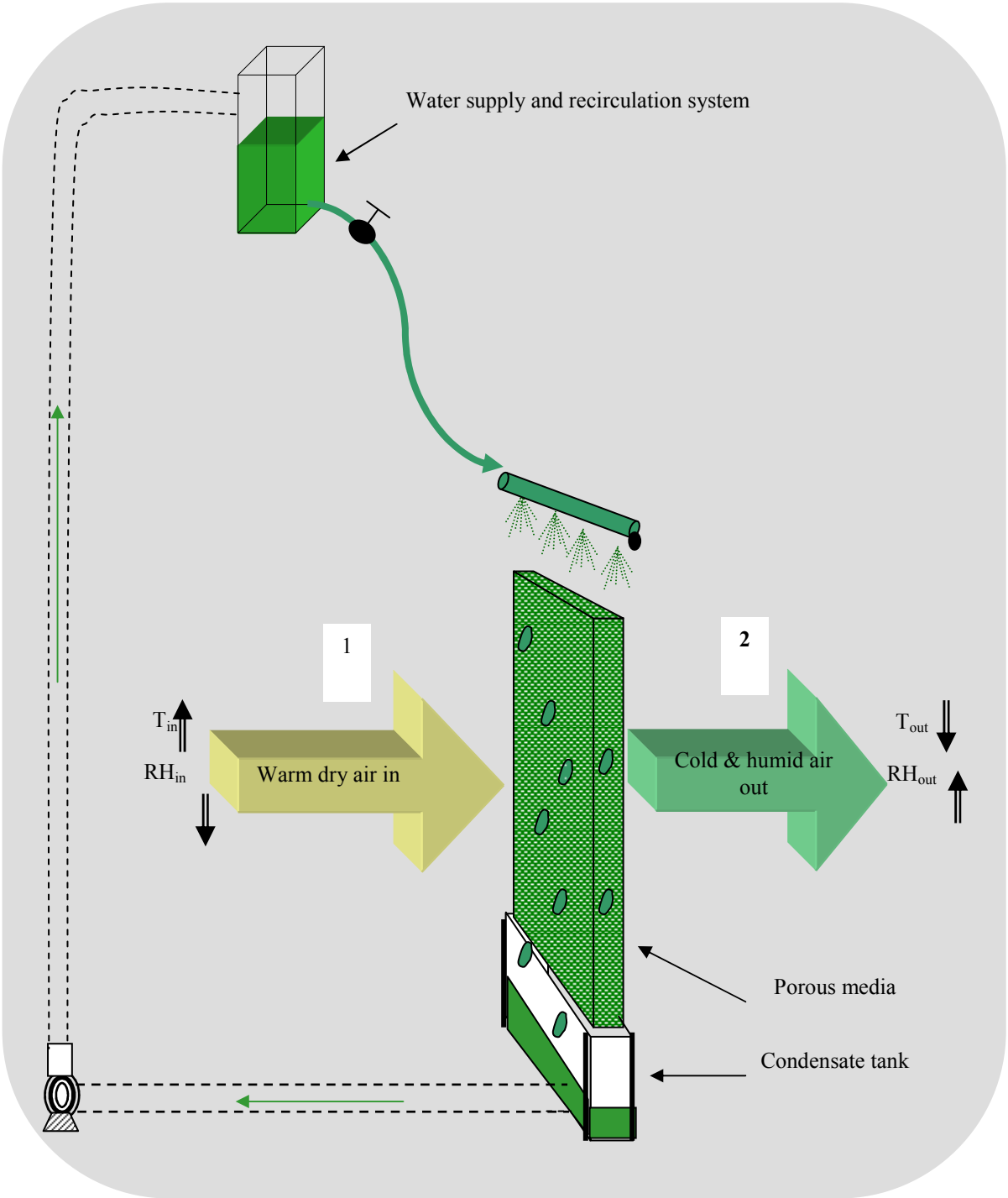

Figure 3.3a Process in direct evaporative cooling system

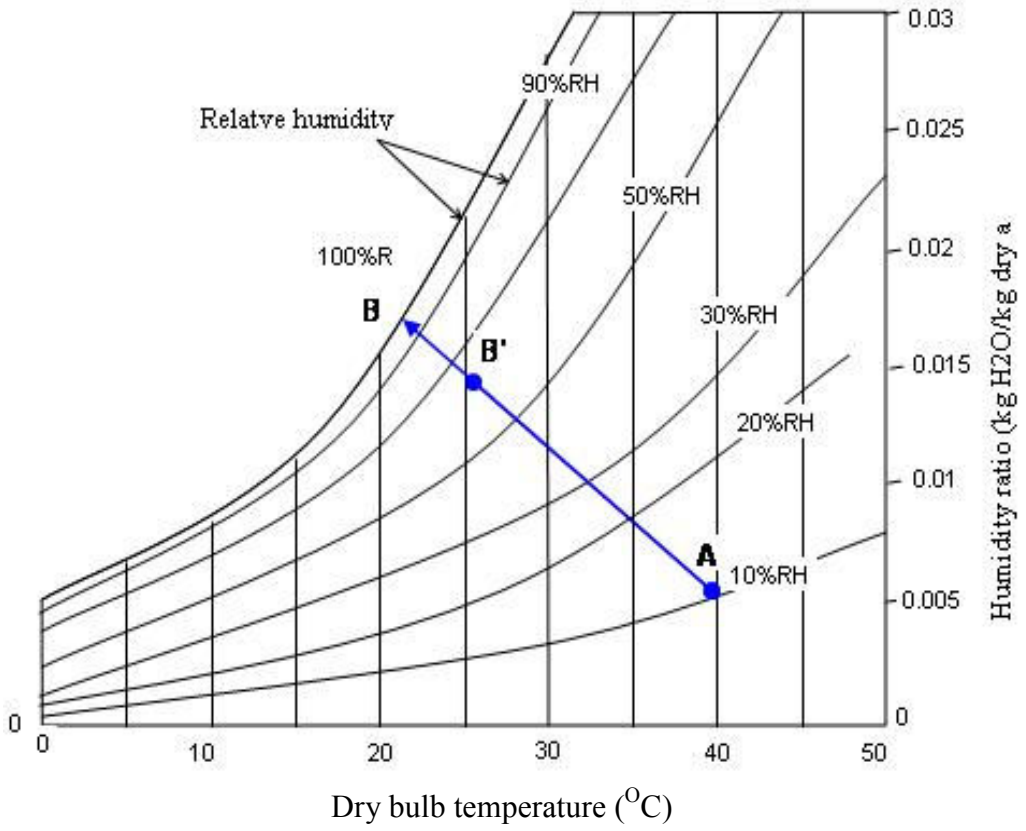

Figure 3.3b Psychrometric representation direct evaporative cooling system

An important application of heat and mass transfer analogy as discussed in the preceding section is to the evaporative cooling process. In the absence of heat addition from any external source, the model will require energy balance between convection heat transfer from the fluid (air) and the evaporative heat loss from the liquid (water) or wet surface. Therefore equation (3-2) from the heat transfer model applies, that is:

$$Q_v = Q_e$$

But for a unit surface area the evaporative heat loss (Q_e) from the wet surface can be taken as the product of the evaporative mass flux (m_v) and the latent heat of vaporisation, that is:

$$Q_e = h_{fg} m_v \tag{3-28}$$

For a unit surface area equation (3-10) becomes:

$$m_v = h_m(\rho_s - \rho_\infty) \tag{3-29}$$

Substituting for m_v, equation (3-29) above becomes

$$Q_e = h_m h_{fg}(\rho_s - \rho_\infty) \tag{3-30}$$

Similarly, for a unit surface area the convection heat transfer can be expressed as:

$$Q_v = h_c(T_s - T_\infty) \tag{3-31}$$

3.4.1 Minimum attainable cooling temperature from the system

The minimum temperature that can be achieved in an evaporative cooling process occurs when the air stream becomes saturated as indicated at state B in Figure3.3b. Thus because evaporative cooling is a constant wet–bulb temperature process, the minimum temperature that can be achieved is the wet-bulb temperature of the air at the inlet condition of the system. That is the saturation temperature at sate 1 as shown in Figure 3.3a. However; this depends on the saturation efficiency of the system. The saturation efficiency of direct evaporative cooler is the ratio of the real decrease of the dry bulb system temperature between the inlet and outlet to the maximum theoretical decrease that the dry bulb temperature would reach if the system was 100% efficient and the outlet air was saturated. Under this ideal condition the outlet dry bulb temperature would be equal to the wet bulb temperature of the inlet air.

The minimum possible temperature that air can attain under the evaporative cooling process is the wet bulb temperature (T_{wb}). (Carmago et al, 2003) subject to the saturation efficiency of the system. Generally for both the direct and indirect evaporative cooling process the system performance can be based on the saturation efficiency (η_{sat}), defined in the expression given below: (Santamouris and Asimakapoulos, 1996, Qiu and Saffa, 2006).

$$\eta_{sat} = \frac{T_{db,in} - T_{db,out}}{T_{db,in} - T_{wb,in}} \tag{3-32a}$$

Where for an evaporative cooling system:

$T_{db,in}$ - Is the dry bulb temperature at inlet

$T_{db,out}$ - Is the dry bulb temperature at outlet

$T_{wb,in}$ - Is the wet bulb temperature at the inlet

Under real situation 100% saturation efficiency cannot be achieved that is $\eta_{sat}<100\%$. Therefore the situation is such that:

$T_{db,out} > T_{wb,out} > T_{wb,in}$.

However, it is possible to achieve substantial reduction in the outlet dry bulb temperature, $T_{db,out}$. Depending on the ambient conditions it is possible to achieve a saturation efficiency or effectiveness of about 90% for direct evaporative cooling (DEC) and a value between 70% and 80% for an indirect evaporative cooling (IDE). (Camargo et al, 2003, Qiu and Riffat, 2006).

The adiabatic saturation temperature is the minimum that can be achieved and is equivalent to the wet bulb temperature corresponding to the dry bulb temperature at the inlet.

This temperature can be evaluated by transforming equation (3.32a) for the saturation efficiency can therefore be expressed in terms of the inlet and outlet dry bulb temperatures as below:

$$T_{wb,in} = T_{db,in} - \frac{T_{db,in} - T_{db,out}}{\eta_{sat}} \tag{3-32b}$$

Regardless of the saturation efficiency, the wet bulb temperature of the incoming air ($T_{wb,in}$) as indicated in equation (3.32b) can be calculated using the empirical expression given below (Joudi et al, 2000)**.** Under normal pressure and temperature range of atmospheric air, the adiabatic saturation temperature is closely approximated by wet bulb temperature T_{wb}. (Joudi et al, 2000).

$$T_{wb} = 2.265\sqrt{1.97 + 4.3T_{db} + 10^4\omega} - 14.85 \tag{3-33}$$

In the above equation, T_{db} is in ^{o}C. The moisture content ω is expressed in terms of the saturation pressure, P_{sat} and relative humidity Ø as in the following relation:

$$\omega = \frac{0.622\,\phi P_{st}}{1.013 \times 10^5 - \phi P_{sat}} \tag{3-34}$$

Based on equation (3-33) and (3-34) it is clear that the wet bulb temperature (T_{wb}) is dependent upon dry bulb temperature and the relative humidity regardless of the wind velocity. To determine the humidity ratio ω for such mixtures the wet bulb temperature can be used in place of the adiabatic saturation temperature.

Also in a flow channel containing 'N' number of evaporative cooling media, for a given air inlet at temperature $T_{1,}$ the outlet temperature, T_2 is obtained from the following equation (S.B.Riffat & J. Zhu, 2004):

$$T_2 = T_1 - \frac{NQ}{mC_p} \tag{3-35}$$

and

$$T_1 - T_2 = \frac{NQ}{mC_p} \tag{3.36}$$

Figure 3.4 below shows the variation of outlet dry bulb temperatures with the inlet at different values of relative humidity. Equations (3.33) and (3.34) were solved with EES at different in put dry bulb and relative humidity values. This simulation results predicts how the relative humidity affects the out let temperature of a direct evaporative cooling system. It can be observed that for a given constant inlet dry bulb temperature of 43^{O}C the out let is 24.9^{O}C at 10% relative humidity while it became 42^{O}C when the relative humidity was increased to 65 ^{O}C. Hence at higher relative humidity no appreciable cooling effect can be expected from direct evaporative cooling.

Figures 3.5a, 3.5b and 3.5c show timely variations of outlet temperatures with relative humidity for given constant inlet dry bulb temperatures of 43^{O}C, 35^{O}C and 30^{O}C, respectively. In all these cases the trend shows temperature drops reducing with increasing rise in relative humidity as expected. These trends explained the needs for controlling the relative humidity to march expected outlet temperature to be delivered to building space.

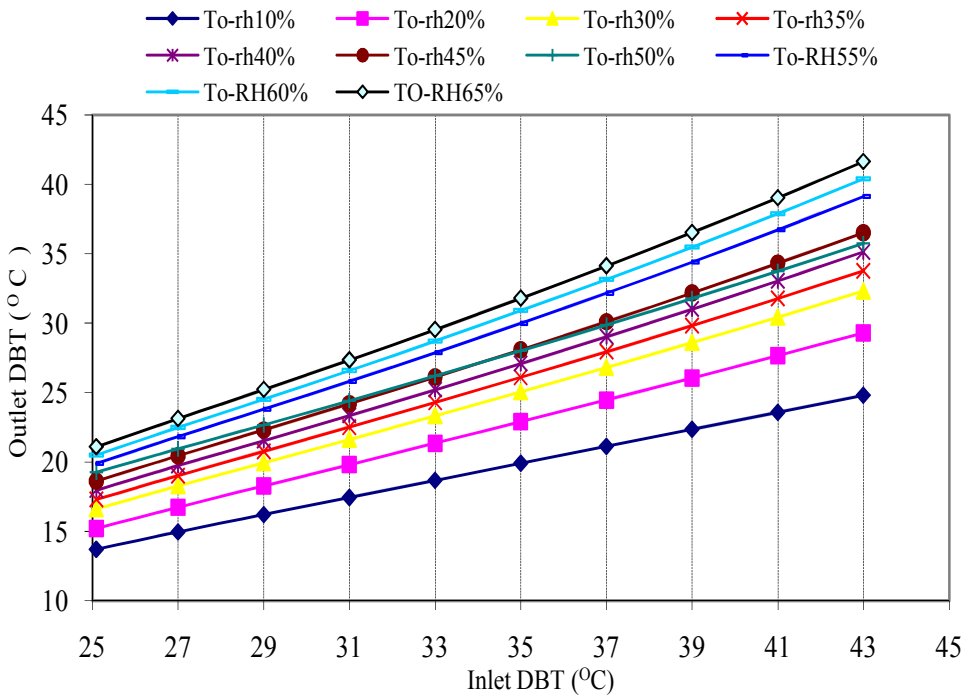

Figure 3.4 Variation of inlet and outlet dry bulb temperature (DBT) at different relative humidity (RH) values.

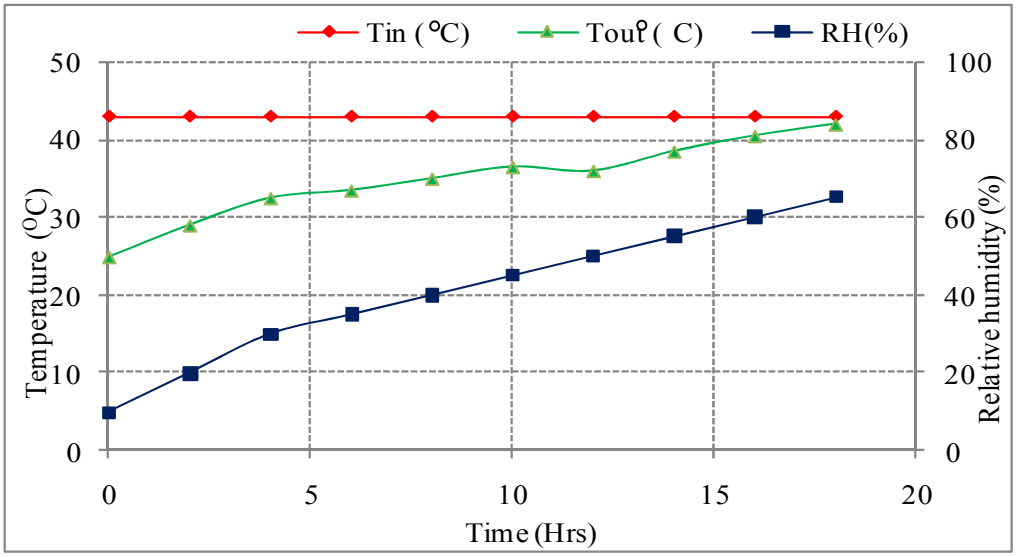

Figure 3.5a Timely variation of outlet temperature with relative humidity (RH) under constant inlet dry bulb temperature, (Tin=43^{O}C constant).

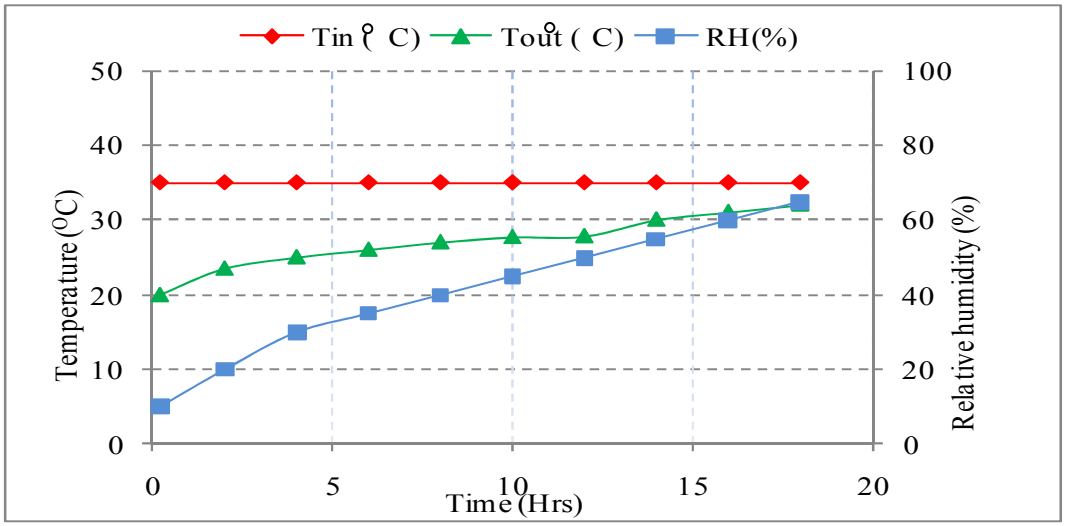

Figure 3.5b Timely variation of outlet temperature with relative humidity (RH) under constant inlet dry bulb temperature, (Tin=35^{O}C constant).

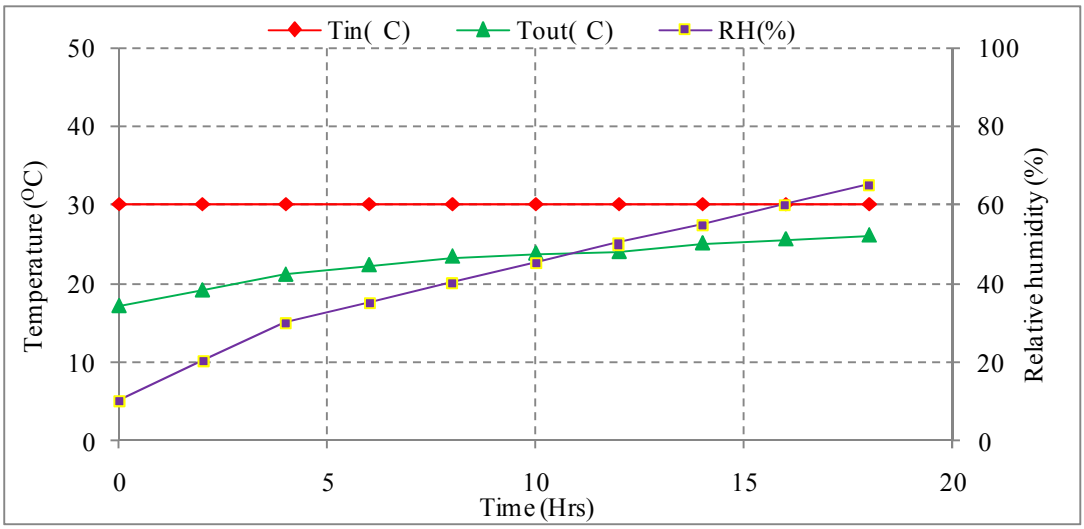

Figure 3.5c Timely variation of outlet temperature with relative humidity (RH) under constant inlet dry bulb temperature, (Tin=30^{O}C constant).

3.4.2 Determination of relative humidity at the system outlet

For an ideal gas mixture relative humidity is defined as the ratio of the partial pressure of the vapour to the saturation pressure of the vapour at the same dry bulb temperature of the mixture (Kenneth, 1999 and Rao, 2003). The relative humidity of the moist air from an evaporative cooling system can therefore be

defined by applying the equation below:

$$\phi = \frac{P_v}{P_g}\Bigg)_{T,P} \tag{3-37a}$$

Where p_v and p_g represent the actual vapour pressure and the saturation pressure at the same temperature respectively.

Assuming that dry air and vapour in a given mixture both behave as ideal gases enables the equation for relative humidity to be expressed in terms of specific volumes (or densities) as well as partial pressures as shown below:

$$\phi = \frac{p_v}{p_g} = \frac{RT_v / v_v}{RT_g / v_g} = \frac{v_g}{v_v} = \frac{\rho_v}{\rho_g} \tag{3-37b}$$

Both humidity ratio and relative humidity can be related in the following expression:

$$\phi = \frac{p_v}{p_a} = \frac{p_a \omega}{0.622 p_g} \tag{3-37c}$$

Also equation (3-17) or (3-18) can be applied to calculate the relative humidity of the system.

The saturation pressure p_g can be obtained as a function of temperature in the saturation temperature table for water. However for the purpose of design calculations this relation can be applied in an equation format given below (Kenneth, 1999):

$$\ln[p_g/\text{bars}] = 12.1929 - \frac{4109.1}{(T/\text{K}) - 35.50} \tag{3-37d}$$

Where: T is the temperature in Kelvin.

3.4.3 Cooling capacity

To evaluate the cooling capacity of an evaporative cooling process the system is modelled in Figure 3.6a. In the unit dry air is passed through the wet porous media. Due to the low relative humidity part of the water evaporates on having contact with the wet surface. The energy required for the evaporation comes from the air and it is cooled. At the same time the air gained increase in specific humidity and the relative humidity as well. Evaporative cooling as mentioned earlier is equivalent to an adiabatic cooling process. The path of the process closely follows a constant wet-bulb temperature line on a psychrometric chart as shown in Figure 3.6b.

On a psychrometric chart constant enthalpy and constant wet bulb temperature lines are parallel. It is therefore accurate to represent an evaporative cooling process either as of constant enthalpy or constant wet bulb temperature.

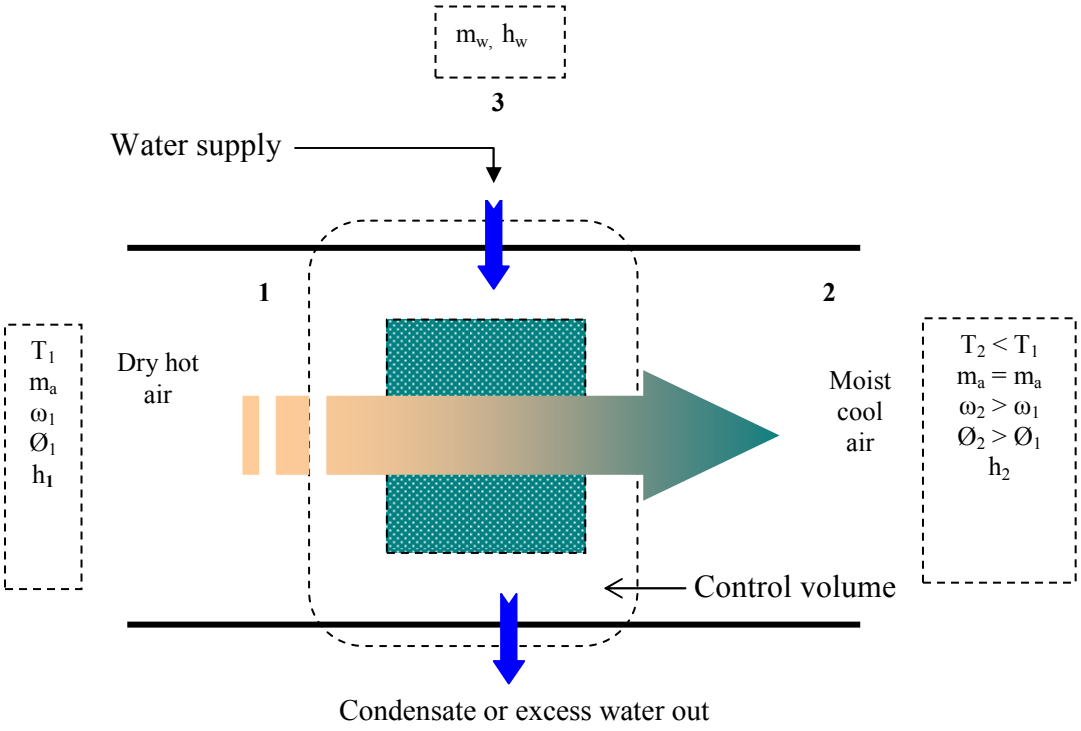

Figure 3.6a Schematic of a porous medium exposed to evaporative cooling process

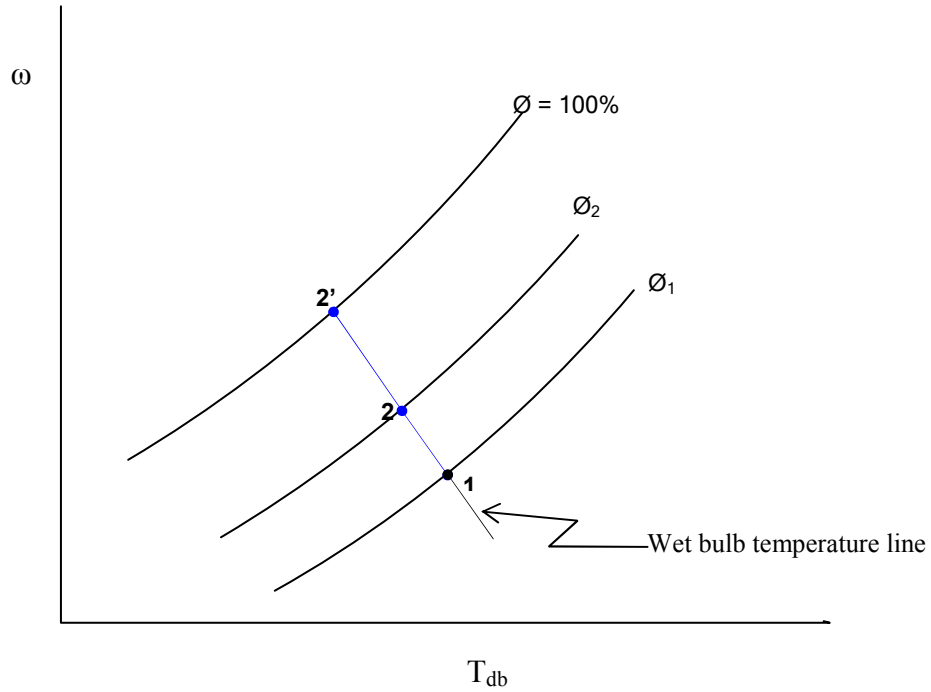

Figure 3.6b Evaporative cooling process on a psychrometric chart (Kenneth,1999)

Assuming steady state, adiabatic, and no heat or work gain, the performance of the system can be obtained by applying the mass and energy balance to the system as follows:

- **Mass balance:**

Mass balance for the dry air:

$$\dot{m}_{a1} = \dot{m}_{a2} = \dot{m}_a \tag{3-38a}$$

Mass balance for water:

$$\dot{m}_{v1} + \dot{m}_w = \dot{m}_{v2} \tag{3.38b}$$

But

$$\omega = \frac{\mathrm{m_v}}{\mathrm{m_a}} = \frac{M_v P_v}{M_a P_a} \tag{3-38c}$$

Therefore dividing the mass balance equation with the air flow rate we have:

$$\frac{\dot{m}_{v1}}{\dot{m}_a} + \frac{\dot{m}_w}{\dot{m}_a} = \frac{\dot{m}_{v2}}{\dot{m}_a} \tag{3-38d}$$

Applying the definition for humidity ratio (ω) the above relation becomes:

$$\omega_1 + \frac{\dot{m}_w}{\dot{m}_a} = \omega_2 \tag{3-38e}$$

$$\dot{\mathrm{m}}_\mathrm{a}\omega_1 + \mathrm{m_w} = \dot{\mathrm{m}}_\mathrm{a}\omega_2 \tag{3-38f}$$

Alternatively:

$$\dot{\mathrm{m}}_\mathrm{w} = \dot{\mathrm{m}}_\mathrm{a}(\omega_2 - \omega_1) \tag{3-38g}$$

- **Energy balance:**

Assuming negligible changes in kinetic and potential energy and no work on or by the system (Figure 3.6a) the steady state energy balance is given as (Rao, 2003).

$$h_1 + (\omega_2 - \omega_1)h_{w,3} = h_2$$

or

$$(h_1 - h_2) + (\omega_2 - \omega_1)h_{w,3} = 0 \tag{3-39a}$$

h_w is the specific enthalpy of liquid water or the condensate and h_w = $\mathrm{h_f}$ corresponding to the saturation temperature of the air at exit. In equation (3-39a) above, for flow within the porous media the second term in the LHS is very small compared to the first term and is therefore considered negligible. The equation therefore reduces to:

$$h_1 - h_2 = 0 \tag{3-39b}$$

The above equation also satisfies the relation for adiabatic saturation. However, cooling capacity of the system can be expressed in terms of mass flow rate and the enthalpy change across the system as shown below (Ebrahim, 2007):

$$Q_c = \dot{m}_a (h_1 - h_2) \tag{3-39c}$$

Also for direct evaporative cooling system the change in the specific enthalpy of the air can be obtained as a function of the outlet and inlet dry bulb temperature of the air stream as shown in the following equation (El-Dessouky et al 2000).

$$\Delta h = (h_1 - h_2) = Cp(T_1 - T_2) \tag{3-39d}$$

Therefore for a given mass flow rate of air the above relation becomes:

$$\Delta h = \dot{m}_a (h_1 - h_2) = \dot{m}_a Cp(T_1 - T_2) \tag{3-39e}$$

The enthalpies of the dry air can be obtained from ideal gas table for air.

Cp represents specific heat capacity of the dry air at constant pressure.

Expressing the cooling capacity in terms of differences in enthalpies and humidity ratios we obtain ((Rao, 2003) :

$$\dot{Q} = \dot{m}_a (h_1 - h_2) - \dot{m}_{a1} h_w (\omega_1 - \omega_2) \tag{3-40a}$$

Thus:

$$\dot{Q} = \dot{m}_a [(h_1 - h_2) - h_w (\omega_1 - \omega_2)] \tag{3-40b}$$

The heat loss from the air required for the water evaporation or the cooling capacity of the system can also be determined by the application of the following empirical correlations (R. Tang and Y. Etzion, 2005).

$$Q_{ews} = (0.7581 + 0.4257v)\,(P - \phi P_a)^{0.7} \quad (3\text{-}41a)$$

and

$$Q_{efs} = (0.2253 + 0.2464v)(P - \phi P_a)^{0.82} \quad (3\text{-}41b)$$

for the evaporation from a wetted surface and the free water surface respectively. Where:

Q_{ews} is the heat loss due to water evaporation from a wetted surface.

Q_{efs} is the heat loss due to water evaporation from a free water surface

v is the wind or air velocity over the surface (m/s).

ϕ -is the relative humidity (%).

P and P_a (in N/m^2) represent the saturated vapour pressures of the air at surface temperature and the ambient air temperature in (^oC) respectively. The saturated vapour pressure is given by the following expression.

$$P + 3385.5\ x\ Exp[-8.0929 + 0.97608(T + 42.607)^{0.5}] \quad (3\text{-}42)$$

Using the above model a simulation was carried out with a computer program written in Engineering Equation Solver (EES) with an input dry bulb temperature ranging from 25^OC to 45^OC. Typical cooling capacity simulation results for the wet surface and free water surface are shown in Figures 3.7a, 3.7b and 3.7c under very low, medium and higher relative humidity values respectively. The simulation results enable the performance to be predicted for comparison with experimental results. For the runs under very low and medium steady state relative humidity values of 10% and 50% respectively the cooling capacity steadily increased with the increase in the inlet dry bulb temperature.

However, for 70% relative humidity the cooling capacity decreased to minimum attainable with increasing inlet dry bulb temperature as shown in Figure 3.7c. This behaviour is what is expected from direct evaporative cooling system for either free water of wet surface cooling media used.

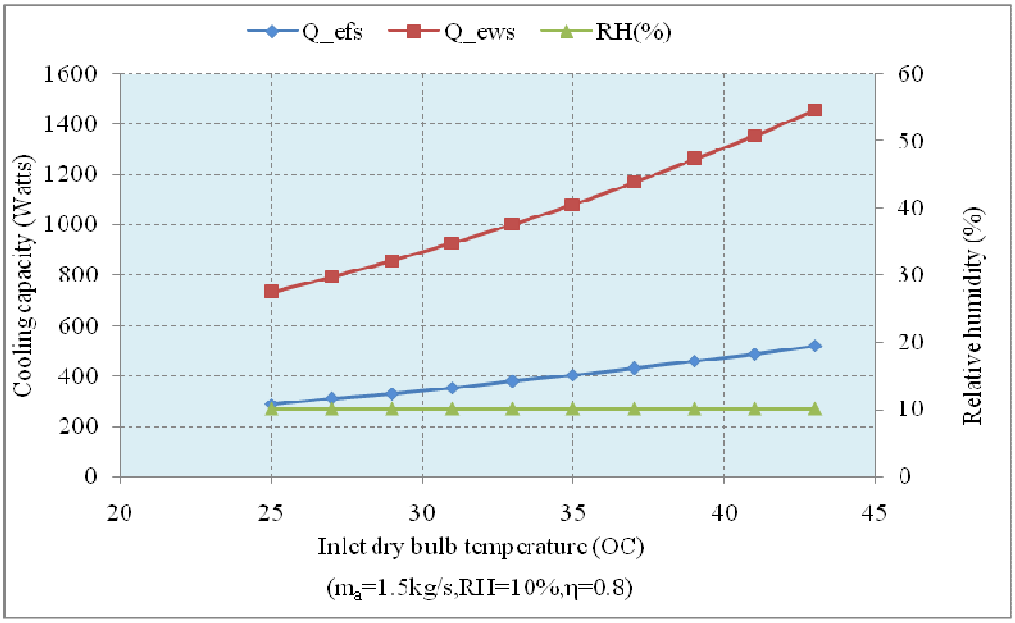

Figure 3.7a Variation of cooling capacity with inlet DBT for both wet and free water surfaces under low constant relative humidity condition

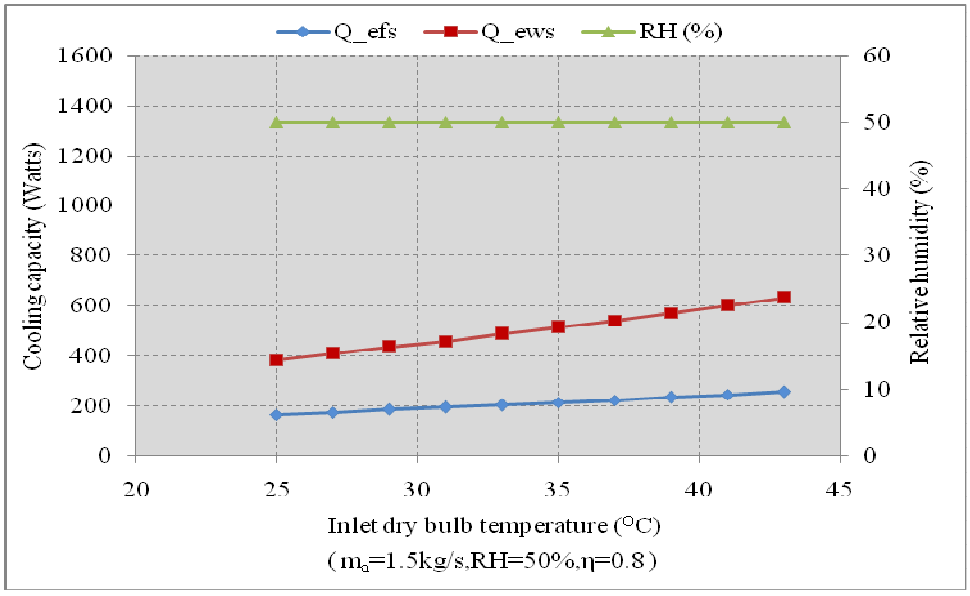

Figure 3.7b Variation of cooling capacity with inlet DBT for both wet and free water surfaces under medium constant relative humidity condition

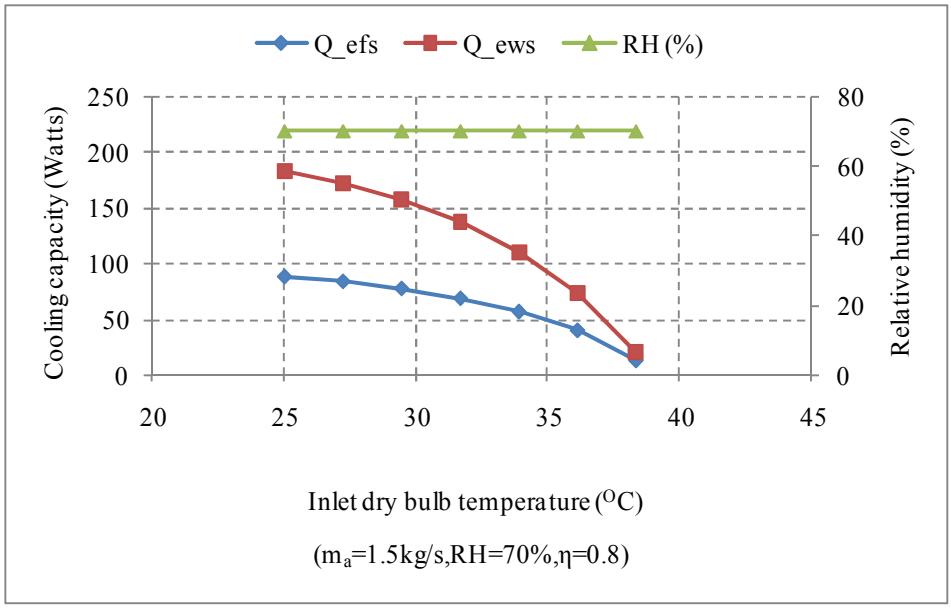

Figure 3.7c Variation of cooling capacity with inlet DBT for both wet and free water surfaces under high constant relative humidity condition.

3.4.4 Rate of water evaporation or water consumption

In evaluating the performance of evaporative cooling system either direct, indirect or combination total evaporative water mass is one of the parameters of importance. Others are available cooling temperature and the required cooling time (Qiu and Riffat, 2006).

Basically the water consumption or requirement of an evaporative cooling system can be evaluated by the application of the equation (3-38g), that is: (Rao, 2003 and Moran, 1995).

$$\dot{m}_w = \dot{m}_a(\omega_2 - \omega_1)$$

The rate of water evaporation, $\dot{m}_w$ (kgm^{-2} s^{-1}) can also be evaluated in terms of mass transfer parameter, vapour pressure difference and relative humidity as expressed in the following equation (Tang et al, 2004, Qiu and Riffat, 2006):

$$\dot{m}_w = h_m(P_w - \phi P_a) \qquad (3\text{-}43)$$

The above equation indicates a linear function of the vapour pressure difference. Ø is the relative humidity.

In a different analysis it was shown that water evaporation rate initially increased with the increase of surface water temperature but the rate gradually decreases with the increase in surface water temperature. It can therefore be expressed in the following new **e**xponential equation (Tang and Etzion 2004).

$$m_c = h_m (P_w - \phi P_a)^n \tag{3-44}$$

The value of the exponent, 'n' in the equation is less than 1.

In the above equation P_w and P_a are the saturation vapour pressures at the respective temperatures T_w and T_a. Also the value of the exponent n is 0.7 when the evaporation is from a wetted surface and 0.82 when it is from a free small water surface such as pond, etc. Coefficient (h_m) is related to wind velocity (Tang and Etzion, 2004). Based on the above the correlations for calculating the water evaporation rate or water consumption taking the wind velocity in to consideration are as follows:

For a wetted surface:

$$m_c = (0.7581 + 0.42572v) \times (P_w - \phi P_a)^{0.7} / h_{fg} \tag{3-44a}$$

For a free water surface:

$$m_c = (0.2253 + 0.24644v) \times (P_w - \phi P_a)^{0.82} / h_{fg} \tag{3-44b}.$$

where: v represents the wind or air flow velocity in m/s.

For moist air the dew point temperature, T_{dp} ($0<T_{dp}<65^oC$), in degrees Celsius, is empirically expressed in terms of relative humidity and the vapour pressure:

$$T_{dp} = 26.13722 + 16.988833 \ln(\phi P_a) + 1.04961[\ln(\phi P_a)]^2 \tag{3-44c}$$

Where, P_a is the saturated vapour pressure of the air corresponding to T_a.

To calculate the saturation vapour pressure of the air at any temperature the following equation can be used.

$$P = \exp[-8.0929 + 0.97608(T + 42.607)^{0.5}] \quad \text{(3-44d)}$$

$(0<T_{dp}<65^{o}C)$ in Hg.

or

$$P = 3385.5\exp[-8.0929 + 0.97608(T + 42.607)^{0.5}] \quad \text{(3-44e)}$$

$(0<T_{dp}<65^{o}C)$ in N/m^2

Similar to the cooling capacity model discussed above, engineering equation solver (EES) software was used to write a program with which the water consumption rate was predicted. Typical simulation results for wet and free water surfaces with dry bulb temperature input range of 25 – 45 ^{o}C are shown in Figure 3.8a. The model can be applicable to predict the water consumption of a wetted porous ceramic surface for comparison with experimental results.

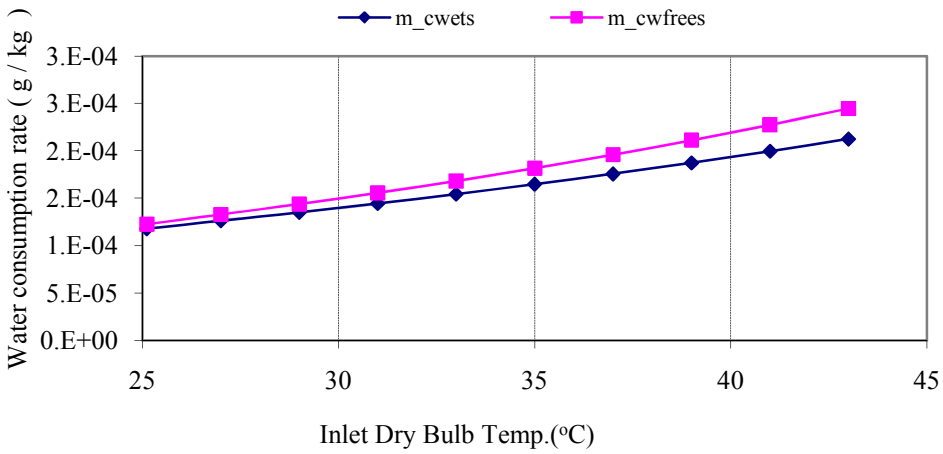

Figure 3.8a Variation of water consumption rates with inlet DBT for both wet and free water surfaces

The variation of the value of water consumption rate in the simulation results obtained with EES using equations (3-44a) and (3-44b) was observed as shown in Figure3.8a. Similarly the same trend was observed under constant relative

humidity as shown in Figure3.8b. This phenomenal behaviour possibly may be due to the different boundary layers of vapour density over the type of surface.

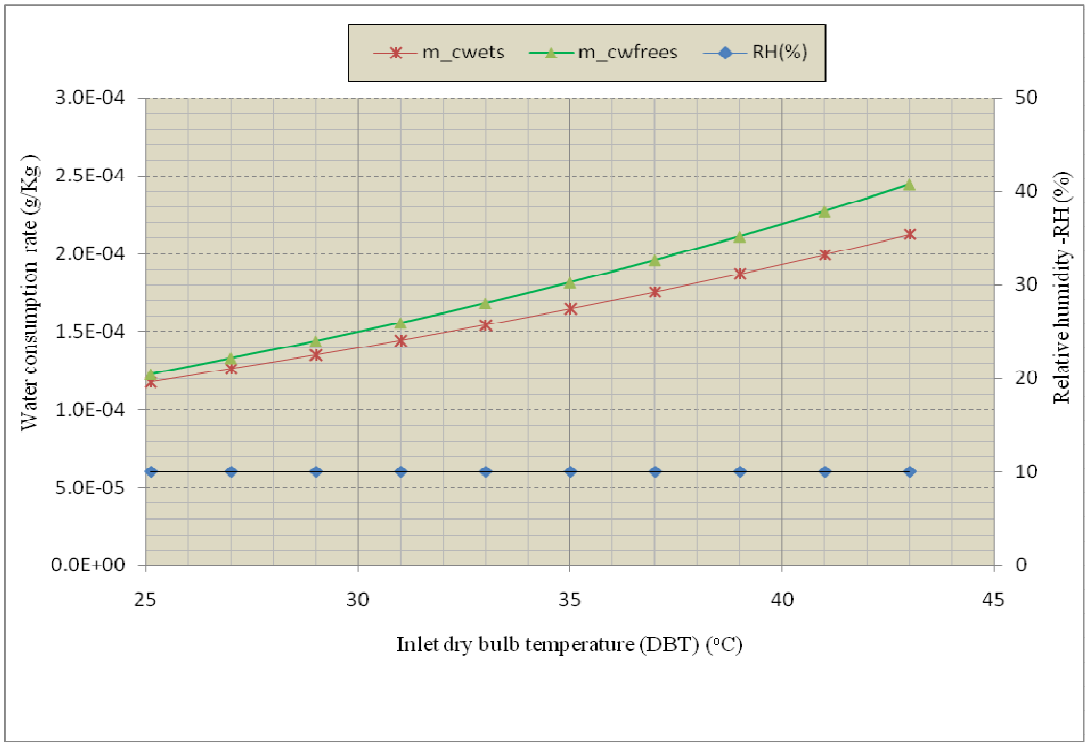

Figure 3.8b Variation of water consumption rates with inlet DBT for both wet and free water surfaces under constant relative humidity condition

The above profiles were obtained based on rough wet towel surface and the exposed free water surface. It was shown that the water evaporation rate or water consumption of the system also depends on the wind speed. It is higher from a wetted surface than that from a free water surface when exposed to very low wind velocity (V<0.5m/s). When the wind speed is high a reversed situation was observed (Tang et al, 2004). Therefore the type of surface and wind speed affects the water evaporation hence water consumption rate of the system.

Also the value conforms to the relations that the exponent n is 0.7 when the evaporation is from a wetted surface and 0.82 when it is from a free small water surface such as pond, etc. (Tang and Etzion, 2004).

3.4.5 System effectiveness

Under ideal situation the lowest temperature which will correspond to ideal system effectiveness of 100% will be equal to the wet bulb temperature corresponding to the inlet dry bulb temperature of the air. This cannot be attained in actual condition as the minimum temperature will be at T_{out} as represented on a psychrometric chart, Figure 3.9.

Generally for a given mass of air subjected to temperature change, the sensible heat transferred is determined by:

$$\delta Q_s = m_a C_p dT \tag{3-45}$$

Where: m_a is the mass flow of air and dT the temperature difference.

But the total humid specific heat capacity of the air –vapour mixture is given as: $C_p = C_{pa} + wC_{pv}$

Equating the rate of sensible heat transfer in terms of temperature change and air flow rate, equation (3-45) to the rate of heat transfer in terms of convective heat transfer coefficient given in equation (3-5 page 65), we respectively have:

$$h_c dA(T_s - T_\infty) = mC_p dT \tag{3-46}$$

The integral form of equation (3-46) above is given below:

$$\frac{h_c}{mC_p}\int_0^A dA = \int_{T_{in}}^{T_{out}} \frac{dT}{(T_s - T_\infty)} \tag{3-47}$$

Integrating the above expression for the entire process considering temperatures at the inlet and outlet, yields:

$$1-\frac{T_{in}-T_{out}}{T_{in}-T_s}=\exp\left[-\frac{h_c A}{mC_p}\right] \tag{3-48}$$

Where $T_s=T_{wb}$ and Cp is the total humid specific heat capacity of the air – vapour mixture ($C_p = C_{pa} + wC_{pv}$).

Since wet bulb temperature (T_{wb}) is the lowest achievable in direct evaporative cooling (DEC), then system effectiveness can be expressed in terms of the wet bulb temperature as shown in the following equation:

$$\varepsilon_{DEC} = \frac{T_{in} - T_{out}}{T_{in} - T_{wb}} \tag{3-49c}$$

However, efficiency or effectiveness correlation for a direct evaporative cooling system have been developed as a function of the air mass flow rate and the packing thickness of the evaporative cooling media of the system (El-Dessouky et al, 2004). The developed correlation whose accuracy is 97.3% is shown in the following expression:

$$\varepsilon_{DEC} = 108.8\ (\frac{\dot{m}_w}{\dot{m}_a})^{-0.077}\,\delta^{0.287} \tag{3-49d}$$

The above correlation is applicable for the following ranges.

$$0.21 \le \frac{\dot{m}_w}{\dot{m}_a} \le 2.09$$

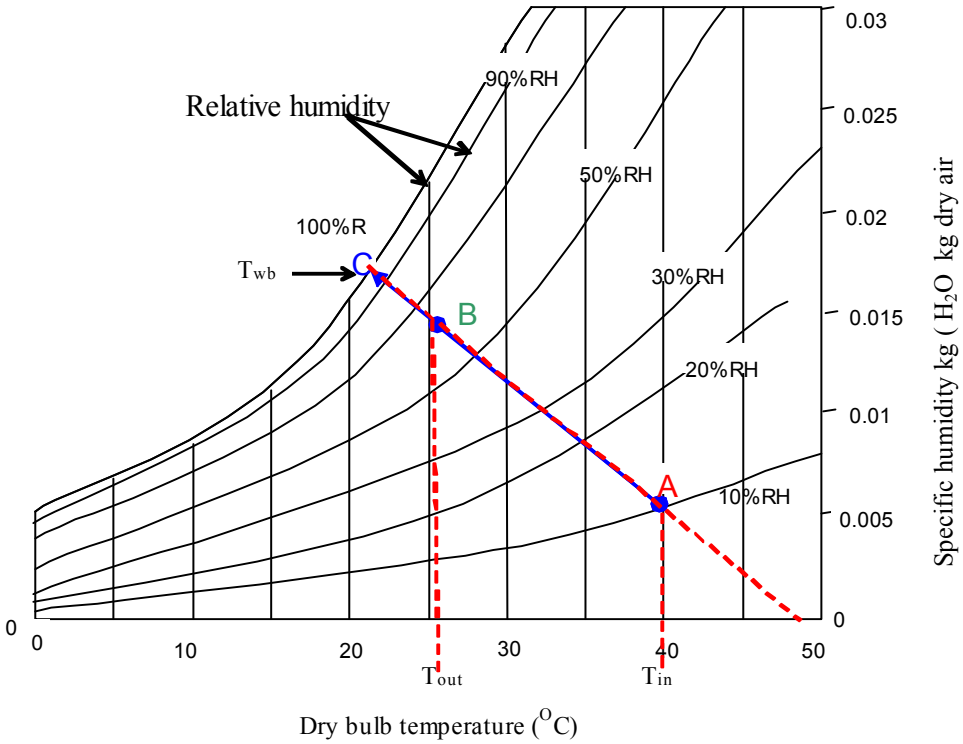

Figure 3.9 Psychrometric representations for temperatures in effectiveness model

3.5 Indirect and Combined Mode Evaporative Cooling Models

In the direct evaporative cooling (DEC) the lower temperature required to be supplied to the building space is always associated with high level of relative humidity which may not be within the acceptable comfort levels. Hence the development of either indirect (IDEC) or combined direct and indirect methods of evaporative cooling (DEC/IDEC). Each should be able to supply cooling air at lower temperature and acceptable levels of relative humidity. In this research study both direct and indirect evaporative cooling methods were investigated. Therefore there is need to have a model for analysing and evaluating the performance of these types. The models developed for the basic psychrometric properties in section 3.3 are applicable to these systems as such only the performance parameters are modelled in this chapter.

3.5.1 Introduction to indirect evaporative cooling process

An indirect evaporative cooler consists of wet side and dry side with wetted impervious layer in between them through which heat transfer takes place. Heat is transferred or extracted from the air contained in the dry side through the layer to the wet side to enhance the water evaporation from the surface of the wet side. The cooled primary air from the dry side is the one to be introduced to a conditioned building space and is often termed as the product or supply air. The secondary air in the wet channel referred to as the process or working air which contained moisture can be channelled out of the conditioned space or passed through desiccant adsorption wheel to remove the moisture.

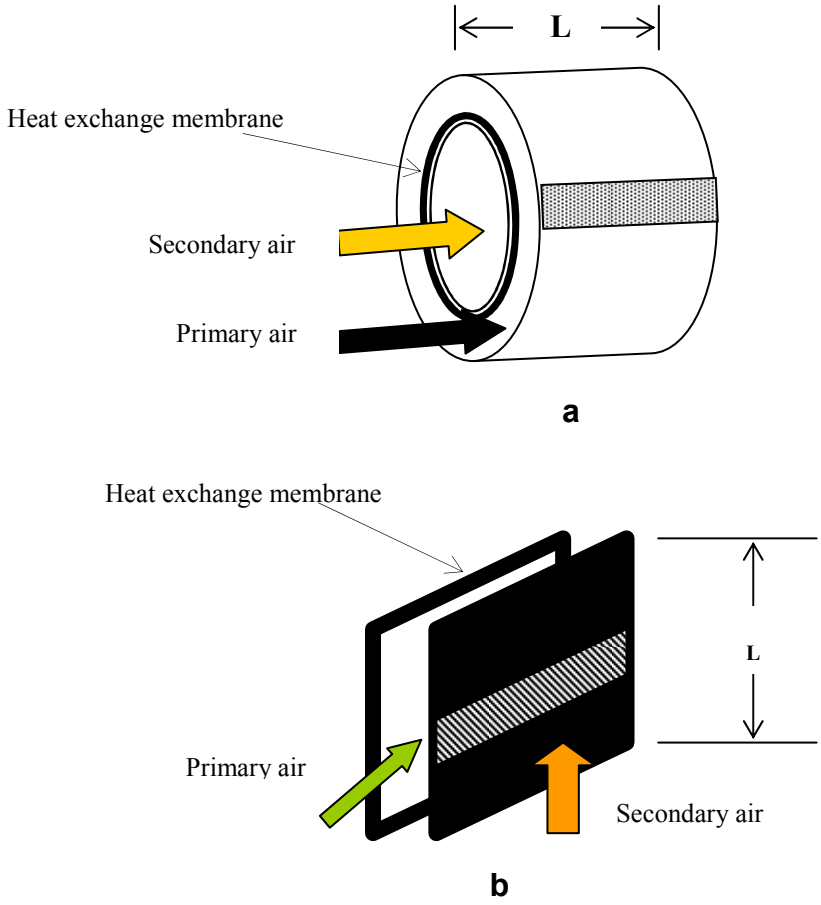

Figure 3.10 Indirect evaporative cooling processes
(**a**-concentric tubes channel type, **b**-flat surface channel type)

The air flow passage can be through gab in between two concentric tubes or flat channels as shown in Figure 3.10a and 3.10b respectively. The air passages are classified as the primary and the secondary air passages for the dry and wet surfaces respectively.

Figure 3.11 is the psychrometric representation of indirect evaporative cooling process employing the wet and dry air flow channels respectively on paths AB'B and AC'C. It shows the ideal and real conditions. Ideally the air temperature in the dry channel could be cooled to the wet bulb temperature of the incoming air. The air in the dry channel however maintains constant specific humidity line. In reality it will not but rather attain the actual value at C'. The actual cooling path is therefore A'B'C' instead of the ideal ABC.

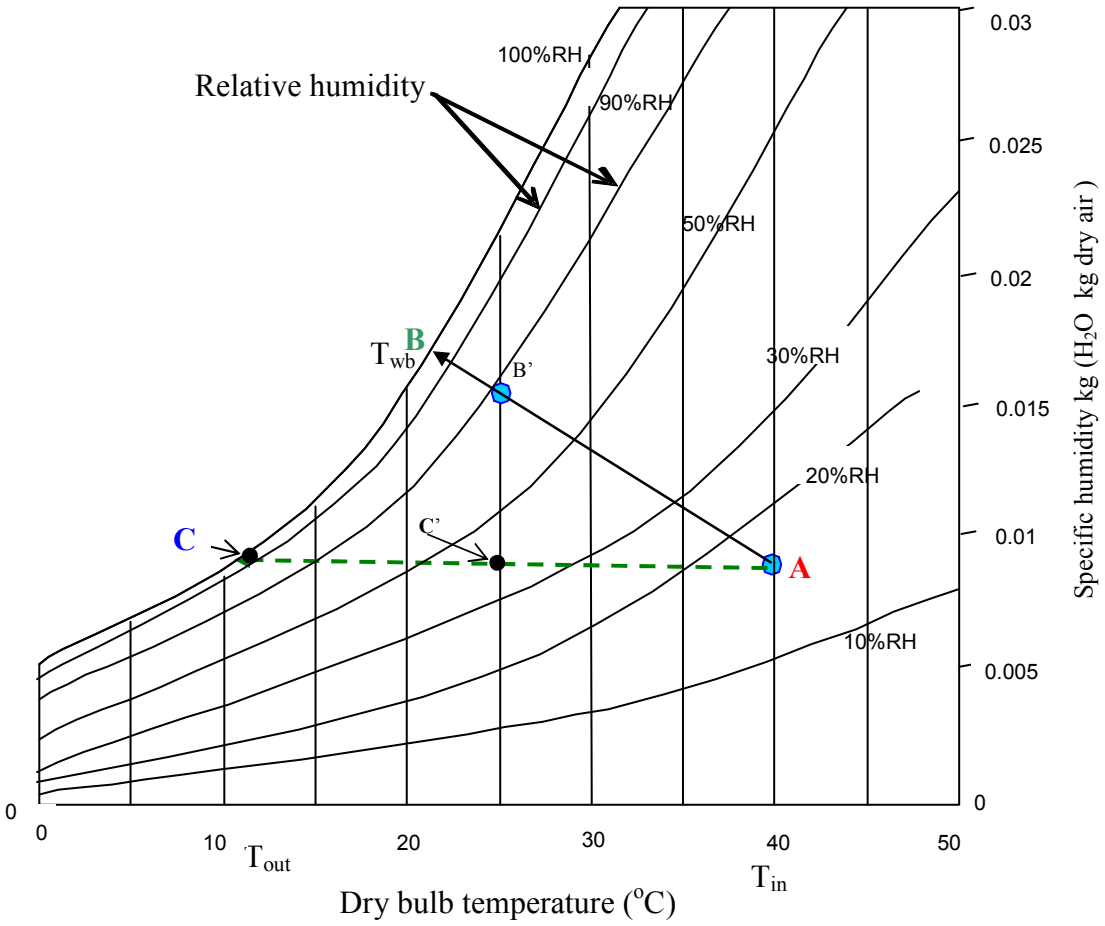

Figure 3.11 Psychrometric cooling process for an indirect evaporative cooling system

3.5.2 Theoretical model for indirect evaporative cooling process

To design, predict the performance of an indirect evaporative cooler and optimise the system an effective heat exchanger is required. Therefore the total heat transfer to the inlet and outlet temperatures of the fluids (air), the overall heat transfer coefficient and the effective surface area must all be related.

The model for an indirect evaporative cooling process was based on the following hypothesis as given by other researchers, (Chongqing, et al 2006):

1. There is no heat transfer between the indirect evaporative cooler and the surroundings. The process is therefore adiabatic.

2. The flow is steady and incompressible and the viscous dispensation is negligible.

3. In each channel or passage the mass flow is constant.

4. The latent heat of vaporisation of water is constant ($\lambda = 2.501$kJ/kg).

5. The water is distributed uniformly over the wet channel and wets the entire surface.

6. The temperature at the air water interface is assumed to be the bulk water temperature.

Considering an indirect evaporative cooler, practically the saturation of the air in the wet channel is not accomplished adiabatically as assumed. In indirect evaporative cooling the process an equilibrium temperature, termed as equivalent temperature (T_{eqv}) develops. It is defined as the temperature that water attains in an indirect evaporative cooler and it enables the total heat flow from the water or to the interface to be determined. This temperature which allows the global indirect evaporative cooling process to be reduced to an adiabatic saturation process replaces that of the water or only the wetted surface, (Alonso et al, 1998).

3.5.2.1 Determination of out let temperature for IDEC

To obtain the outlet temperature of an indirect evaporative cooler (IDEC) the following equation can be applied (Alonso et al., 1998):

$$(T_{wi} - T_{2i^*})h_{wi} + ((T_{2i} - T_{2i^*})h_{2i} = \lambda K_{di}(X_{2i*} - X_{2i}) \quad (3\text{-}50)$$

In indirect evaporative cooling we are dealing with exchange of heat between the wet and dry air streams through a heat exchanger with an infinite surface area. The flow can either be parallel or counter. However, parallel flow is more convenient to operate because initial air intake can be at the same point for both working and product air as shown in Figure 3.12a.The temperature profile along the tube of the heat exchanger in the system is represented in Figure 3.12b.

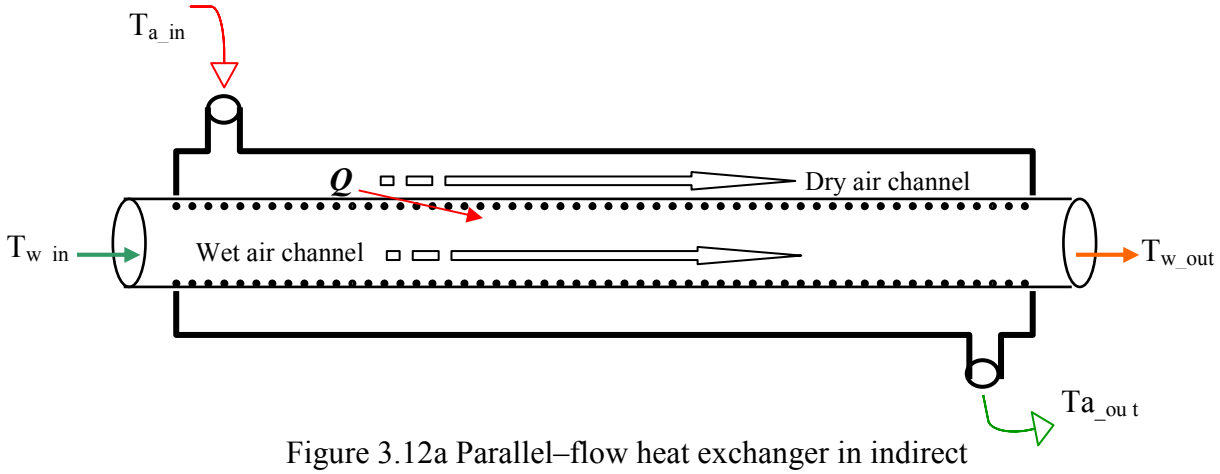

Figure 3.12a Parallel–flow heat exchanger in indirect evaporative cooling system

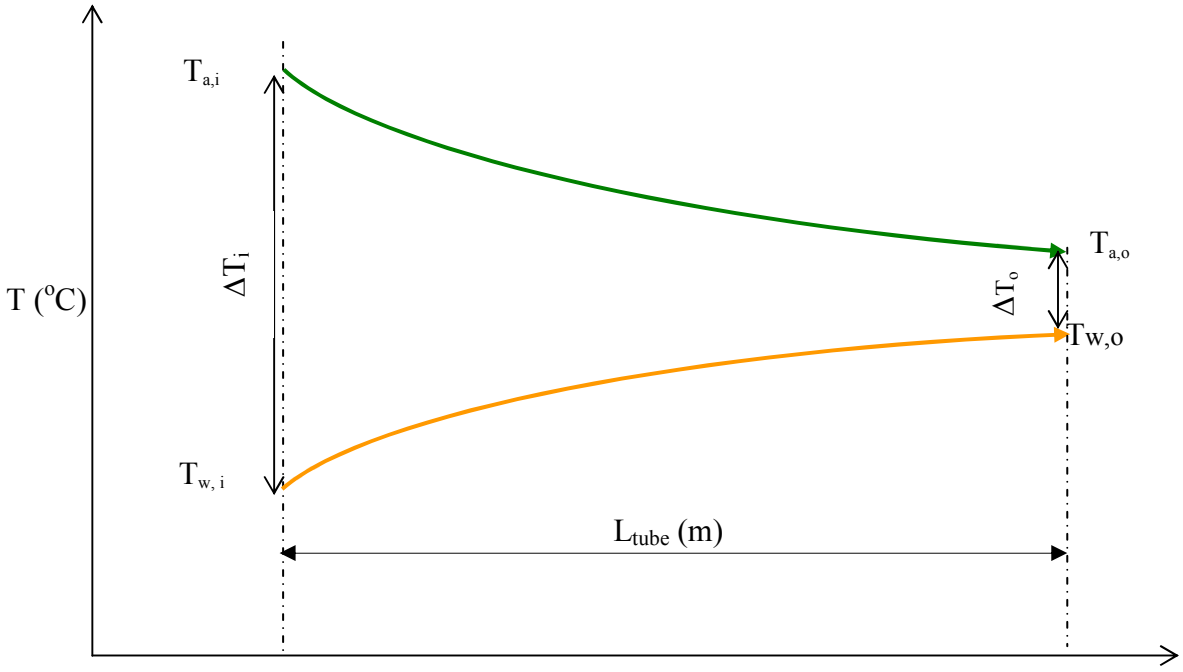

Figure 3.12b Temperature profile of parallel–flow heat exchanger in indirect evaporative cooling system

The performance model for indirect evaporative cooling is described in the following sections.

3.5.2.2 Cooling capacity of indirect evaporative cooling (IDEC)

Also for IEC consisting of wet and dry air channels the cooling capacity can be evaluated from the following simplified energy balance equation.

$$Q_{iec} = Q_w = Q_a \qquad (3\text{-}51)$$

The above energy balance can be return in terms of the respective enthalpies of air flowing through wet and dry channels as follows:

$$Q_{iec} = \dot{m}_w \left(h_{wi} - h_{wo} \right) = \dot{m}_a \left(h_{ao} - h_{ai} \right) \qquad (3\text{-}52)$$

Where in the expression ‘h’ refers to enthalpy and not heat transfer coefficient.

By considering the specific heat capacities the energy balance equation becomes:

$$Q_{iec} = \dot{m}_w Cp_w (T_{w,in} - T_{w,out}) = \dot{m}_a Cp_a (T_{a,in} - T_{a,out}) \quad (3\text{-}53)$$

Relating equations (4.3) to (4.5) we have:

$$Q_w = \dot{m}_w Cp_w (T_{w,in} - T_{w,out}) \quad (3\text{-}54)$$

$$Q_a = \dot{m}_a C p_a (T_{a,in} - T_{a,out}) \quad (3\text{-}55)$$

For the exchange of heat between the wet and dry channels the temperature difference at a given location can be expressed as:

$$\Delta T = T_w - T_a \quad (3\text{-}56)$$

Since heat transfer involved varies along the entire surface area of the heat transfer layer separating the dry and wet channels we then require the mean temperature difference, ΔT_m .The cooling capacity or thermal load can therefore be expressed in terms of the effective heat transfer area, overall heat transfer coefficient and the mean temperature difference. The relationship is shown below for a parallel flow heat exchanger.

$$Q_{iec} = A \times U \times \Delta T_m \quad (3\text{-}57)$$

Where, ΔT_m is the appropriate 'mean temperature difference' and will be defined as the 'log mean temperature difference (LMTD)'.Therefore equation (4-9) becomes:

$$Q_{iec} = A \times U \times LMTD \quad (3\text{-}58)$$

When the air flow along the dry and wet channels is a counter flow, then the LMTD in equation 3.58 is defined as:

$$LMTD = \frac{T_{a,in} - T_{a,out}}{\ln\left[\frac{R}{R + \ln(1 - RP)}\right]} \quad (3\text{-}59a)$$

R and P in the above equations are given as:

$$R = \frac{T_{w,in} - T_{w,out}}{T_{a,in} - T_{a,out}} \quad (3\text{-}59b)$$

$$p = \frac{T_{a,in} - T_{a,out}}{T_{a,in} - T_{wb}} \quad (3\text{-}59c)$$

The overall heat transfer coefficient, U, in equation (3-57) is defined by the following relation**:**

$$\frac{1}{U} = \frac{1}{h_{cw}}\frac{A_o}{A_i} + R_{fw}\frac{A_o}{A_i} + \frac{A_o\delta}{A_i\lambda}R_{fa}\frac{1}{h_{ca}} \quad (3\text{-}60)$$

The waterside or wet side heat transfer coefficient contained in the above equation is obtained from the Dittus- Bolter equation given below:

$$h_{cw} = 0.023(\mathrm{Re}_w)^{0.8}(\mathrm{Pr}_w)^{0.4}\left(\frac{\lambda_w}{d}\right) \quad (3\text{-}61)$$

In the above equation the Reynolds number is defined as

$$\mathrm{Re_w} = (\rho_w v_w d)/\mu_w \quad (3\text{-}62a)$$

And the Prandtl number is defined as follows:

$$\mathrm{Pr_w} = (\rho_w Cp_w)/\mu_w \quad (3\text{-}63b)$$

3.5.2.3 System effectiveness / efficiency

The system effectiveness (Maisotsenko) or efficiency can be evaluated by applying the following expression:

$$\eta_{cooling} = \frac{T_{s,in} - T_{s,out}}{T_{s,in} - T_{wb}} \quad (3\text{-}64)$$

However, indirect evaporative cooling system efficiency correlation (ε_{IEC}) is given in the following expression (El-Dessouky et al, 2004):

$$\varepsilon_{IEC} = 1.0819A^{0.185}(\mathrm{Re}_w)^{0.0181}(\mathrm{Re}_a)^{0.254} \quad (3\text{-}65)$$

Where:

A - effective heat transfer area of the heat exchangers of the indirect evaporative cooler (m^2)

Re_w and Re_a represent the Reynolds number for the water and air flowing through the wet and dry channels of the indirect evaporative cooler respectively. These dimensionless numbers are defined in the following expressions:

$$Re_w = \frac{(\rho_w v_w d)}{\mu_w} \tag{3-66a}$$

and

$$Re_a = \frac{(\rho_a v_a d)}{\mu_a} \tag{3-66b}$$

From the above relation it can be observed that the effectiveness or efficiency of indirect evaporative cooler depends on the Reynolds number of the flowing fluid as well as the effective heat transfer area of the heat exchanger. For our own case the water flow rate is negligible when compared with the air flow rate because the water only wets the surface of the wet flow channel. So air is our main medium of heat.

3.5.2.4 COP of the system

The coefficient of performance (COP) is defined as:

COP = cooling capacity /input power

That is:

COP = cooling capacity / (fan power + pump power)

For eliminating the use of pump the COP becomes:

COP = cooling capacity / fan power.

3.5.3 Combined indirect/direct evaporative cooling system ($\varepsilon_{IDEC/DEC}$):

For the combined indirect/direct evaporative cooling system, efficiency correlation is based on the heat transfer area of the IEC heat exchanger part, the Reynolds numbers for water and air inside and outside IEC heat exchange tubes, the thickness or parking density of the DEC and mass flow rate of water and air in the DEC parking as given below (El-Dessouky et al, 2004):

$$\varepsilon_{IEC}/\varepsilon_{DEC} = 0.95A^{0.743}(Re_w)^{-0.112}(Re_a)^{0.247} \quad (3\text{-}67)$$

3.5.4 Regenerative evaporative coolers

In the case of series of regenerative evaporative coolers the lowest theoretical air temperature that can be obtained is the dew point temperature corresponding to the ambient. Under this situation the efficiency is defined in the expression shown below (Erens and Dreyer, 1991):

$$\eta_{sat,dp} = \frac{T_{db,in} - T_{db,out}}{T_{db,in} - T_{dp,in}} \quad (3\text{-}68)$$

Where $T_{dp} = T_{dew\ point}$

3.6 IDEC heat exchanger design considerations

In the performance analysis of the indirect evaporative cooling system having heat exchanger the LMTD described above can be used and is the easiest method when inlet and outlet temperatures of the fluid which in this case is air are known. That is given the type of fluid, temperatures and specified flow rates the LMTD method can be applied to size the heat transfer effective surface area (A) of the system. This will include the tube diameter; length and

the number of tubes. If the heat exchanger dimensions of the IDEC system are given while the cooling capacity and the outlet temperatures are desired, then the performance calculation will be performed using a different method.

The easier method in this case is the 'Number of Transfer Units' (NTU) effectiveness method because using LMTD method will require iterations. The 'Number of Transfer Units' (NTU) is a dimensionless parameter and is defined in the following expression:

$$NTU = \frac{UA_a}{m_a Cp_a} \tag{3-69}$$

For moist air the specific heat capacity contained in the above equation (3-69) is defined as (Cp_{ma}) in the following expression:

$$Cp_{ma} = \mathrm{Cp_a} + w_a Cp_v [kJ/kg^oC] \tag{3-70}$$

The simplified model for obtaining indirect evaporative cooler performance based on NTU method was developed, (Chengqin and Hongxing, 2006) and the simplified model for determining the indirect evaporative cooler performance developed by Erens and Dreyer (1993).

The following relations can be used to determine cooler area corresponding to a required cooling load.

$$\mathrm{A_o} = \frac{\mathrm{m_a}}{\mathrm{h_D}} \ln\left(\frac{\mathrm{i_{asw} - i_{ai}}}{\mathrm{i_{asw} - i_{ao}}}\right) \tag{3-71}$$

The surface area can be expressed in terms of overall heat transfer coefficient as shown below:

$$\mathrm{A_o} = \frac{\mathrm{m_p C_{pp}}}{\mathrm{U_o}} \ln\left(\frac{\mathrm{T_{pi} - T_{wm}}}{\mathrm{T_{po} - T_{wm}}}\right) \tag{3-72}$$

The value of overall heat transfer coefficient U_o [Wm-2K-1] contained in equation (3-72) can be calculated from the equation given below:

$$U_o = \left(\frac{1}{h_p} + \frac{t_p}{k_p} + \frac{1}{h_w} \right)^{-1} \quad (3\text{-}73)$$

Similarly from equations (3-71) and (3-72) it is shown that:

$$i_{ao} = i_{asw} - (i_{asw} - i_{ai}) e^{-NTU_a} \quad (3\text{-}74)$$

and

$$T_{po} = T_{wm} + (T_{pi} - T_{wm}) e^{-NTU_p} \quad (3\text{-}75)$$

Where the $NTU_p = \frac{A_o U_o}{m_p C_{pp}}$ and $NTU_a = \frac{A_o h_D}{m_a}$

The value of T_{wm} that can be applied in equations to calculate the outlet conditions can be iteratively obtained by using the following expression, (Erens and Dreyer, 1993):

$$T_{wm} = T_{pi} - \frac{m_a (i_{asw} - i_{ai})(1 - e^{-NTU_a})}{m_{cpp} (1 - e^{-NTU_p})} \quad (3\text{-}75)$$

Detailed correlations applicable for the determination of heat and mass transfer coefficients as well as non dimensional associated relations are given in literature (Liao and Chiu,2002; Kloppers and Kroger,2005; RenandYang, 2006; Bilal and Zubair,2006; Heidarinejad et al.,2008).

3.7 Summary

In this chapter the basic heat transfer governing equations involved during evaporative cooling process has been discussed and theoretically modelled. The important parameters which consist of temperatures, specific and relative

humidity, density, enthalpy, specific heat capacities and other basic psychrometric parameters which are always required in the performance evaluation of any evaporative cooling system were modelled.

In addition to the general parameters, performance evaluation model for direct evaporative cooling system was presented. This allows for proper analysis and the system performance evaluation.

Also reviews on theoretical relations for indirect evaporative cooling process have been presented in this chapter. These consist of procedures for performing the system analysis based on the heat exchanger performance analysis models. The performance models considered procedures which can be applied. These are the Log Mean Temperature Difference method (LMTD) and the effectiveness - Number of Transfer Units (NTU) methods. The LMTD method can be used when the inlet and outlet temperatures of the dry and wet air channels are given or determined from the energy balance. However if the type and size of the systems heat exchanger are given then NTU performance calculation method can be employed to determine the cooling capacity and outlet temperatures of the system.

CHAPTER 4

Investigations on Porous Ceramic Direct Evaporative Cooling Systems *(supporting-frame and stacking configurations)*

4.1 Introduction

In this chapter experimental investigations on porous ceramic evaporators were carried out. The experimental tests were based on the high porosity ceramic evaporators identified to consistently perform better in comparison with the low and medium porosity prototypes (Ibrahim et al, 2003).The work here allowed extended investigations on the porous ceramic based evaporators and comparison of the experimental performance with some empirical model predictions discussed in chapter 3. These give more bases for the choice of porous ceramics for evaporative cooling applications in buildings. The desire is to have system operating at low cost, energy and water consumption accompanied with use of simple technology based on new materials and methods.

4.2 System Description

The porous ceramic evaporators for these experiments were all closed - hollow rectangular units. They were selected to suite the “hanging” or “supporting frame” and “stacking” tests configurations. While the supporting frame set-up consists of individual units of ceramic evaporators the stacking configurations was formed by assembling two units of different geometric dimensions. Descriptions of the prototypes used for the experiments are discussed in the following sections.

4.2.1 The supporting-frame ceramic evaporators' experimental units

For the supporting frame the porous ceramic evaporators were supported by aluminium frame making five rows of 10 ceramic evaporators spaced 70mm apart. Each rectangular ceramic unit has 400mmx200mmx35mm volume and a nominal wall thickness of 5mm as shown in Figure 4.1a. Figure 4.1b is the photograph of the unit. The configuration is termed as the supporting frame because the porous ceramic evaporators were supported on aluminium supporting frames as illustrated in Figure 4.1c.The entire frame structure is then covered with ply wood to make a chamber. The chamber can be attached to the building with a provision of air inlet and outlet. The inlet should be from the ambient while the out let should be directly to the building interior. Figure 4.1d shows the set up photographs and the data measuring sensors tree. The data taker provided with channels expansion modules to accommodate more sensors was used as in Figure 4e. Figure 4.1f shows the drip water supply tube to evaporators.

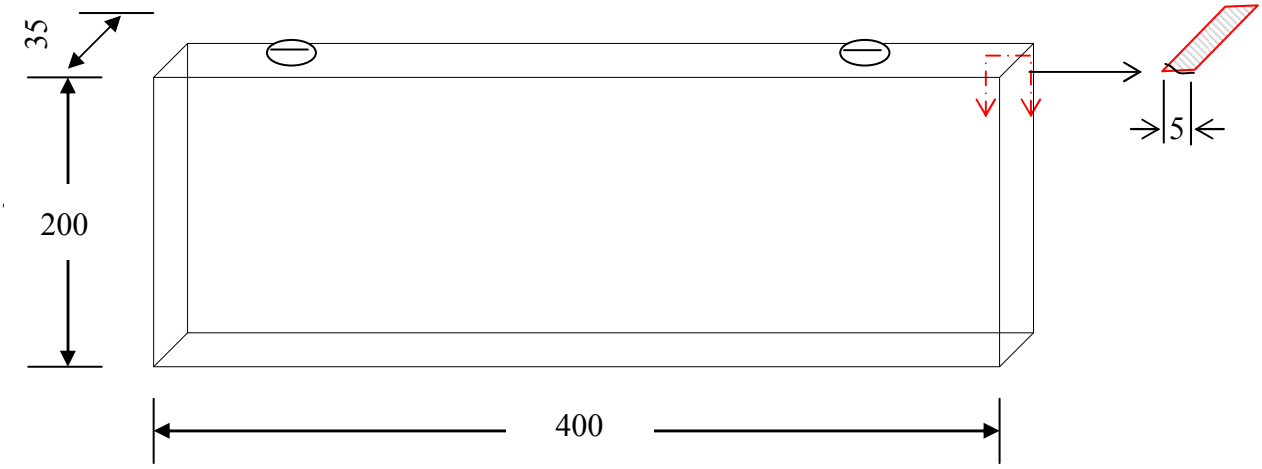

Figure 4.1a Geometric dimensions of a porous ceramic evaporator for hanging option (dimensions in mm)

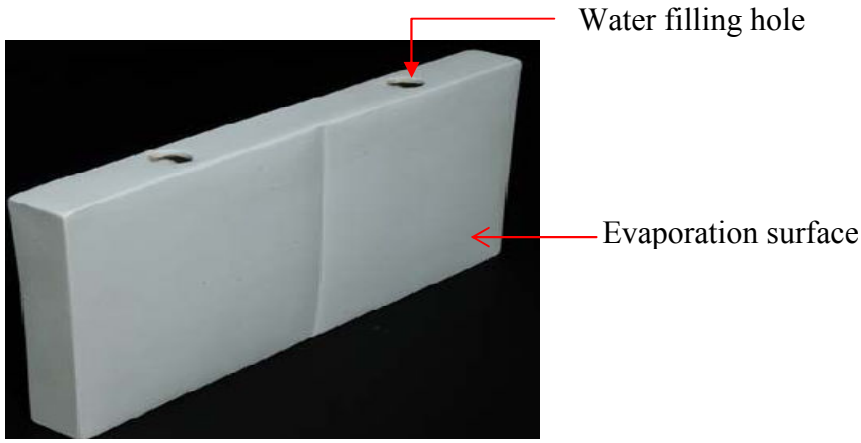

Figure 4.1b Photograph of a porous ceramic evaporator
for 'hanging tests' set-up

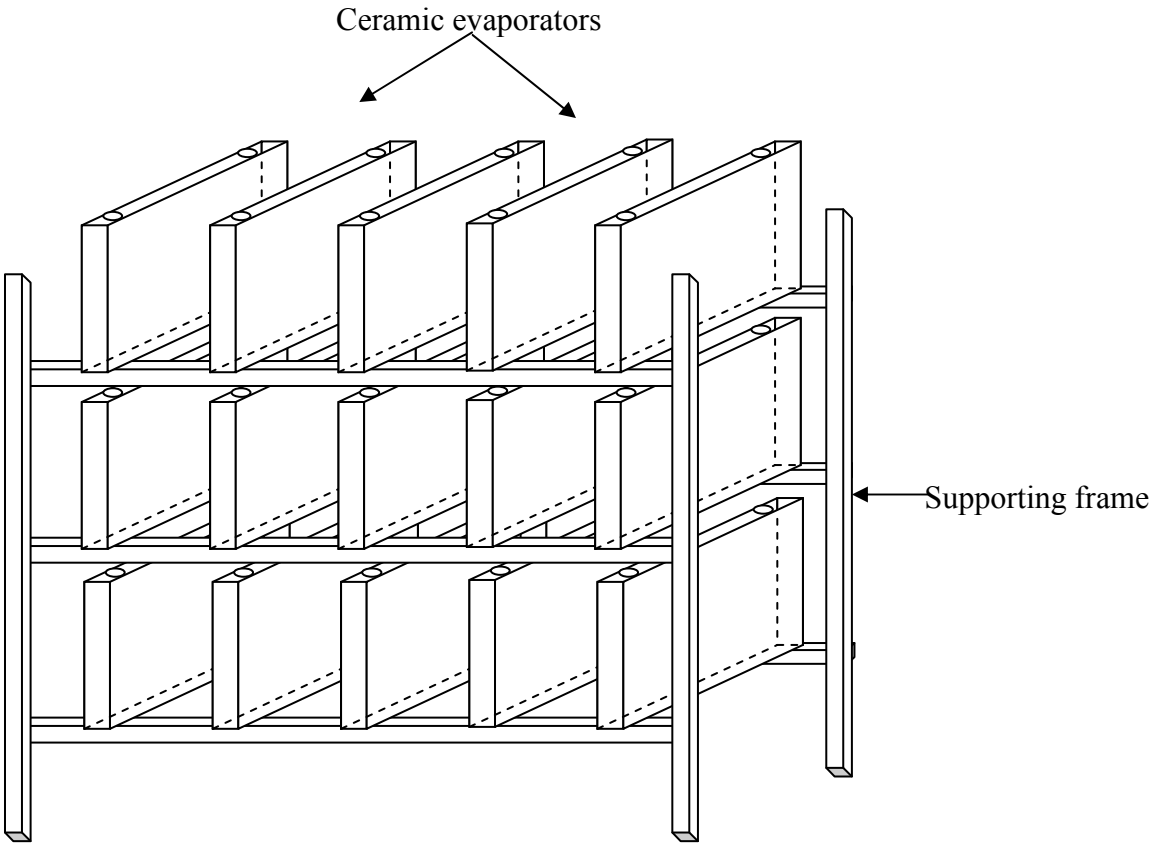

Figure 4.1c Supporting frame system configuration

Figure 4.1d Supporting frame system configuration and measurements set up

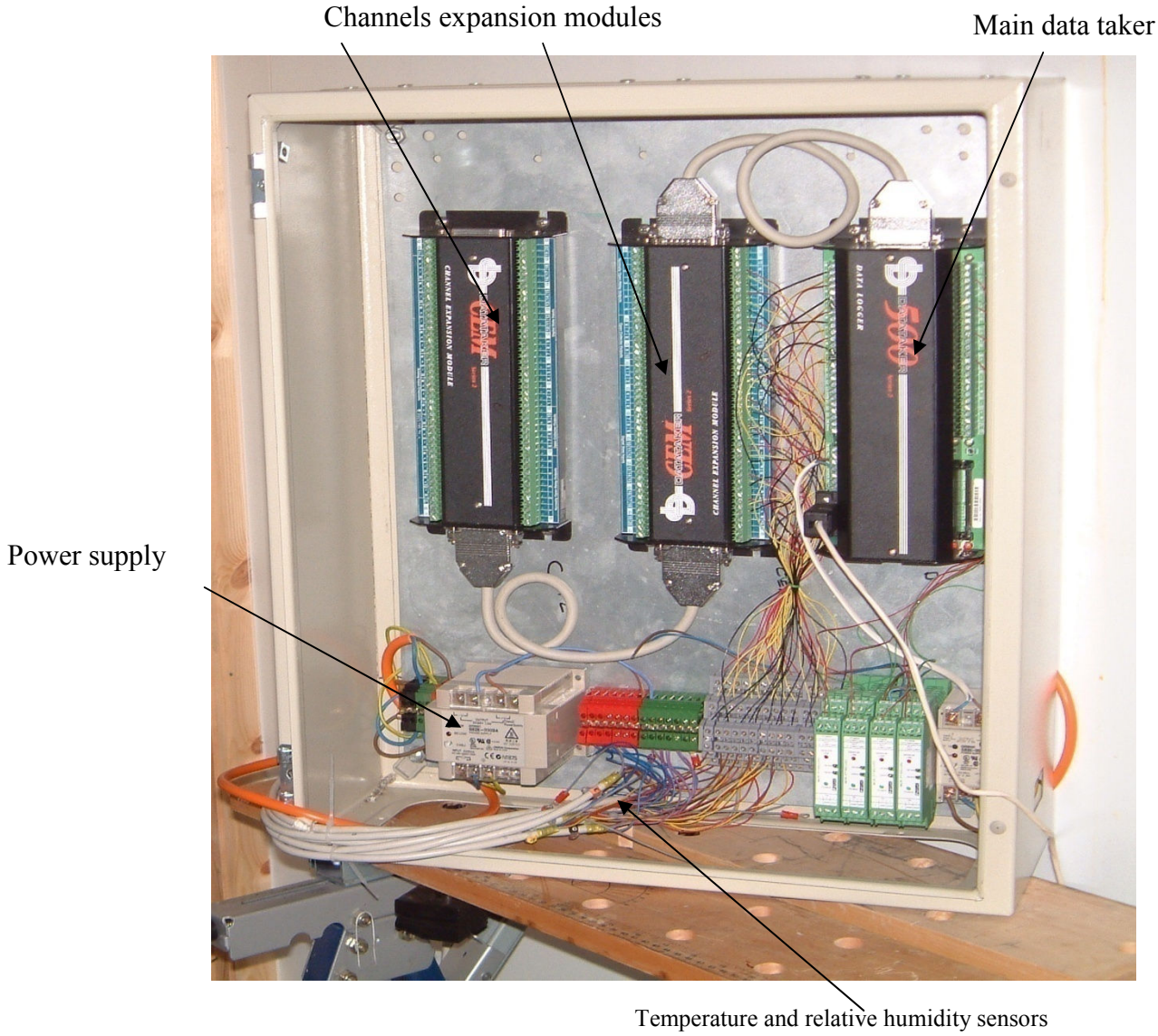

Figure 4.1e Data taker with channels expansion modules set up

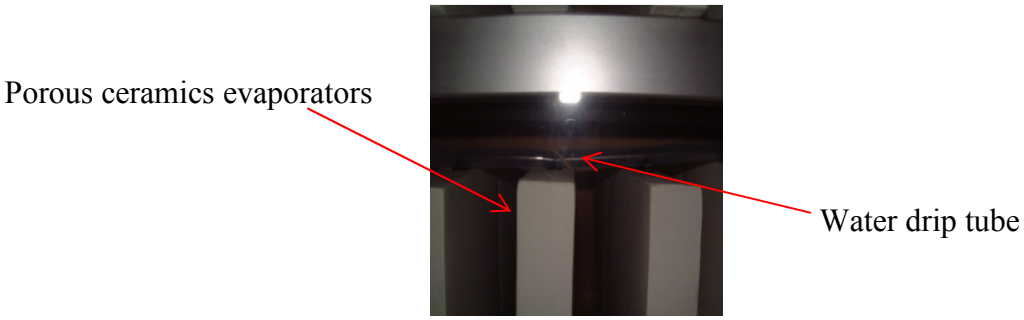

Figure 4.1f Drip water supply arrangement for filling the porous ceramics

4.2.2 The stacking ceramic evaporator's experimental units

The "stacking" option consists of two types of rectangular closed hollow porous ceramic evaporators. The first type has a volumetric dimension of 410mmx210mmx80mm while the second type has 145mmx210x80mm, length x height x width, respectively. For each the nominal wall thickness was 5mm.Figure 4.2a shows the schematic drawing of the ceramic units. Figures 4.2b and 4.2c shows the photographs of the units' front and back evaporative surfaces respectively. Figure 4.2d shows how the individual units can be stacked for assembly in the evaporative cooling chamber and Figure 4.2e shows the photograph of the same process. After stacking the the assembled structure stands in a condensate tank with the top opening for water feeding as in Figure 4.2f which shows both the front and back evaporative cooling surfaces of the system.

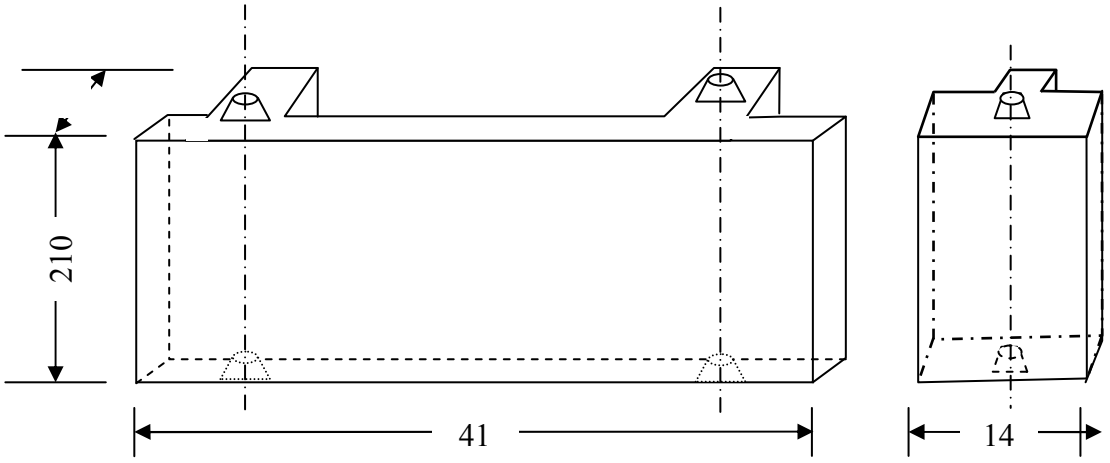

Figure 4.2a Schematic diagram of ceramic evaporators for wall or stacking test configuration

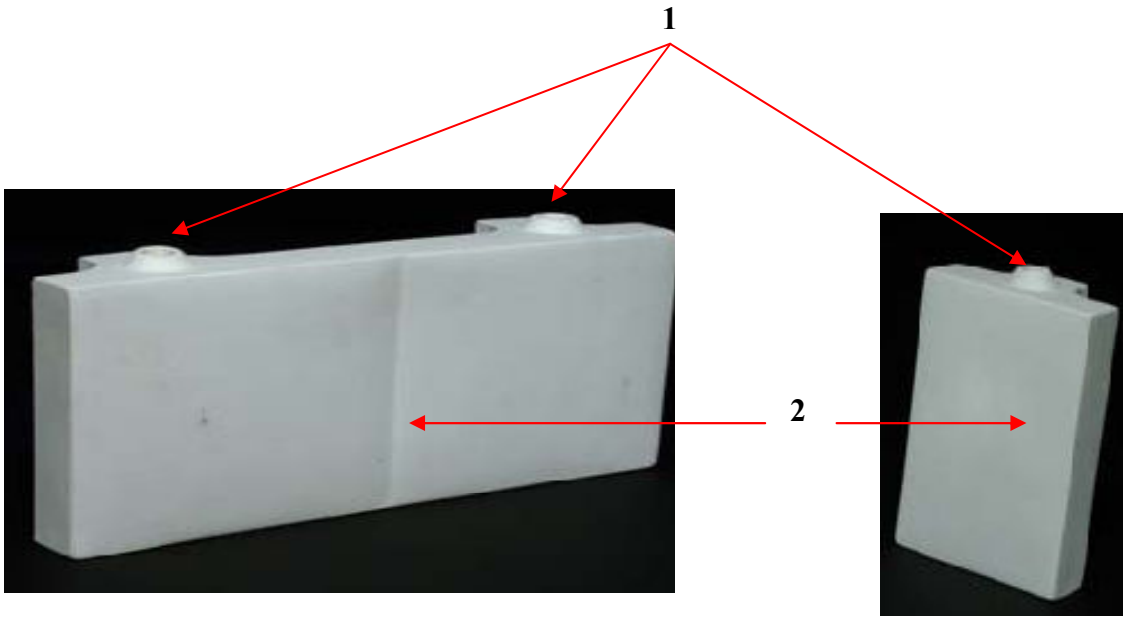

Figure 4.2b Photograph of ceramic evaporators for stacking test configuration front surface area (1-water feeling holes, 2-evaporation surface)

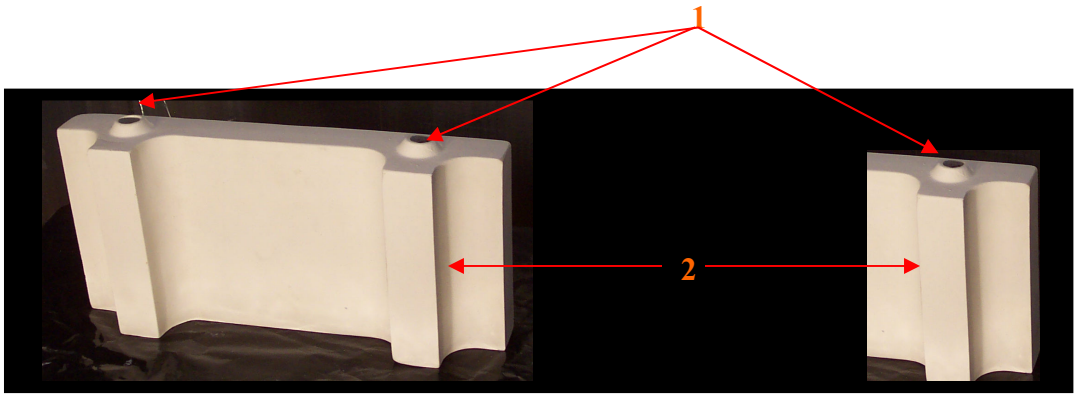

Figure 4.2c Photograph of ceramic evaporators for wall or stacking test configuration back surface area (1-holes, 2-evaporation surface)

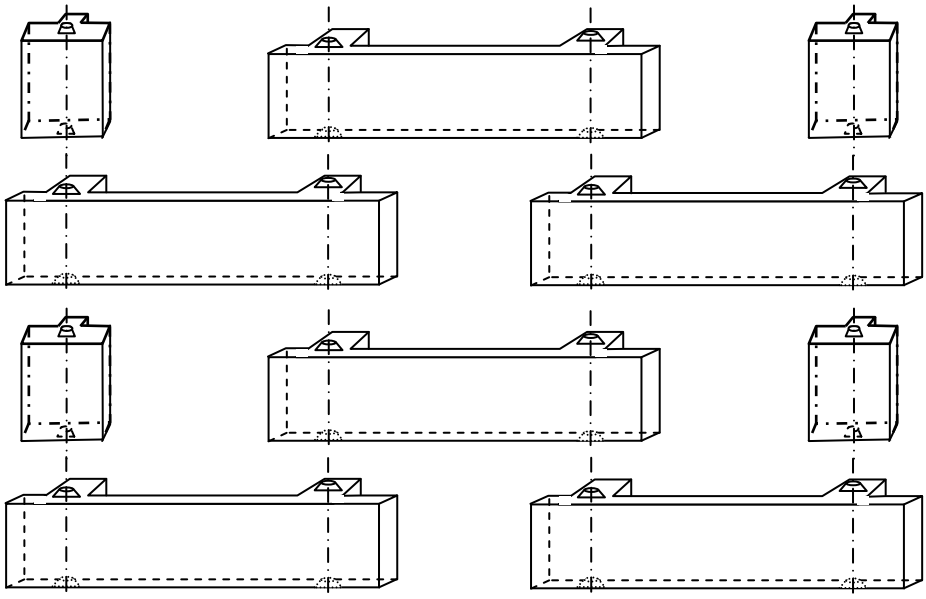

Figure 4.2d assembling individual units for the stacking system experiment

Figure 4.2e Process of assembling individual units for the stacking system experiment

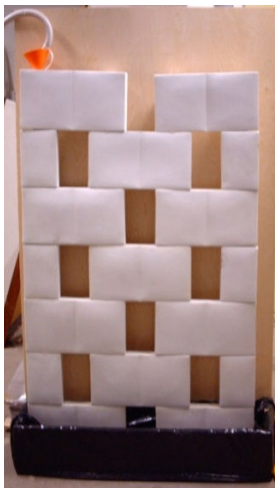

Front surface

Back surface

Figure 4.2f The front and back evaporative cooling surfaces of the stacked system in condensate tank

4.3 Experimental Procedure

Experiments for the performance evaluations were conducted in an environment control chamber. The chamber was partitioned to create an indoor and outdoor space conditions as shown in Figure 4.3. To prevent heat exchange between the indoor and outdoor spaces the barrier between the two was made with a thermal insulation material. The indoor has a space volume of 3m width x 2m length x 2.1m height. A rectangular chamber containing porous ceramic evaporators was installed along the partition. Air coming from the outdoor condition passes through the ceramics chamber and then to the indoor space where the cooling effect would be required. Outdoor air temperature and relative humidity were simulated with the help of the environmental chamber controls and then passed to the evaporative cooling chamber as inlet conditions. Corresponding changes were monitored in the indoor space.

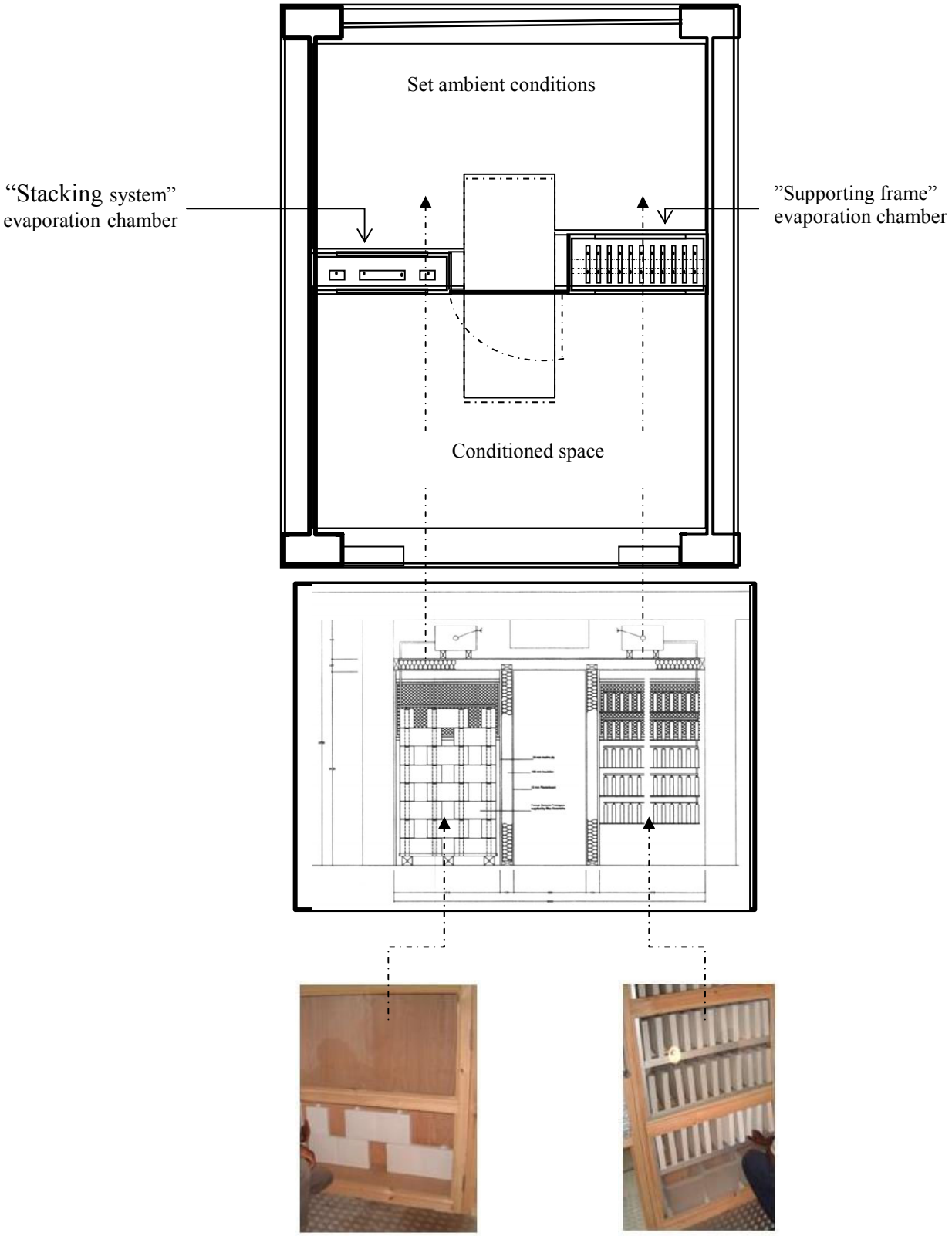

Figure 4.3 Plan and front elevation of the experimental set-up and the assembly of the porous ceramic evaporators units

Air temperatures and relative humidity (RH) were monitored for both inlet and outlet using VAISALA HMP45A relative humidity and temperature probes. Each probe has measurement range of -50^{O}C to + 50^{O}C, accuracy of ±0.2K and 0 to 100%, accuracy of ±2%, for temperature and RH respectively. Type T thermocouple temperature sensors were used for the water contained in the ceramic cooler and at different points on their surfaces. Air volume flow rate was measured using an orifice plate meter.

Experimental data acquisition and logging was carried out using DT500 data taker and expansion modules to accommodate enough temperature and relative humidity sensors. These instruments are shown in Figure 4.4(a, b and c).

Different wall and roof integration options and how outside ambient air can be cooled through the porous ceramics and then be delivered to a room space can be used. For this experiment wall integrated option was adopted. Several porous ceramic evaporators were arranged in a duct which has an inlet and out let air path connecting the ambient and the inside of a building space. Finally the humid air can be exhausted out of the room. The general air flow pattern across the porous ceramic evaporators was in accordance with the system integration in to building as illustrated in Figure 4.5. Different values of air temperatures and relative humidity were set at inlet and corresponding outlet values were recorded after passing through the evaporative cooling chamber. Each set was tested in the same environment chamber partitioned to simulate and provide inlet temperature and relative humidity values. Technical specifications of the sensors with the data taking and logging programme are respectively shown in appendices AIIa and AIIb.

Figure 4.4 Tests measuring instruments:
a-DT500 data taker.
b-Vaisala HMP45A relative humidity and temperature sensor
c-PT100 temperature sensor.

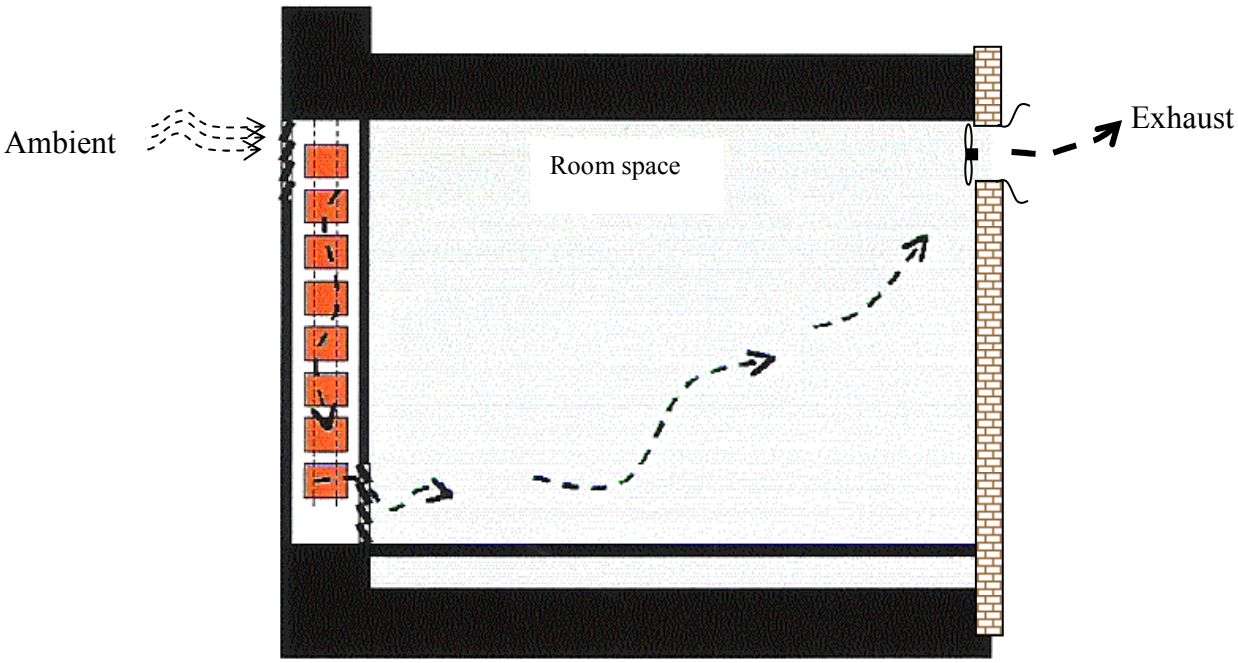

Figure 4.5 Diagram of Inlet and outlet air flow pattern through the wall integrated experimental evaporation chamber containing

4.4 Test Results and Performance Analysis on each System

Experimental performance tests were conducted to analyse different parameters that are crucial in evaluating the performance of evaporative cooling process. Typical test results at different values of inlet temperature, relative humidity and corresponding outlet conditions were recorded. At the same time effect of different air flow rates were investigated. Based on these results the following parameters were calculated using appropriate theoretical expressions as discussed in chapter 3.

- Temperature drop across the system.

-Relative humidity increase.

-Cooling capacity of the system.

- Water consumption.

-Effectiveness of the system

4.4.1 "Stacked-wall" system configuration results and discussions

The stacked wall system configuration consists of the porous evaporators stacked one on top of the other in an evaporation chamber as shown in Figure4.6. Test runs were conducted by setting the environment chamber allowing experiments at different but constant inlet conditions consisting of constant inlet temperatures, relative humidity values and air flow rates.

Also prior to attaining steady state, instantaneous ambient air inlet parameters were monitored with corresponding outlet values. This is a representation of

the actual behaviour of the environmental situation where the ambient temperature, relative humidity and wind speed continue to vary with time.

Corresponding outlet values obtained from the tests are shown in Table 5.1. The air volume flow rate was 140m^3/hr. It was measured using Sulzer AG orifice plate meter having a measuring range of 50 to 430m^3/h and an accuracy of ±5m^3/h. The probe was installed within the exhaust air duct from the conditioned room. The air flow was control by regulation the speed of the air circulation fan moving the air from the evaporative cooling chamber across the room and then expelled out from the room.

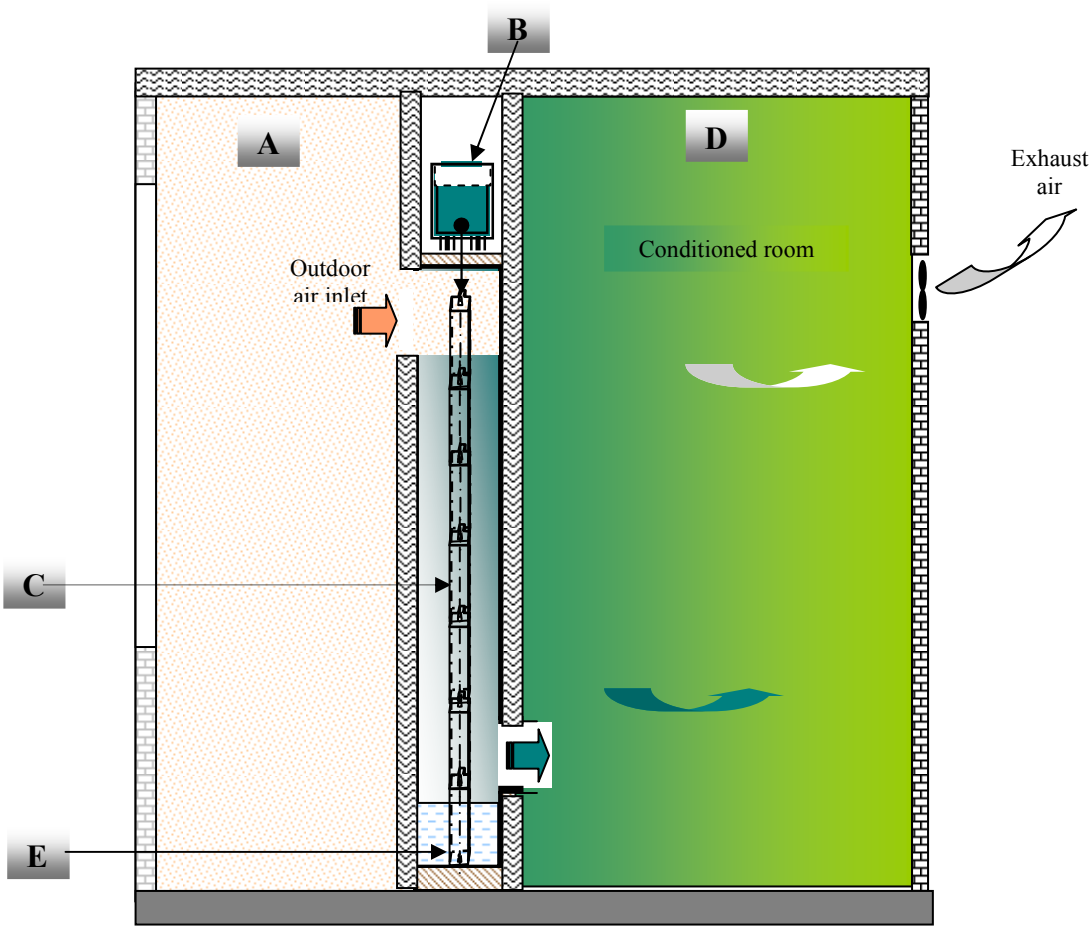

Figure 4.6 Stacking system configurations [A-environmental chamber set conditions, B-water supply tank to porous ceramics, C-stacked evaporators in evaporation chamber, D-room space cooled

Table 4.1 Experimental data for different air temperature and relative humidity values for stacking wall system configuration

DBT_{in} (^oC)	DBT_{out} (^oC)	RH_{in} (%)	RH_{out} (%)
25.9	24.4	46.5	59.9
26.0	24.3	46.9	60.0
27.0	24.3	47.3	60.1
31.5	25.6	34.4	51.7
32.0	27.1	35.8	52.7
34.0	27.5	35.1	53.4
36.0	30.3	38.7	57.1
38.0	30.8	35.5	55.2
40.0	33.6	37.9	56.5
42.0	33.9	36.9	56.9
43.8	34.6	33.9	57.0

4.4.1.1 Inlet and outlet temperature profiles

The temperature drop across the ceramics evaporative cooling chamber was observed. First instantaneous values were recorded before the steady state tests in the environmental control chamber. Figure 4.7a shows the instantaneous variation of the inlet and outlet temperature values with time. The difference between the two is also plotted to indicate the respective temperature drop at each instance. This is shown as ΔTdb_out in the chart. The temperature drop increased with increasing inlet or ambient air temperature. For inlet temperature range of 25.9^{o}C – 43.8^{o}C a drop of 1.5^{o}C – 9.2^{o}C was recorded with the highest value corresponding to the maximum inlet temperature. The

temperature drop profile representing the differences between inlet and outlet values is also shown on the same graph. It represents the difference between the inlet and outlet values.

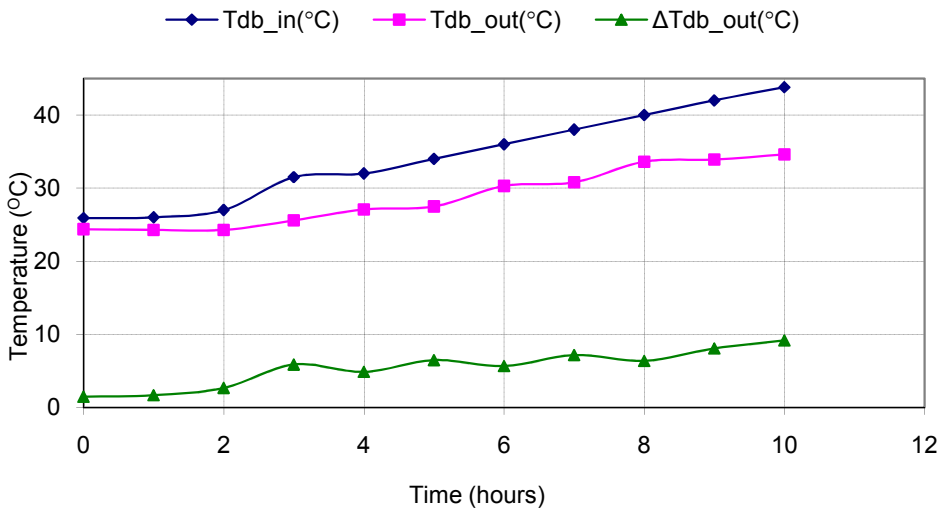

Figure 4.7a Inlet and outlet dry bulb temperatures variation with time (instantaneous)

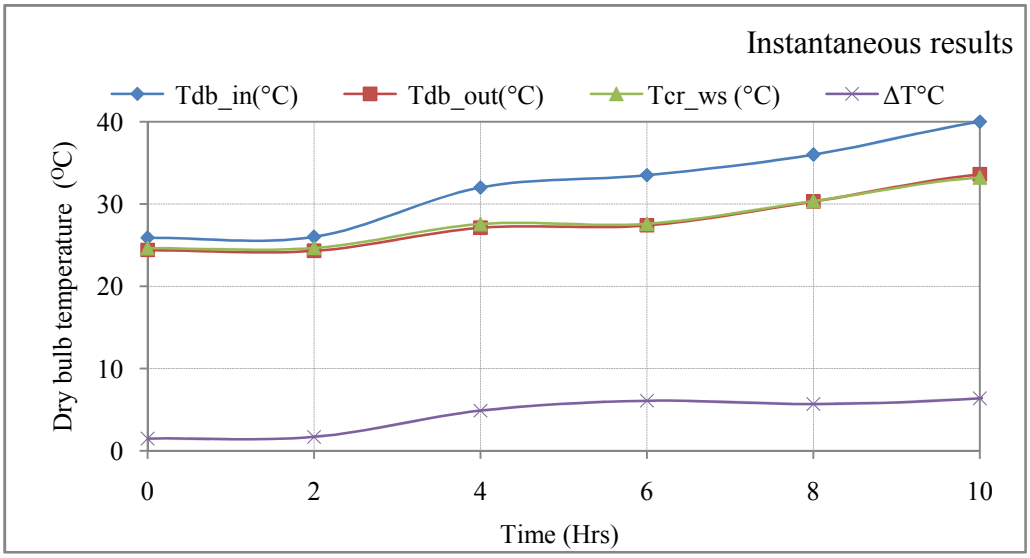

Figure 4.7b Instantaneous variations of inlet and outlet dry bulb temperatures with time for air and the porous ceramic wet surface (Tcr_ws) including temperature drop (ΔT) profile

Under steady state, inlet dry bulb temperature and relative humidity were set at constant values under the same air flow rate. Corresponding outlet values were recorded and results shown for different test runs as discussed below.

First, figure 4.7c shows general inlet and outlet temperature profiles under different test runs ranging from 26°C - 44°C. The trends show continues difference between inlet and outlet temperature values from the lower inlet up to the highest experimental limits. However, the temperature drop kept on increasing with the increase in the inlet temperature depicting the behaviour of direct evaporative cooling using other cooling pad materials. Under these test the temperature drop varies from about 1.3°C to 7°C corresponding to 26°C to 44°C, respectively.

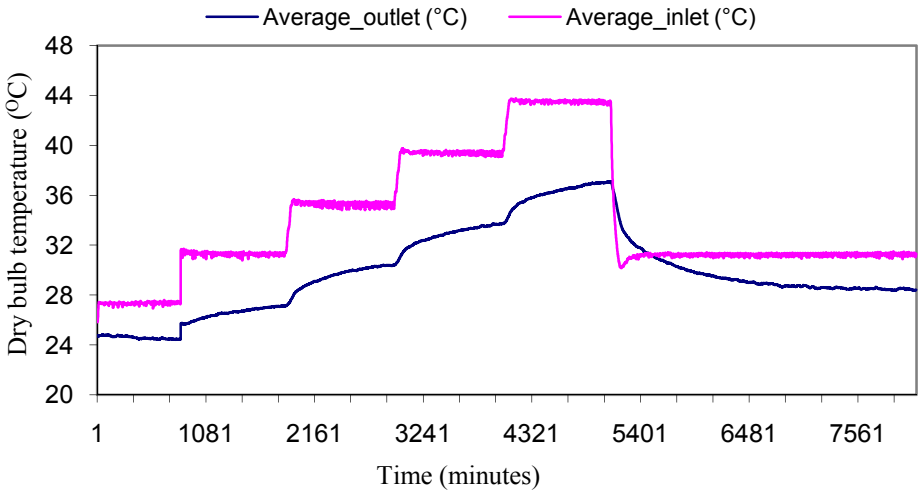

Figure 4.7c General inlet and outlet dry bulb temperature profiles for different test conditions for the stack or wall prototype system.

Results of the subsequent test runs under constant inlet dry bulb temperature and relative humidity values are shown in Figures 4.7d to Figure 4.7i.

In all these cases the results showed the difference between inlet and outlet temperatures increases with increasing in the inlet temperature values.

However, the effect of relative humidity was also observed. The increase in the relative humidity at outlet reduces the outlet dry bulb temperature.

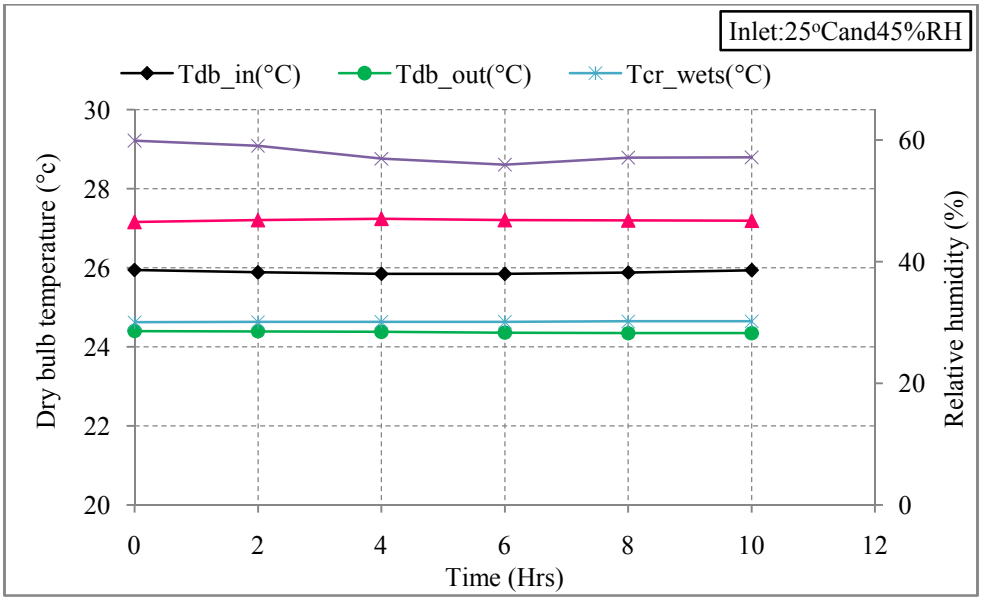

Figure 4.7d Variation of inlet and outlet dry bulb temperature under 25°C and 45% constant inlet ambient conditions

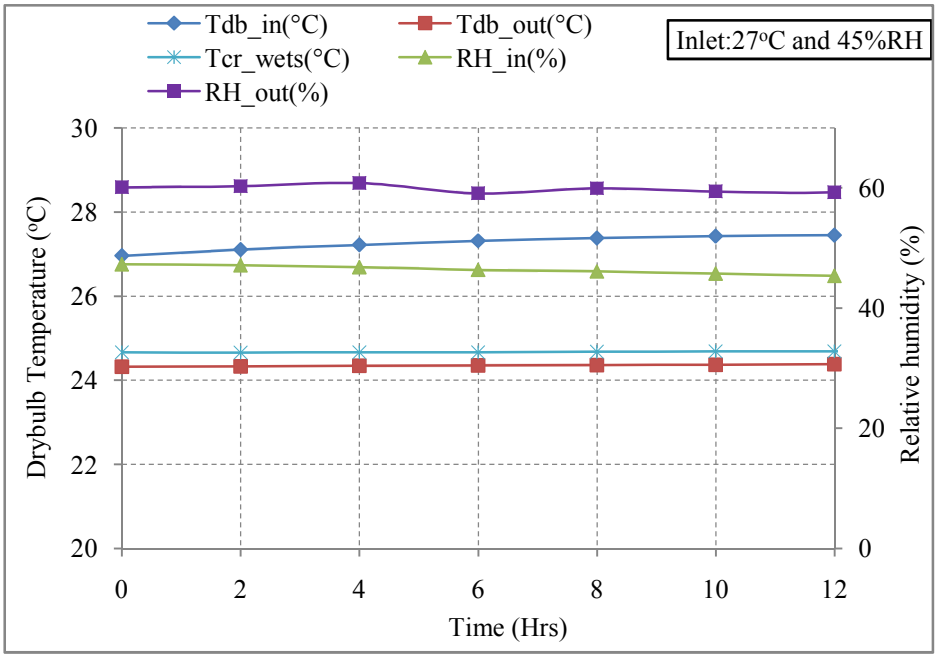

Figure 4.7e Variation of inlet and outlet dry bulb temperature under 27°C and 45% constant inlet ambient conditions

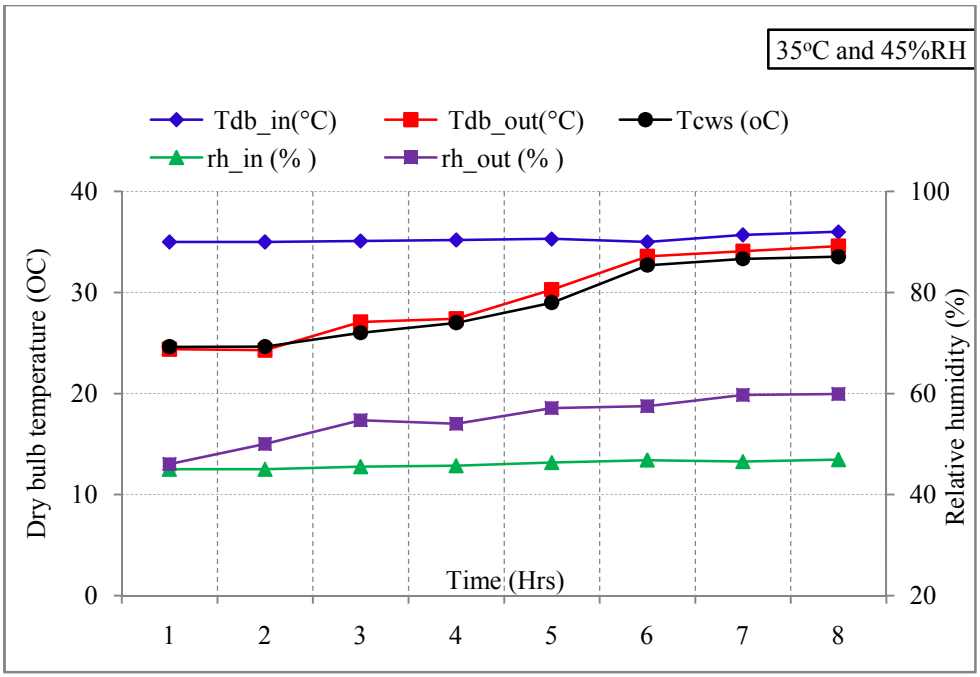

Figure 4.7f Variation of inlet and outlet dry bulb temperature under 35oC and 45% constant inlet ambient conditions

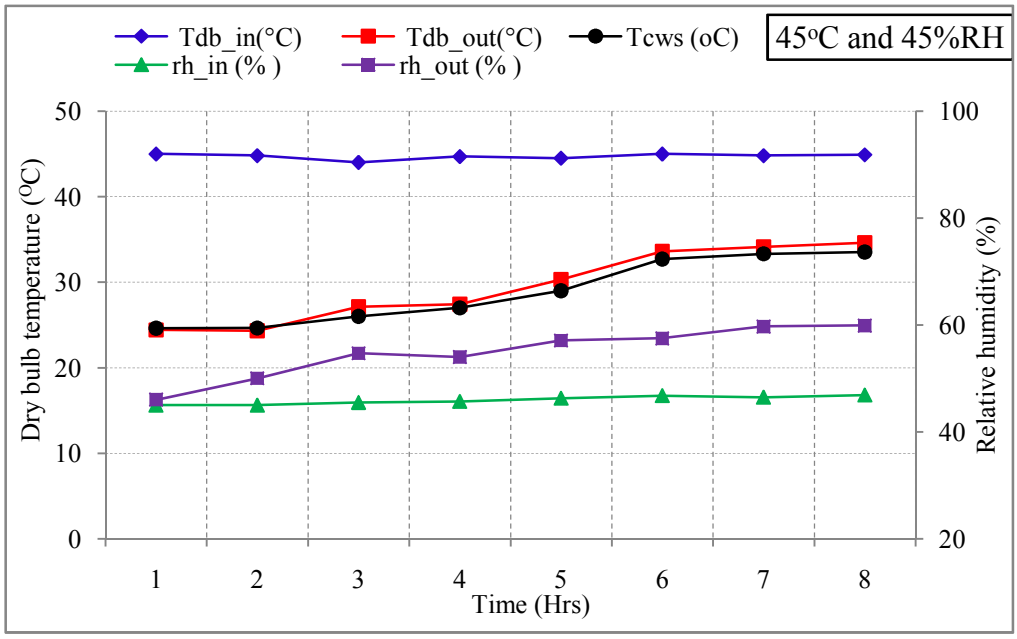

Figure 4.7g Variation of inlet and outlet dry bulb temperature under 45ºC and 45% constant inlet ambient conditions

Additional test results were conducted by lowering and maintaining the inlet relative humidity value to 35% in combination with different inlet dry bulb temperature values. These results are shown in Figures 4.7g to 5.7i.

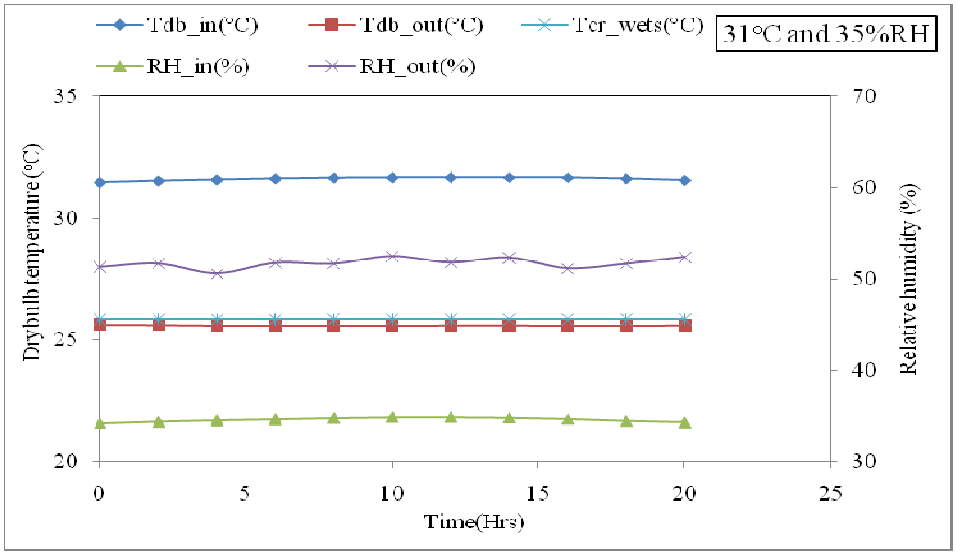

Figure 4.7h Variation of inlet and outlet dry bulb temperature under 31°C and 35% constant inlet ambient conditions

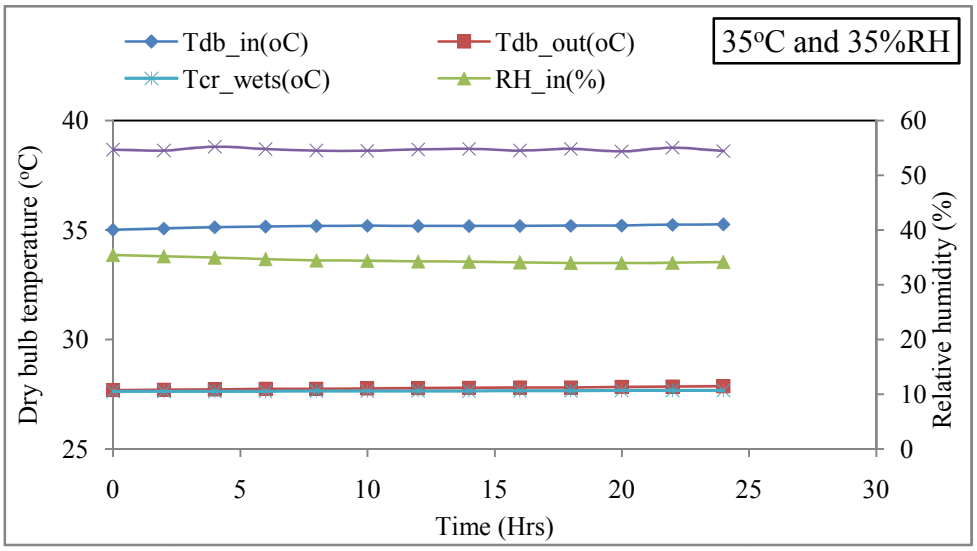

Figure 4.7i Variation of inlet and outlet dry bulb temperature under 35°C and 35% constant inlet ambient conditions

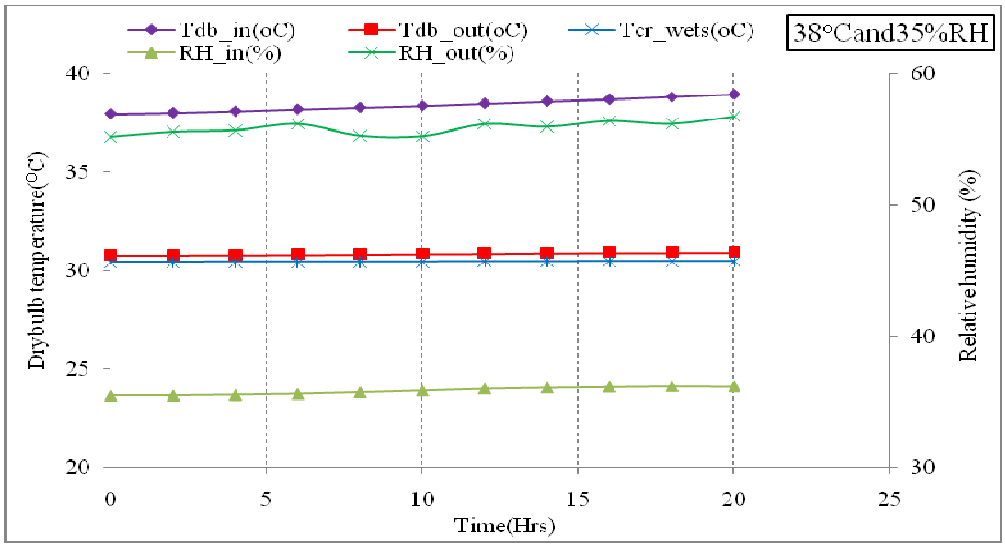

Figure 4.7j Variation of inlet and outlet dry bulb temperature under 38°C and 35% constant inlet ambient conditions

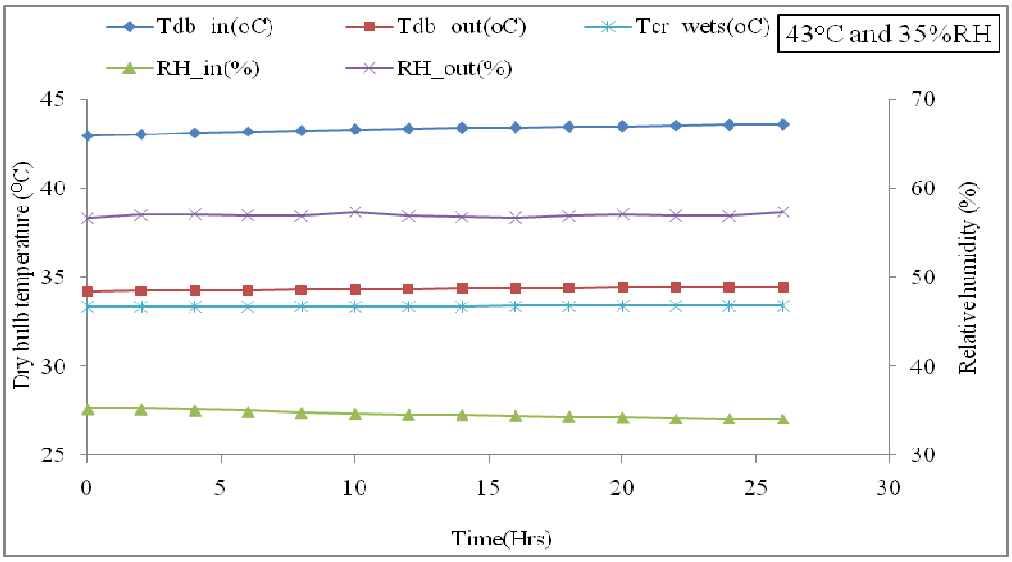

Figure 4.7k Variation of inlet and outlet dry bulb temperature under 43°C and 35% constant inlet ambient conditions

4.4.1.2 Ceramic evaporators' surface temperature profiles

Figure 4.7b shows variation of inlet temperature with the outlet and the porous ceramics surface temperature for the instantaneous results obtained.

It is observed that the outlet temperature does not vary much with the ceramic surface temperature. However the difference increases along with the increase in temperature drop between the inlet and the outlet. Similar trends were observed for all the test runs as shown in Figures 4.7c to Figure 4.7j. A difference between the outlet temperature and the ceramic surface temperature was averagely:

- $0.2 < T_{ws} < 1.1^{o}C$. This indicates that the cooling air exits the evaporative cooling chamber at a temperature very close to the surface temperature of the porous ceramics.

4.4.1.3 Inlet and outlet relative humidity profiles

Variation of the inlet and outlet relative humidity with time is also shown in Figure 4.8. For inlet relative humidity range of 34% - 47%, corresponding increase of 13% - 23% was observed at the outlet which is an inlet or supply air to the room.

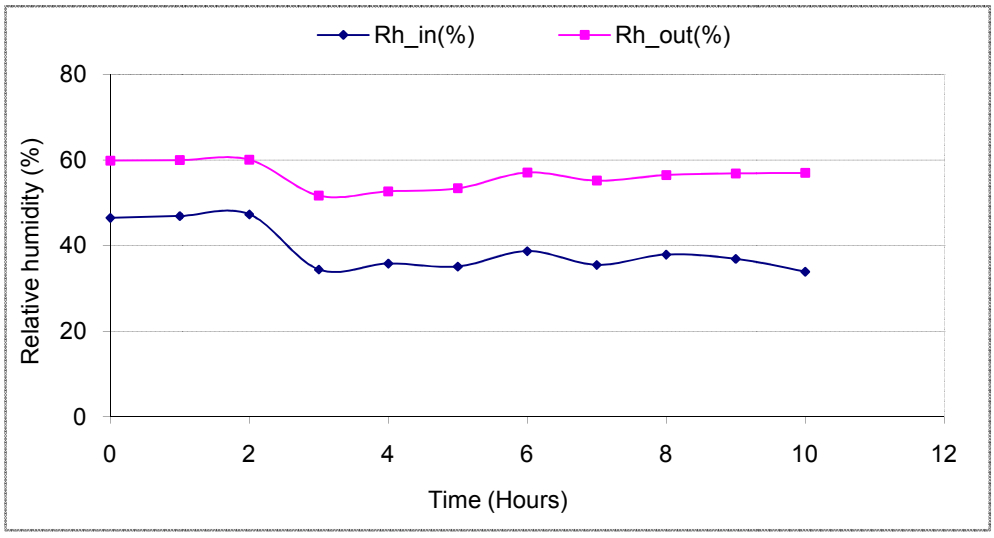

Figure 4.8 Variation of inlet and out relative humidity with time

4.4.1.4 System cooling performance

The specific cooling capacity of the system was plotted on Figure 4.9a. It showed the cooling performance to increase with increase in inlet and out let temperature variation for a given air mass flow rate. It is also sensitive to sudden increase or decrease in temperature drop. However, maximum cooling capacity of 179.8W/m^2 was calculated at 10^{o}C dry bulb temperature drop and 23.1% rise in relative humidity across the evaporative cooling chamber of the system. The result virtually agrees but not exactly the same with the value of 178.4W/m^2 based on wet surface empirical model, equation 3.49c in chapter 3, (Etzion et al, 2003). [sp.cooling exp] represents the experimental result while [sp.cooling_model] is based on the empirical model.

Figure 4.9b shows the cooling capacity profiles under the steady state inlet dry bulb temperature of 35^{o}C with corresponding outlet dry bulb temperature of 27.5^{o}C, averagely.

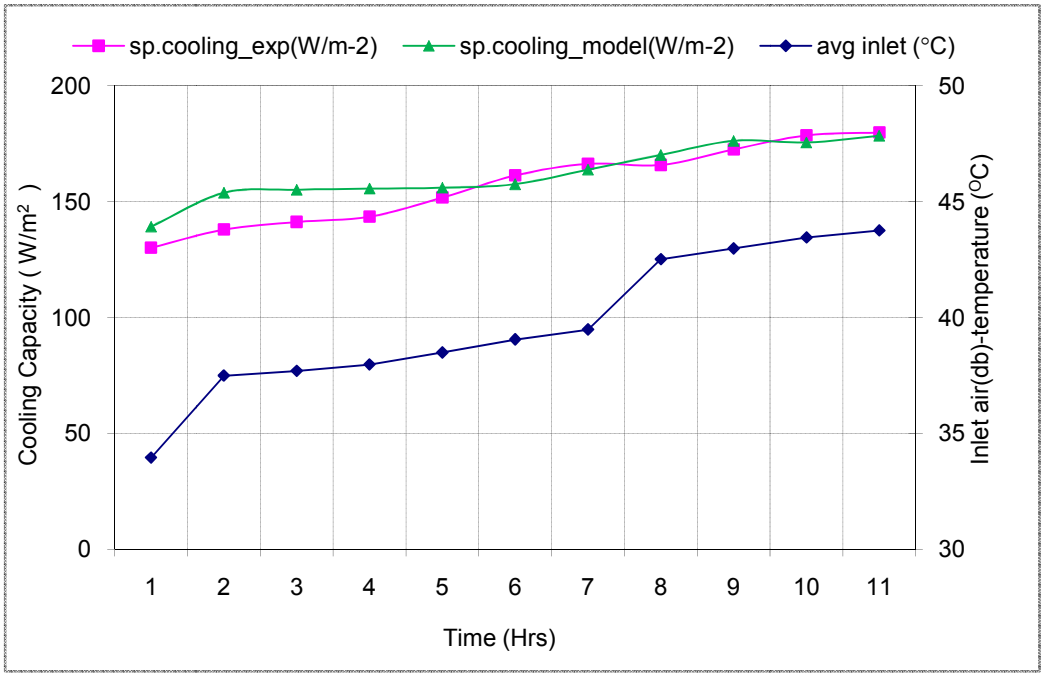

Figure 4.9a Effect of inlet air DB-Temperature on the cooling capacity for the experimental and modelling results

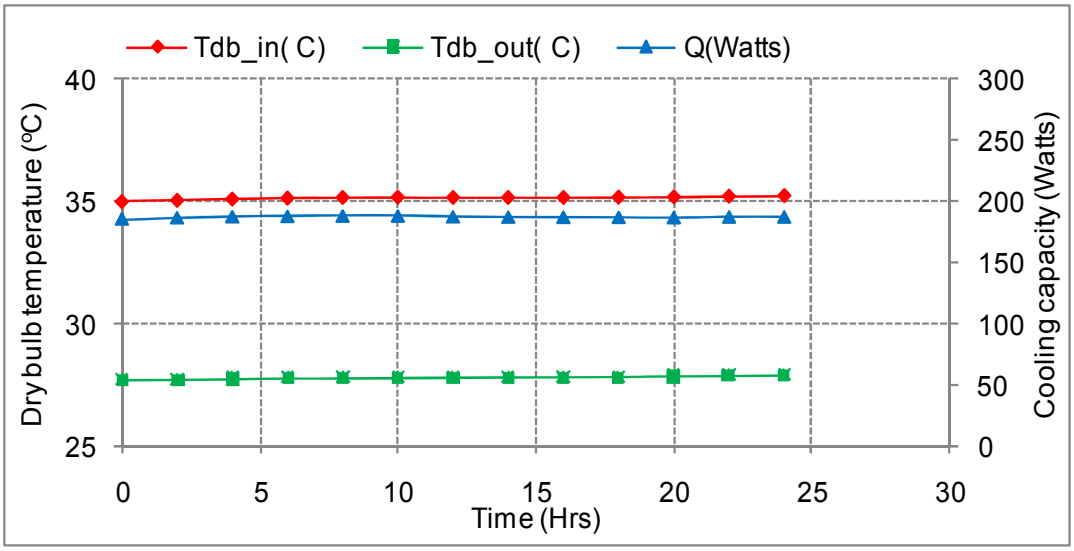

Figure 4.9b Diurnal temperature drop and cooling capacity profile under steady state test condition

4.4.1.5 Effect of vapour pressure difference on cooling performance

Ambient to saturated vapour difference (P_s-P_a), is a parameter expressing the force driving water evaporation from wetted porous ceramic surface. While ambient vapour pressure, P_a is a measure of the amount of water vapour present in the air, the corresponding saturated vapour pressure, P_s is the maximum amount that could be held and is a function of temperature, (Ibrahim et al 2003). It is therefore a very important parameter that affects cooling capacity of evaporative cooling system. In this investigation effect of the ambient to saturated vapour difference on cooling capacity of the system is plotted on Figure 4.10. It shows that the cooling capacity of the system increases with an increase in the ambient to saturated vapour pressure. For saturation to ambient vapour difference of 17.9mb and 59.4mb, the cooling rate showed 35W/m^2 and 180W/m^2, respectively.

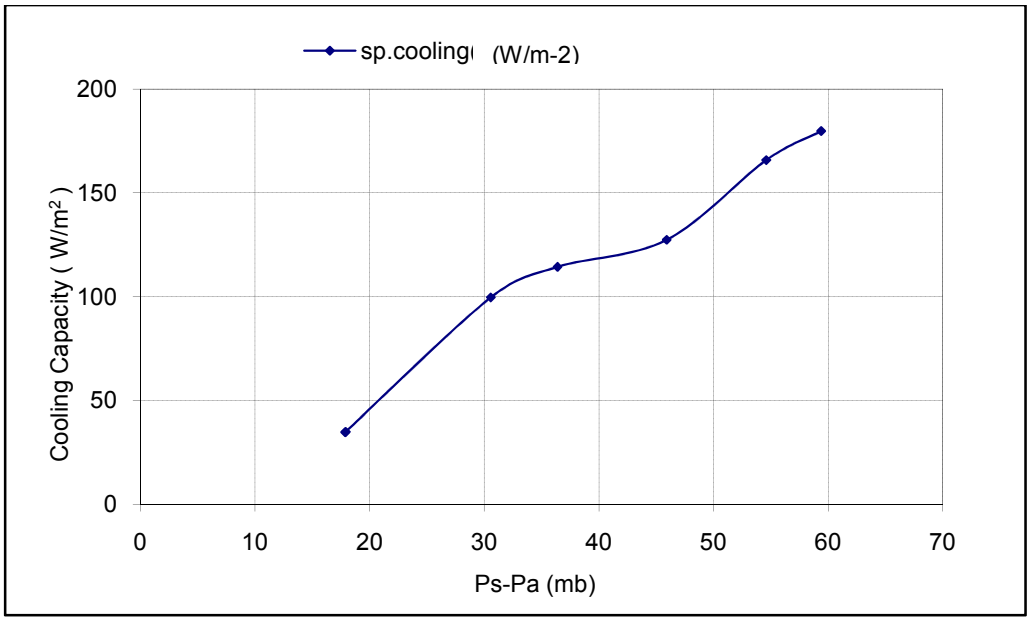

Figure 4.10 Variation of ambient and saturation vapour pressure difference with cooling capacity

4.4.1.6 Water consumption

Table 4.2 contains the experimental results for the water consumption analysis of the system. Figure 4.11a plots show the instantaneous differences between air inlet and outlet temperatures variation with the water consumption rate. The maximum water consumption rate of 0.012g/s occurred at the maximum temperature difference or drop of 9.2^{o}C corresponding to ambient air inlet temperature of 43.8^{o}C. Comparing with empirical model under the same condition a value of 0.072g/s was calculated. This big difference is because the evaporative wet surfaces were not of the same material.

Similarly the effect of relative humidity on the water consumption rate is shown on Figure 4.12b. Though the relative humidity change remains virtually constant because of the higher value at both inlet and outlet, the water evaporation rate reduces.

Table 4.2 Experimental and model results for system water consumption rate

Tdb_in(°C)	Tdb_out(°C)	rh_in (%)	rh_out (%)	Tws (°C)	$\dot{m}_{ws}$ (g/s)
25.9	24.4	46.5	59.9	24.6	0.05776
26.0	24.3	46.9	60	24.6	0.05716
32.0	27.1	35.8	52.7	27.5	0.06860
33.5	27.4	34.7	54	27.6	0.06685
36.0	30.3	38.7	57.1	30.3	0.06973
40.0	33.6	37.9	56.5	33.2	0.07615
42.5	34.1	35.2	57.6	33.3	0.07279
43.8	34.6	33.9	57	33.5	0.07195

T_{db_in} −Air dry bulb temperature in to the evaporative cooler
T_{db_out} −Air dry bulb temperature out of the evaporative cooler
$rh_{\_in}$ −Air relative humidity at inlet to evaporative cooler
$rh_{\_o}$ −Air relative humidity at outlet of the evaporative cooler
T_{ws} -Dry bulb temperature of the ceramic evaporator surface
$\dot{m}_{ws}$ -Water consumption rate based on experiment

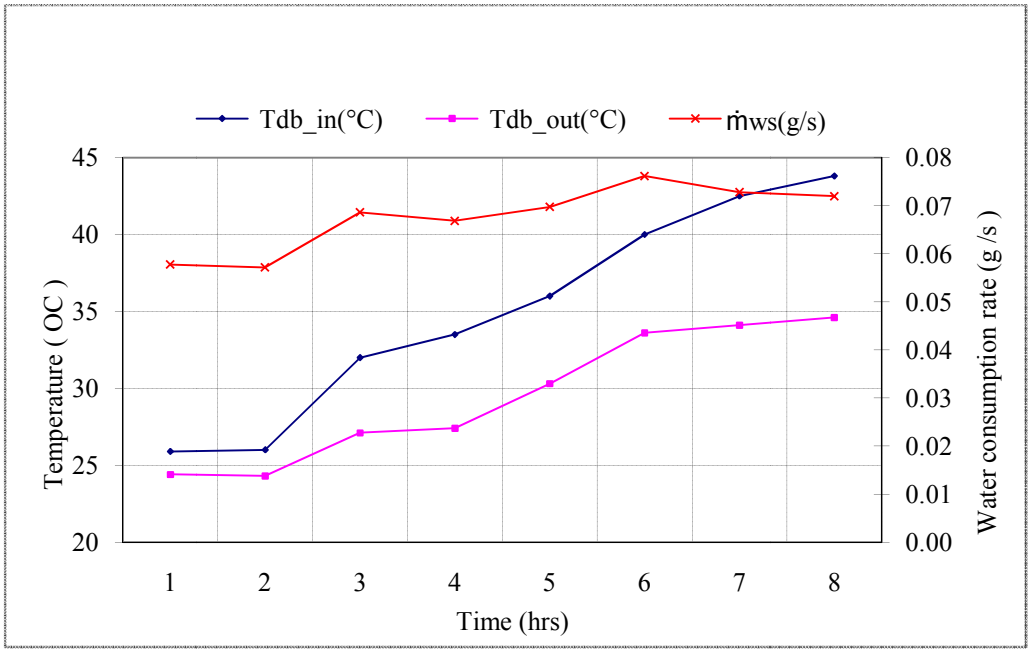

Figure 4.11a Effect of inlet and outlet temperatures on water consumption

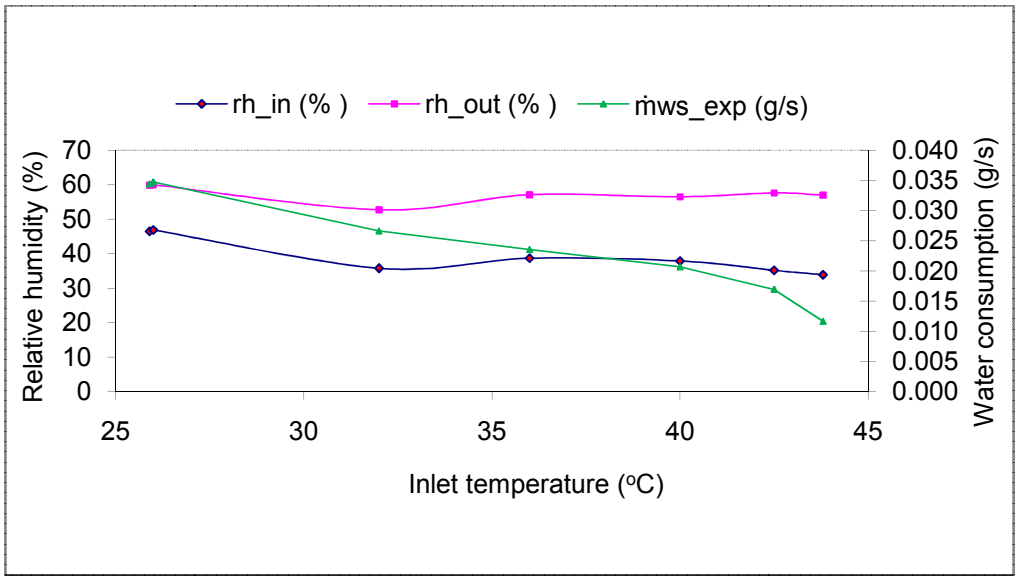

Figure 4.11b Effect of relative humidity increase on water consumption rate

4.4.1.7 Effectiveness of the system

Effectiveness was calculated by applying effectiveness equation 3.49c described in Chapter 3 on the experimental after obtaining the corresponding wet bulb temperature values by using a psychrometric calculator. Results for instantaneous inlet temperature values are shown in Table 4.3a and plotted on Figure 4.12a. In this test a value of over 60% was recorded. This implied that the system supplied temperature at a value over 60% of the inlet wet bulb temperature. The effectiveness increases with increasing ambient air inlet temperature. In this case it varies from 21% to 66.3% corresponding to the minimum and maximum inlet of 27°C and 44.1°C, respectively. Figure 4.12b shows the variation of inlet temperature with outlets at different chosen values of effectiveness. From the figure it can be seen that the predicted maximum effectiveness of 90% corresponds to the maximum temperature difference across the system inlet and outlet boundaries.

Effects of other operating parameters on effectiveness are discussed below.

Table 4.3a Experimental and model results for system effectiveness

Time (hours)	Tdb_in (°C)	Tdb_out (°C)	Twetbulb_in (°C)	$\Delta Td_{bin-out}$ (°C)	ΔTdb_{in-wb} (°C)	ε (%)
0	27.0	24.8	16.5	2.2	10.5	21.0
2	28.9	25.5	18.26	3.4	10.64	32.0
4	31.o	26.1	19.98	4.9	11.02	44.5
6	33.1	27.0	21.78	6.1	11.32	53.9
8	35.3	28.2	23.09	7.1	12.21	58.1
10	37.4	29.5	24.15	7.9	13.25	59.6
12	39.6	30.9	25.64	8.7	13.96	62.3
14	41.8	32.4	27.12	9.4	14.68	64.0
16	44.1	33.7	28.42	10.4	15.68	66.3

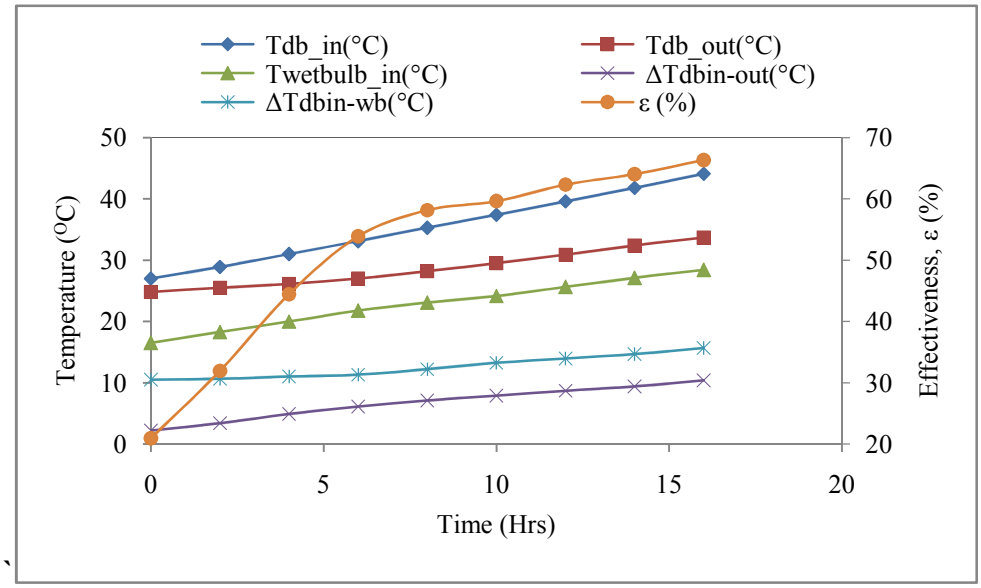

Figure 4.12a System effectiveness at different inlet ambient temperatures and outlet values and the wet-bulb temperature profile

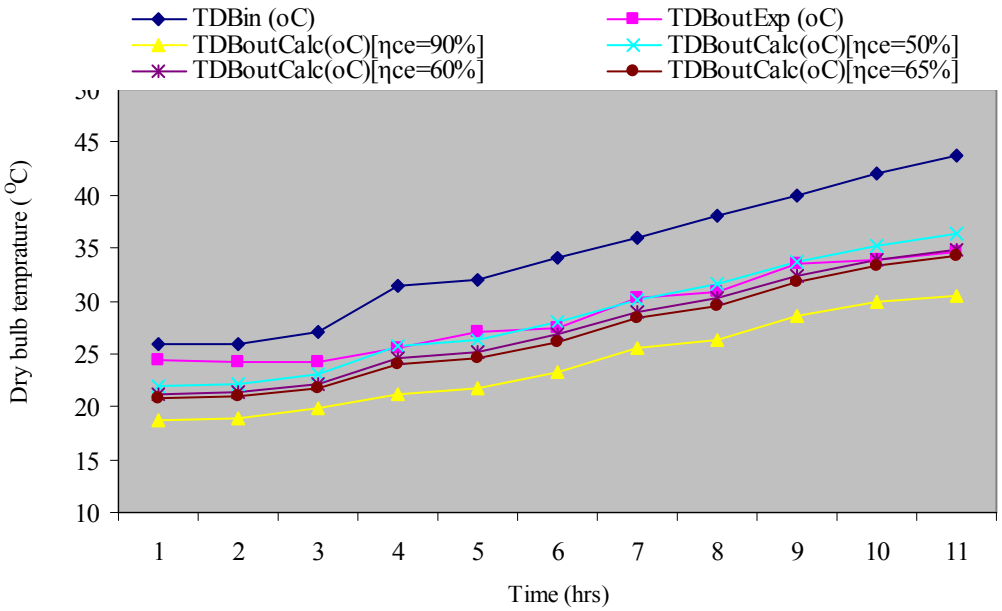

Figure 4.12b Timely variation of inlet dry bulb temperature with outlet at different effectiveness settings

4.4.1.8 The impact of inlet and outlet temperatures with effectiveness

The impact of inlet and outlet temperature on the system effectiveness is demonstrated on Figure 4.12c. It can be seen that the effectiveness increases with the rising temperature difference. The maximum value of over 60% system effectiveness occurred at the maximum temperature difference or drop attained. Therefore as the temperature difference increases as a result of higher dry bulb temperature at the inlet the effectiveness also tend to gain higher value. The continuous change of the result with time shows a real behaviour under natural environment where the ambient parameters sometimes significantly change with the time and steady state can hardly be attained. This trend is therefore recorded in this research to reflect the unsteady state instantaneous values. This behaviour requires the system to be operated within an environment where ambient inlet temperature is always high.

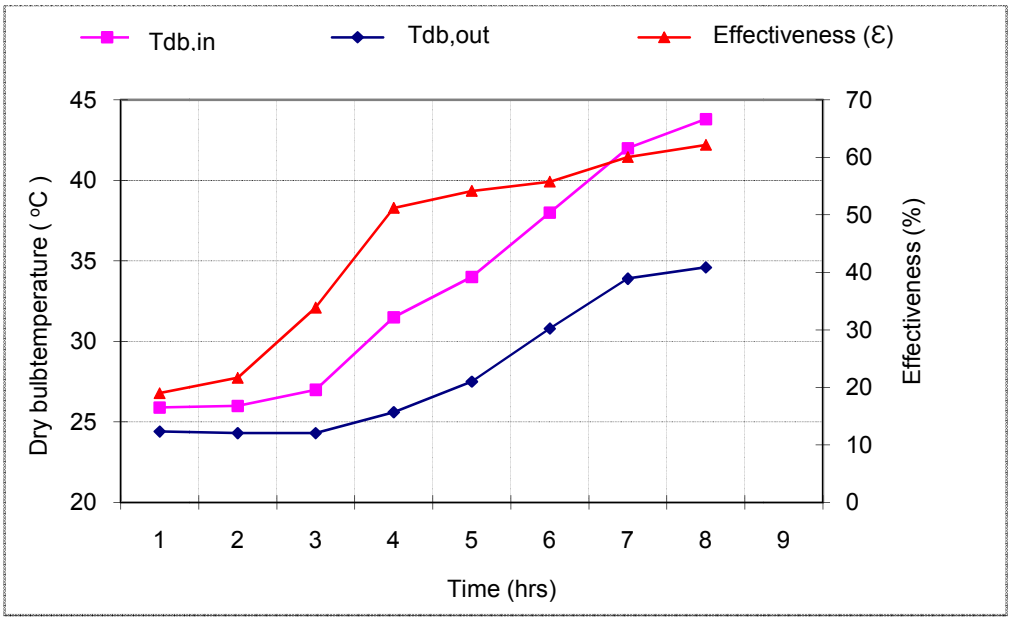

Figure 4.12c Variation of inlet and outlet dry bulb temperature with system effectiveness (instantaneous results)

4.4.1.9 The impact of inlet and outlet relative humidity with effectiveness.

Table 4.3b presents the experimental results for the inlet and outlet relative humidity with the corresponding calculated values of effectiveness.

These results are shown plotted in Figure 4.13d. As the variation between inlet and outlet relative humidity increases the water consumption also increases. For this system the maximum system effectiveness of approximately 63% corresponds to the maximum relative humidity rise of 23.1%. The characteristic also shows virtually a constant change in the effectiveness along side with constant relative humidity changes across the porous ceramics evaporative cooler.

Table 4.3b Experimental results for the inlet and outlet relative humidity and calculated effectiveness.

RH_{in} (%)	RH_{out} (%)	$\varepsilon\_{exp.}$(%)
46.5	59.9	19.01
46.9	60.0	21.7
47.3	60.1	33.9
34.4	51.7	51.2
35.1	53.4	54.2
35.5	55.2	55.8
36.9	56.9	60.1
33.9	57.0	62.2

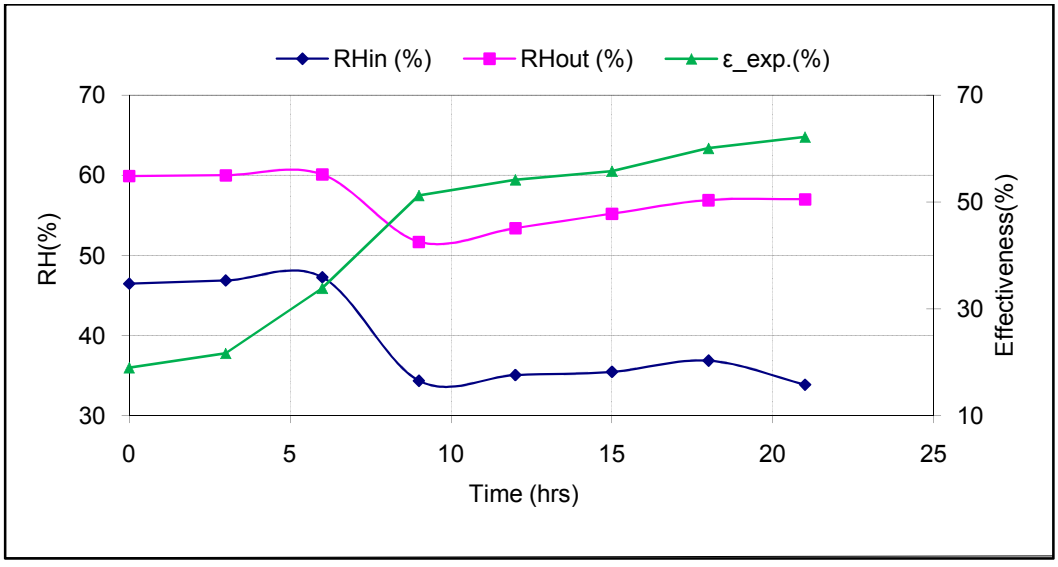

Figure 4.12d Impact of inlet and outlet relative humidity (RH) on effectiveness

4.4.2 "Supporting-frame or hanging" system configuration

To evaluate the performance of the supporting frame configuration the system was subjected to experimental tests in the same environmental control chamber as the stacking system. The tests were conducted at volume flow rate of 145m^3/hr. The total effective area of the ceramic evaporators which were assembled in rows on supporting frames as shown in Figure 4.13a and Figure 4.13b was 10.0m^2. Test results for different inlet dry bulb temperatures and relative humidity with corresponding outlet values were recorded as and the mean results are shown in Table 4.4. With these results the system performance was evaluated with the application of theoretical formulae and some modelling correlations applicable to direct evaporative cooling system (DECS).

Table 4.4 Experimental data for air inlet with corresponding outlet values.

T_{db_in} (°C)	T_{db_out} (°C)	T_{wb_in} (°C)	$rh_{\_in}$ (%)	$rh_{\_out}$ (%)	ΔT_{db} (°C)	Δrh (%)
31.3	25.9	23.15	50.5	82.6	5.4	32.1
34.6	26.6	24.95	46.1	84.6	8	38.5
36.3	28.8	26.62	47.4	83	7.5	35.6
37.8	29.1	27.53	46	85	8.7	39
41	31.7	30.16	46.1	85.3	9.3	39.2
44.3	34.3	32.71	45.5	86	10	40.5

T_{db_in} - Air dry bulb temperature in to the evaporative cooler
T_{db_out} - Air dry bulb temperature out of the evaporative cooler
T_{wb_in} - Air wet bulb temperature corresponding to inlet temperature
$rh_{\_in}$ - Air relative humidity in to the evaporative cooler
$rh_{\_out}$ - Air relative humidity out of the evaporative cooler
ΔT_{db} - Dry bulb temperature drop across the cooler
Δrh - Relative humidity increase across the cooler

Related parameters needed such as wet bulb and dew point temperatures, enthalpy, humidity ratio, specific humidity were obtained using Psychrometric chart and the Psychrometric calculator(5.12-Psycal98;LinricCompany,Bedford, NH,USA). The performance parameters analysed from the results include:

- Temperature drop across the system.
- Relative humidity increase.
- Cooling capacity of the system.
- Water consumption.
- Effectiveness of the system.

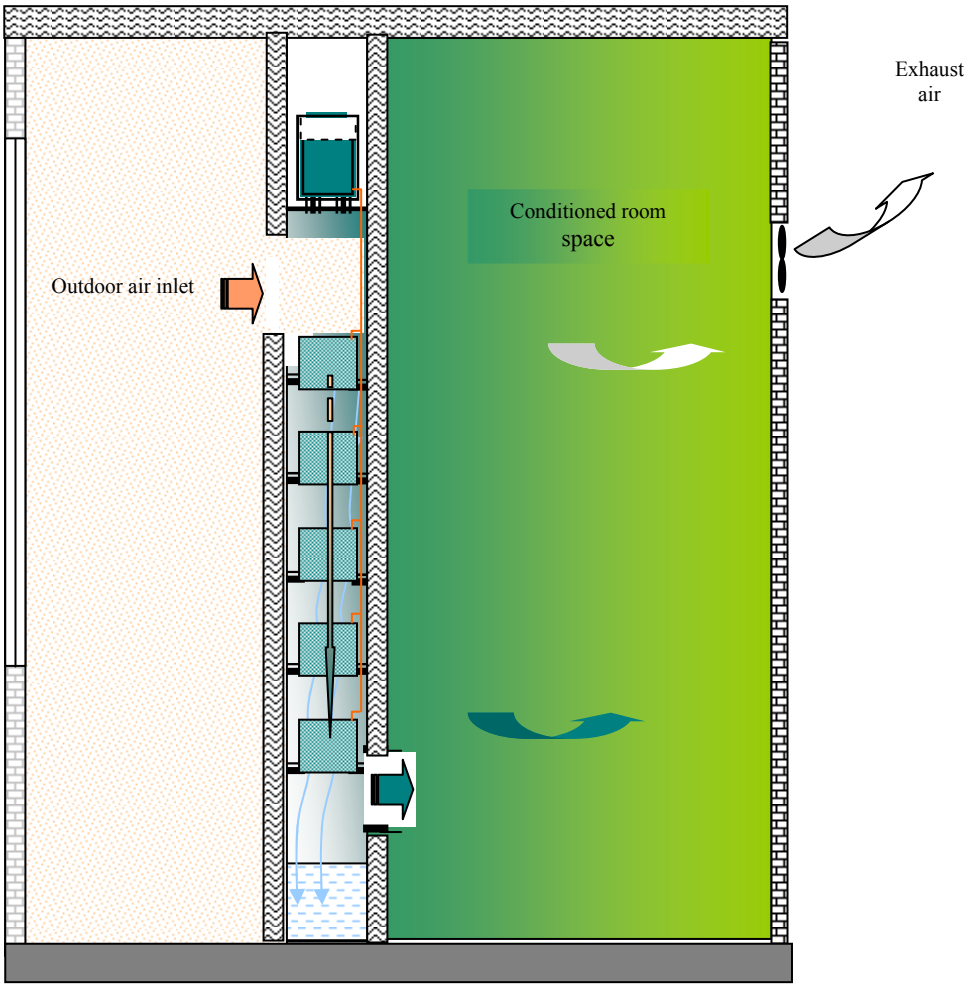

Figure 4.13a Experimental layout for the hanging system configuration

Figure 4.13b Experimental rig for the hanging system configuration

4.4.2.1 Temperature drop across the system.

Temperature distribution across the system is shown in Figure 4.14. It consists of the air inlet dry bulb temperature ranging from 36^{o}C to 44.3^{o}C with corresponding wet bulb temperature and the outlet dry bulb temperature. The periodic change was due to the continuous rise in inlet conditions before attaining steady state. The results are therefore a particular instant. From the results the following observations were made:

- As the inlet ambient air passes across the surface of the ceramic evaporators there was continuous decrease in air temperature ranging from 5-10^{o}C with the highest temperature drop of 10^{o}C corresponding to the highest air inlet dry bulb temperature of 44.3^{o}C.

- The outlet temperature constantly decreases, approaching the wet bulb temperature of the inlet air. An average difference of 1.9°C above the wet bulb temperature was observed.

The system is therefore capable of achieving low outlet temperature close to the inlet wet bulb temperature of the incoming air.

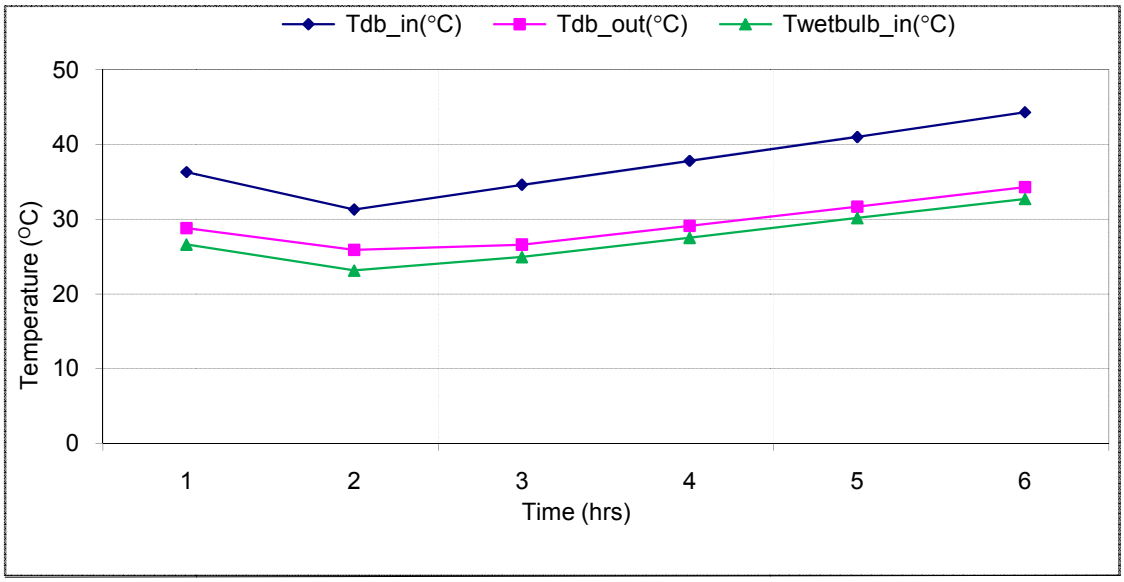

Figure 4.14 Time-averaged dry bulb and wet bulb temperature distributions across the system

4.4.2.2 Relative humidity profiles.

Figure 4.15 shows the timely variation of inlet and outlet relative humidity (RH) across the system. Because of the high level of RH condition at the inlet the varying increase at the outlet remains virtually constant. With an ambient inlet range of 45.5% - 50.5% the variation showed corresponding range of 83% - 86% at the outlet conditions. The increase in relative humidity was therefore 32% - 40.5% as the outlet conditions were approaching saturation. These inlet dependent out let conditions were above the comfort relative humidity level requirements in a building space.

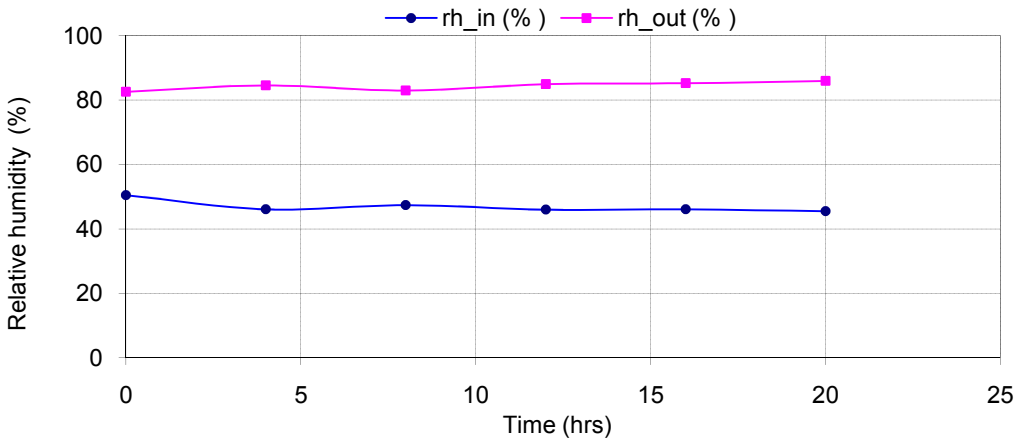

Figure 4.15 Diurnal variation of inlet and outlet relative humidity across the system

4.4.2.3 Combined dry bulb temperature and relative humidity profiles.

Figure 4.16 shows the combined temperature and relative humidity profiles at the inlet and outlet operating conditions of the system. The main characteristic of this result is that the air temperature decreases while the relative humidity increases between the inlet and outlet boundaries of the system. It can be observed that the increase in relative humidity is virtually proportional to the decrease in dry bulb temperature as more clearly shown in Figure 4.17. Based on experimental results, the linear relationship between the temperature drop and the relative humidity rise across the system is as shown in the following expression.

$$\Delta RH = 1.8766\Delta T + 21.93$$

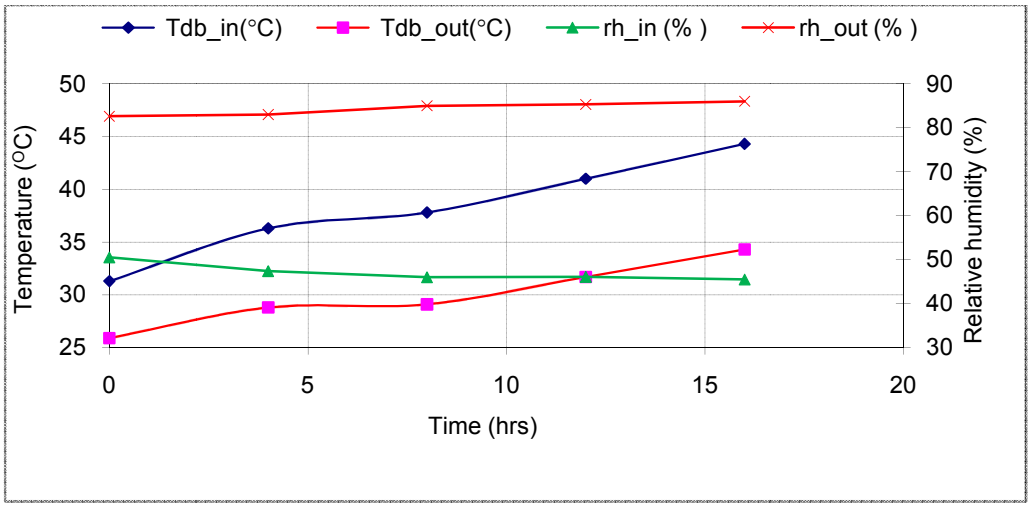

Figure 4.16 Distribution of air inlet dry bulb temperature and relative humidity with corresponding outlet values across the system with time

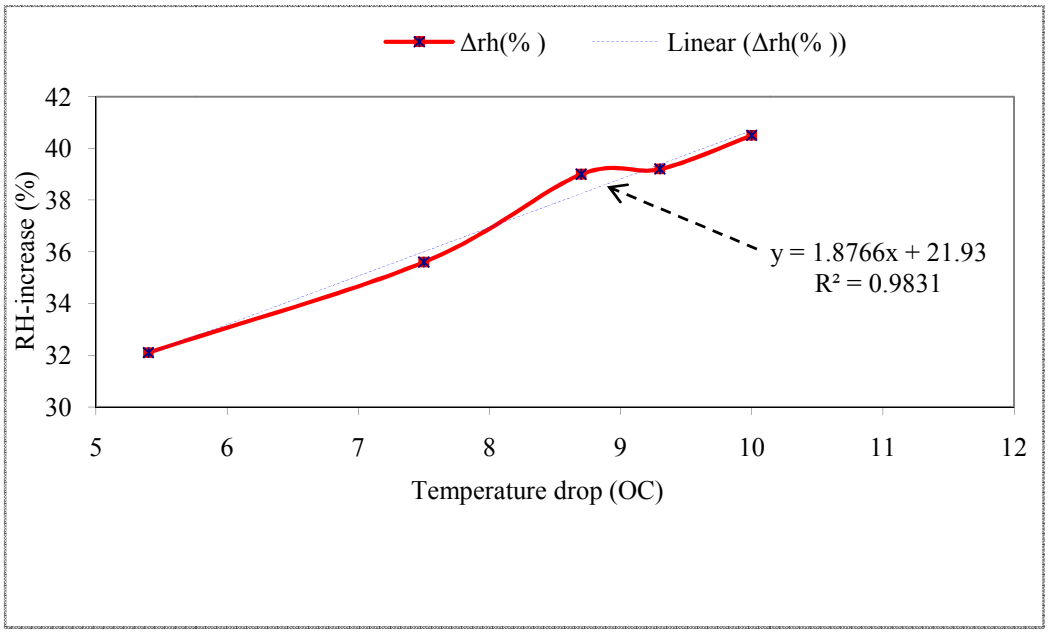

Figure 4.17 Variation of temperature drop with relative humidity (RH) increase across the system

4.4.2.4 System cooling capacity

For this system configuration cooling capacity was calculated using equation (16) based on the results shown in Table 5.4.

Figure 4.18 shows variation of cooling capacity with different values of air velocities ranging from 0.3m/s to 2m/s.The trend shows that the cooling capacity increases linearly with increasing air velocity and the rate of increase shows 141.21W/m^2 per 1m/s. From the figure the following trend correlation was deduced: $Q_{cws} = 141.21v + 251.46$

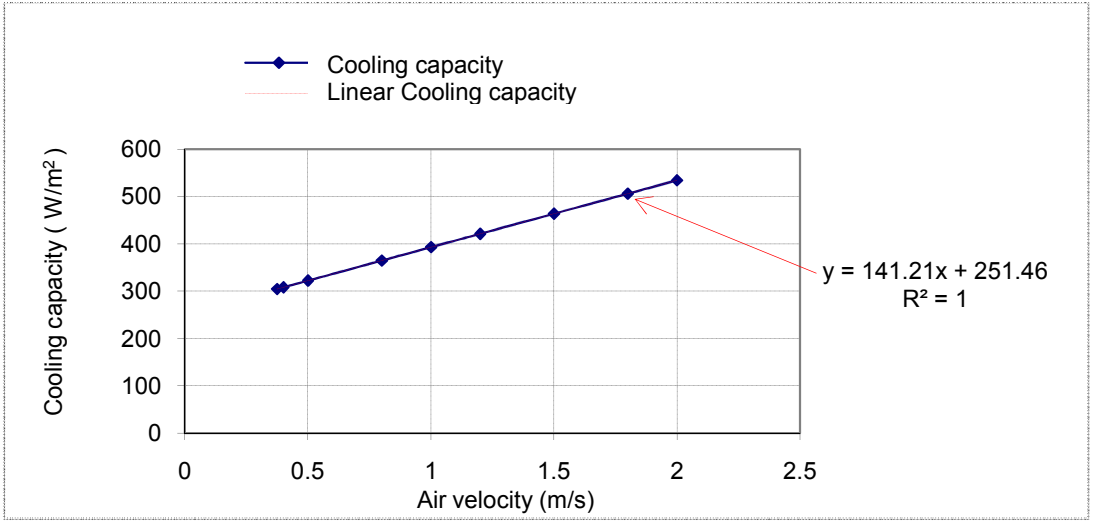

Figure 4.18 Variation of air velocity with system maximum cooling capacity

4.4.2.5 Cooling capacity experimental and theoretical model results

Figure 4.19 represents comparison between experimental data and the theoretical model prediction. In both cases the cooling capacity increased with increase in air inlet dry bulb temperature. The maximum cooling capacity attained for the experimental data was 426.52W/m^2 corresponding to the maximum air inlet temperature of 44.3^{o}C.

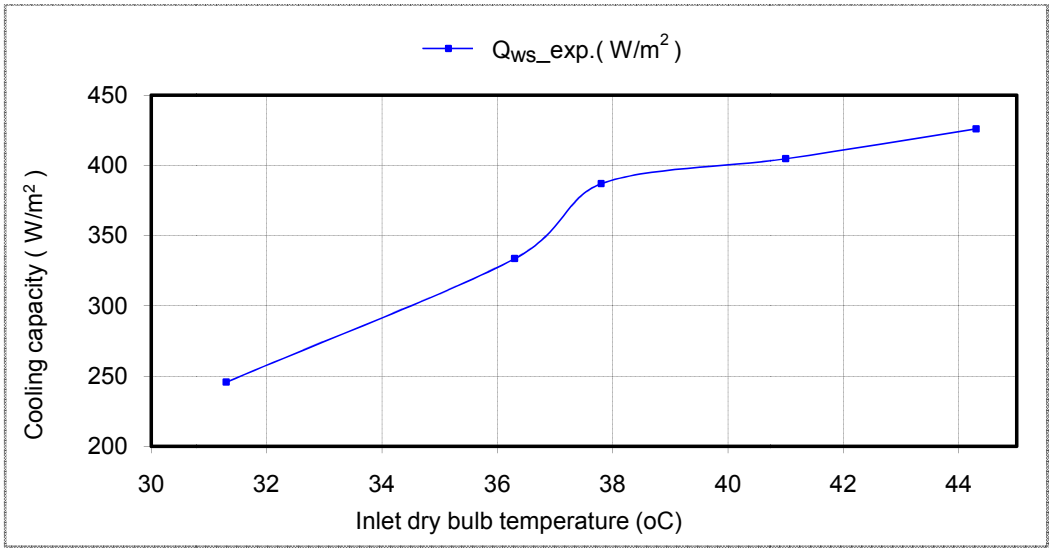

Figure 4.19 Inlet temperatures versus experimental cooling capacity

4.4.2.6 Water consumption results

The system water consumption was calculated and the experimental data in Table 4.4. Figure 4.20 shows that as the difference between air inlet and outlet temperature increases the water consumption rate reduces. This is because the higher temperature drop lowers the temperature of the ceramic evaporator surface, hence lowers the evaporation rate.

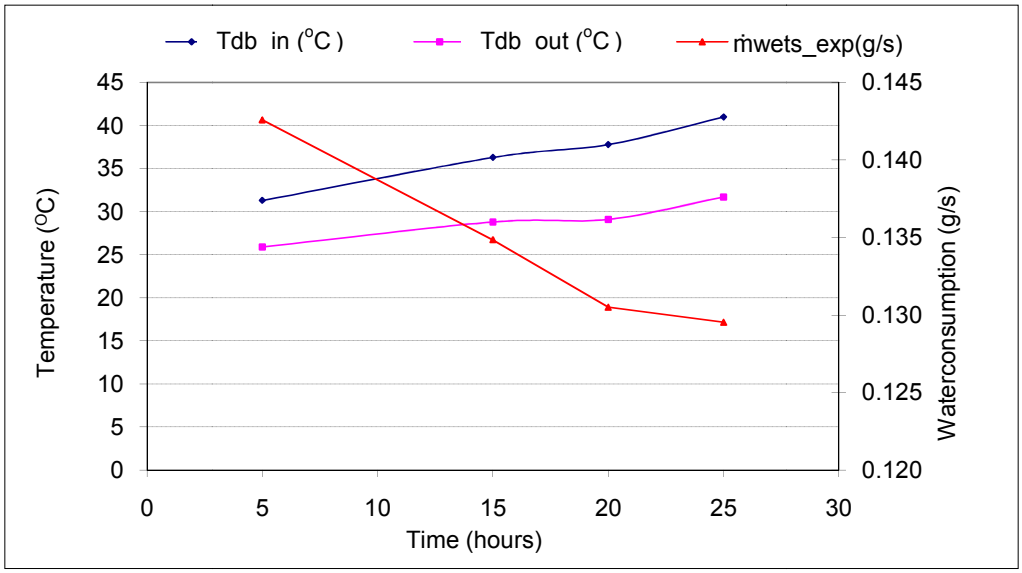

Figure 4.20 Timely variation of inlet and outlet temperature with water consumption rate

Similarly the effect of relative humidity on the water consumption rate is shown on Figure 4.21. Though the relative humidity change remains virtually constant because of the higher value at both inlet and outlet, the water evaporation rate reduces.

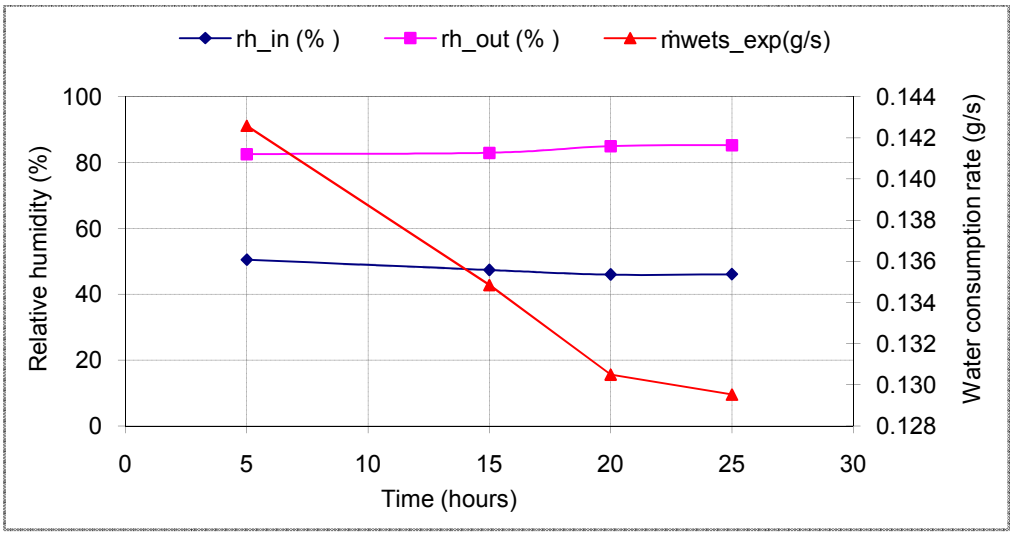

Figure 4.21 Timely variations of inlet and outlet relative humidity with water consumption rate

4.4.2.8 System effectiveness

Effectiveness or cooling efficiency of the system increases with increase in the inlet air temperature and corresponding cooling capacity as shown in Figure 4.22a**.** Following same trend as the cooling capacity the increase virtually remains constant after an inlet air temperature of 38^{o}C. The maximum effectiveness of 86% was attained at a maximum inlet air temperature of 44.3^{o}C. In this test therefore the system supplied temperature at 86% of the inlet wet bulb temperature that is approaching the desired theoretical value of over 90% expected for a typical direct evaporative cooling system (DECS).

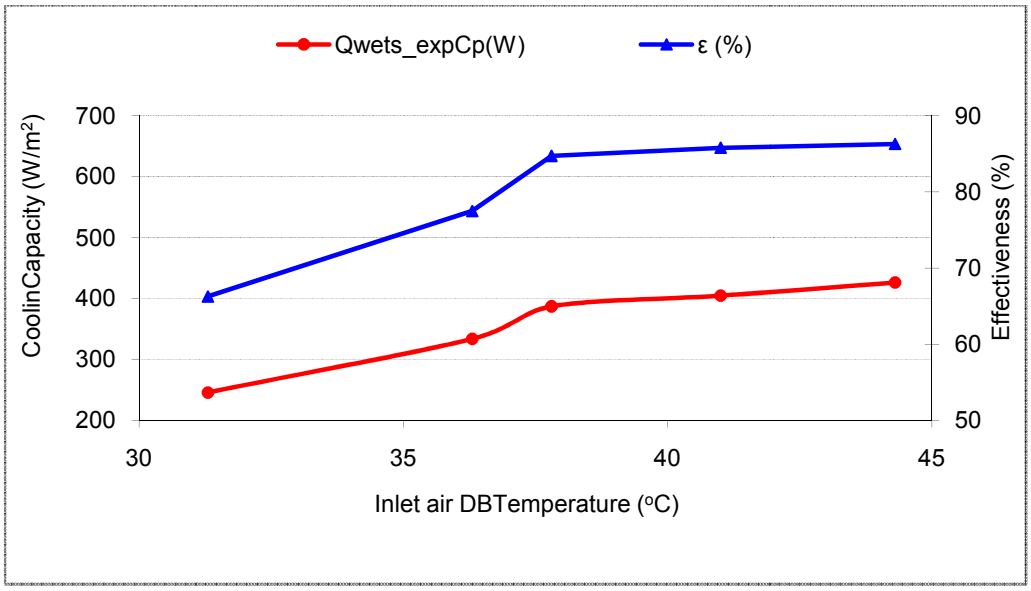

Figure 4.22a Variation of inlet air dry bulb temperature with cooling capacity and effectiveness (for supporting frame at 145m^3/hr)

Figure 4.22b shows the timely variation of the ratio of the cooling capacity to effectiveness ratio with inlet temperature under the constant inlet of 35°C and 35% relative humidity. The relationship with the constant inlet relative humidity is shown in Figure 4.22c.

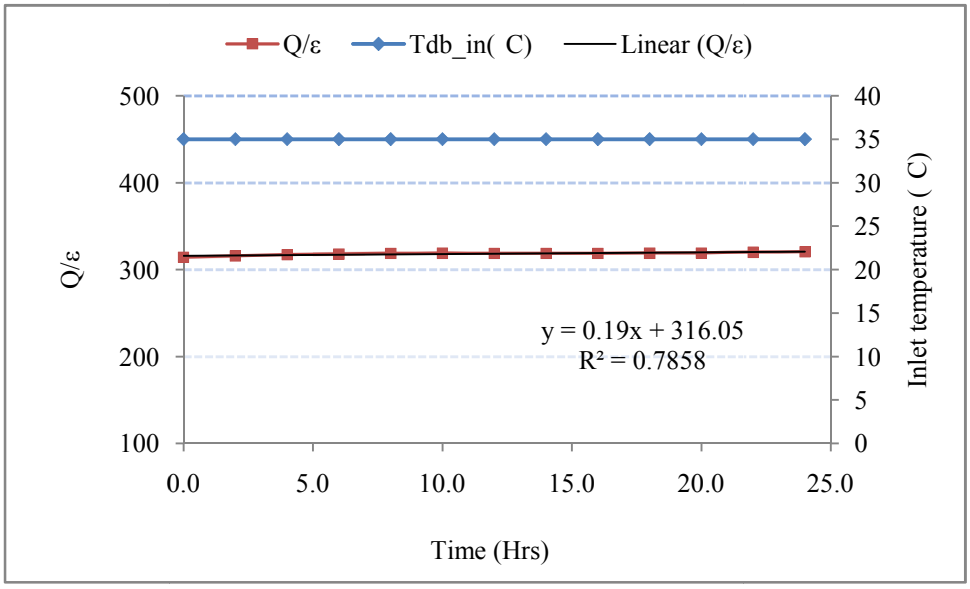

Figure 4.22b Relation of cooling capacity to the effectiveness ratio Q/ε with constant dry bulb inlet temperature of 35°C

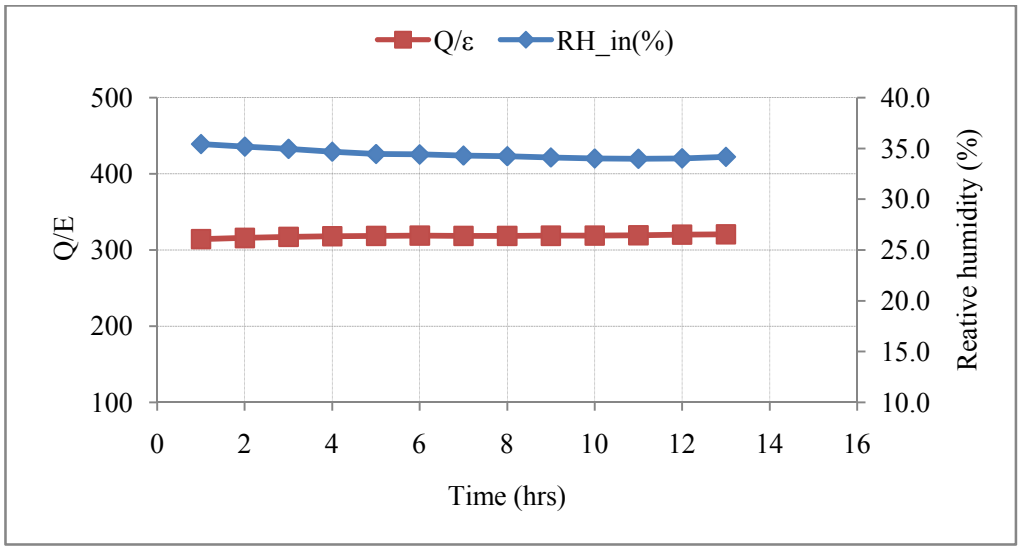

Figure 4.22c Relation of cooling capacity to the effectiveness ratio Q/ε with constant inlet relative humidity of 35%

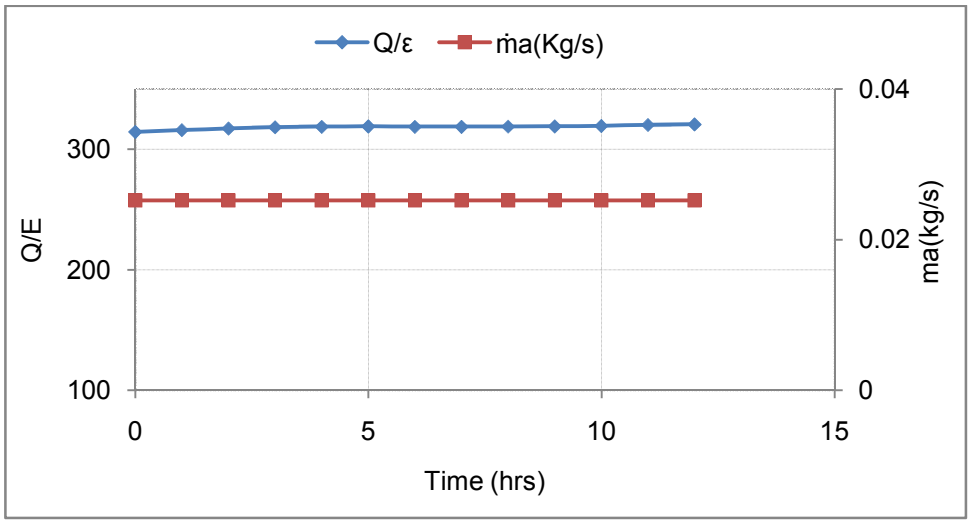

Figure 4.22d Relation of cooling capacity to the effectiveness ratio Q/ε with constant air flow rate

4.4.3 General comparison between both systems with empirical models.

In comparison, the supporting frame system configuration has twice the effective evaporative surface area as that of the stacking system.tha is, $10m^2$ compared to $5m^{2,}$ respectively. Also during the tests the systems were not exposed to the same initial dry bulb temperature and relative humidity levels as

the control chamber failed to stabilise the elevated moisture generated by the supporting frame system being the first set up to be experimented on. However, the comparison is based on the system specific cooling capacity, water consumption and system effectiveness/efficiency. Table 4.5 is the summarised data for these performance parameters.

Table 4.5 Comparative performance results for the stacking and supporting systems

Parameter	System type/Configuration			
	Stacking		Supporting-frame	
	Exp.	Model	Exp	Model
$\Delta T_{db\text{-}max}$ (^{O}C)	9.2	-	10	-
$\Delta rh\text{-}_{max}$ (%)	23	-	40.5	-
$Q_{ws\text{-}max}$ (W/m2)	179.8	178.4	426.52	304.3
$_{Mws\text{-}max}$ (g/s)	0.012	0.072	0.145	0.531
η_{max} (%)	62.2	90	86	90
Area (m^2)	5	-	10	-
Vol.FlowRate(m^3/hr)	140	-	145	-

4.4.3.1 Comparative cooling capacity

Figure 4.23 shows the cooling capacity chart for the two systems and the empirical model results. It can be seen that the cooling capacity for the supporting frame system is more than twice that of the stacking type.

The higher value tallies with the area which was two times. However the stacking type is more closely to the theoretical model results unlike the

"supporting frame" system which shows about 30% increase as compared to the empirical model. The increase from the supporting frame system was basically because of the large surface area exposed to evaporation.

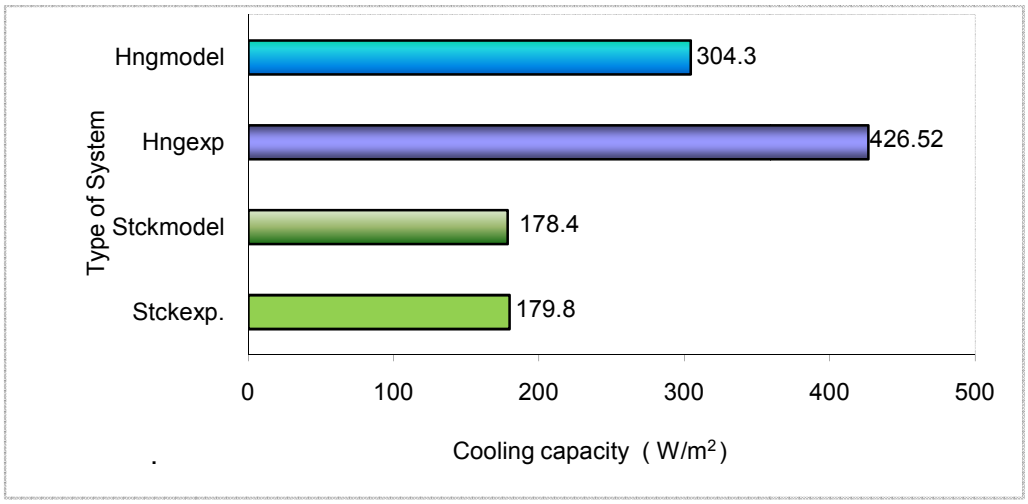

Figure 4.23 Experimental and model comparative performance chart for cooling capacity for the two systems

4.4.3.2 Comparative water consumption

A comparative result for the water consumption is shown in Figure 4.24. Both systems demonstrated very low water consumption in comparison with the model. Each system shows about 30% of its model prediction as can be seen on the figure. Here also the effect of evaporative surface area is clearly demonstrated. It can be observed that the empirical model (Hngmodel) and experimental (Hngexp) results for the supporting frame or hanging system which was twice the area turned out to be more than twice the value of the water consumption for the stacking type model (Stckmodel) and experimental (Stckexp) results.

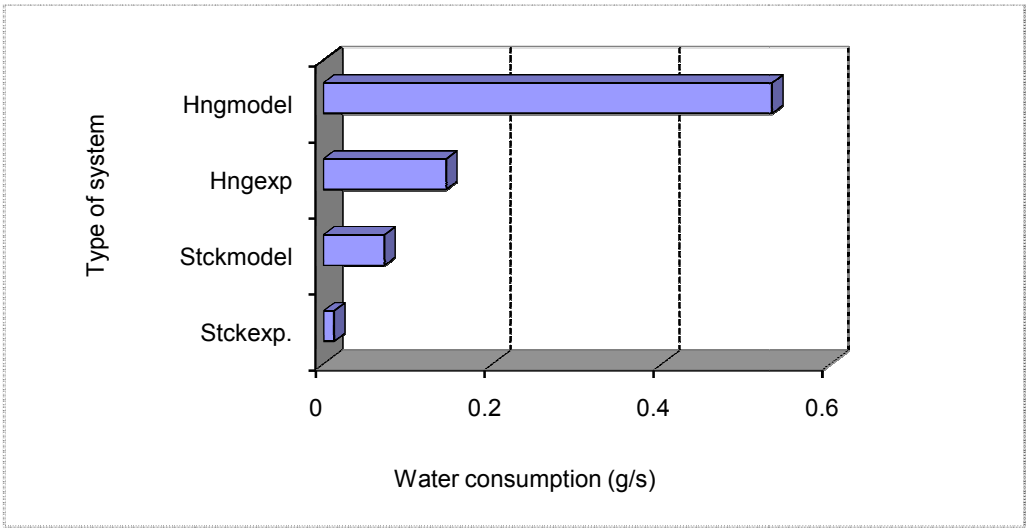

Figure 4.24 Comparative water consumption results

4.4.3.3 Comparative system effectiveness/efficiency

Comparative system effectiveness is demonstrated on Figure4.25. The hanging system approaches the theoretical efficiency of a direct evaporative cooling system with a value of 86% out of 90%. The efficiency of the stacking arrangement whose effective area was 50% less than that of hanging gave a value of 62.2%. Therefore increase in the evaporation surface area of the porous ceramics generates higher system effectiveness.

4.5 Effects of outlet parameters on room space

The effect of the outlet temperature and relative humidity values were monitored at different areas of the 3mx2mx2.1m room space created within the experimental chamber. For the supporting-frame system the outlet temperature range of 27-29 ^{O}C was observed from the floor to ceiling with corresponding relative humidity values of about 65-76%. The high outlet relative humidity was affected by the inlet values which were high at 45% to 50% hence not dry.

The room therefore turned out to exceed the comfort requirements and the stratification within the entire room was approximately uniform. Also the cumulative effect of the surface areas of the evaporators generated higher relative humidity more than required within the experimental room space. In the case of stacking configuration lower values of outlet temperature and relative humidity flowing across the room were observed. This was because the inlet relative humidity was lower and also the moisture emitting surface area was smaller. Therefore the room condition was within the comfort limits.

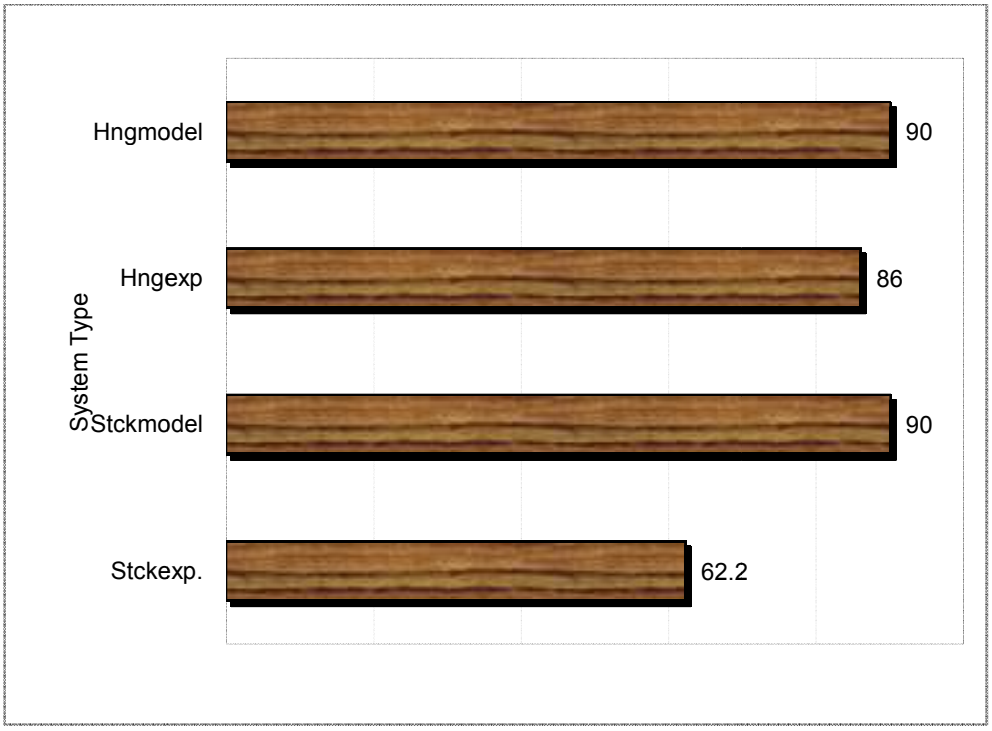

Figure 4.25 Comparative experimental and empirical model charts for the effectiveness of the two systems

4.6 System application

Having carried various experiments and performance analysis of the results evaporative cooling using porous ceramics can be applied to cool buildings.

The evaporative cooling chamber will be integrated so that all incoming air will be passed through the chamber containing the ceramic evaporators. The water supply to the evaporators can be by gravity from a tank erected on top of the evaporative cooling chamber. There should be continuous flow of air across the room to prevent accumulation of humid air in to the building interior. Figure 4.26 shows the typical system configuration in which the entire evaporative cooling chamber is attached to a building.

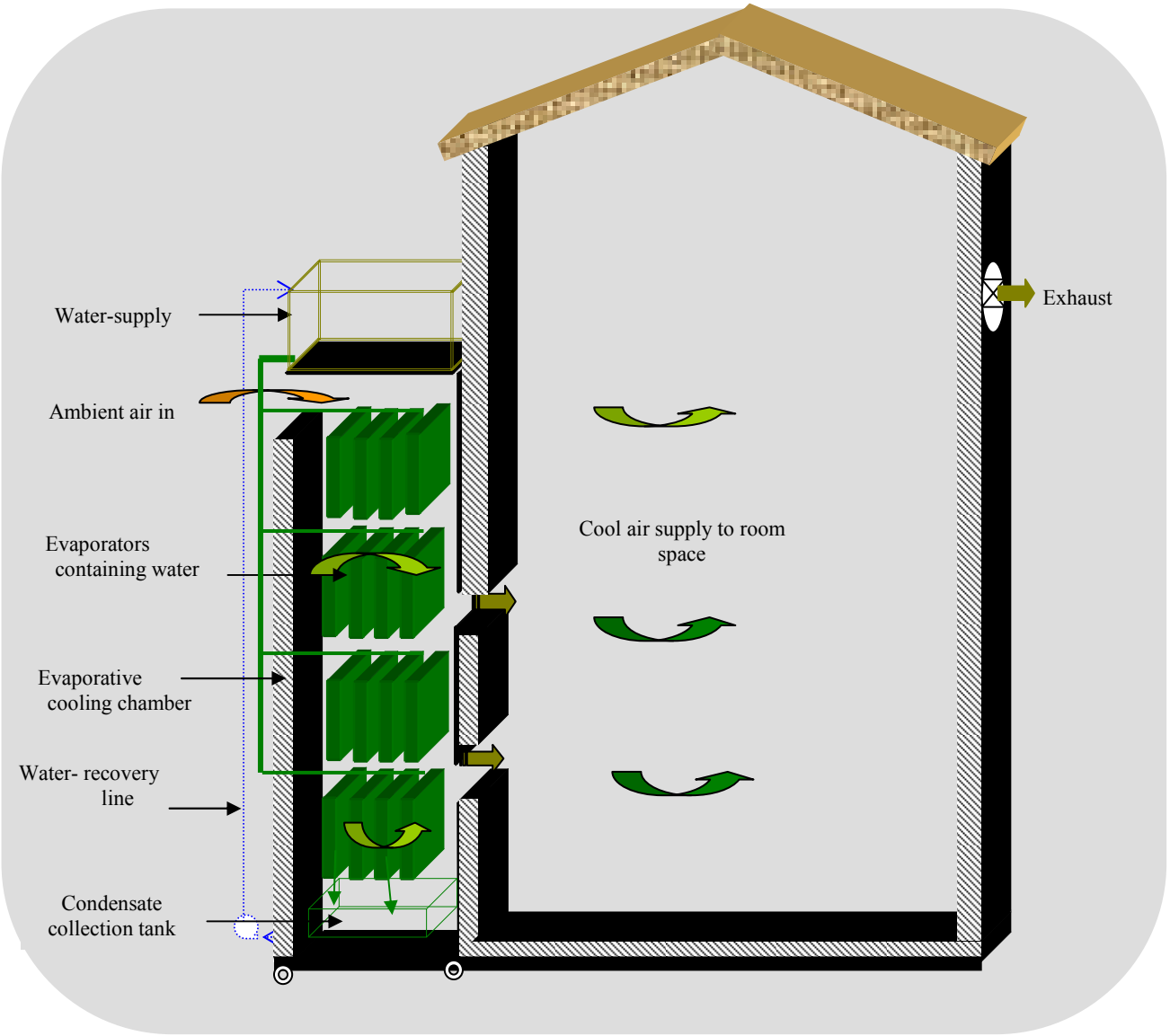

Figure 4.26 Schematic arrangement of "porous- ceramics" evaporative cooling unit attached to cool building space

4.7 Summary

This chapter discussed experimental work on evaporative cooling using porous ceramic evaporators for two types of system configuration. The systems were classified according to the way installed in the evaporative cooling chamber and were termed as the stacking wall and the hanging or supporting frame system configuration. Each of the systems was tested in an environmental control chamber under varying inlet dry bulb temperature, relative humidity and air flow. The data recorded was then analysed and main performance features compared with empirical model results. For each of the systems significant temperature drop was recorded. Temperature drop of 9.2^{o}C and 10^{o}C for the stacking and hanging configurations were respectively observed. The relative humidity outlet values were affected by the initial inlet conditions and the effective surface area of the ceramic evaporators.

One of the novel features observed in this research is the fact that the water consumption from ceramic evaporator surface is much less than other evaporative cooling systems. Comparison with theoretical model developed for water consumption rate of a wet surface showed considerable lower consumption when ceramic containers were used for evaporative cooling.

Also by making a batch feed by gravity the use of water circulating pump is eliminated. The novel advantage here is less energy consumption, little noise due to pump and ease of operational maintenance. Comparatively the two systems showed similar values of cooling capacity on the basis of their effective surface areas.

From the operational and maintenance perspective the hanging system has more advantage because failure of a single evaporator or row can not affect the

others. In terms of water feeding the stacked wall arrangement was easier because of the interconnection of the feeding holes.

Research and development of porous ceramic evaporators have shown that the technology can be applied for cooling of office and domestic buildings in the hot and dry parts of the world. Mathematical model equations are very helpful in evaluating the performance of the system for a more effective sizing and optimisation.

The experimental and theoretical analysis presented in this chapter provides a guide in the selection, sizing, improvements and applications of porous ceramics to match different capacities of building space evaporative cooling requirements.

CHAPTER 5

Experimental Investigation of Integrated Porous Ceramics Evaporative Cooler with Thermoelectric Cooler

5.1 Introduction

Evaporative cooling using porous ceramic was experimentally investigated as discussed in chapter 4. Encouraging results in terms of temperature reduction and cooling effectiveness were reported. In this work thermoelectric based cooling unit was integrated in to the evaporative cooling system containing porous ceramic evaporators. The warm inlet air cooled in the porous ceramics' evaporative cooling chamber was passed over the hot-side fins of the thermoelectric cooling device to act as a better heat sink. This increased the coefficient of performance, (COP) and is a measure of reducing high humidity associated with direct evaporative cooling applications. It also minimises material failure resulting from higher temperature generated at the hot side when a thermoelectric unit is in operation. The system was subjected to various psychrometric test conditions consisting of varying the inlet temperatures and relative humidity. Typical test results showed that the cold side temperature of thermoelectric unit was $5^{o}C$ lower and the hot side was $10^{o}C$ lower, respectively when operated on the wet and dry porous ceramics evaporative cooling chamber. The overall system performance is discussed and presented in this chapter.

5.2 Materials

The major materials used in these investigations are the porous ceramic and a thermoelectric base cooling unit and are described in the following sections.

5.2.1 The porous ceramic evaporation unit

For this work similar units of porous ceramic evaporators (Elfatih et al, 2003) used in the previous investigations in chapter 4 were used. Such unit is shown in Figure 5.1.

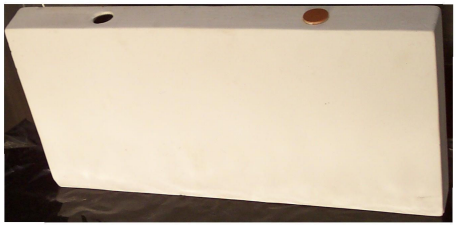

Figure 5.1Typical porous ceramic evaporator used as heat sink

5.2.2 Description of thermoelectric cooling system

Thermoelectric device works on the basis of Peltier effects to achieve cooling or heating. This means that when a DC source passes through a cell made of **n**-and **p**-type semi conductor materials, one of the junctions will be cooled while the other becomes heated depending on the direction of the current as illustrated in Figure 5.2. Therefore the device requires a power source and heat sinks to dissipate the energy generated or absorbed at the two junctions. (Omer et al, 2001). The use of thermoelectric for air conditioning is becoming more popular because they are environmentally friendly. However there is still need for improving the cooling capacity and efficiency of their performance.

For this research a standard 2kW electric fire already modified to house a thermoelectric cooling device that was rated to deliver 440W of cooling in summer was used. Figure 5.2b shows a photograph of the electric fire.

The housing for the thermoelectric unit can be seen at the rear of the fireplace. To integrate this with evaporative cooling the heat sinks fins of the thermoelectric cooler was attached to evaporative cooling chamber containing porous ceramic evaporators.

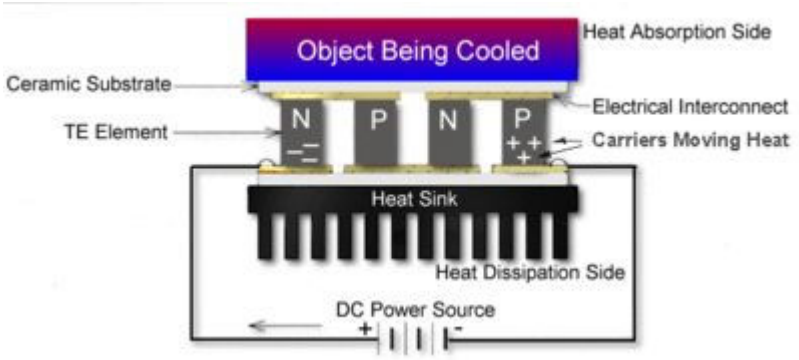

Figure 5.2a Schematic details of a typical thermoelectric cooling system (Thermoelectric Reference Guide)

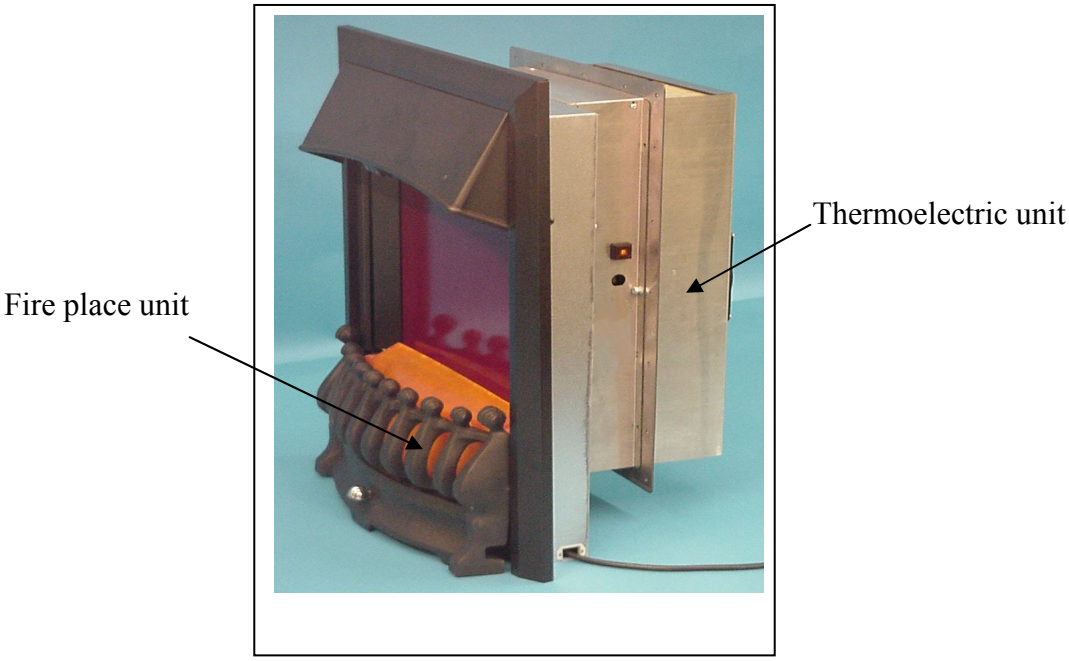

Figure 5.2b Photograph of the electric fire with thermoelectric unit

5.2.2.1 Thermoelectric heat sink.

Two ways of improving TEC efficiencies or COP are improving the material used in constructing the TE and provision of better or very effective hot-side heat sinks while the former has to be at the design and manufacturing stages the latter can be applied to the existing commercial systems. Figure5.3a shows the basic structure of a thermoelectric unit and Figure5.3b shows the exposed unit with cooling fins. A heat sink is a vital component of a thermoelectric air conditioning (TEAC) system that has a very important role in the total system performance. The overall performance of TE systems are related to the temperature of a heat sink and should therefore be given careful consideration. The COP of TEAC can be raised by improvement of thermoelectric materials and optimum design of the hot side heat sinks, (Riffat et al, 2005).

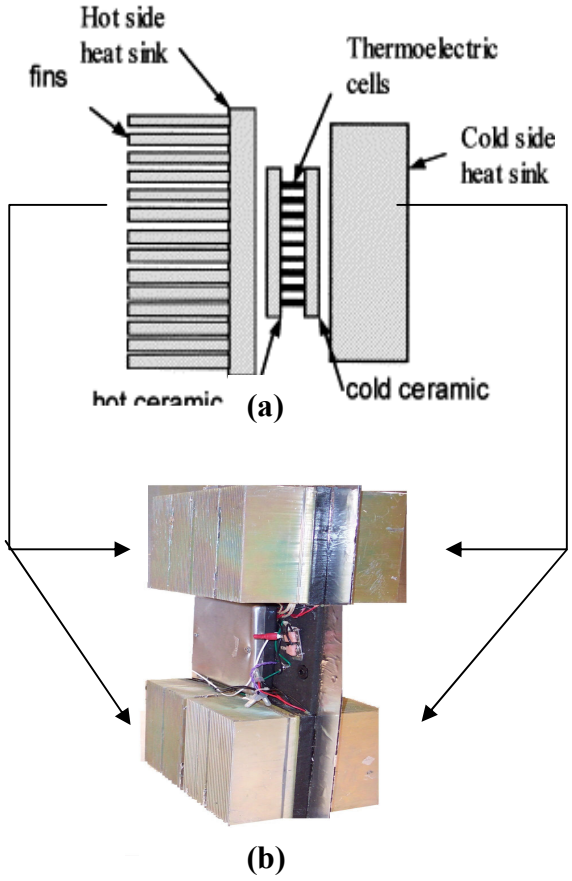

Figure 5.3 Structure of a thermoelectric system

The best heat sink is the one that can absorb unlimited quantity of heat with little increase in temperature. However in reality this cannot be possible since it is always desirable to minimise the temperature of the heat sink. Temperature rise of 5^{o}C to 15^{o}C above ambient (or cooling fluid) is typical for many thermoelectric applications. A fan or blower can be used to remove the waste heat from the TE heat sinks and dissipate to the ambient. For optimum performance in this case the housing of an axial fan should be mounted a distance of 8-20mm from the fins. Figure5.4 shows a typical cooling arrangement using a fan, (Thermoelectric Reference Guide). Also the heat transfer from the two junctions of a thermoelectric cooler can be of many forms as shown in Figure 5.5 (Omer et al. 2001). Other configurations may be considered depending on the application. As can be seen in the figure heat sinks can be air, liquid, solid cooled or a combination of different fluids but they are generally categorised as air- cooled and liquid-cooled heat sinks.

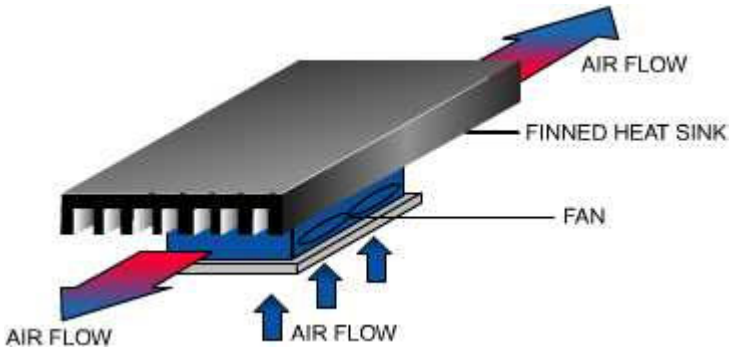

Figure 5.4 Typical forced convection heat sink showing preferred air flow (Thermoelectric Reference Guide)

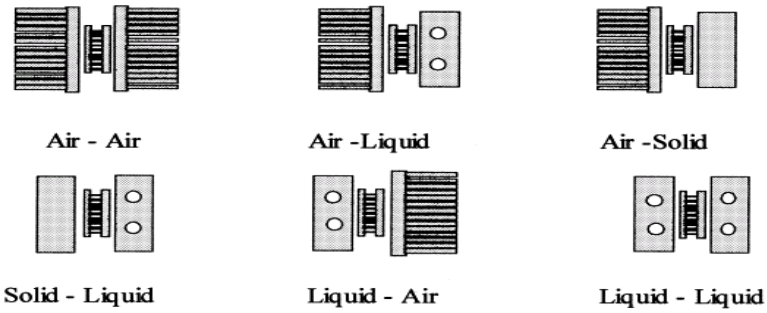

Figure 5.5 Different heat sinks from the junctions of thermoelectric module

Air movement in air–cooled heat sinks can be achieved by natural or forced convection. Natural convection heat sinks are only useful for low power applications and mostly have a thermal resistance greater than 0.5^{o}C/W and often exceeding 10^{o}C/W. The following considerations are vital when installing a natural convection heat sink:

(1) Long dimension of the fin should be in the direction of air flow and not perpendicular to it.

(2) All significant physical obstructions to air flow should be avoided. The forced convection heat sink is probably the most commonly heat sinking method in thermoelectric cooling.

The thermal resistance falls within a range of 0.02 to 0.05^{o}C/W. Liquid cooled heat-sinks can provide the highest thermal performance per unit volume and can also exhibit a very low thermal resistance between 0.01 and 0.1^{o}C/W if properly designed (Thermoelectric Reference Guide).However, it me be complex and may require more maintenance for a long term operations. Based on the above classifications, the natural convection and forced convection for air cooled heat-sinks is shown in Figure 5.6(a) and (b). The liquid heat sinks also include forced convection water and heat pipe construction as shown in Figure 5.6(c) and 5.6(d) respectively (Riffat and Qiu, 2006).

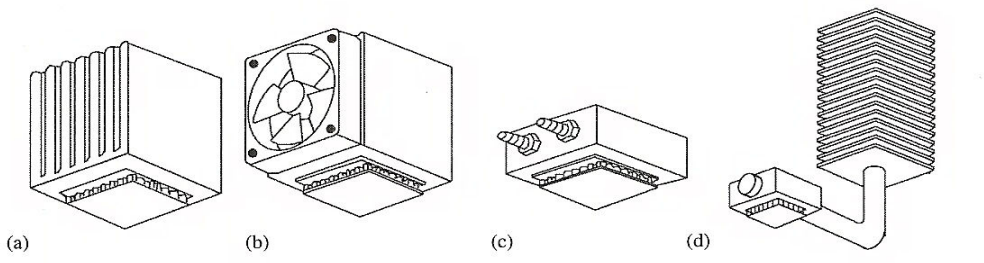

Figure 5.6 Different designs of heat sinks

5.2.3 Description of thermoelectric integrated system

This is a new idea of using air cooled by evaporation to act as a heat sink for thermoelectric air cooling applications. The method can be expanded and applied to conventional power plants with possible prospects of reducing the water consumption than the conventional cooling towers methods. The novel integrated system is schematically shown in Figure 5.7a and the air flow diagram in Figure 5.7b. The system consists of a chamber containing porous ceramic evaporators and an overhead water supply tank. This chamber is made up of a rectangular wooden box of 70cm x 50cm cross-section and a vertical height of 165cm, mounted on wheels for easy movement if required. It is thermally insulated outside with a 25mm-thick polyethylene insulation sheet to make the system function under adiabatic condition. The water from the tank fills the evaporators to provide wet surfaces required for evaporation. At the bottom of the box is a condensate tank, which collects the condensate falling from the surface of the evaporators. The thermoelectric unit is a commercial Valor model-802 type. A wooden casing was made to accommodate it and then insulated at the outside after it has been attached to the evaporative cooling chamber. It was installed such that the hot fins project in to the outlet channel of the evaporative cooling chamber.

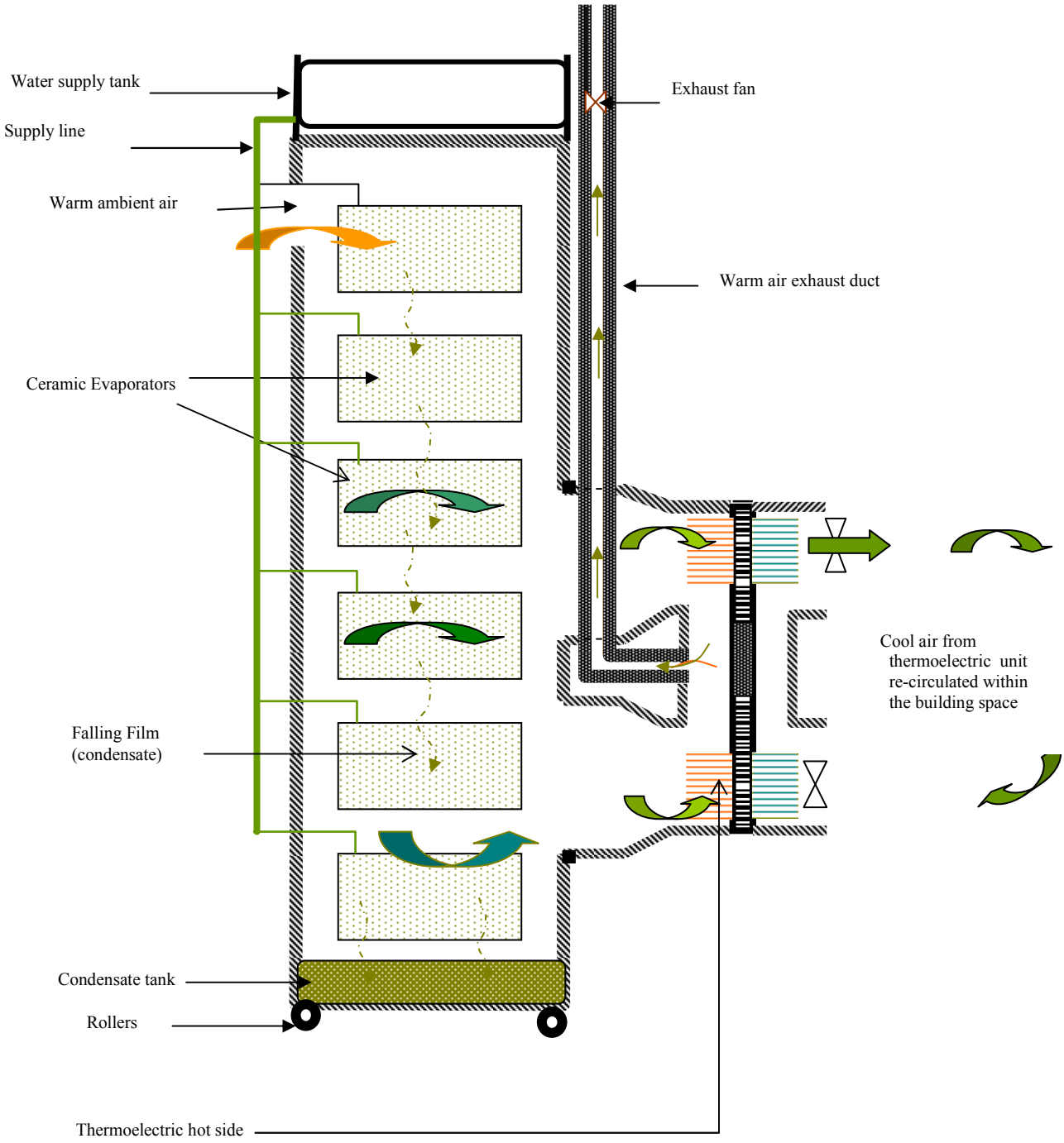

Figure 5.7a Section of ceramic evaporators and thermoelectric integrated cooling system

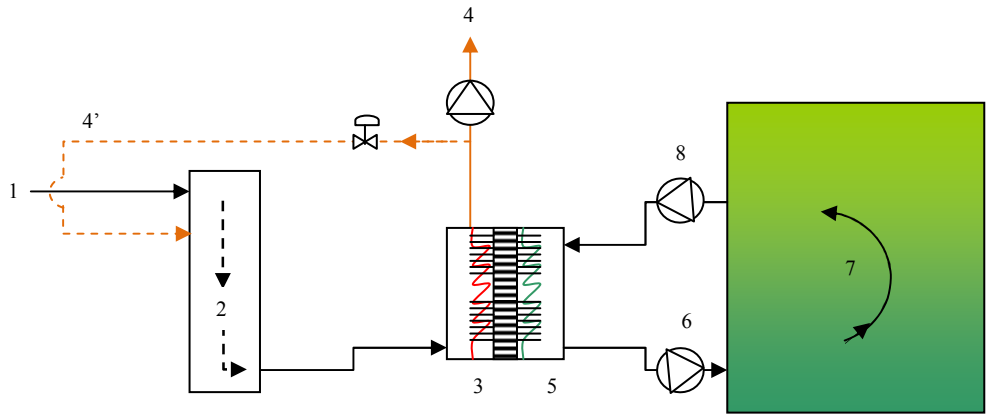

[Key: 1-ambient air inlet; 2-porous ceramics' evaporative cooling unit; 3-heat-sink fins of the thermoelectric unit; 4-warm air exhaust from TE heat-sink; 4'-exhaust air returned to inlet; 5-cooling fins of the thermo electric unit; 6-cooled air from the TE; 7-space being cooled; 8-returned air to TE]

Figure 5.7b Porous ceramics evaporative cooler and thermoelectri (TE) combined system air flow schematic diagram.

5.3 Performance Calculation Model

Detailed mathematical model was developed for the simulation and performance evaluation of a thermoelectric system, (Riffat et al, 2006) and based on the model the following relationships were selected.

- Heat balance equations across the heat sink:

$$T_c = T_{in} - Q_c R_c \quad \text{(for cooling mode)} \tag{5-1}$$

$$\text{Therefore, } Q_c = (T_{in} - T_c) / R_c \tag{5-2}$$

$$T_h = Q_h R_c + T_{in} \quad \text{(for heating mode)} \tag{5-3}$$

$$\text{Therefore, } Q_h = (T_{in} - T_h) / R_c \tag{5-4}$$

The parameters defined above are expressed in terms of heat sink resistance, (R_c).This parameter can therefore obtained by rearranging any of the equations.

- Average temperature of the cold and hot sides of the thermoelectric modules:

$$T_m = (T_h + T_c)/2 \quad (5\text{-}5)$$

- Temperature difference between the cold and hot sides of the thermoelectric modules:

$$\Delta T = (T_h - T_c) \quad (5\text{-}6)$$

- Power consumption, that is the input electric power is:

$$P = Q_h - Q_c) \quad (5\text{-}7)$$

- Calculation of coefficient of performance (COP) of the system:

Figure 5.7c is performance model diagram of the thermoelectric air-conditioning unit showing the temperatures and heat flows involved in the system operation. The coefficient of performance is calculated based on these parameters, (Riffat and Qiu, 2004).

Basically, the coefficient of performance (COP) of a typical thermoelectric cell system in cooling mode is given as the ratio of the cooling capacity of the system to the electrical energy input to the thermoelectric cells as defined below (Omer et al, 2001).

$$COP = \frac{Q_c}{P} \quad (5\text{-}8a)$$

In the above expression, Q_c *is* the cooling capacity in the cooling mode, while P is the electric power input to the thermoelectric.

However, under the cooling mode operation of a thermoelectric cooler, the following parameters are involved Riffat and Qiu, 2004, and2006):

- The cooling capacity, $Q_c = (mc_p)_c(T_{c,out} - T_{c,in})$.

- The heat rejected in the hot-side heat sink, $Q_h = (mc_p)_h(T_{h,out} - T_{h,in})$.
- The input electric power, $P = Q_h - Q_c$.

Therefore the cooling mode COP_c is expressed as:

$$COP_c = \frac{Q_c}{P} = \frac{1}{\frac{(T_{h,out} - T_{h,in})}{T_{c,out} - T_{c,in}} C_r - 1} \quad (5\text{-}8b)$$

Where, Cr iss the heat capacity ratio and is defined as:

$$C_r = \frac{(mc_p)_h}{(mcp)_c}$$

The heating mode COP_h, is given as:

$$COP_h = \frac{Q_h}{P} = 1 + COP_c \quad (5\text{-}8c)$$

Also the maximum or optimum coefficient of performance of a simplified model can be expressed as a function of cold side, hot side temperatures and the figure of merit of the thermoelectric material, that is T_c, T_h, and z, respectively (Gao et al, 2000 and Riffat et al, 2000).That is:

For cooling mode, $COP_{c,opt}$:

$$COP_{c,opt} = \frac{T_c}{T_h - T_c}\left(\frac{\sqrt{1+ZT_m} - \frac{T_h}{T_c}}{\sqrt{1+ZT_m}+1}\right) \quad (5\text{-}9a)$$

Similarly for heating mode the optimum coefficient of performance can be expressed as:

$$COP_{h,opt} = \frac{T_h}{T_h - T_c}\left(1 - 2\frac{\sqrt{1+ZT_m}-1}{ZT_m}\right) \quad (5\text{-}9b)$$

Where: Tm is the average temperature as defined in equation (5-5).

Z is a comprehensive parameter describing the thermoelectric characteristics. It is the figure of merit and its value relates to the physical properties of the thermocouple material. The greater its value, the better the thermo electrical material is. It is defined as:

$Z=\acute{\alpha}^2/K_tR_t$ [1/K]

Where: ά is Seebeck coefficient [Volts/Kelvin]

K_t total thermal conductance of thermoelectric components [Watt/cm Kelvin]

R_t total electrical resistance of thermoelectric components (resistivity) [Ohm cm].

Typical approximate figure of merit (Z) for the following thermo electric materials at different temperatures are shown in Figure 5.7d (Ferrotec, 2001-2008):

-Bismuth Telluride (Bi_2Te_3),

-Lead Telluride (PbTe),

-Silicon Germanium (SiGe),

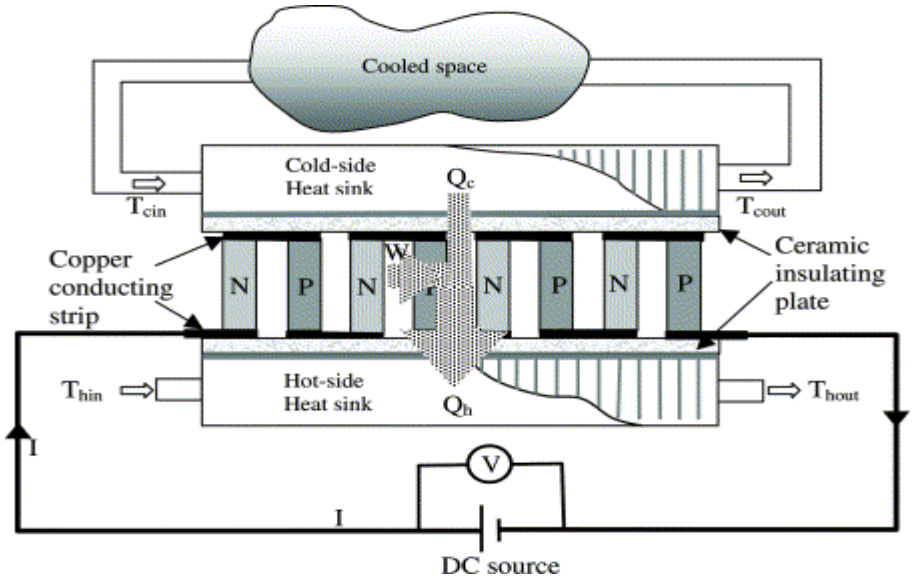

Figure 5.7c Performance model schematic of the thermoelectric air-conditioning system

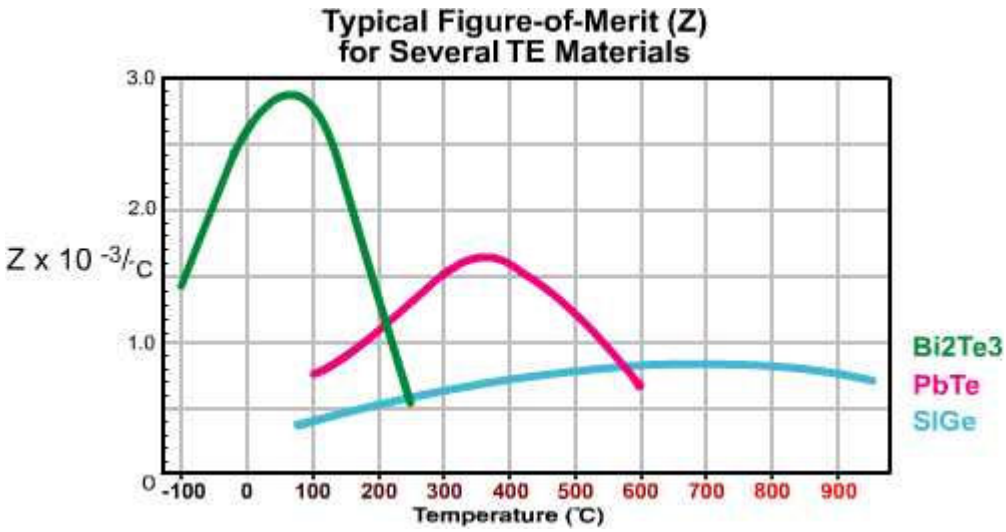

Figure 5.7d Approximate figure of merit (Z) values for some thermoelectric materials at various temperatures (Ferrotec (USA) Corporation- http://www.ferrotec.com/technology/thermoelectric/thermalRef02/)

Typical material property coefficients and geometry factor for modelling thermoelectric system are shown in Appendix, Ac5.

5.4 Experimental Set-Up

5.4.1 Description of the experimental set-up

In the present experiment thermoelectric unit is integrated in to the porous ceramic evaporators' evaporative cooling system. The system integration concept is illustrated in Figure 5.7a. It is shown that the air cooled in the porous ceramics evaporative cooling chamber is passed over the hot fins of the thermoelectric cooling device to act as a heat sink. The thermoelectric device is therefore modified from its usual casing and then provided with an air exhaust duct and another casing that makes it more suitable for coupling to evaporative cooling chamber. It was attached so that the hot fins receive cool air from the out let of the evaporative cooling chamber and dissipated to the ambient as demonstrated in Figure 5.8.

Porous ceramics required for the experiment were well secured in the evaporative cooling chamber as partly shown in Figure 5.9. The experimental set up is shown in Figure 5.10 showing a mobile chamber containing porous ceramic evaporators. The chamber had a door for opening and closing to inspect the ceramic coolers. An overhead water supply tank was provided on top of the chamber box. In this way water is supplied to the ceramic evaporators through a feed line by gravity. A condensate tank was located at the bottom for periodic monitoring and control of the condensate level.

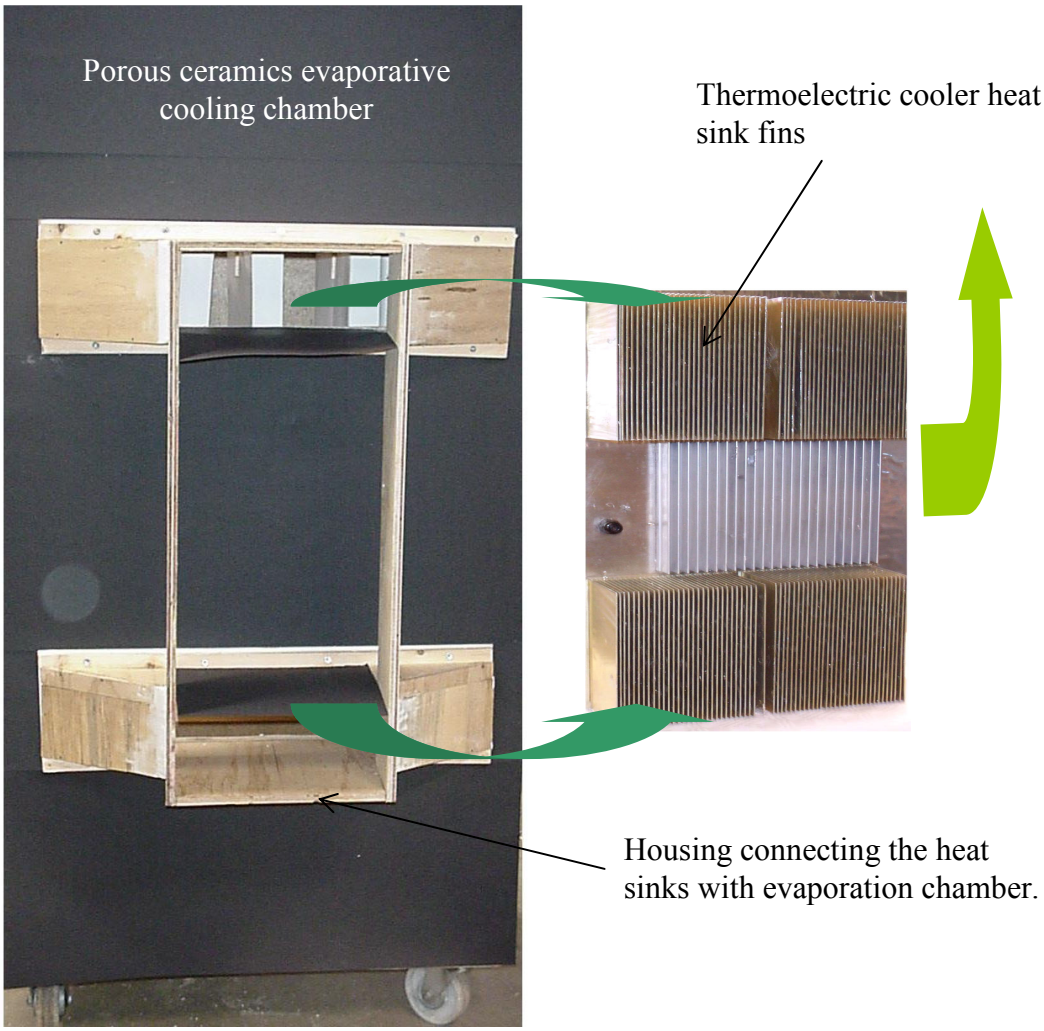

Figure 5.8 Housing for attaching TE heat sinks to porous ceramics evaporative cooling chamber

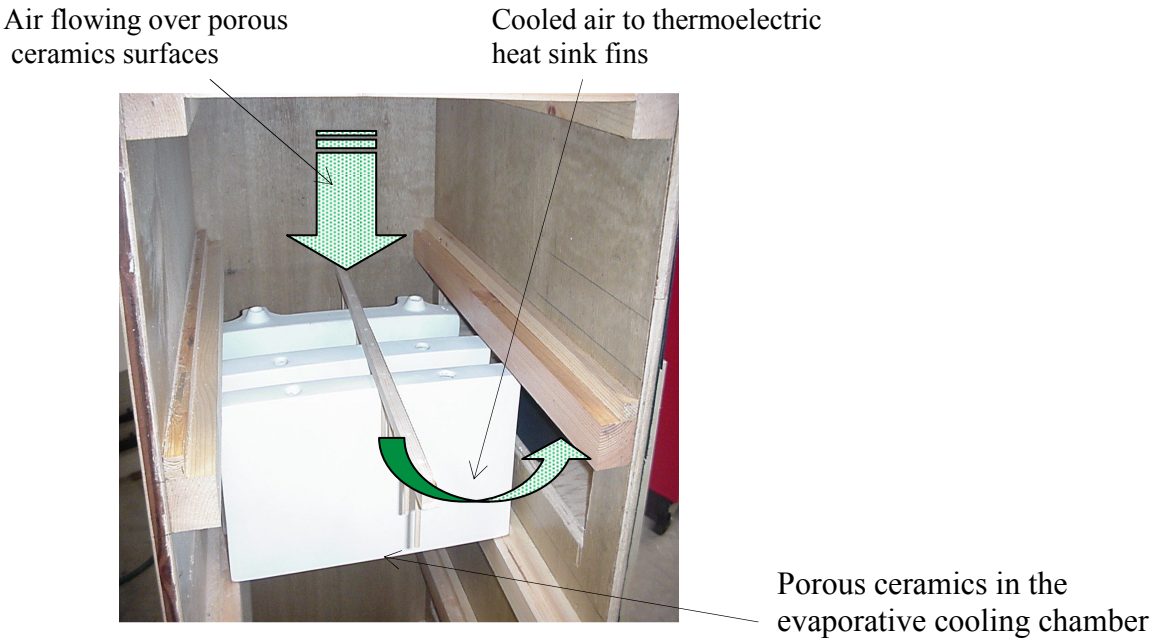

Figure 5.9 Porous ceramics arrangement in the evaporative cooling chamber

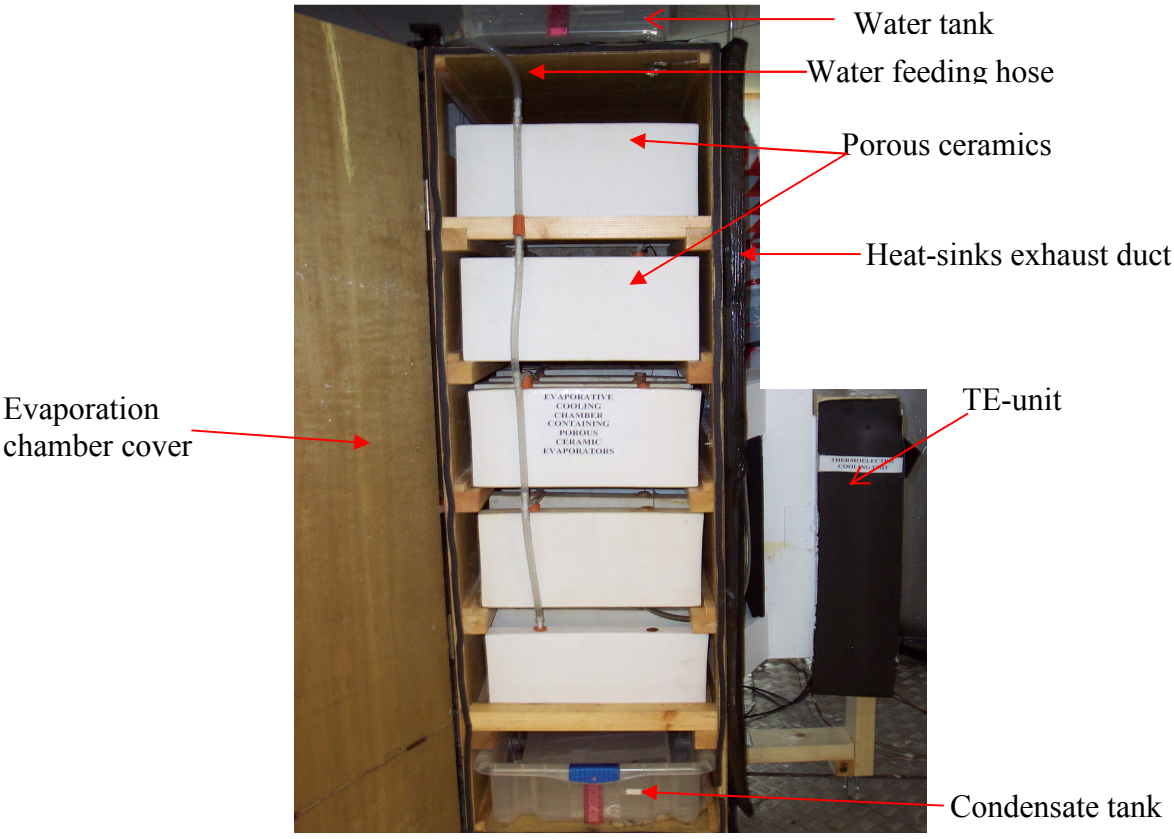

Figure 5.10 Porous ceramics and TE integrated experimental unit. (ceramics chamber opened).

5.4.2 Experimental procedure

Having prepared the experimental set up as discussed, the system was insulated as shown in Figure 5.11.Temperature, relative humidity and air flow measuring instruments used for the porous ceramics experiments in chapter 4 were used here as well. The temperature and relative humidity sensors located at different points of the integrated system were connected to the data taker with channels expansion modules as shown in Figure 5.12. To investigate the performance of the integrated evaporative- thermoelectric cooling system the following tests were carried out:

- Running the system on dry basis first. These tests were conducted at different settings of the dry – bulb temperature and relative humidity in the climatic chamber without filling the ceramics with water to obtain wet surface for the evaporative cooling.
- Running the system after filling the porous ceramic evaporators assembled in the evaporative cooling chamber with water. Again tests were conducted at different settings of the dry – bulb temperature and relative humidity in the climatic chamber. For comparative analysis the same climatic conditions as above were maintained.
- The System was tested at varying input power to thermoelectric unit.
- Maintaining the input power to the thermoelectric unit constant but varying the airflow rate through the entire system.
- All the above tests were conducted at different DBT and RH settings in the climatic chamber.

The environmental chamber was partitioned so as to separate the set ambient temperature and relative humidity values from the building space required to

be cooled. Insulation was also provided to minimise the infiltrations of theses separated temperature and relative humidity set values.

The warm humid air from the thermoelectric hot side was channelled out. Each dry test was carried out for not more than an hour to prevent overheating of the thermoelectric element, while the wet tests were conducted for several hours and no sign of overheating was noticed.

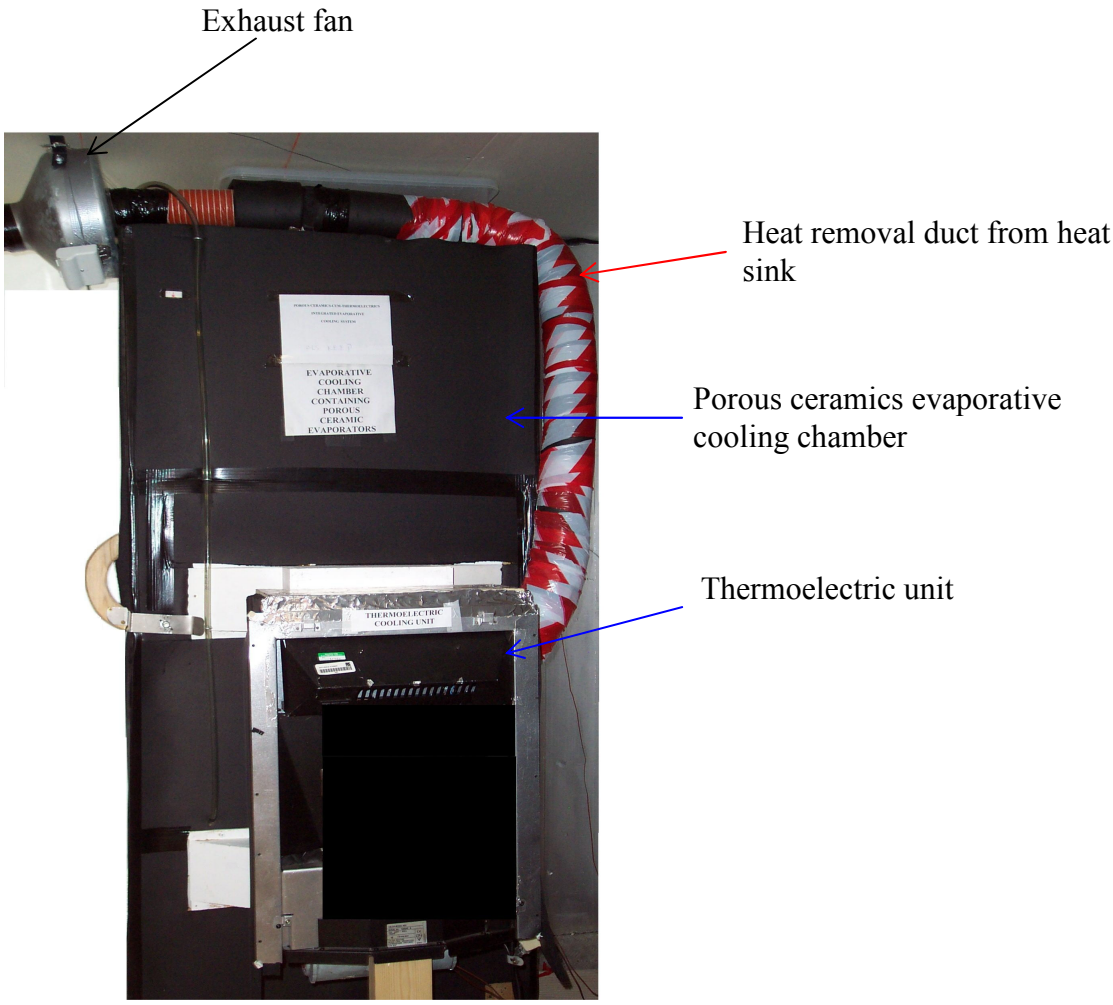

Figure 5.11 Complete system insulated for tests

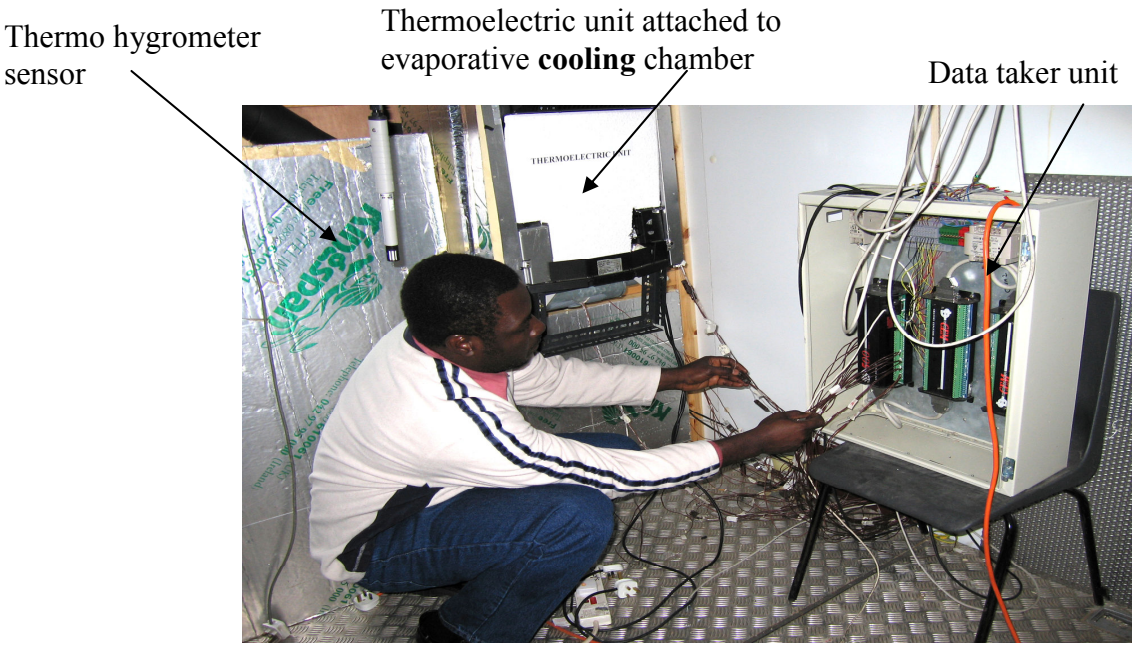

Figure 5.12 Data taker and thermoelectric experimental set-up

5.5 Results and Discussions

First experimental tests were conducted on the thermoelectric unit when the porous ceramics contained in the evaporative chamber were not filled with water. The heat sink fins of the thermoelectric cooler were exposed to dry evaporative cooling chamber. This test was therefore termed as dry test. Under this test, timely variation of cold-side with hot-side temperatures of the system was recorded as well as their respective differences with the ambient shown in Figure 5.13a. Results under this test showed temperature drop between constant ambient and cold side of 20^{o}C, temperature rise between ambient and hot side of 17^{o}C and difference between hot side and cold side of 34^{o}C.

Table 5.1 Results under dry test condition for constant set ambient temperature of 35^{o}C and relative humidity of 40%.

Time (minutes)	$T_{ambient}$ (°C)	$RH_{ambient}$ (%)	$T_{coldside}$ (°C)	$T_{hotside}$ (°C)
0	35	40	21.041	20.577
2	35	40	15.243	32.69
4	35	40	13.076	40.213
6	35	40	13.018	43.695
8	35	40	13.693	45.59
10	35	40	14.356	46.874
12	35	40	14.979	47.689
14	35	40	15.48	48.337
16	35	40	15.52	48.863
18	35	40	15.861	49.283
20	35	40	16.177	49.625
22	35	40	16.428	49.909
24	35	40	16.681	50.141
26	35	40	16.902	50.37
28	35	40	17.09	50.57
30	35	40	17.226	50.774
32	35	40	17.328	50.895
34	35	40	17.432	51.017
36	35	40	17.566	51.166
38	35	40	17.669	51.288
40	35	40	17.747	51.359

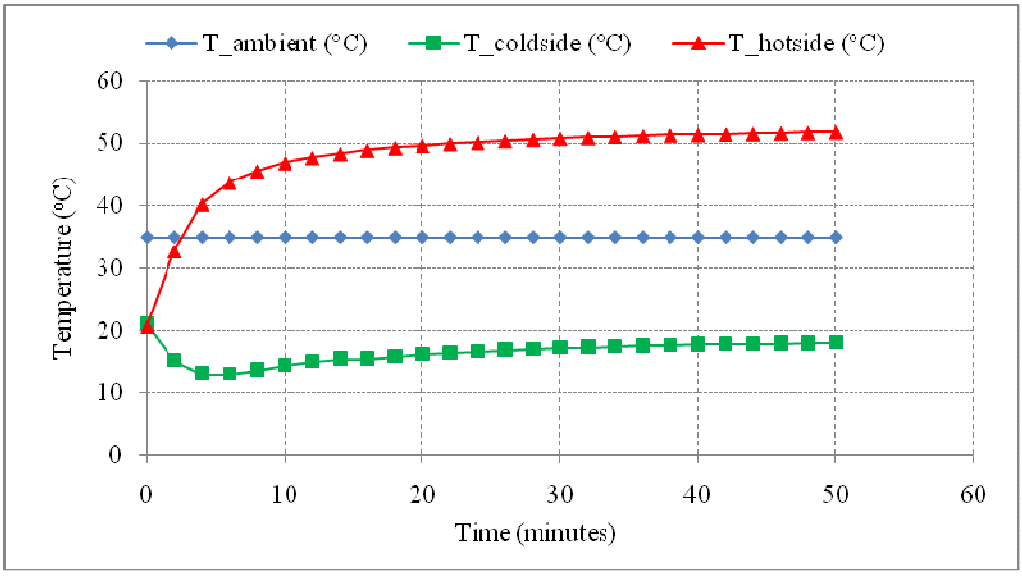

Figure 5.13a Difference between hot and cold sides temperatures of the thermo electric unit under dry test condition (i.e. when the porous ceramics were not filled with water)

Figure 5.13b shows the distribution of both the temperature and relative humidity for the system in relation to the set inlet conditions of 30°C and 40% for temperature and relative humidity respectively after attaining steady state. The system stabilises at a maximum hot side temperature of 52°C and cold side temperature of 18°C that is having a temperature difference of 33°C, which results in low coefficient of performance. This also shows a need for better heat sink to prevent material failure due to over-heating when long-term system operation is required.

After the dry test discussed above, the porous ceramics in the evaporative cooling chamber were then supplied with water to provide wet surfaces for the evaporative cooling. This is termed as wet test. Variation of the temperature and relative humidity values were recorded. Temperature

profiles of these results are plotted in Figures 5.14a. In this case the hot side and cold side temperatures stabilises at 13.2°C and 42°C, respectively.

These values are lower than the above stated values for the dry–tests. Dry tests as mentioned were the tests carried out before filling the ceramic evaporators with water. Also here the COP value of about 1.4 was calculated using equation 5-8b as shown in Figure 5.14b. A bar chart representation of the comparative performance result is shown in Figure 5.15. The results showed that after running the system under wet test the temperature drops were found to be 5°C and 10°C for the cold and hot side respectively lower than the tests conducted under the dry tests. Figure 5.16 shows the gradual temperature rise and cooling to equilibrium in relation to initial set the ambient temperature, sometime after the test run.

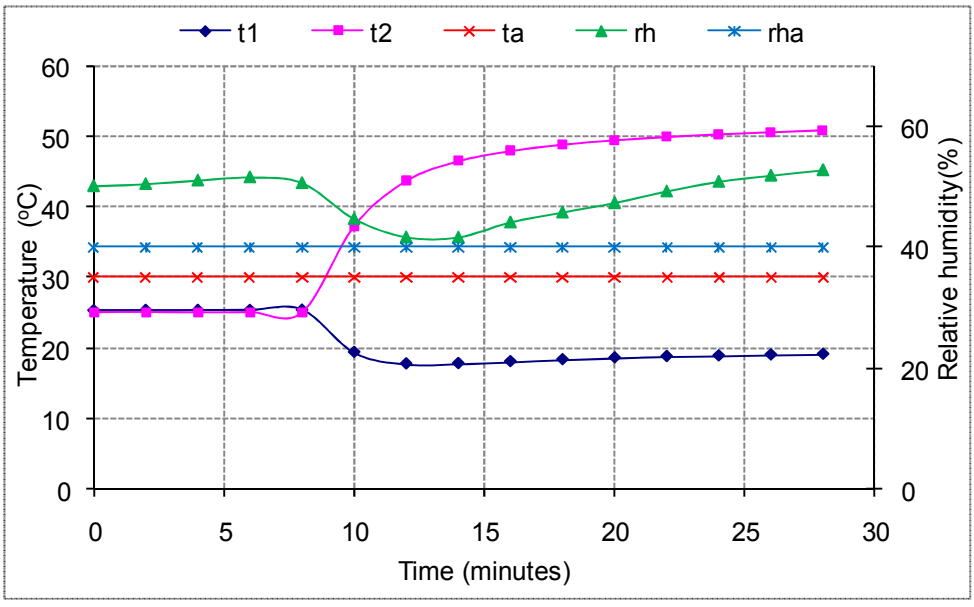

Figure 5.13b Variation of temperature and relative humidity under dry test [t1-coldside, t2-hotside, ta-ambient temperature, rh-relative humidity at thermoelectric exit, rh-ambient RH]

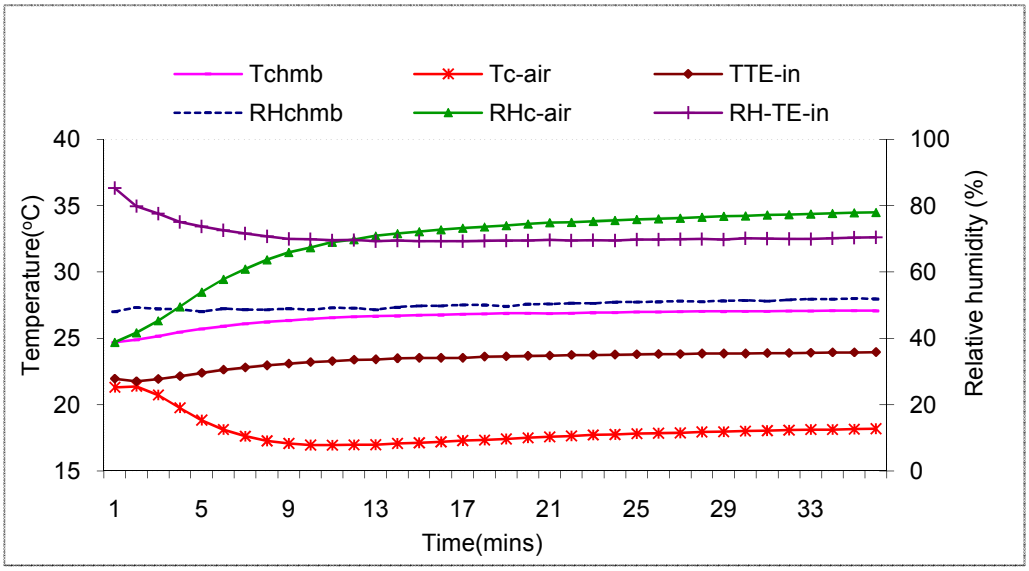

Figure 5.14a Temperature and relative humidity variations with time for the integrated system under wet- running condition

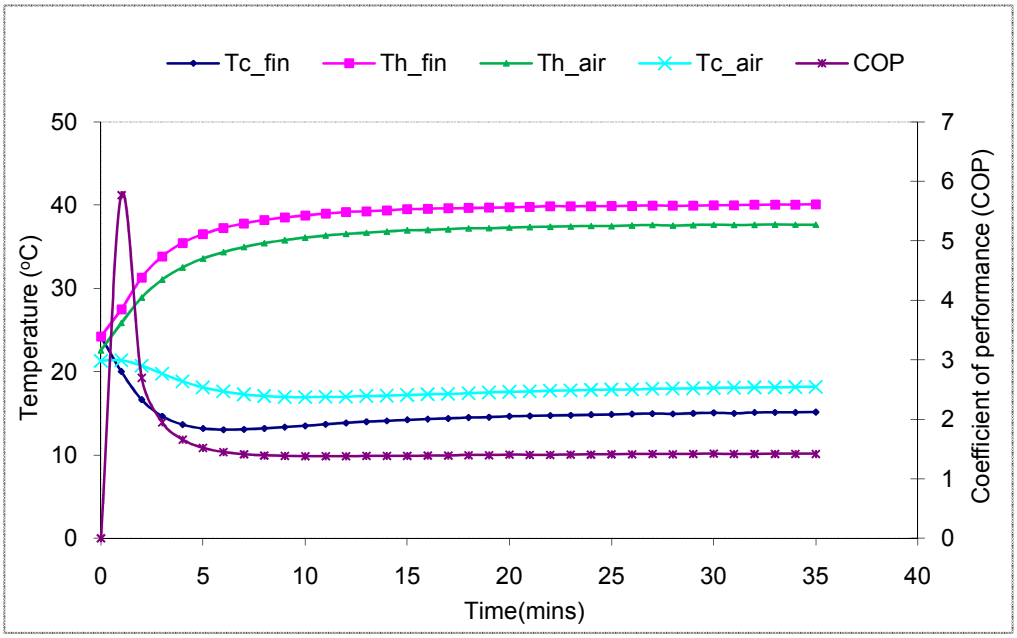

Figure 5.14b Timely variation of hot-side and cold-side temperatures for the thermoelectric pellets and the corresponding surrounding air when ruuning with evaporative cooling heat-sink (wet test case).

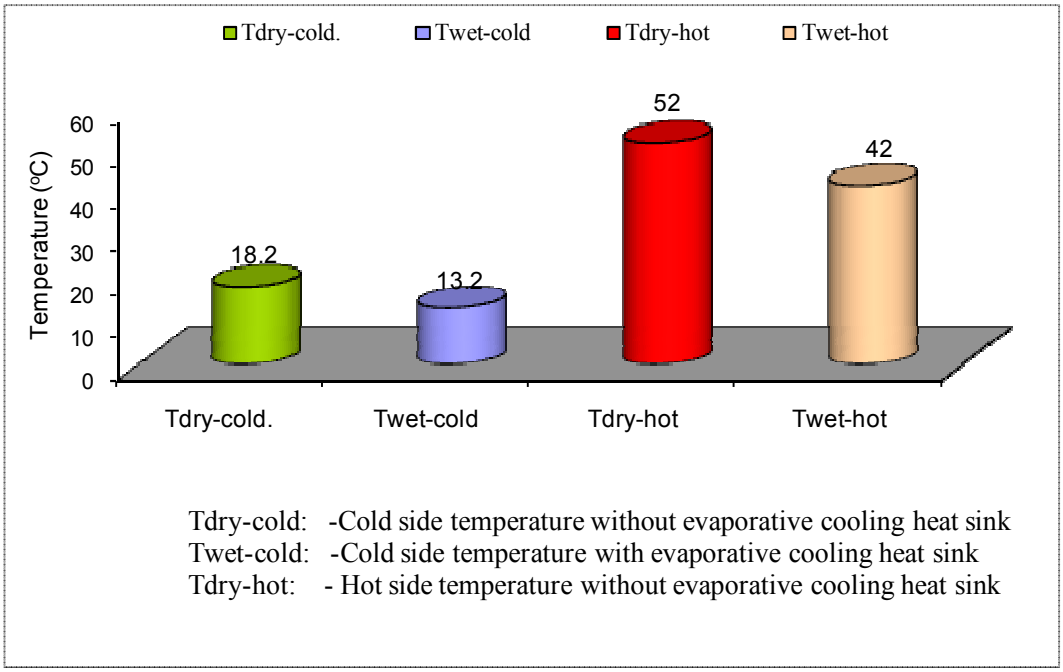

Figure 5.15 Comparative temperature profiles for TE test with dry and wet evaporative cooling chamber

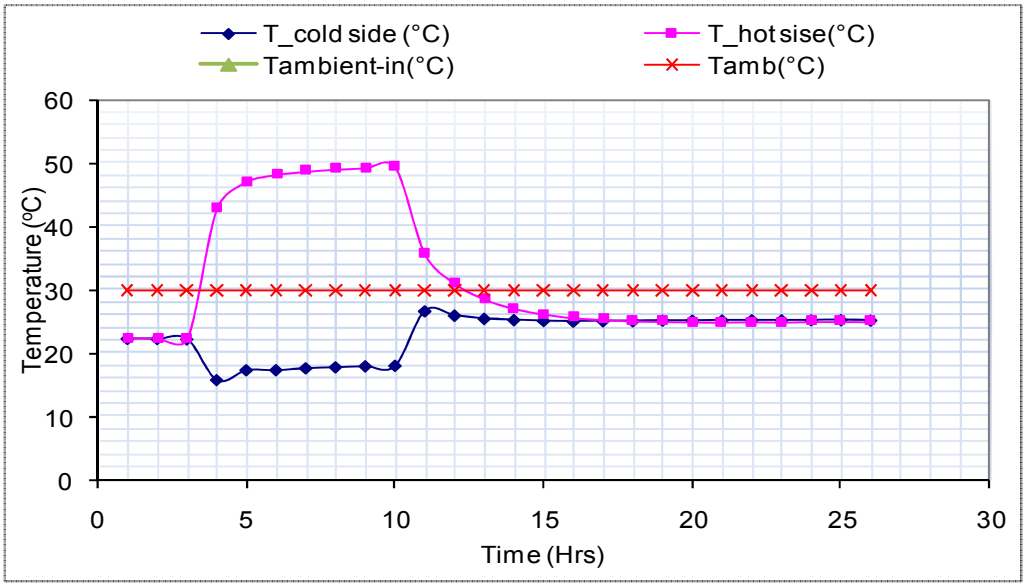

Figure 5.16 System hot side and cold side temperature difference during and after operation

5.6 Summary

Tests results and other reports have indicated the suitability of evaporative cooling in situation where increase in humidity can be acceptable. However, integrating the system with thermoelectric unit provides brighter prospects for the application of the system under different environments. The results obtained from these tests gave an indication on the need for having an integrated system, which can provide cooling within acceptable degree of temperature and relative humidity variations.

In this novel integrated system the evaporative cooling part provides the sink temperature needed for improving the efficiency of the thermoelectric cooler. This indicates that the system can also be applicable as a heat sink for other thermal devices and does not require continuous water circulation. Hence this is a new contribution to knowledge that has not yet been exploited in these types of research investigations.

CHAPTER 6

Development and Performance Investigation of Novel Fibre-Tubes Indirect Evaporative Air Cooler

6.1 Introduction

Direct evaporative cooling often results in increased relative humidity, which may lead to poor thermal comfort. Indirect evaporative cooling offers a solution but its efficiency requires improvement. A novel idea of using horizontal tubes arrangement has been considered. In this case, it is not necessary to use a pump to supply the water required to moisten the evaporative cooling surface area.

A horizontal system has been constructed and tested under various temperatures, relative humidity values and air flow rates. Results showed that a 6-10^{o}C temperature drop between the inlet and outlet of the product (supply) air could be achieved without too much rise in relative humidity. The increase in relative humidity of the product (supply) air was much less than that of the working air. The novel fibre tube evaporative cooler has the potential to cool a building space with very little addition of moisture.

6.2 Material Selection

Fibrous materials are widely used for evaporative cooling but these have only a limited capillary effect (Al-Sulaiman, 2000). If the cooler is to be positioned vertically, periodic or continuous spraying with water is required during operation. This process adds to power consumption, noise, vibrations and

increases system running costs, as well as construction and operational complexity. In order to select a suitable material the water absorption experiment was conducted on different paper materials that are readily available, environmentally safe and some can be from recycled items.

6.2.1 Paper samples water-absorption comparison tests

Initially ten different paper samples were vertically supported in a tank containing water at the base. They were all subjected to the same test conditions and allowed sufficient time to attain maximum surface wetting height from the base level of the water tank. The sample papers as can be seen in Figure 6.1 are as follows:

(A) Psychrometric energy core (PEC) paper, which was brought from ISAW Company

(B) Micro Heat & Mass Cell Cycle Core (MHM3C) paper comes from a building respirator prototype;

(C) C-kitchen towel;

(D) Toilet hand towel;

(E) Newspaper;

(F) Packing cardboard with vertical channels;

(G) Packing cardboard with horizontal channels;

(H) Aluminium foils lining paper-inner surface;

(I) Waxed paper cover for (F)

(J) Waxed paper covers for (G)

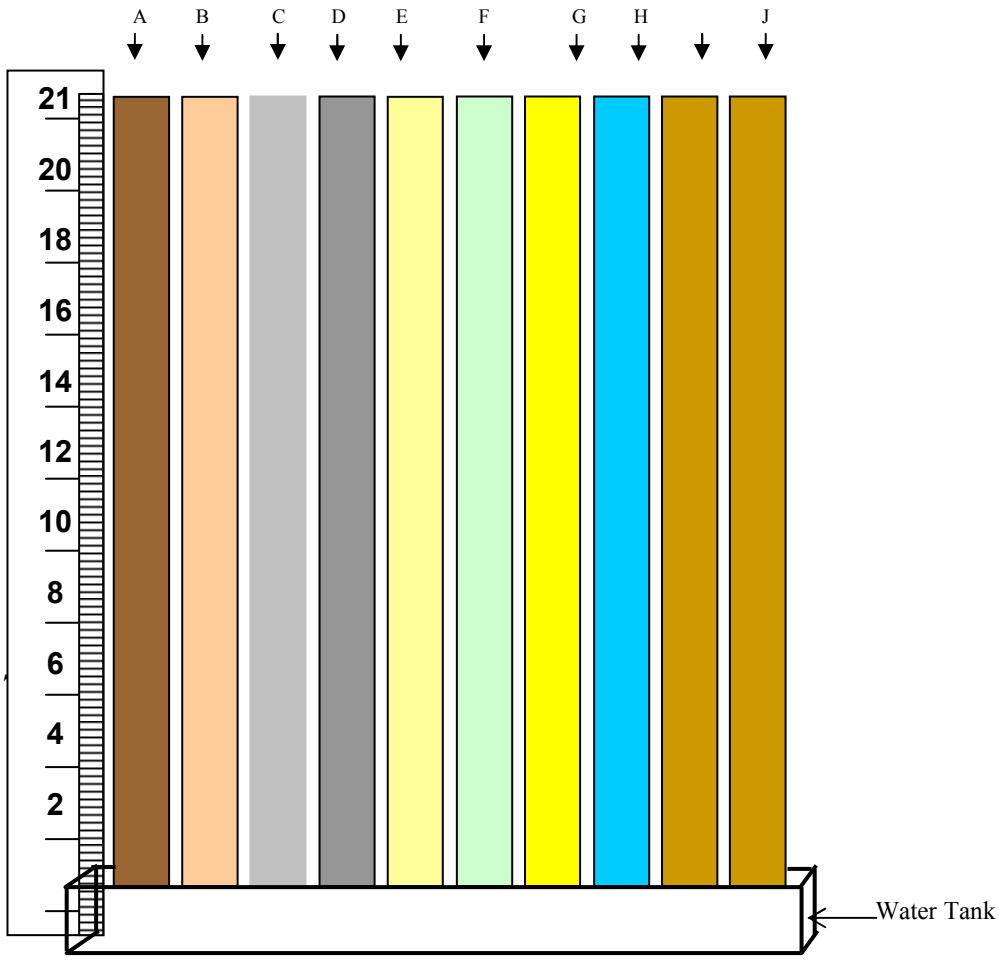

Figure 6.1 Arrangement of paper materials samples for comparative water sorption height tests

6.2.2 Paper samples comparative test results and selection

Out of the nine samples subjected to tests four were found to have attained higher "wet heights" as compared to others. However samples I and J were too low to show any significant reading as could not absorb much moisture. Based on the test results, the measured height of wetted surface from water level is shown in Figure 6.2(a) and 6.2(b). From the tests, C-kitchen towel and D- toilet hand towel are better in water-absorption than A, B. They are also easily to

obtain and are flexible enough to be lined around any tubular surface. Therefore C is selected for this novel evaporative air cooler.

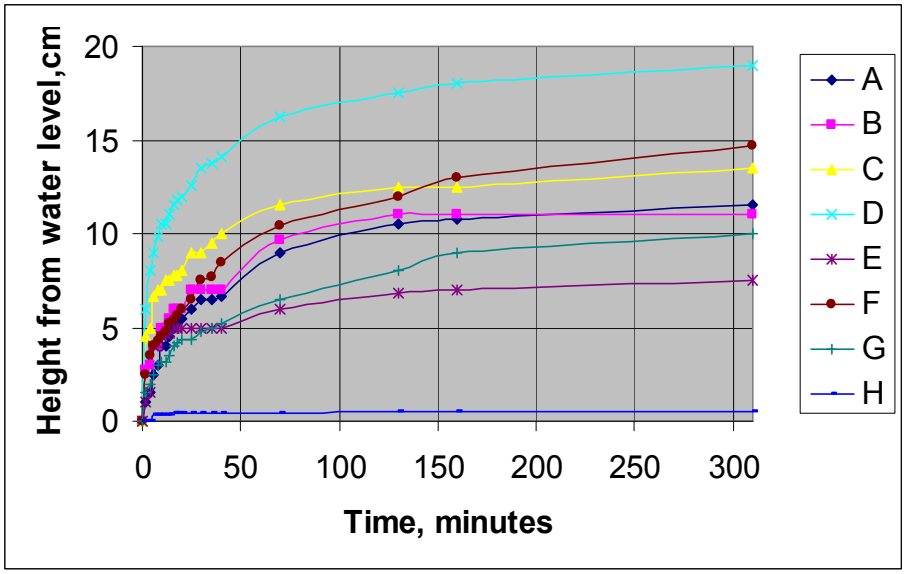

Figure 6.2(a)

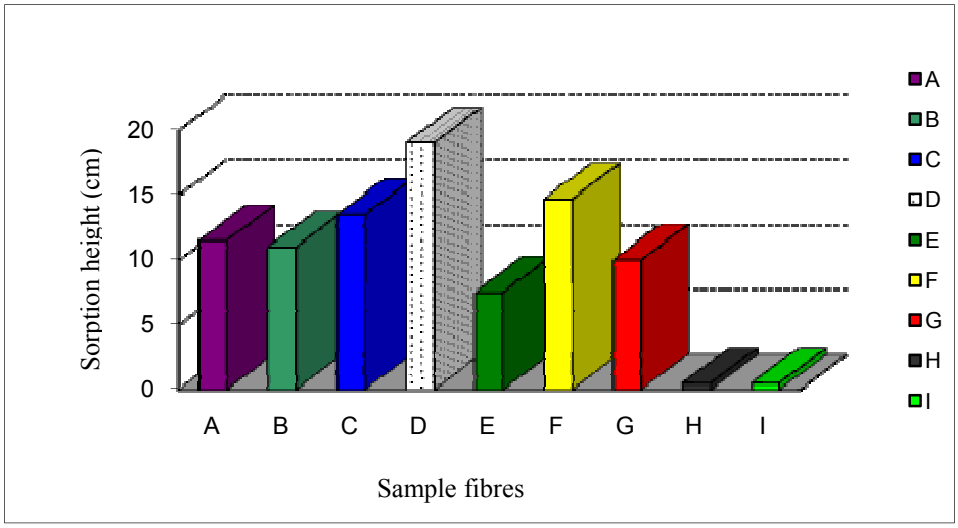

[Key: A-Psychrometric energy core (PEC) paper; B-paper from building respirator; C-kitchen towel; D-Toilet hand towel; E-newspaper; F-packing cardboard with vertical channels; G-packing cardboard with horizontal channels; H-aluminium foil lining paper]

Figure 6.2(a) and 6.2(b) Attainable water sorption heights of different fibre materials

6.3 System Design Features and Construction

Following the selection of the water absorbing material for the cooler as described in the above section the system was then constructed in different stages. Basically the evaporative cooler was made of arrangement of concentric tubes as shown schematically in Figure 6.3 and then assembled in the casing as shown in Figure 6.4

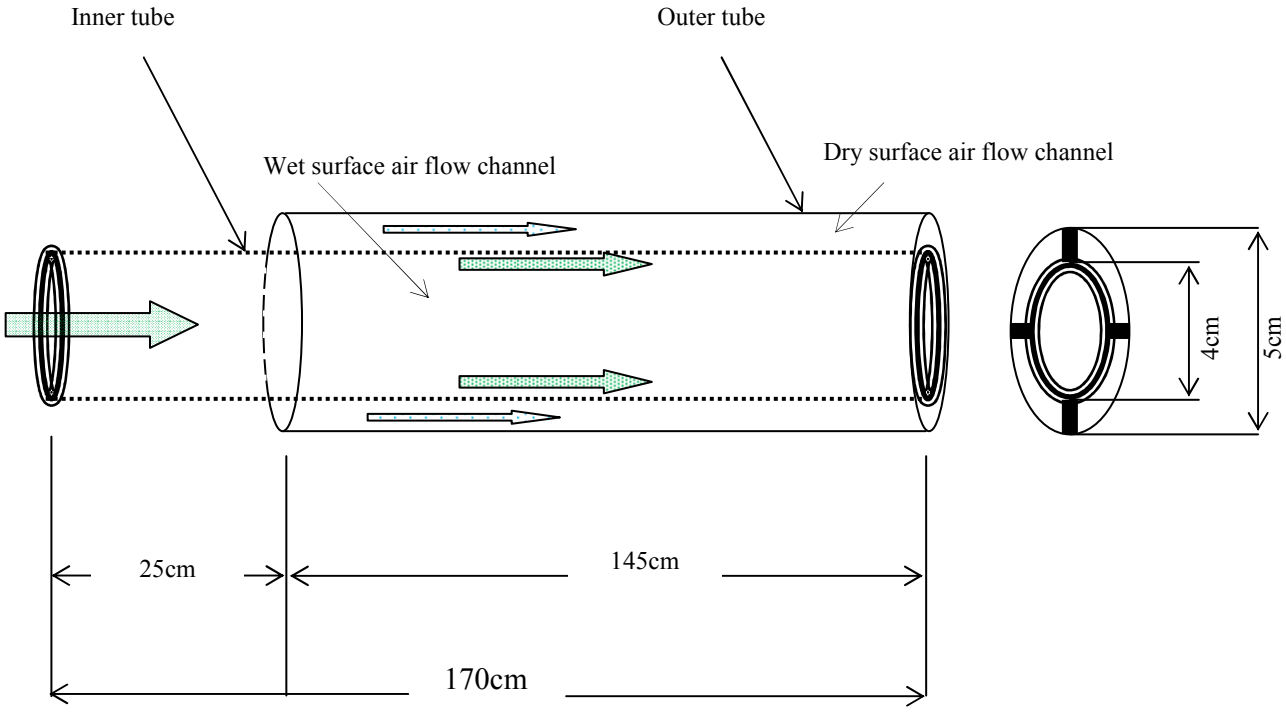

Figure 6.3 Air flow channels and dimensions of the concentric tubes for the evaporative cooler

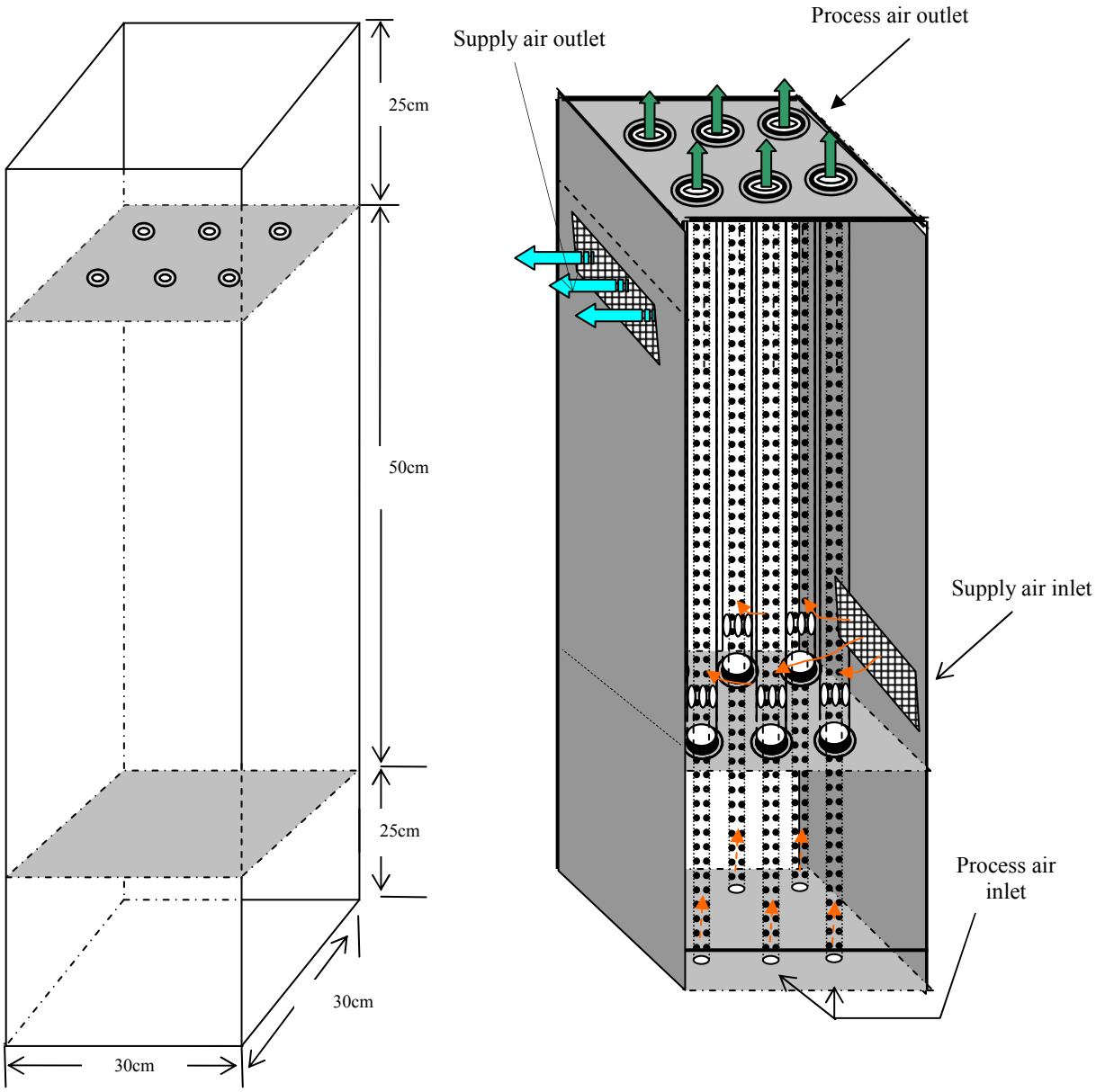

Figure 6.4 Dimensions of the casing and arrangement of the tubes forming the evaporative cooler unit

The tubes preparations formed the main part of the evaporative cooler and construction of each tube involved seven stages which are shown in Figure 6.5 and described as follows:

- (1) Cut the required length of the perforated tube for supporting the paper material which will be applied to form the wet surface of the

evaporative cooler. Each tube has a length (L) of 145cm and a diameter (d) of 4cm.

- (2) Cut the steel tube to form the outer casing. This tube has the same length of 145cm as the above but with a bigger diameter of 5cm.Each end of this outer casing was provided with three holes to make inlet and outlet for the dry air.
- (3) The selected water absorbing paper for making the wet surface was then cut to the required size. It has (L) as the length and (πd) as the width for wrapping around the perforated tube.
- (4) The impermeable paper was cut to the same dimension as that of the above wet surface paper material.
- (5) With the help of thermal adhesive, the wet – surface paper was glued to the impermeable paper.
- (6) The combined wet surface paper and impermeable paper set was wrapped around the perforated supporting frame. This impermeable surface formed the outer surface of the tube and it is the surface area through which the dry air flows.
- (7) The wrapped perforated tube was then inserted in the bigger tube to form a set of concentric tubes. The inner tube formed the wet channel and the annular opening between these tubes formed the dry channel.

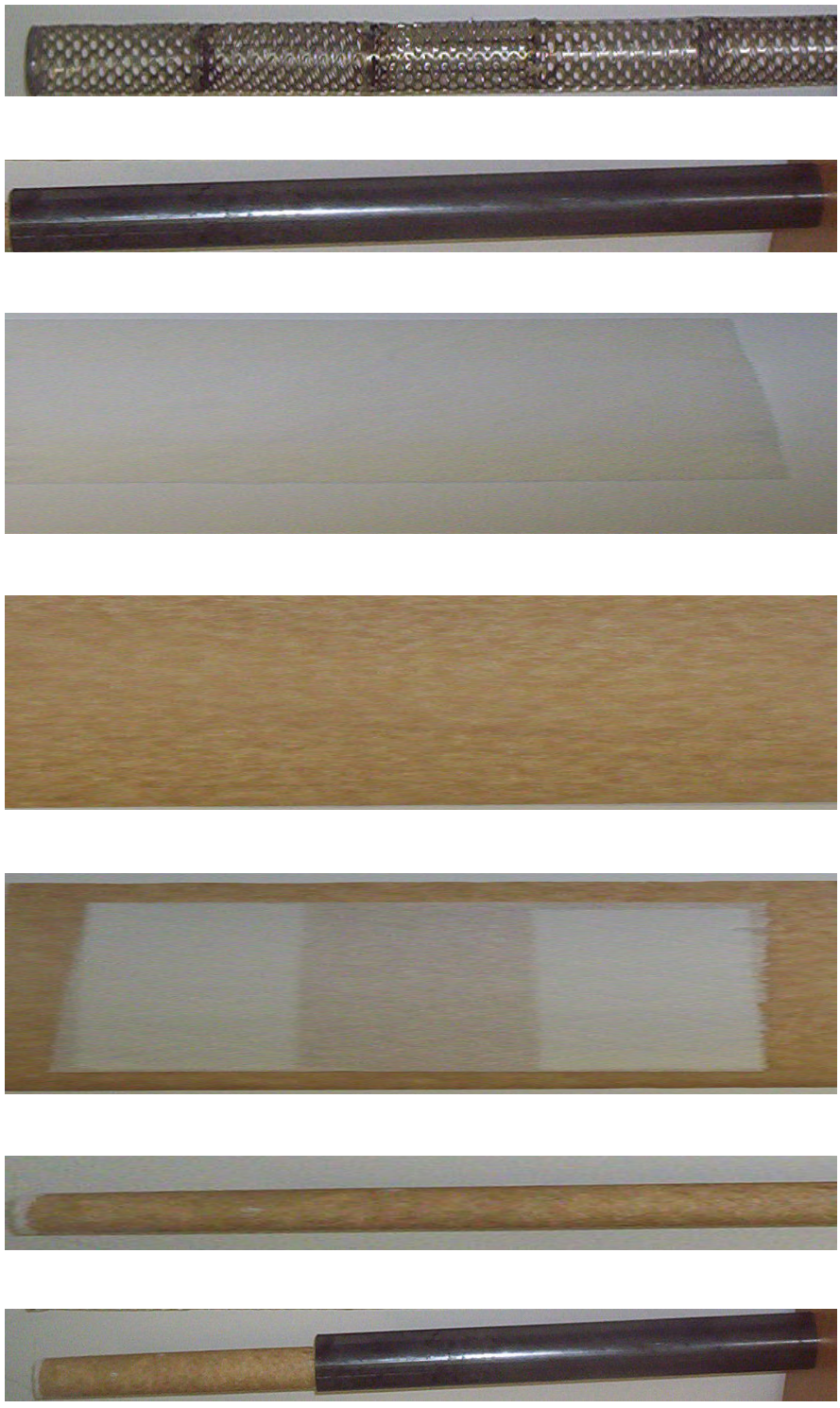

Figure 6.5 Seven steps involved in the construction of evaporative cooler concentric tubes

The seven stages described above made up a complete singular tube for the cooler. The cooler consists of six such tubes arranged in two rows of three

enclosed in a wooden frame as shown in Figure 6.6. Figure 6.7(a) shows the working air outlet after passing through the wet channel holes shown in Figure 6.7(b).

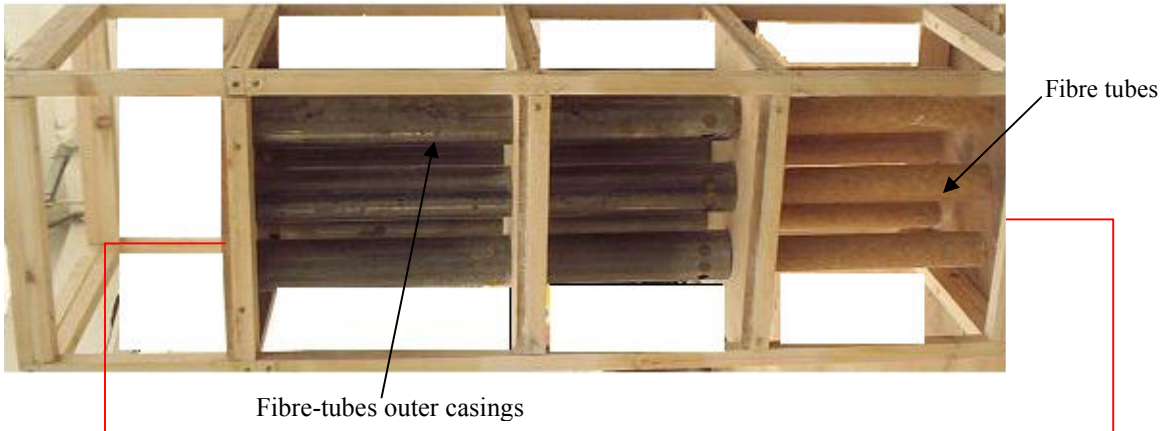

Figure 6.6 An array of the fibre tubes assembled in a wooden frame

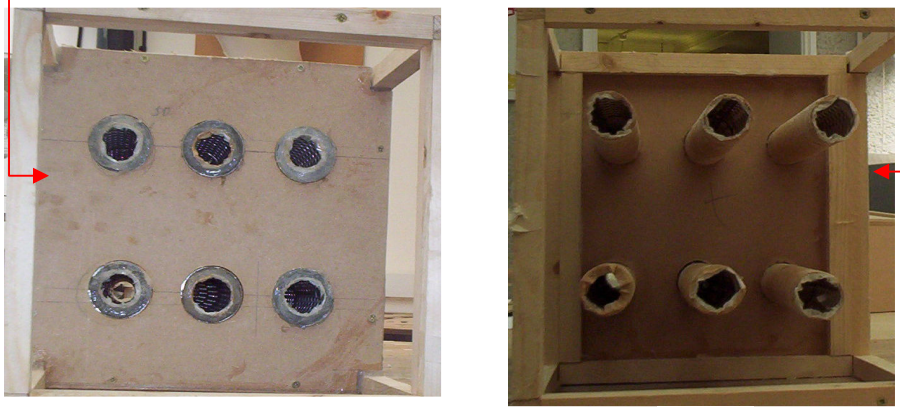

(a) **(b)**

Figure 6.7Inlet, (**b**) and outlet (**a**) provisions for the wet-air channel

Having secured the tubes in the wooden frame, the structure was then entirely covered with a wooden casing to form a rectangular box as shown in Figure 6.8. It can easily be mounted like a typical window room air conditioner. Provisions were made for the flow of working and product or supply air

through annular passages of the tubes. To effect the movement of air fans were installed at the inlet and exhaust positions.

One of the fans was located at the end as shown in Figure 6.9 to aid the intake of the working air which becomes humidified.

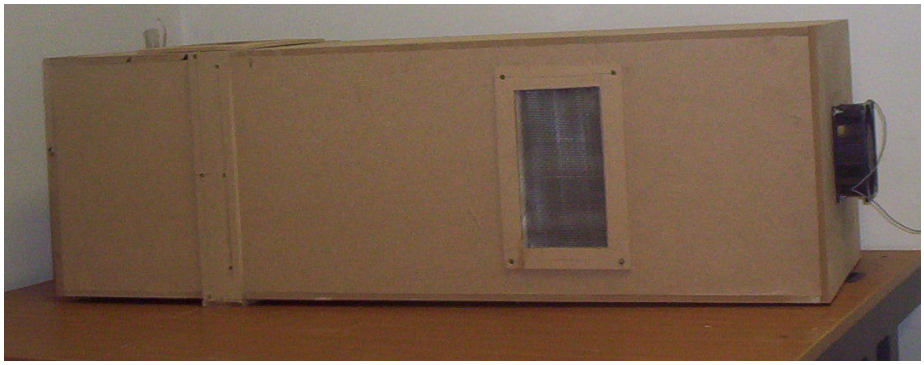

Figure 6.8 Array of tubes enclosed in a wooden casing making up the fibre tubes evaporative cooler

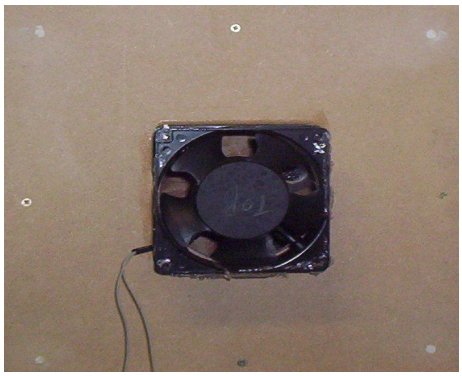

Figure 6.9 Working air intake fan mounted at the end of the cooler to aid the expulsion of the humid air

6.4 Working Principle of the System

This novel tube evaporative cooler can be categorised to operate under indirect evaporative cooling principle. In this case the primary or product air is supplied over the dry outer surface of the fibre tube while the secondary or working air flows inside the tube over the wet inner surface as shown in Figure 6.10. This enables the moistened fibre to absorb heat from the air flowing through

the outer channel by conduction because of the direct contact by thermal adhesion between the wet fibre and the dry impermeable paper membrane. Consequently, evaporation within the inner or wet channel is enhanced. However, the wet bulb temperature of the cooling or process air cannot be greater than the dry bulb temperature of the air being cooled which is the air required to supply the building space to be cooled. The working process through the assembled evaporative cooler box is shown in Figure 6.11.

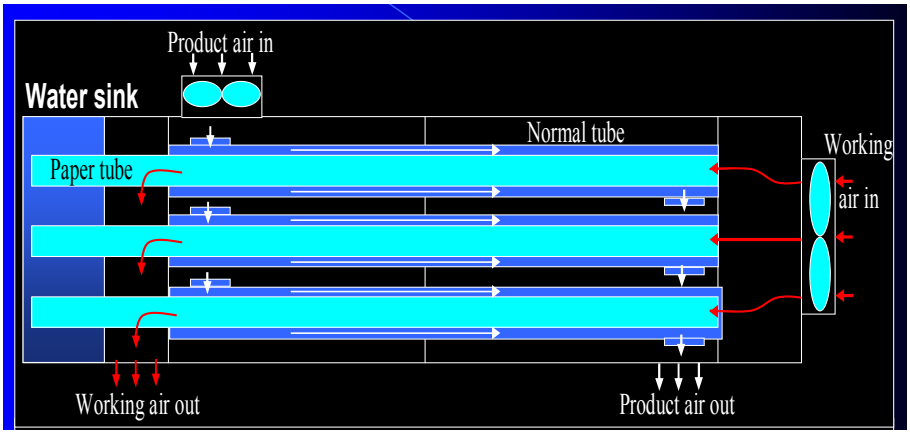

Figure 6.10 System air flow process within the inner wet channel and outer dry channel

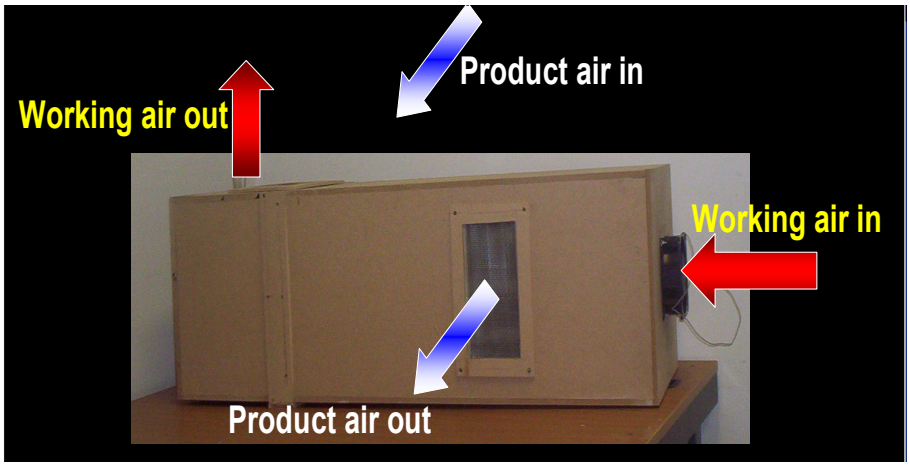

Figure 6.11 Working process of the encased tubes evaporative air cooler

Figure 6.12 below shows the entire system components and the system operation cycle. The flow paths for both the cooling and the cooled air are shown in the figure.

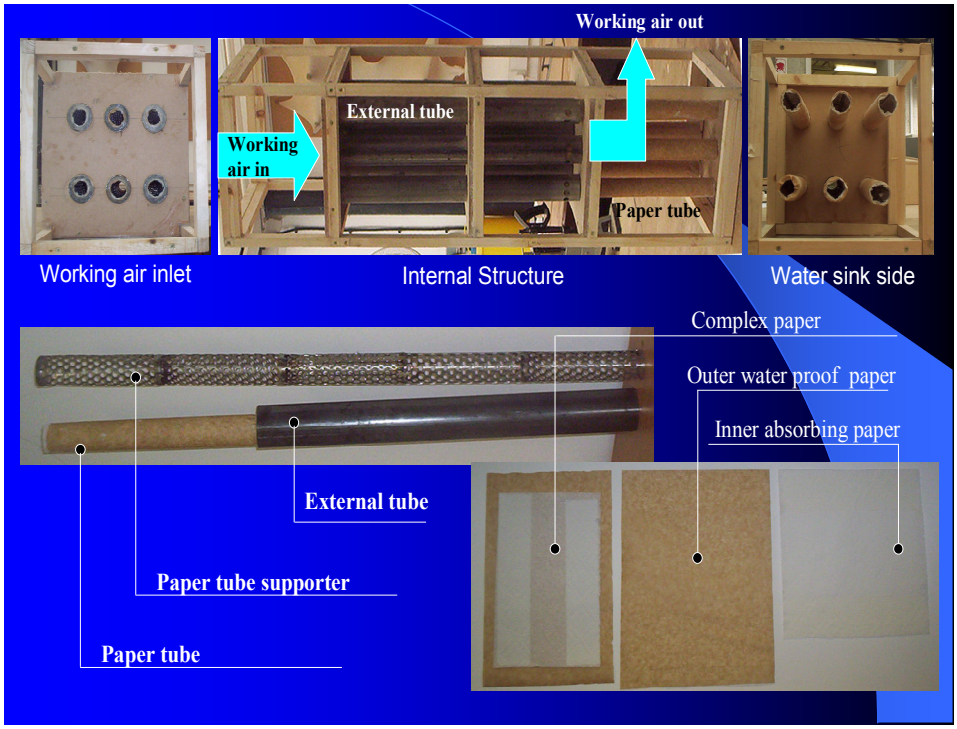

Figure 6.12 Pictorial representations of complete system components and the working principle

6.5 Description of the Experimental Set-up and Tests

The assembled evaporative cooler in Figure 6.9 was coupled to an outlet air flow rectangular duct as shown Figure 6.13. The duct allowed for proper measurements of the air flow at different sections and air flow velocities. It has a cross-sectional area of 10cm x 20cm and a length of 120cm. Both the inlet temperature and relative humidity values were monitored by installing HMP4 combined temperature and relative humidity sensors. A DT500 data taker was used to record the data via a data logger installed in the computer. Data taker

expansion modules were used to accommodate sufficient channels for different points monitored. This set up is shown in Figure 6.14.

The complete experimental set up consisting of the evaporative cooler unit, data taker set and monitoring computer are shown in Figure 6.15. Supply air velocity was recorded using hot wire anemometer (RS 327- 0640). The system was tested within inlet dry-bulb temperature range of 22^{o}C - 41^{o}C and starting inlet relative humidity as low as 10%. Corresponding outlet values were monitored over a certain period of time.

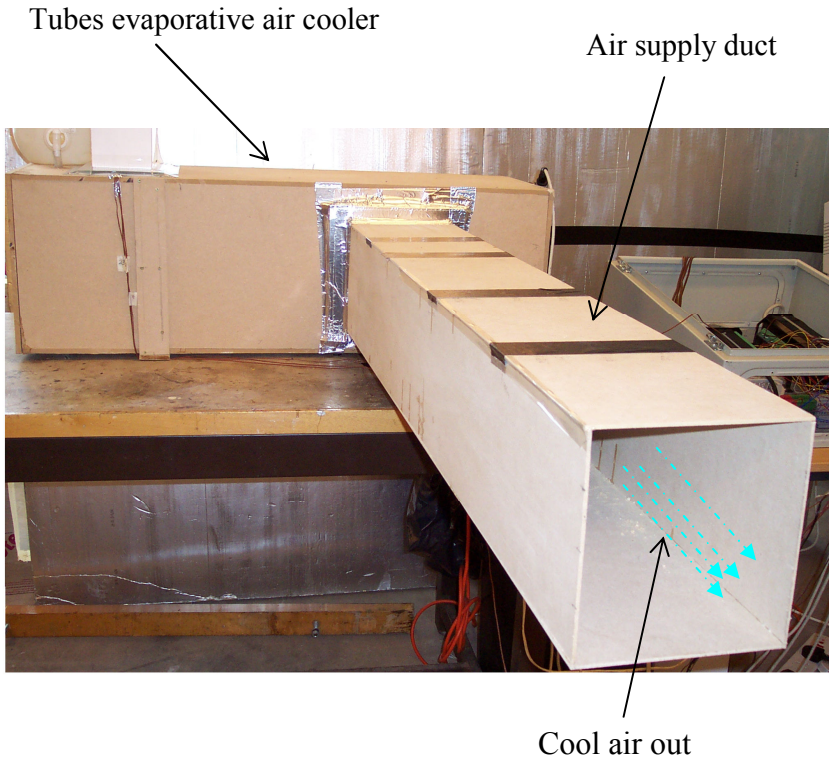

Figure 6.13 Tubes evaporative cooler coupled to cool air supply duct for experimental tests

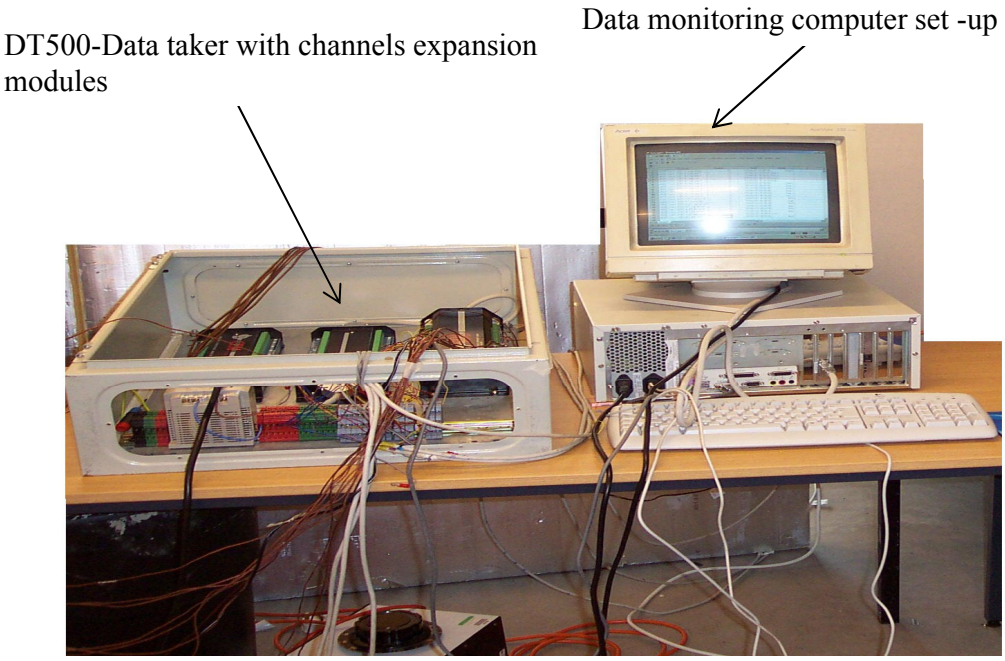

Figure 6.14 Experimental data recording set up

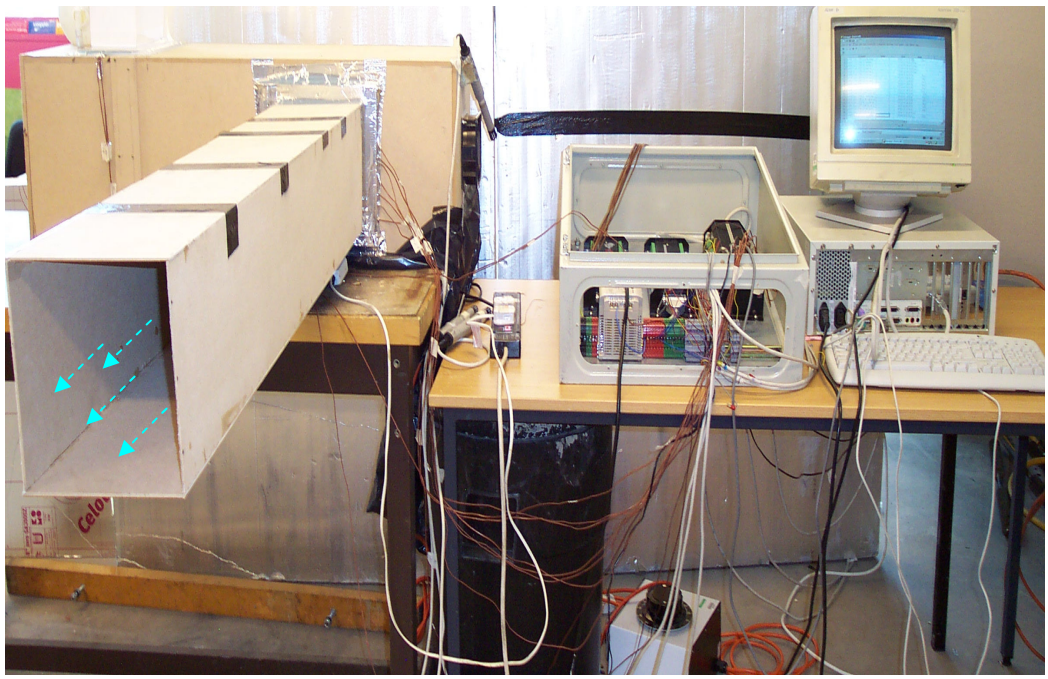

Figure 6.15 Tubes evaporative air cooler instrumented experimental test set

6.6 System Performance Calculations Model

Ideally the product or supply air temperature from the dry surface could reach the wet bulb temperature but in reality this is virtually difficult to achieve. That is, ideally, $T_{\text{product-ou}}=T_{\text{wetbulb}}$ (6-1a)

But in reality or for the actual working of the system the following relation holds: $T_{\text{product-ou}} \geq T_{\text{wetbulb}}$ (6-1b)

However, the cooling air should not be saturated. Ideally the working process should be such that the heat reduction of the cooled air is equal to the heat increase of the cooling air. Assuming that the entire process is adiabatic so there is no loss of cooling to the surrounding, and then the heat reduction of the cooled or supply air is equal to the heat increase of the cooling or working air. This is represented in the following thermodynamic expression:

$$m^*_A (h_{Ain} - h_{Aout}) = m^*_B (h_{Bin} - h_{Bout}) \quad (6\text{-}2)$$

From equation (2) above the ratio of the mass flow rate between the cooled or supply air and the cooling or process air can therefore be expressed as follows:

$$\frac{m^*_A}{m^*_B} = \frac{(h_{Bin} - h_{Bout})}{(h_{Ain} - h_{Aout})} \quad (6\text{-}3)$$

One of the assumptions for the ideal and theoretical working process of the system is that, the ratio of the mass flow rate between the cooled (working) air and cooling (supply) air should satisfy the equation (6-3) above.

Other assumptions are as follows:-

-No cooling loss from the fibre material to the surrounding.

-Appropriate dry channel and wet channel dimensions for completing this process.

For a given ratio of the mass flow rate between cooled air and cooling air as expressed, the enthalpy of exhausted air at exhaust condition can be obtained by rearranging equation (6-3) as shown below.

$$h_B = m^*_A/m^*_B = (h_{Ain} - h_{Aout}) + h_B \quad (6\text{-}4)$$

Thermodynamically, for any indirect evaporative cooling system, either operating ideally or real while neglecting the fan or pump and water temperature entering or gain losses, the cooling capacity, (Q_o) can be evaluated from the following energy balance equation. It can be expressed in terms of enthalpies and the corresponding mass flow rates (Maisotsenko, 2003).

$$Q_o = m^*_A (h_{Ain} - h_{A,out}) = m^*_B (h_{B,out} - h_{B,in}) \quad (6\text{-}5)$$

Where:

Q_o - is the cooling capacity (Watts)

Also the cooling capacity can be evaluated by writing the energy balance equation in terms of temperatures, humidity ratio and latent heat as shown below:

$$Q_o = m^*_{product} C_p (t_{product,in} - t_{product,out}) = m^*_{exhaust} [L(w_{exhaust,out} - w_{exhaust,in}) + Cp(t_{exhaust,in} - t_{exhaust,out})] \quad (6\text{-}6a)$$

$$Q_o = m^*_A Cp(T_{Ain} - T_{A,out}) = m^*_B [L(w_B,out - w_B,in) + Cp(T_B,_{in} - T_{B,out})] \quad (6\text{-}6b)$$

The mass flow rate for the working (cooling) and product (supply) air can generally be obtained by the application of the following continuity equation assuming steady follow between the inlet and out let of the system:

$$m^* = \rho_{in} A_{in} V_{in} = \rho_{out} A_{out} V_{out} \quad (6\text{-}7)$$

Water consumption of the fibre material:
Based on the air state point obtained in the previous expression, the water consumption can be evaluated by applying the following expression:

$$Q_{wf} \; - \; m^{*}_{B} \, (\omega_{B\text{-}wet} \; - \; \omega_{B\text{-}in}) \tag{6-8}$$

The system effectiveness or efficiency:

The system effectiveness or efficiency can be evaluated by also applying the following expression Riffat and Oliveira, et al (2000), (Al-Sulaiman, 2000):

$$\eta_{cooling} = \frac{T_{s,in} - T_{s,out}}{T_{s,in} - T_{wb}} \tag{6-9}$$

6.7 Test Results and Discussion

The performance of the fibre–tube evaporative air cooler was determined by carrying out a number of experimental tests. The inlet temperature and the relative humidity were varied and the corresponding outlet magnitudes were recorded. These include testing the system under dry condition, that is without water and then conducting tests when the water was supplied to wet the fibre material tubes making up the cooler. The system has a common air inlet both for the primary or working air and the secondary or the product air. Tests were also carried out to investigate the effect of changing the air flow rate. The following sections discuses results of the tests under different conditions.

6.7.1. Dry test

This test is termed as dry as it was conducted without providing water to wet the fibre evaporative cooling surface. It formed the basis for observing the evaporative cooling effect of the fibre material when moistened with water using horizontal supply arrangement. Based on these performance tests, very

little drop in temperature was recorded, hence the cooling effect was virtually absent in comparison with the prevailing ambient conditions. Results of this test are shown in table 6.1 and plotted in Figure 6.16. Both the working and supply air conditions at the inlet and outlet remained almost constant throughout the test period. Under steady state the average ambient inlet temperature of 22.4^{o}C and relative humidity of 39.8% left the system at average values of 22.1^{o}C and 43.8% from the wet air channel. Corresponding values of 21.6^{o}C and 42% outlet temperature and relative humidity respectively were recorded for the dry air channel.

Table 6.1 Temperature and relative humidity results for the dry test case (un-wetted evaporative cooling surface).

T_in (°C)	RH_in (%)	Twet_out (°C)	Tdry_out (°C)	RHwet_out (%)	RHdry_out (%)
22.2	39.9	22.1	21.6	44.1	42.1
22.1	39.9	22.1	21.6	43.9	42.1
22.1	39.9	22.1	21.6	43.8	42.0
22.2	39.9	22.1	21.6	43.9	42.0
22.3	40.1	22.1	21.6	43.6	41.9
22.5	40.4	22.1	21.6	43.8	42.0
22.6	39.5	22.1	21.6	43.5	42.0
22.5	39.4	22.1	21.6	43.7	42.1
22.5	39.4	22.0	21.6	44.0	42.0
22.5	39.4	22.0	21.6	43.9	42.0
22.4	39.5	22.1	21.6	43.9	41.9

T_in	Set ambient inlet temperature
RH_in	Set ambient inlet relative humidity
Twet_out	Out let temperature from the wet air channel (process or working air)
Tdry_out	Out let temperature from the dry air channel (product or supply air)
RHwet_out	Out let relative humidity from the wet air channel
RHdry_out	Out let relative humidity from the dry air channel

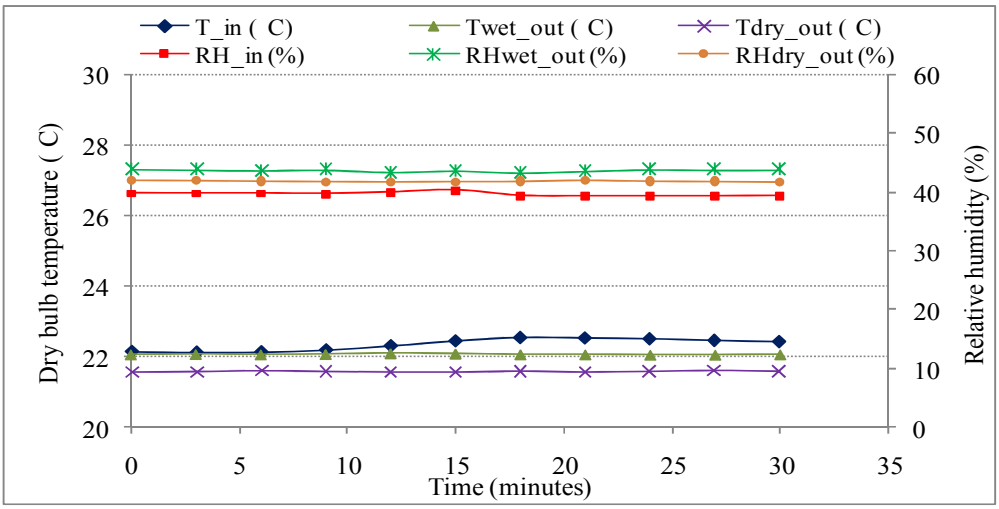

Figure 6.16 Inlet and outlet temperatures and relative humidity variations for the dry test.

6.7.2. Wet test

Wet tests were conducted after the system was supplied with water to moisten the fibre in the tubes. Effects of different performance parameters based on wet tests are discussed in the following sections.

6.7.2.1 Temperature effects

The results are shown in Figure 6.17. It was observed that the temperature drop between the inlet and outlet conditions was almost equal for the working and supply air with the working air having a slightly lower temperature in the order of 1-3^{o}C. Operating the system with an inlet temperature range of 20^{o}C to 41^{o}C produced a temperature drop of 7^{o}C to 14^{o}C for both the working air (wet channel) and the supply or product air (dry-channel). These results suggested effective heat transfer between the working air flowing over the moistened surface and the product or supply air flowing over the dry surface membrane attached to the wet fibrous material.

Table 6.2: Temperature and relative humidity results for the wet test case (wetted evaporative cooling surface).

Twater(°C)	T_in (°C)	RH_in (%)	Twet_out (°C)	Tdry_out (°C)	RH_{wet_out} (%)	RHdry_out (%)
15.9	38.5	20.0	22.0	24.8	65.2	45.0
16.0	38.5	19.9	22.0	24.9	64.8	44.9
16.0	38.5	20.0	22.1	24.9	65.0	45.0
16.0	38.5	20.1	22.1	24.9	64.8	45.0
16.0	38.6	19.9	22.1	24.9	64.6	44.8
16.0	38.6	19.9	22.1	24.9	64.7	44.8
16.0	38.6	19.9	22.1	24.9	64.5	44.8
16.0	38.6	19.9	22.1	24.9	64.5	45.0
16.0	38.6	20.1	22.2	24.9	64.6	45.2
16.1	38.6	19.9	22.2	24.9	64.5	45.0
16.0	38.6	20.0	22.2	24.9	64.5	45.0
16.0	38.6	20.0	22.2	25.0	64.2	44.6

Twater	Water temperature
T_in	Set ambient inlet temperature
RH_in	Set ambient inlet relative humidity
Twet_out	Out let temperature from the wet air channel (process or working air)
Tdry_out	Out let temperature from the dry air channel (product or supply air)
RHwet_out	Out let relative humidity from the wet air channel
RHdry_out	Out let relative humidity from the dry air channel

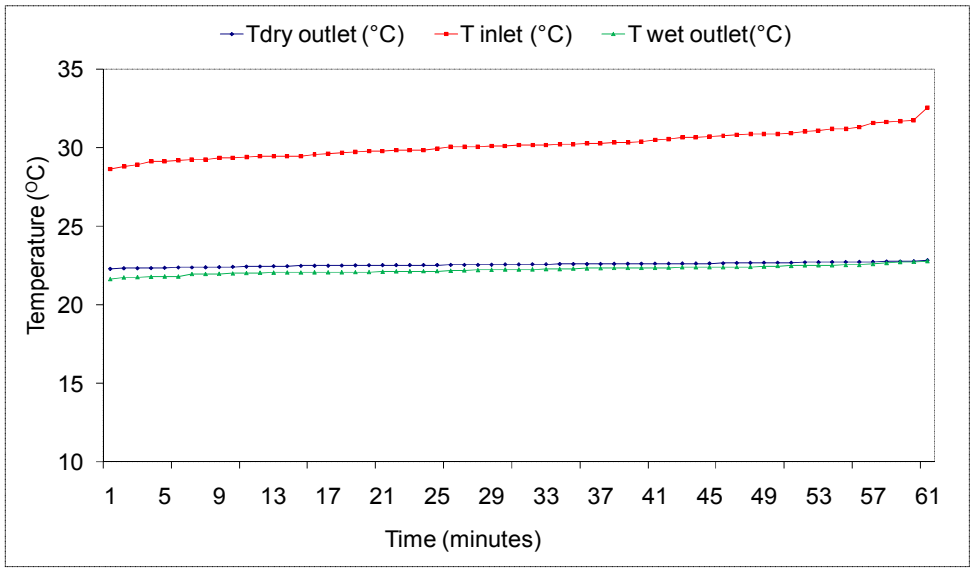

Figure 6.17 Timely variations of inlet and outlet temperatures for the wet (working) and dry (supply) air channels under the wet-test condition

6.7.2.2 Relative humidity effects

Similar to temperature effect test above, corresponding relative humidity outlet conditions were observed. Under very low relative humidity inlet condition significant variation of outlet values were observed for the working or process air and the product supply air. Starting with a very low relative humidity at inlet as plotted on Figure 6.18 the relative humidity increase of about 30% was noticed on the supply or product air (dry air channel). The corresponding increase in relative humidity at the outlet of the process air (wet air channel) was over 70%. This performance indicated the effectiveness of the system in minimising the rise in relative humidity that can be supplied to the building environment. It also showed that even at a very low level of inlet relative humidity the system can provide out let values within the range of comfort limits.

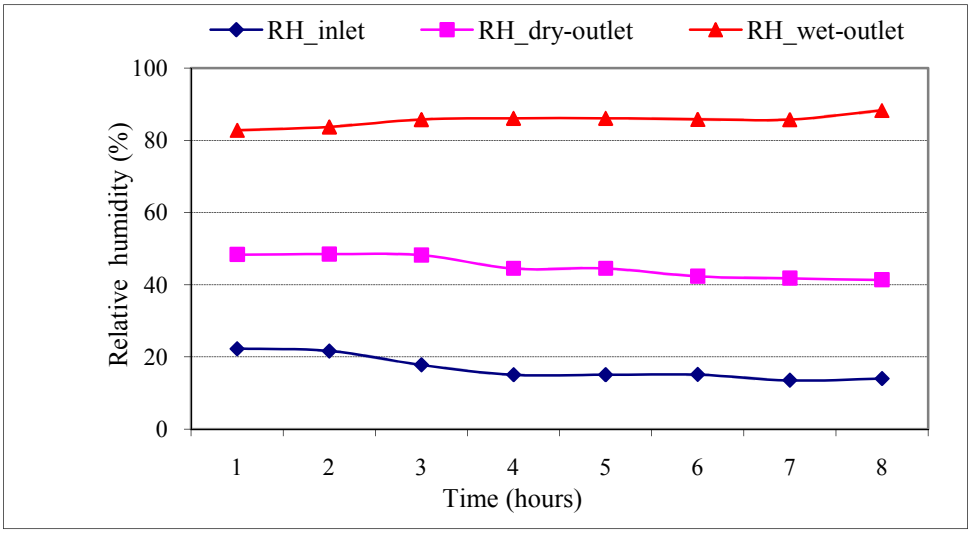

Figure 6.18 Timely variation of inlet and outlet relative humidity for the working and supply air under wet-fibre test condition

In Figure 6.19 different range of both temperature and relative humidity were set at the inlet and corresponding out let values recorded. The test covered a temperature range of 20-41^{o}C. In each case the performance curves showed continuous reduction in outlet temperature values for both the process and supply air. However, the corresponding relative humidity outlet values recorded lower difference in between the inlet and outlet for the supply or product air. At the same time high values were noticed for the working or process air which was directly in contact w3ith the moistened fibre. The combined effect of lower temperature and medium values for relative humidity obtained from the supply air outlet made it to be of comfortable cooling advantage over the process or working air.

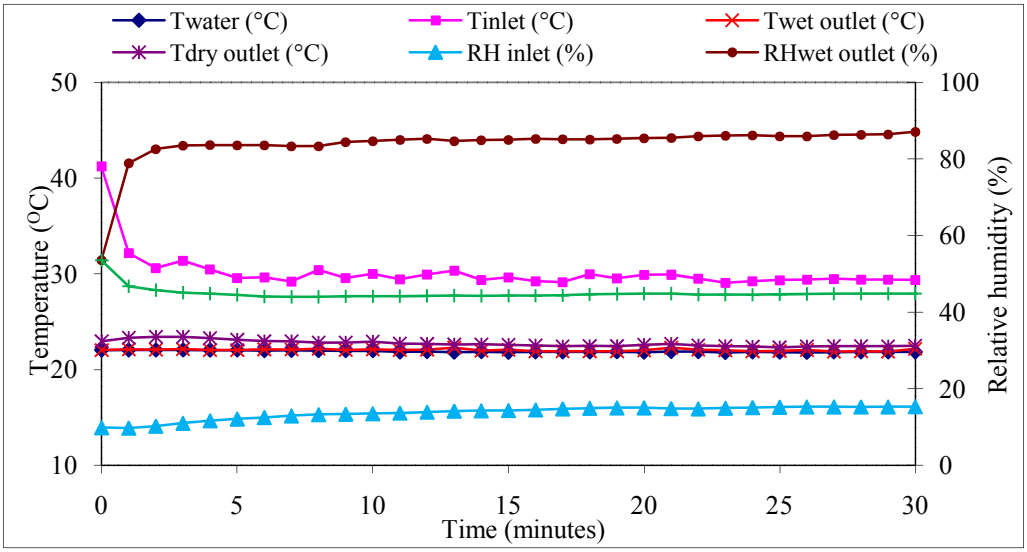

Figure 6.19 Combined effects of temperature and relative humidity at different inlet values under the wet test condition

6.7.3. Cooling capacity.

The cooling capacity was calculated using equation (6-5) based on temperature and relative humidity inlet/ outlet values. A value of 500 Watts was calculated

for the supply air. A corresponding value of less than 50 Watts was recorded for the working or process air. The cooling performance for the supply and process air are shown in Figure 6.20. These were found to increase linearly with the increasing supply air velocity. Also there is a difference in the cooling capacity between the two channels and it became bigger with increasing air flow rate. The main reason for that was due to higher moisture or relative humidity level in the wet or process air channel which makes the enthalpy change between the inlet and outlet from that channel to be small, hence the cooling capacity. In contrast, the enthalpy difference between the inlet and out let of the dry or supply air channel is much higher, resulting in bigger cooling capacity.

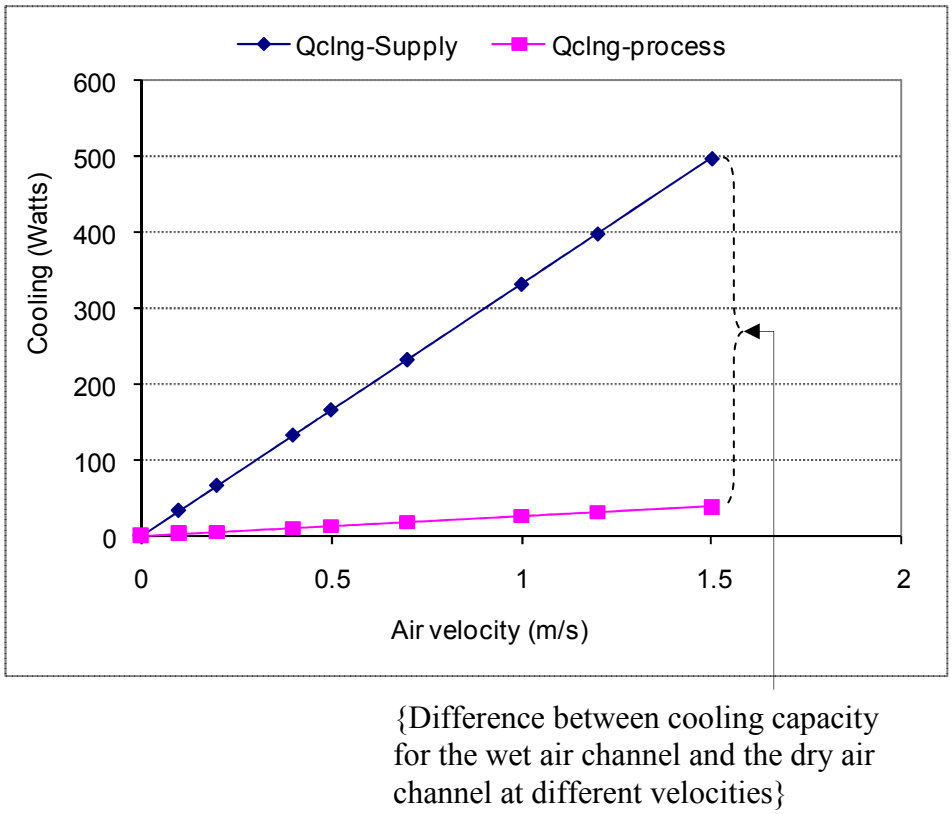

Figure 6.20 Variation of cooling capacity for wet and dry air channels at different air flow rates

6.7.4 Water consumption rate and system effectiveness

The system effectiveness and water consumption were calculated with the results collected at the maximum inlet dry bulb temperature test run as shown in table 6.3.

Table 6.3 Data for the calculation of system effectiveness and water consumption

Air flow channel	T_{inlet}(°C)	RH $_{inlet}$ (%)	T_{outlet}(°C)	RH_{outlet} (%)
Supply or dry air	41.2°C	10%.	23°C	53.3%
Process or wet air	41.2°C	10%.	22°C	88.3%

- **Water consumption rate**

Equation (6-8) was applied to calculate the water consumption rate when system was operated at inlet temperatures of 41.2°C and inlet relative humidity of 10%. Corresponding outlet values were temperature of 23°C and 53.3% for the supply or dry air channel. At the same time, outlet temperature of 22°C and relative humidity of 88.3% were obtained for the working or wet air channel. The calculated water consumption rates based on these results were 0.32g/kg and 0.54g/kg obtained for the supply or dry air channel and the process or wet air channel, respectively as shown in Figure 6.21. Air supplied from the wet channel indicated higher water consumption as well as higher content of moisture.

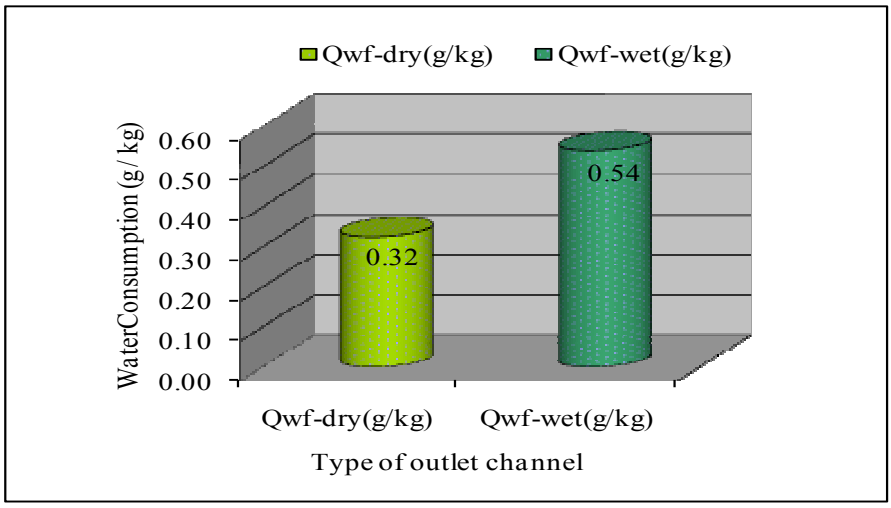

Figure 6.21 Water consumption for the dry air (Qwf-dry) and wet air (Qwf-wet) flow channels

- **Effectiveness**

The system effectiveness was calculated by the application of equation (6-9) using the results shown in table 6.3. The calculated values were respectively 83% and 48 % for the supply or dry air channel and process or wet air channel as shown in Figure 6.22a. This result was obtained at ambient inlet dry bulb temperature of 41.2°C and relative humidity of 10%. Corresponding outlet temperatures were 22°C and 23°C while outlet relative humidity values were 53.3% and 88.3% for the supply (dry) and the wet (process) air channel respectively. First the wet bulb temperature at the inlet was obtained using the Engineering Equation Solver (EES) software as shown on the software's psychrometric plot in Figure 6.22b. It can be observed that the effectiveness due to the dry or supply air channel approaches that of the theoretical value expected for the indirect evaporative cooler. However the effectiveness of the wet channel as can be seen turned out to be about 50% that of the theoretical and the dry air channel. This is attributable to the higher value of the relative humidity from the wet channel.

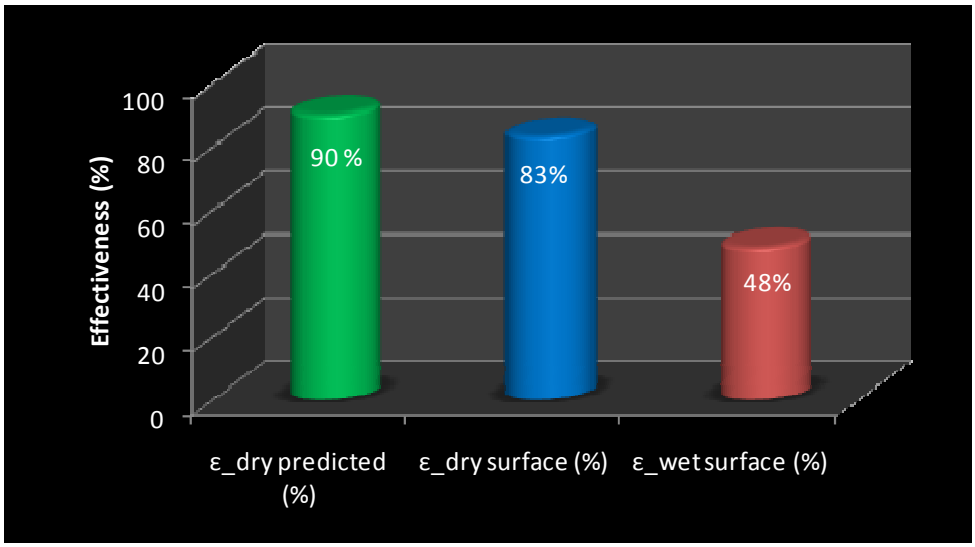

Figure 6.22a Comparative effectiveness for the dry and wet air channels with the theoretical prediction value

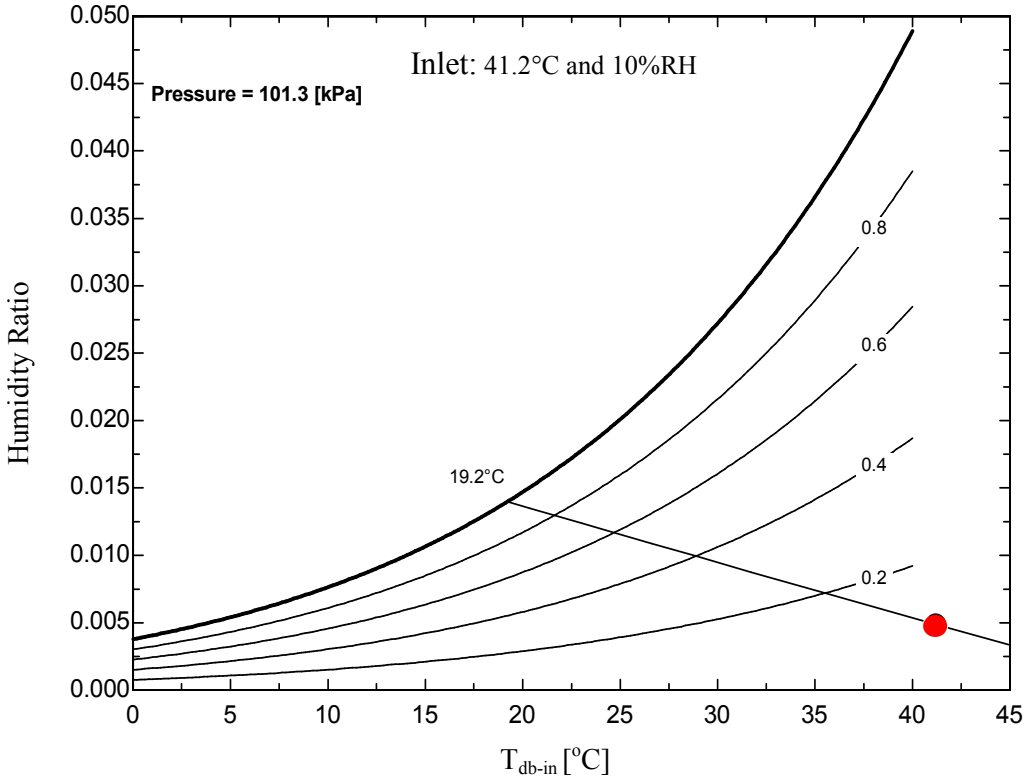

Figure 6.22b Psychrometric plot for Inlet condition of 41.2°C and 10%RH

More experiments were then carried under steady state at a series of temperatures, relative humidity at constant air flow rate as well. Figure 6.22c shows the steady state result when the system was operated under the same inlet temperature of 41°C and RH% relative humidity for longer period than the instantaneous results discussed above. In this case a very much higher value of over (90%) effectiveness was observed. This is because the system was operated at very higher temperature and very low relative humidity.

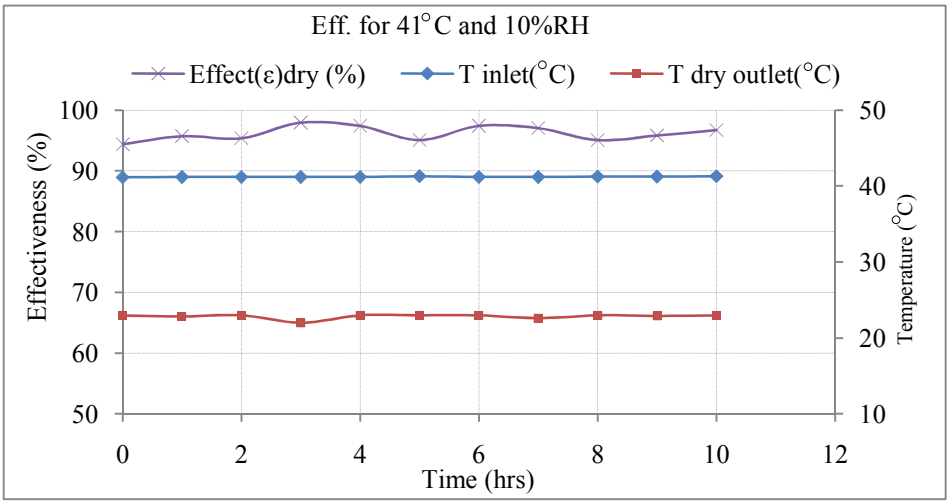

Figure 6.22c Inlet and outlet temperature variation with effectiveness for constant inlet temperature of 41°C and 10% relative humidity

The following additional tests were carried out for different combination of inlet parameters under steady state:

- 30°C temperature and 15% relative humidity.

The corresponding wet bulb temperature for this set is shown in Figure 6.22d. With this value the effectiveness was calculated for both the dry air channel and the wet. Because in this case the relative humidity was increase and the

temperature reduced the value of the effectiveness for both the dry channel and the wet channel reduced and also had very little variation between them.

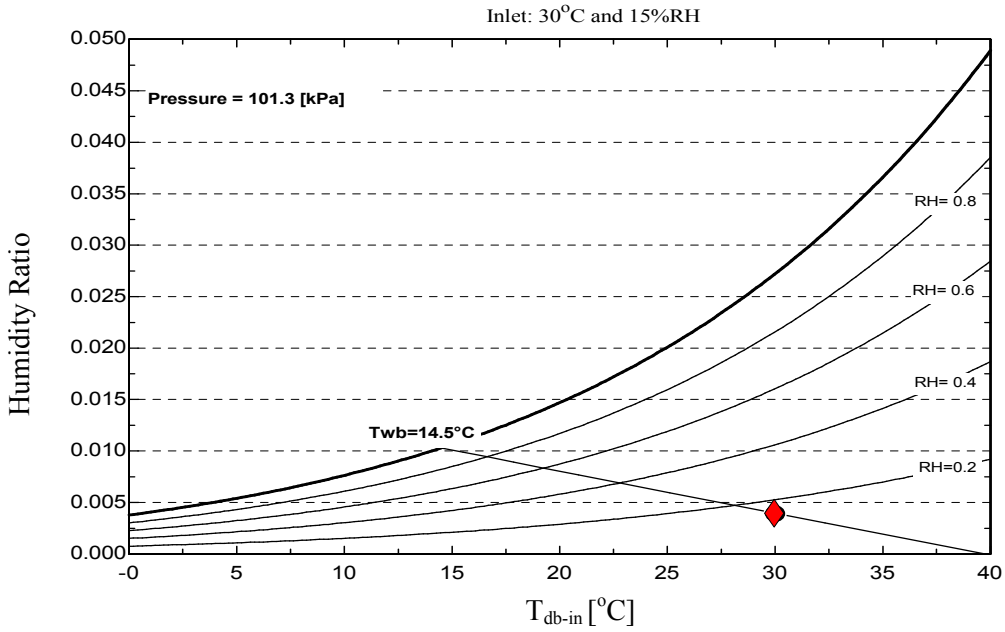

Figure 6.22d Psychrometric plot for 30°C temperature and 15% relative humidity steady state inlet test condition

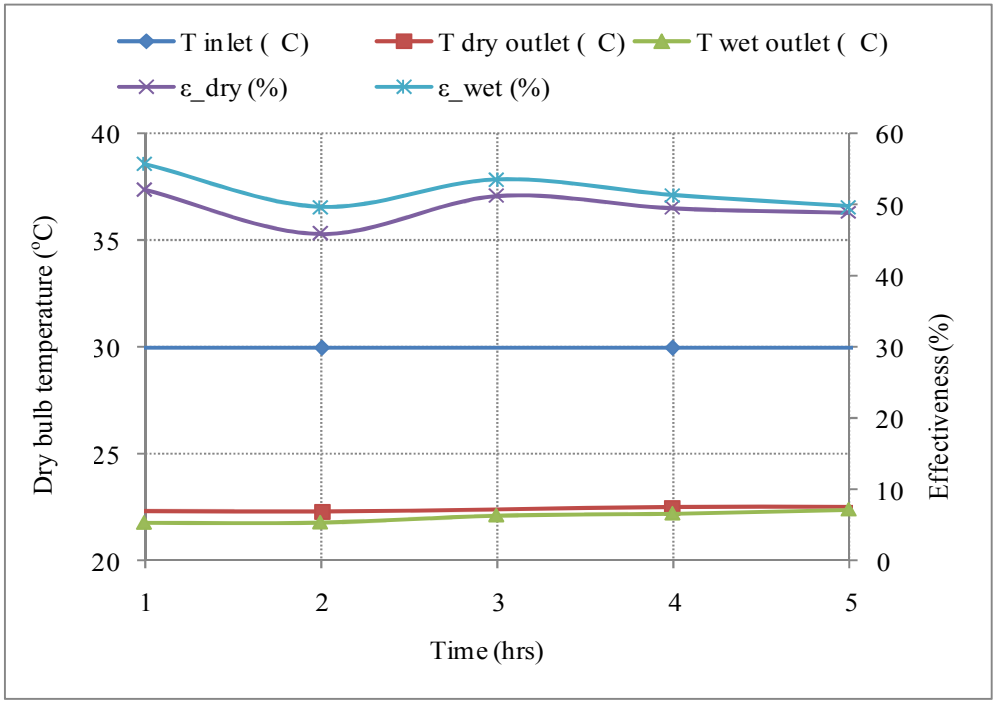

Figure 6.22e Timely variations of inlet and outlet temperatures with system effectiveness for the dry air (ε_dry) and wet air (ε_wet) channels

- 39°C temperature and 20% relative humidity inlets for the dry channel and 24°C and 46% relative humidity for the wet channel.

This test was carried out by operating the system under counter flow. The constant inlet values for each channel were as above. Corresponding wet bulb temperature at the inlets were obtained using EES software and the psychrometric plots shown in Figures 6.22f and 6.22g for the dry and wet air channels respectively.

The effect of steady state test under different inlet conditions for both the dry and wet air flow channels are shown in Figure 6.22h. It can be seen that the wet channel having constant temperature of 24°C and relative humidity of 46% at the inlet had a very low effectiveness with a maximum value of about 21%. Simultaneously the dry channel with constant inlet temperature of 39°C and relative humidity of 20% obtained effectiveness of 61.7%. At the outlet the air from the dry channel had average temperature drop of 13.65°C while the drop from the wet channel was averagely 1.42°C.

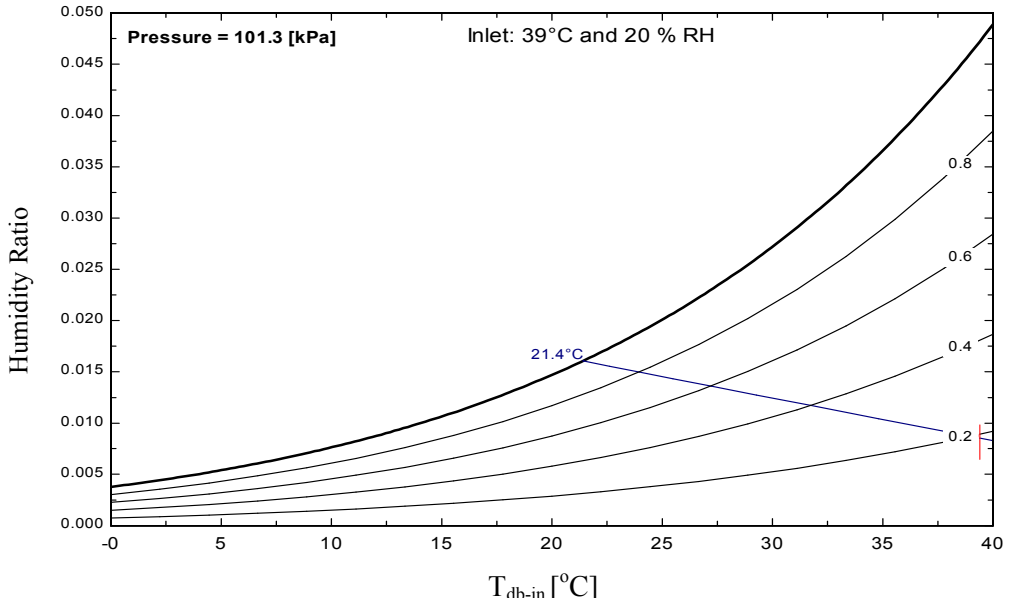

Figure 6.22f Psychrometric plot for 39°C temperature and 20% relative humidity steady state inlet test condition.

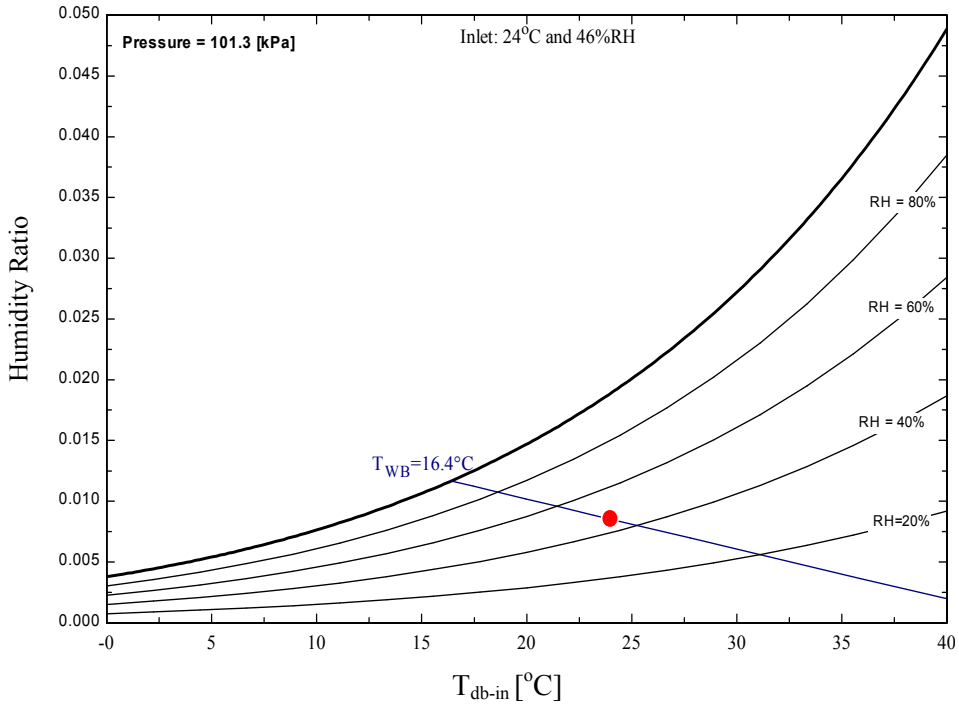

Figure 6.22g Psychrometric plot for 24°C temperature and 46% relative humidity steady state inlet test condition.

For this reason the counter flow should be made simple so as to keep the inlet through the dry channel at low temperature and medium relative humidity while the inlet to the supply or dry air channel can be maintained at higher dry bulb temperature and low relative humidity.

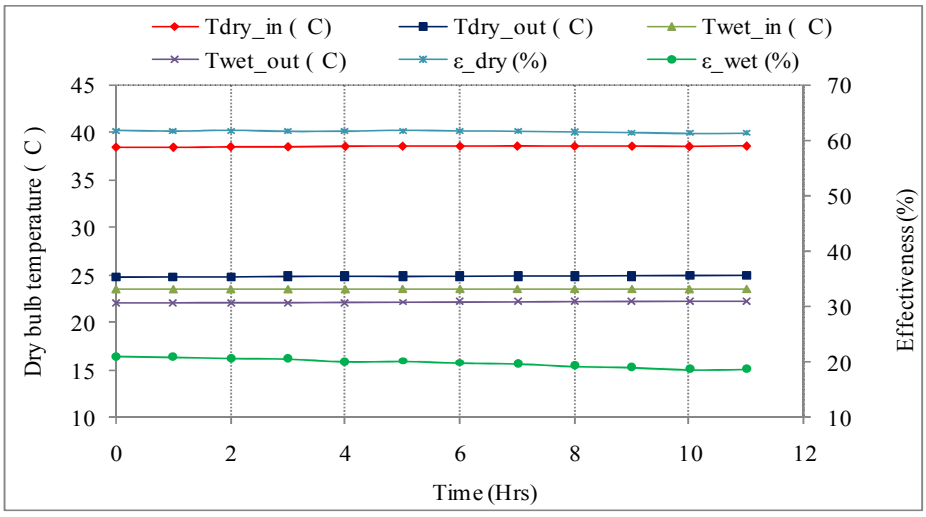

Figure 6.22h Effects of different inlet values $T_{dry,in}$ of 39°C and $RH_{,dry\_in}$ 20%; T_{wet_in} 24°C and RH_{wet_in} 46%

6.8 Psychrometric representation of system performance

Psychrometric representation of the system performance was shown for mixed and unmixed outlet air properties after passing through the evaporative cooling process. The plots were obtained using iGet Psyched^{TM} psychrometric programme worksheet as described in the following sections.

6.8.1 Representation of cooling path for separate dry and wet air

The properties of the air channels operating in the evaporative cooler are shown on the psychrometric chart in Figure 6.23. It represents system performance showing the temperature, relative humidity and corresponding enthalpies from an initial inlet dry-bulb temperature of 41^{o}C and a relative humidity as low as 10%. Starting at A the inlet, A-B represents the supply air with exhaust values of dry-bulb relative humidity and enthalpy values while A-C represents the working air properties.

It should be observed that the supply air remains within psychrometric comfort zone while the working air is out of it because of the high gain in relative humidity raising the moisture content in the air.

It should be observed that the dry air channel have moisture increase but less than 50% of the wet channel as shown by (x) and (y) lines respectively in Figure 6.23. The increase in the dry channel can be due to many factors. Among them is the fact that any lowering of temperature will raise relative humidity and further lowering can lead to condensation on the surface of the heat transfer membrane. Secondly the boundary layer material used for heat transfer might not be perfectly impermeable. So some moisture might diffuse through it. Also there can be a minor material failure to allow some moisture to

leak from the wet channel to the dry channel thereby causing moisture rise in that channel.

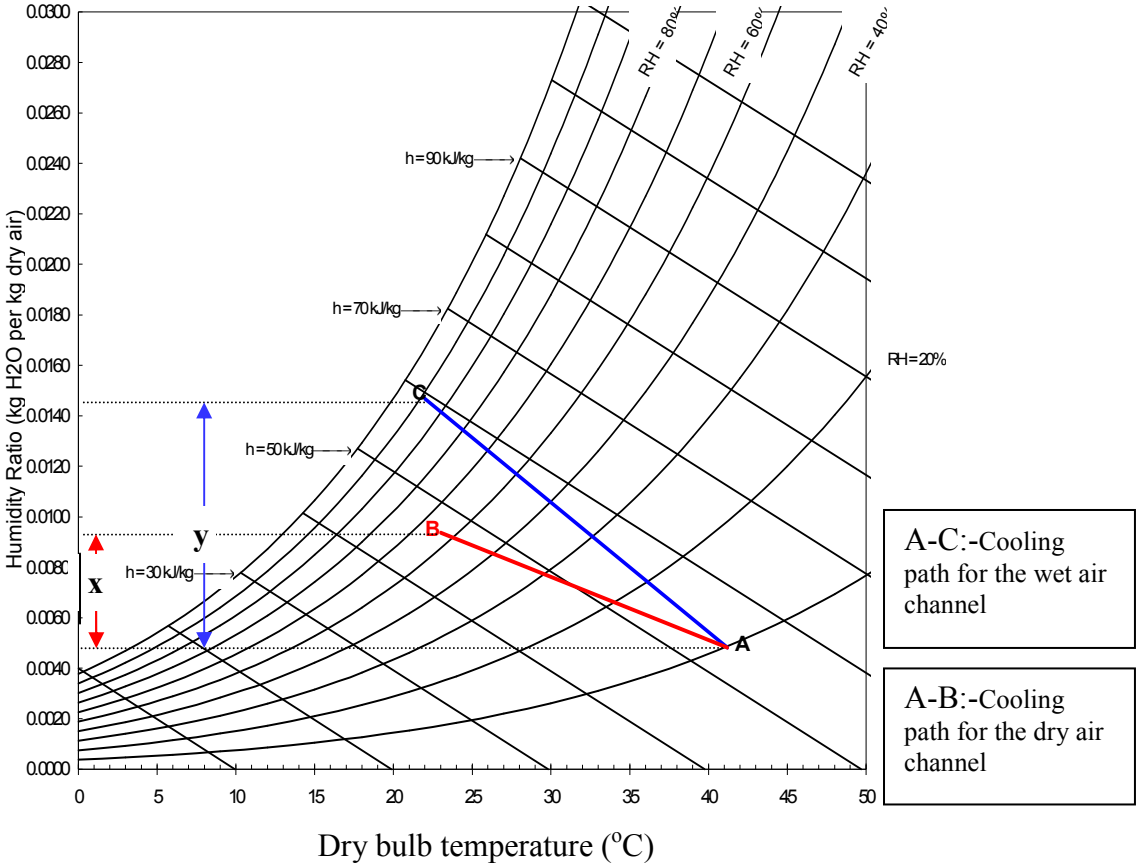

Figure 6.23 Typical representations of supply (dry) and working (wet) air performance on a psychrometric. A-B shows supply air while A-C shows working air

6.8.2 Representation of cooling path for dry, wet and mixed air.

Similarly in this case the plots were plotted using a version of Get Psyched™ psychrometric worksheet. As indicated in Figure 6.24 starting at A the inlet, A-B represents the supply air, A-D represents the working air and A-C represents the product of mixing both the supply and the process air. The supply air remains within the psychrometric comfort zone, while the working air outside because of the high gain in relative humidity raising the moisture content of the

air. In some cases, the values from the mixture can be tolerated. The comfort zone is based on ASHRAE Standard-55-2004.

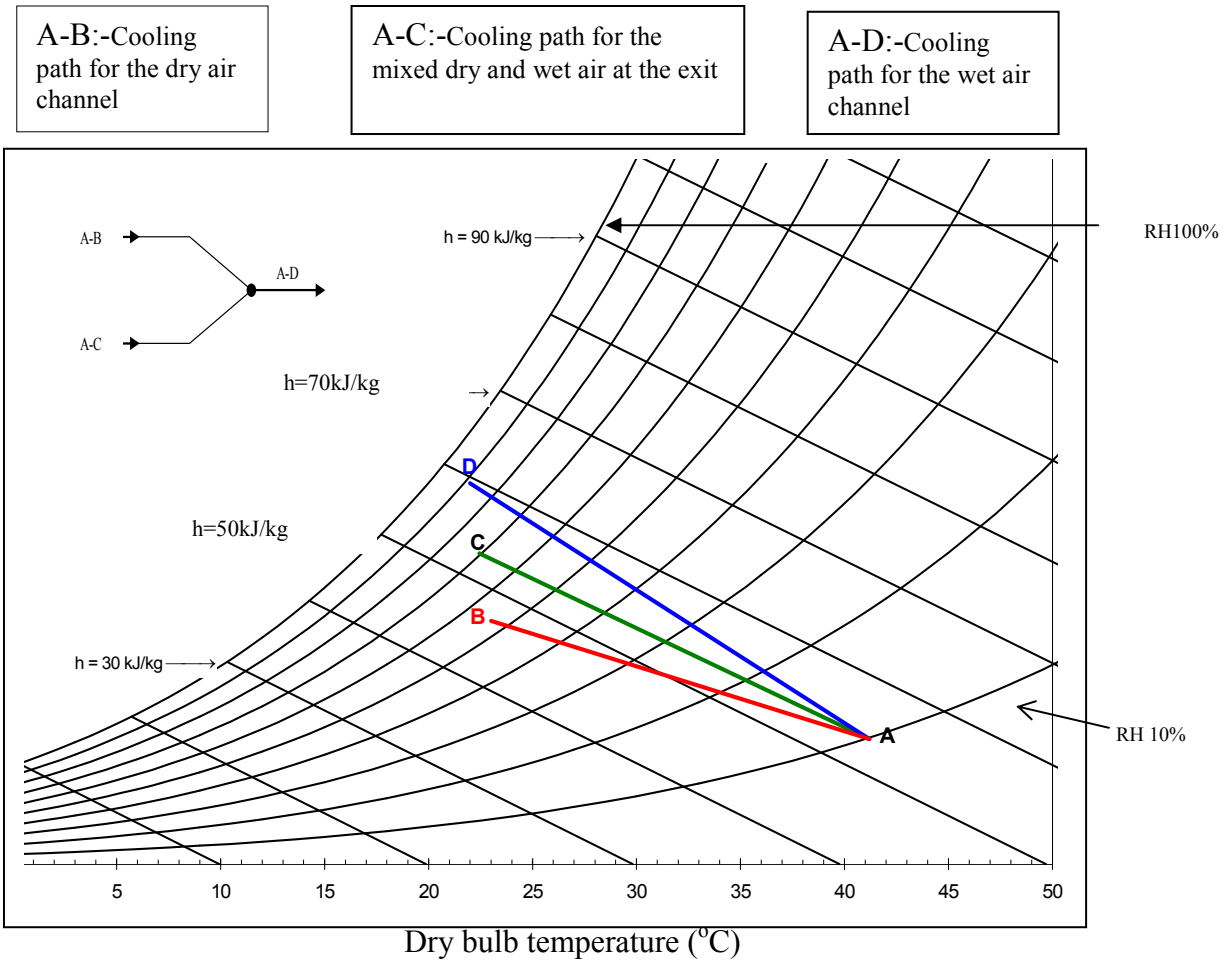

Figure 6.24 Working, supply and mixed air channels plotted on psychrometric chart

6.9 Applications of the Novel Concentric Tubes Evaporative Cooler

The cooler can be used either as an indirect, direct or combined mode depending on the humidity level limit on a desired application. The possible applications are discussed in the following sections.

6.9.1 Indirect application.

This application is suitable where cooling is required with little increase in relative humidity. The areas consist of home, offices and some industrial buildings. As can be seen in Figure 6.12 of section 6.4, the unit can be installed as a simple window air conditioner. However, where ever it is installed should be provided with adequate ventilation ensuring continuous exchange of fresh air passing through the system inlet to the space to be cooled and then exhausted. Operating the system in this form will eliminate possible accumulation of moisture that may be associated with the little increase in the relative humidity to cause discomfort. When the system is to be operated under the indirect mode on the air from the supply channel will be directed to the desired space while the highly moistened process air will be channelled away from entering.

6.9.2 Direct application.

In areas cooling and humidification is required than depending on the level of humidity desired the systems direct operation mode can be utilised. Here the air delivery channel can be changed so that the working air can directly be admitted to the space requiring cooling and humidification. The larger version of this can therefore has applications in textiles and related industries. However it will not be suitable in storage areas where cool and dry environment is the basic requirement.

6.9.3 Combined direct and indirect application.

Another important application is to use the system based on combined mode operation. Here both the supply and the process or working air can be allowed to mix at the outlet just before being supplied in to the cooling space.

The resultant out let values of temperature and relative humidity takes the average value of each as can be observed in the psychrometric chart in Figure 6.24, above. The application of this can be on canopies, parasols or other roof structures with open space below that enables free movement of air in different directions. In such environment relative humidity cannot build up. The average values of the temperatures and relative humidity for both the working and supply air are provided as they appear to be within the psychrometric comfort limits.

6.9.4 Development of a prototype for parasol cooling application

Encouraging results obtained from the box-type novel horizontal tubes evaporative cooler as discussed in the previous sections proved viable and therefore led to the development of a prototype for parasol cooling applications. Drawing of this new development is illustrated in Figure 6.25. It consists of integrating the tubes cooler in a parasol set-up. The system can have dry channel air directed under the parasol roof while humid air can be channelled out as shown in the figure. If the environment is hot and dry then cooling air from the wet channel can be used or combination of the wet and dry. On the other hand if the area is humid then only cooling air from the dry channel can be used. A fan installed in housing is located at the centre of the parasol tent, Figure 6.26. The arrangement is flexible to allow for the opening

and closing of the parasol as shown in Figure 6.27. Constructions of the tubes were similar to the box type. The paper tubes are inserted in to the outer tubes axially to create the dry and wet air channels as shown in Figure 6.28.

All the components constructed for the parasol application are displayed in Figure 6.29.

Figure 6.30 shows the system installed on a parasol to demonstrate its application on such structures having roof and open underneath like the reception or living rooms commonly found in rural areas of Africa.

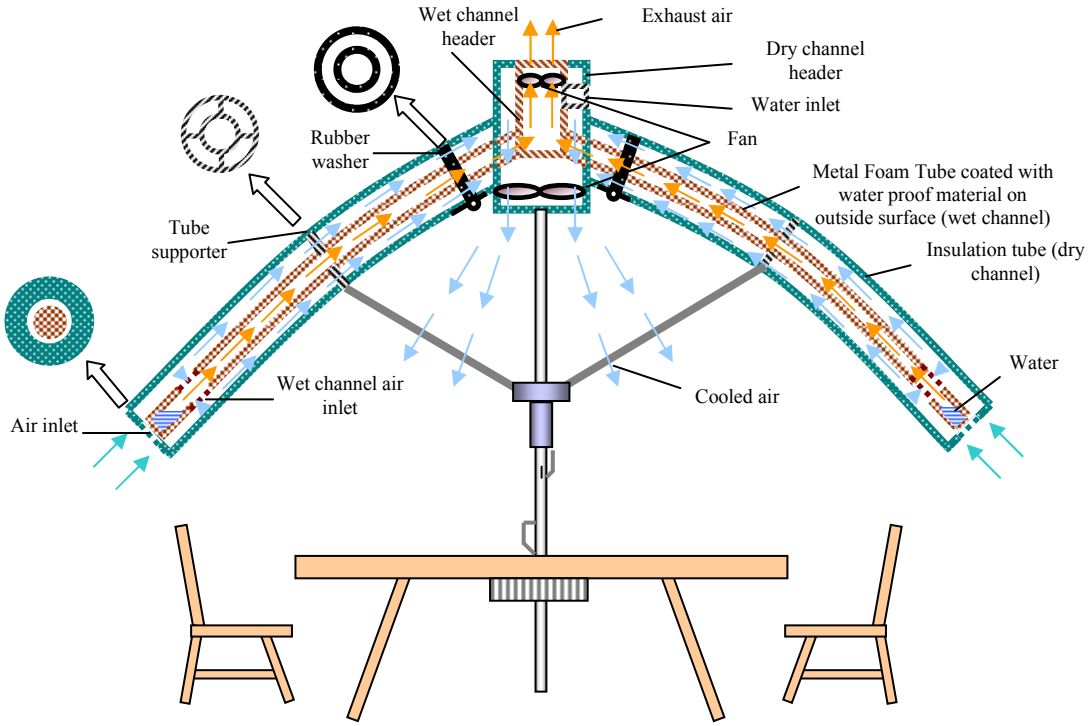

Figure 6.25 Sketchmatic illustration of tubes evaporative cooler for parasol

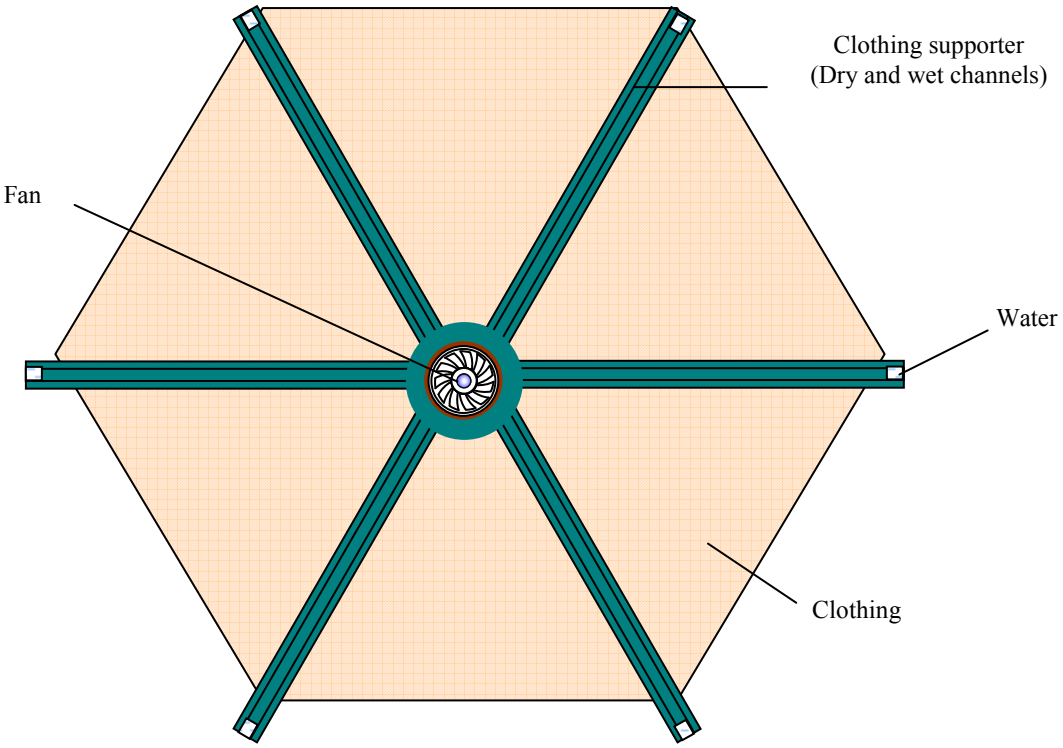

Figure 6.26 Top View of the tubes on parasol and the central air fan

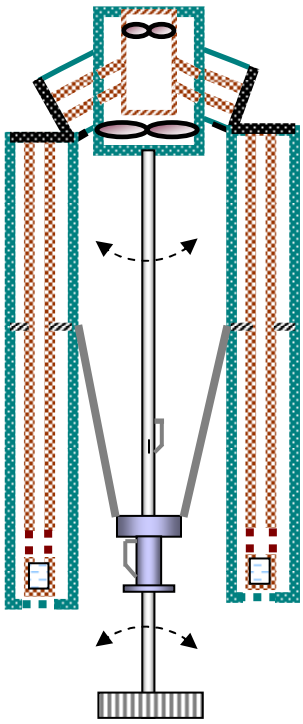

Figure 6.27 View of a parasol opening and closing mechanism

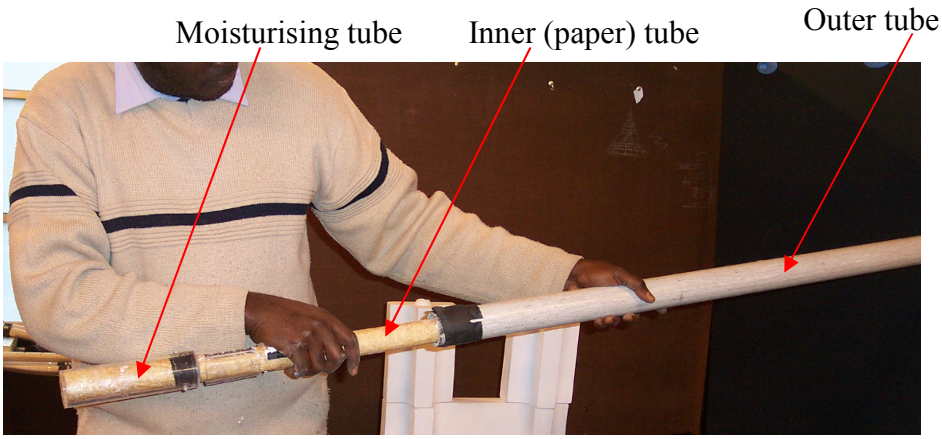

Figure 6.28 Placing the inner paper tubes axially in the outer tube.

Figure 6.29 Components of the tubes evaporative air cooler for parasol

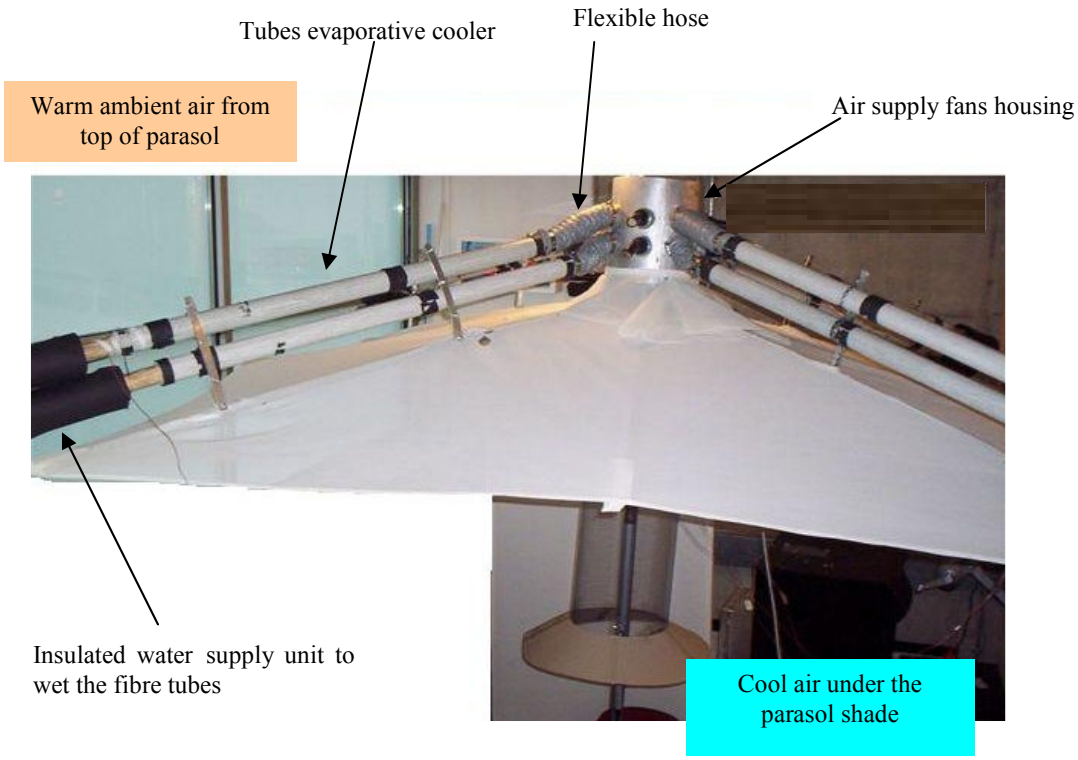

Figure 6.30 Constructed system installed on a parasol

6.10 Summary

Too high or too low a level of temperature and relative humidity in a building space leads to poor thermal comfort and can affect the productivity of a workforce. Conventional air conditioning systems consume large quantities of fossil fuels for their operations. The fibre-tube evaporative cooling system is environmentally friendly and can operate in either a direct, indirect or

combined mode. The system could be developed for application in homes, offices factories where cooling with or without humidification is required.

The test run under counter flow mode with each of the channels at different inlet conditions resulted in higher effectiveness for the dry dir channel. However the parallel flow arrangement is simpler to construct and operate. Also further work needs to be done and test the counter flow system for very long time periods of experimentations.

Among the novel features of this system are:

- Low water consumption
- Less energy consumption as no extra power is required to run a pump
- Virtually noise free making the system to be semi – passive.
- Greatly minimised vibration effects on the building structure.
- The system can be used in humid, semi-humid or dry environment. In the humid environment only air from the dry channel can be used while in semi- humid or dry environment the outlet dry and wet air can be allowed to combine.

CHAPTER 7

Conclusions and recommendations for further works

7.1 Introduction

Research and development in evaporative cooling have been going on for decades but still investigations are continuing for improvements. The technology is environmentally friendly and has the potential of minimising the dependency on hydro chlorofluorocarbons (HCFCs) and chlorofluorocarbons (CFCs) based conventional air conditioning systems. Interest in new methods and materials to find solutions to the problems associated with evaporative cooling is receiving the attention of researchers in order to make the technology more attractive. In the light of the above this research was embarked upon and investigated novel evaporative cooling systems based on direct and indirect evaporative cooling methods.

The research initially carried out a review on evaporative cooling processes comprising of direct, indirect, combined direct and indirect and also desiccant based types. The review covered status and developments in evaporative cooling using porous ceramics. Theoretical studies covering the heat and mass transfer as well as psychrometric associated with evaporative cooling were presented because of their relevance in the modelling and performance evaluation of the novel evaporative cooling systems investigated.

The research then focussed on the following novel evaporative cooling systems.

7.2 Investigation on Novel Direct Evaporative Cooling using Porous Ceramics

Developments and experimental investigations were carried out on two configurations consisting of different prototypes of porous ceramic evaporators. The prototypes were classified as the "stacking wall" and the suspended or "supporting frame" test configurations. They were all subjected to direct evaporative cooling tests through a duct constructed in environment chamber. On each test configuration the effects of inlet dry bulb temperature, relative humidity and inlet air flow rates were monitored. With the corresponding output results overall performance of the systems were evaluated. Each of the two prototypes was installed to cool a room space of 3m x 2m floor area and a height of 2.1m that is approximately a volume of $12m^3$.

Test results on the "stacking wall" configuration indicated the temperature drop of 1.5 -9.2^O C. For inlet relative humidity range of 34%-47% corresponding increase of 13% - 23% was observed at the outlet of the system. These results affected the effectiveness of the system. In this test 62.2% effectiveness was calculated which was less than the 90% effectiveness expected of a direct evaporative cooling system. The total effective surface area of the ceramic evaporators for this set up was $5m^2$. In comparison with theoretical model the performance showed better agreement in terms of cooling capacity. $179.8W/m^2$ and $178.4W/m^2$ were calculated for experimental and the theoretical model results, respectively. Then investigation on the "Supporting–frame" or "hanging system" followed. The set up for this test consists of porous ceramic evaporators with total effective surface area of $10m^2$ supplying a room of the same space volume as above. Results showed that maximum temperature drop

of 10^{o}C with corresponding relative humidity increase of 40.5%. The system performance showed cooling capacity of 426.52W/m^{2}, water consumption rate of 0.145g/s and effectiveness 86%. The resulting outlet temperature and relative humidity across the system were affected by the inlet conditions especially the relative humidity.

Comparison between the two systems and effects on room space was carried out. While results from the stacking wall configuration whose effective surface area was 80% of the floor area of the room almost conform to the comfort limits, the supporting frame whose total effective area was almost twice the floor area of the room performed above comfort requirements because of the higher humidity it generated in the building space. The overall results proved the prospects of porous ceramics for evaporative cooling application with very little water consumption as well as room for improvements.

7.3 Integration of Porous Ceramic Evaporative Cooling with Thermoelectric Cooler

In this research the evaporative cooling effect from the novel porous ceramics was applied as a heat sink to thermoelectric cooler to explore its possible potential as a heat sink for thermal power plants applications. A typical requirement is to limit the heat sink temperature above the ambient to 10^{o}C to 20^{o}C. Based on this research the cold side temperature of thermoelectric unit was 5^{o}C lower and the hot side was 10^{o}C lower, respectively when operated on the wet and dry porous ceramics evaporative cooling chamber. This integration allowed cooled humidified air from porous ceramic evaporators to be used as a

heat sink which is a novel technique as compared to the conventional methods of using air or water.

7.4 Novel Indirect Evaporative Cooling Using Horizontal Paper Tubes

A novel idea of using a horizontal arrangement has been considered. In this case, it is not necessary to use a pump to supply the water to moisten the evaporative cooling surfaces. A horizontal system has been constructed and tested under various temperatures, relative humidity values and air flow rates. Results showed that a $6^{o}C$ - $10^{o}C$ temperature drop between the inlet and outlet of the product (supply) air could be achieved without an unwanted rise in relative humidity. The increase in relative humidity of the product (supply) air was much less than that of the working air. The fibre tube evaporative cooler has the potential to cool a building space with very little addition of moisture.

7.5 Contribution to Knowledge and Novel Features

The novel features or originality of this research which contribute to knowledge include the following:

- The study and experimental work on different shapes and configurations of porous ceramic evaporative cooling system and analysed theoretically based on heat transfer and other psychrometric properties for evaporative cooling.
- Operation and application of evaporative cooling systems without continuous use of water recirculation pumps.
- Exploring the possibility of using evaporative cooling as heat sink for other thermal operations in which heat-sinks are required.

7.6 Recommendations for Further Works

Some experimental results when compared with the theoretical model predictions showed distinct differences mostly due to experimental errors. These provide an opportunity for further investigations to improve and optimise the performance of different methods and materials for evaporative cooling applications. Therefore the following further works are recommended to be carried out in the future:

- Investigate the performance of different geometric shapes of the conventional porous ceramic water coolers in different areas for space cooling applications.
- Effects of the resulting humidified air in human health and building should be well investigated and a better integration of the system in building structure.

2-Application of porous ceramic evaporative cooling systems as heat sinks integrated with power plants condensers can be carried out. This minimises water consumption and power requirements of huge recirculation pumps.

3-For the horizontal tubes indirect evaporative cooling system the research can be extended and the system applications be widened. More modelling and computational fluids dynamic (CFD) analysis can be performed to evaluate suitable parameters that can match a given cooling load. In this research the application of the system was demonstrated on the roof of a parasol. Applications on roof of other building spaces can be investigated.

System environmental and social costs benefit analyses should be incorporated in further investigations.

REFERENCES

A

Acedo, A.L., *Storage life of vegetables in simple evaporative coolers*. Tropical Science, 1997. **37**: p. 169-175.

Acedo, A., *Ripening and disease control during evaporative cooling storage of tomatoes.* Tropical Science, 1997. Vol.**37**: p.209-213.

Ahmed, C.S.K., P. Gandhidasan, and A.A. Al Farayedhi, *Simulation of a hybrid liquid desiccant based air-conditioning system*. Applied Thermal Engineering,1997,**17**(2):p.125-134.

Ahmed, C.S.K., et al., *Exergy analysis of a liquid-desiccant-based, hybrid air-conditioning system.* Energy, 1998. **23**(1): p.51-59.

Alonso, J.F.S.J., et al., *Simulation model of an indirect evaporative cooler.* Energy and Buildings, 1998. **29**(1): p. 23-27.

Al-Sulaiman, F., *Evaluation of performance of local fibers in evaporative cooling.* Energy Conversion and Management, 2000. **43**: p. 2267-2273.

Amir Abbas Zadpoor, and Ali Hamedani Golshan, *Performance improvement of gas turbine cycle by using desiccant based evaporative cooling system.* Energy, 2006. **31**(14): p.2652-2664.

Armbruster, R. and J. Mitrovic, *Evaporative cooling of falling water film on horizontal tubes*. Experimental Thermal and Fluid Science, 1998. **18**(3): p.183-194

Ashish Shukla, G.N. Tiwari and M.S. Sodha, *Experimental study of effect of an inner thermal curtain in evaporative cooling system of a cascade greenhouse.* Solar Energy, 2008. (82)1: p. 61-72

Armando C. Oliveira, et al, *Thermal Performance of a novel air conditioning SystemUsing Liquid dessican*t. Applied Thermal Engineering, 2000. 20: P. 1213-1223.

ASHRAE, *ASHRAE Handbook-HVAC Systems and Equipment, SI Edition, ASHRAE, Inc., Atlanta, USA. 2004.*

ASHRAE-ANSI/STANDARD-55. *Thermal environmental conditions for human occupancy.* ASHRAE, Atlanta, USA. 2004.

AZEVAP, *Engineered solutions in evaporative cooling*, *http://www.azevap.com/* [27 April 2007].

B

Badran, A.A., *Performance of cool towers under various climates in Jordan.* Energy and Buildings, 2003. **35**(10): p. 1031-1035.

Baruch Givoni, *Passive and low energy cooling of buildings*. 1994, New York: Van Nostrand Reinhold.

Belding et al, US patent-Pat No. 5,727,394, 1998

Bilal A. Qureshi, Syed M. Zubair, *A comprehensive design and study of evaporative coolers andcondensers. PartI. Performance evaluation.* International Journal of Refrigeration, 2006. **29**:p.645-658

Brian Ford, *Passive downdraught evaporative cooling: principles and practice.* Environmental Design*,* 2001. **5**(3): p. 271-280.

Brian Ford and Rosa Schiano Phan, *Evaporative cooling using porous ceramic evaporators-product development and generic building integration*. PLEA2003-The20th Conference on passive and low energy architecture, Santiago-Chile, 9-12 November 2003.

B.R. Brooks and D.L. Field, *Indirect evaporative cooling apparatus*, US Patent No.6523604. 2003.

Bucklin R. A., J. D. Leary, D. B. McConnell, E. G. Wilkerson, *Fan and Pad Greenhouse Evaporative Cooling Systems*. http://edis.ifas.ufl.edu

C

Camargo, J.R., C.D. Ebinuma, and J.L. Silveira, *Thermoeconomic analysis of an evaporative desiccant air conditioning system.* Applied Thermal Engineering, 2003. **23**(12): p. 1537-1549.

Camargo, J.R., E.G. Jr, and C.D.Ebinuma, *An evaporative and desiccant cooling system for air conditioning in humid climates*. J.of the Brazil Society of Mech.Sci. & Eng., 2005. **27**(3): p. 243-247

Carmago, J. R., et al., *A mathematical model for direct evaporative cooling air conditioning system.* CIE'NCIA/SCIENCE. Engenharia Termica,n°4, 2003 p.30-34

Chris Gupta, 2004, *Pot-in-pot cooler. http://www.newmediaexplorer.org/chris/2004/04/14/cool_fridge_without_using_electricity.htm*. [2 September 2007].

CIBSE, Guide F, "*Energy efficiency in buildings*", 2nd edition. 2004

Costelloe, B. and D.Finn, *Indirect evaporative cooling potential in air-watersystems in temperate climates.* Energy and Buildings, 2003. **35**(6): p. 573-591.

Chung-Min Liao and Kun-Hung Chiu, *Wind tunnel modelling the system performance of alternative evaporative cooling pads in Taiwan region* Building and Environment. 2002. **37**(2): P.177-187

D

DT500 Data taker.http://www.datataker.com/products/dt500zoom.html[1 July 2004]

Donald W. Abrams, *Low-energy Cooling: A Guide to the Practical Application of Passive Cooling and Cooling Energy Conservation Measures*. 1986, New York: Van Nostrand Reinhold International.

Dreyer, A.A., Erens, P.J.,*Modelling of cooling tower splash pack.* International Journal of Heat and Mass Transfer, 1996. **39**(1): p. 109-123.

El-Dessouky H.T., H.M. Ettouney and W.Bouhamra. *A Novel air conditioning system –Membrane air drying and evaporative cooling*-(Trans IChemE, Vol. 78, PartA, October, 2000).

Erens, P.J. and A.A. Dreyer, *Modeling of Indirect Evaporative Air Coolers.* International Journal of Heat and Mass Transfer, 1993. **36**(1): p. 17-26.

Ecocooling Ltd, *http://www.ecocooling.org* [30 December 2006]

ECOWAS.info (*Nigeria climate*). Copyright 2003-2006 *http://www.ecowas.info/ngaweat.htm*

ERBA evaporative cooler, *http://www.erba-aircooler.com/air_cooler.html* [2006].

Environmental Control systems: Heating, Cooling Lighting. International Edition. McGraw- Hills Inc *1993* pp 201-207.

Elfatih Ibrahim, Li Shao, Saffa B Riffat, *Indirect evaporative cooling of building using porous ceramic systems* – submitted for publication in Building and Environment, Dec *2002*.

Evaporative cooling *Http:en.wikipedia.org/wiki/Evaporative_cooler#Evaporative_coooling* [3 June 2005]

Etzion Y., et al, *Adaptive architecture: Integrating low-energy technologies for climate control in the desert.* Automation in construction, 1997. **6**: p. 417-425.

F

Ford, B., et al., *Cooling without air conditioning - The Torrent Research Centre, Ahmedabad, India*. Renewable Energy, 1998. 15(1-4): p. 177-182.

G

Ghassem Heidaranejad, et al, *Feasibility of using various kinds of cooling systems in a multi-climate country.* Energy and Buildings, 2008. Vol.**40**: p. 1946-1953.

Ghiabaklou, Z., *Thermal comfort prediction for a new passive cooling system.* Building and Environment, 2003. **38**(7): p. 883-891.

Giabaklou, Z. and J.A. Ballinger, *A passive evaporative cooling system by natural ventilation.* Building and Environment, 1996. **31**(6): p. 503-507.

Gomez, E.V., et al., *Description and experimental results of a semi-indirect ceramic evaporative cooler.* International Journal of Refrigeration-Revue Internationale Du Froid, 2005. 28(5): p. 654-662.

Gan, G., S.B. Riffat, and L. Shao, *Performance prediction of a prototype closed-wet cooling tower.* Journal of the Institute of Energy, 2000. **73**(495): p. 106-113.

Ghosal, M.K., G.N. Tiwari, and N.S.L. Srivastava, *Modeling and experimental validation of a greenhouse with evaporative cooling by moving water film over external shade cloth*. Energy and Buildings, 2003. **35**(8): p. 843-850.

Gan, G. and S.B. Riffat, *Numerical simulation of closed wet cooling towers for chilled ceiling systems*. Applied Thermal Engineering, 1999. **19**(12): p. 1279-1296.

GreenConstruction(www.sierragreenhouse.com/gallery/greenhouse.htm
2008 Sierra Greenhouse LLC Placeville CA USA 530-621-1296

H

Heidarinejad, G. et al.,*Numerical simulation of counter-flow wet-cooling towers.*InternationalJournalofRefrigeration(2008), doi:10.1016/j.ijrefrig.2008.10.008

Hisham El-Dessouky, Hisham Ettouney and Ajeel Al-Zeefari, *Performance analysis of two-stage evaporative coolers.* Chemical Engineering Journal, **102**(3): 2004. P. 255-266.

Evaporative cooling/pressurization unit
http://www.kelleysindia.com/pollutioncontrol.htm [3 July 2006]

Evaporative cooling pad in green house
http://ecaaser3.ecaa.ntu.edu.tw/weifang/lab551/vegetable/culturalpractice/Greenhouse%20construction.files/evap_cooling_pad.jpg [15 March 2005]

I
Ibrahim, E., L. Shao, and S.B. Riffat, *Performance of porous ceramic evaporators for building cooling application*. Energy and Buildings, 2003. **35**(9): p. 941-949.

Incropera F. P. and D.P. Dewitt, *Fundamentals of Heat and Mass Transfer* 6 Rev Ed ed. 2006: John Wiley and Sons (WIE).

J
Jose Rui Carmago, et al., *Experimental performance of a direct evaporative cooler operating during summer in Brazilian city*. International Journal of Refrigeration, 2005. **28**: p. 1124-1132.

Joudi, K.A. and S.M. Mehdi, *Application of indirect evaporative cooling to variable domestic cooling load.* Energy Conversion and Management, 2000. **41**(17): p. 1931-1951.

Jones, W.P., *Air conditioning engineering*. Fourth ed. 1994: Butterworth-Heinemann Ltd.

Jorge Facao, Armando Oliveira, *Heat and mass transfer correlations for the design of small indirect contact cooling towers.* Applied Thermal Engineering, 2004. Vol.**24**: p. 1969-1978.

L
Lee D.Y., B.H. Kang, and C.S. Lee, *Regenerative evaporative cooler,* US Patent No.6338258. 2002, Korea Institute of Science and Technology.

Lebrun, J., et al., *Simplified models for direct and indirect contact cooling towers and evaporative condensers*. Building Service Engineering Research and Technology, 2004. **25**(1): p. 25-31.

K
Kloppres, J.C., D.G. Kroger, *The Lewis factor and its influence on the performance prediction of wet-cooling towers.* International Journal of Thermal Sciences, 2005. **44**: p.879-884

M
Mohamed Y.Al-Koheji, *Application of porous ceramics and wind-catchers for direct and indirect evaporative cooling in buildings, in Built Environment*. Ph.D theses, University of Nottingham,UK, 2003.

Maisotsenko Cycle-Technical, *http://www.idalex.com/technology/how it works*.[January 2005].

Mark C. Gillot, *A novel mechanical ventilation heat recovery/heat pump system*. PhD theses, University of Nottingham, UK, 2000.

Munters, the humidity expert, http://www.munters.com [1 January 2007].

Michael J. Moran and Howard N. Shapiro, *Fundamentals of thermodynamics. (3rd edition)* John Wiley & Sons, Inc. New York et al, 1995 (ISBN 0-471-07681-3), pp.46-50].

O
Omer S.A., Riffat S.B., Xiaoli Ma, *Experimental investigation of a thermoelectric refrigeration system employing a phase change material integrated with thermal diode (thermosyphons),* Applied Thermal Engineering,Vol. **21**, 2001, pp. 1265-1271

P
Paschold, H., et al., *Laboratory study of the impact of evaporative coolers on indoor PM concentrations*. Atmospheric Environment, 2003. **37**(8): p. 1075-1086.

Paschold, H.W., *The effects of evaporative cooling on indoor/outdoor air quality in an arid region*, Ph.D. thesis 2002, The University of Texas at El Paso: El Paso, USA.

Palmer, J.D., *Evaporative cooling design guidelines manual for New Mexico schools and commercial buildings*. Funded by DOE. 2002: Albuquerque, New Mexico, USA. p. 1-99.

Pearlmutter, D., et al., *Refining the use of evaporation in an experimental down-draft cool tower*. Energy and Buildings, 1996. **23**(3): p. 191-197.

Prabhata K.S., et al, *Optimum design of double pipe heat exchanger.* International Journal of Heat and Mass Transfer, 2008. 51: p. 2260-2266.

Q
Qiu, G.Q. and S.B. Riffat, *Novel design and modelling of an evaporative cooling system for buildings.* International Journal of Energy Research, 2006. **30**(12):p.985-999.

Guoquan Qiu, *A Novel Evaporative/Desiccant Cooling System.* Ph.D theses University of Nottingham, UK, 2007.

R

Riffat, S., et al., *Thermal performance of a closed wet cooling tower for chilled ceilings: measurement and CFD simulation*. International Journal of Energy Research, 2000. **24**(13): p. 1171-1179.

Riffat, S.B. and H.A. Shehata, *Development of a novel mop fan*. International Journal of Energy Research, 2001. **25**(7): p. 601-619.

Riffat,S.B. ,G.Q.Qiu, and A.C. Oliveira, *Experimental investigation on a liquid desiccant/evaporative cooling system driven by a mop fan impeller.* Applied Thermal Engineering (at press), 2007.

Ren, C. and Yang, H., *An analytical model for the heat and mass transfer processes in indirect evaporative cooling with parallel/counter flow configurations,* International Journal of Heat and Mass Transfer, 2006. **49** p.617-627.

Ren, C.Q., *An analytical approach to the heat and mass transfer processes in counterflow cooling towers.* Journal of Heat Transfer-Transactions of the Asme, 2006. **128**(11): p. 1142-1148.

Riffat, S.B.,Omer,S.A.,Xiaoli Ma, *A novel thermoelectric refrigerating system employing heat pipes and a phase change material- Experimental investigation,* Renewable Energy,Vol.**23**, *2001*,pp.313-323.

Riffat S. B., H.A.Shehata, and P.S.Doherty, *A Novel Evaporative Air Cooler*. Int. of Ambient Energy, 2000. **21**(2): p. 97-108.

Riffat S.B, X.Zhao, *Preliminary study of the performance and operating characteristics of a mop-fan air cleaning system for buildings.*Building and Environment, **42** (2007), p.3241-3252.

Roy S.K., *Postharvest technology of vegetable crops in India*. Indian Horticulture. Jan-June,1989.: p.7678).

S

Saffa Riffat, Armindo Oliveira, Jorge Facao, Guohui Gan, & Prince Doherty, *Themal performance of a closed wet cooling tower for chilled ceilings:measurements and CFD simulation*. International Journal of Energy Research, 2000.Vol.**24**.Septemberpp1171-1179.

Santamouris, M. and D. Asimakopoulos, *Passive Cooling of Buildings*. 1996, London: James & James.

Singh, A.K., et al., *Energy conservation in a cinema hall under hot and dry condition.* Energy Conversion and Management, 1996. **37**(5): p. 531-539.

Sodha M.S., N.K.Bansal, and P.K.Bansal, *Solar passive building*. Science & Design 1986: Pergamon Press.

S.E. J. Telchuk, L.H. Brown, and D.F. Gerdes, *Air washer/scrubber*, US Patent No 4328012. 1982.

S.K.Wang, *Handbook of air conditioning and refrigeration*. 2 ed. 2001: The McGraw-Hill Companies, Inc.

T

Tang, R.S. and Y. Etzion, *On thermal performance of an improved roof pond for cooling buildings*. Building and Environment, 2004. **39**(2): p. 201-209.

Tang, R. and Y. Etzion, *Comparative studies on the water evaporation rate from a wetted surface and that from a free water surface*. Building and Environment, 2004. **39**(1): p. 77-86.

Tang, R.S. and Y. Etzion, *Cooling performance of roof ponds with gunny bags floating on water surface as compared with a movable insulation*. Renewable Energy, 2005. **30**(9): p. 1373-1385.

Tang, R.S., Y. Etzion, and E. Erell, *Experimental studies on a novel roof pond configuration for the cooling of buildings*. Renewable Energy, 2003. **28**(10): p. 1513-1522.

V

Vaisala HUMICAP Probes HMP45A/D, *http://www.vaisala.com/instruments/products/humidity/modules/hmp45ad* [15 June 2004].

W

Wikipedia,EvaporativeCoolers http://en.wikipedia.org/wiki/Evaporative_cooler#Evaporative_cooling[May 2006]

William J. McGuinness, Benjamin Stein, *Building Technology –Mechanical and Electrical Systems*-2nd edition. c1977. Published by John Wiley &Sons

X

Xiaoli Ma, *Investigation of Novel thermoelectric refrigeration system*, PhD thesis, University of Nottingham, UK, 2004.

Xiaoli Ma *Estimation of an air conditioning system combining psychrometric energy core (PEC) and a liquid desiccant* (report submitted to the School of the Built Rnvironment University of Nottingham, UK, 2004).

Z

Zhang, L.Z. and J.L. Niu, *A pre-cooling Munters environmental control desiccant cooling cycle in combination with chilled-ceiling panels*. Energy, 2003. **28**(3): p. 275-292.

Zhao, X., Shuli Liu, and S.B. Riffat, *Comparative study of heat and mass exchanging materials for indirect evaporative cooling systems*. Building and Environment, (2007),doi:10.1016/j.buildenv.2007.11.009.

Zhao, X., J.M. Li, and S.B. Riffat, *Numerical study of a novel counter-flow heat and mass exchanger for dew point evaporative cooling.* Appl. Therm.Eng. (2008),doi:10.1016/j.applthermaleng.2007.12.006.

APPENDIX I

Air Properties on Psychrometric Chart

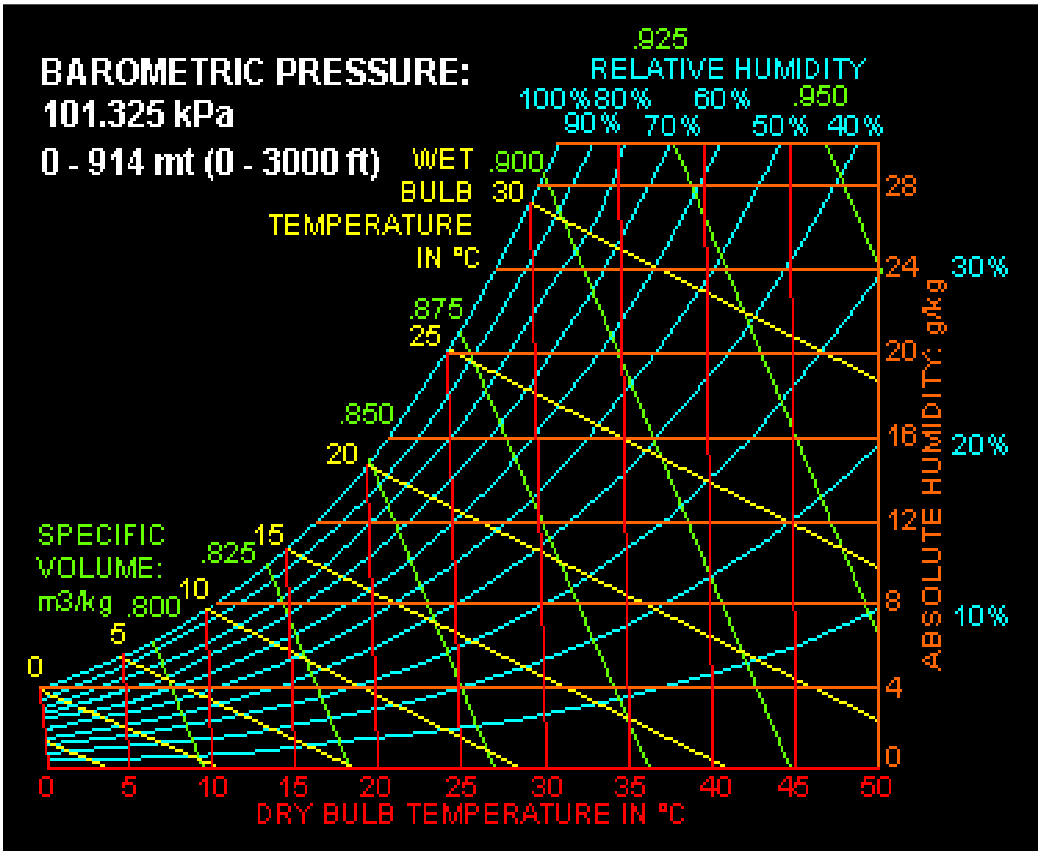

Figure-AI: Psychrometric chart

APPENDIX IIa

Specifications for Vaisala HUMICAP Humidity and Temperature Probes HMP45A

In the experiments carried out during the researchHMP45A hygrometer sensors were used to measure the temperature and relative humidity of air. The sensors were designed for a wide range of instrumentation (e.g. data logger, laboratory equipment and weather stations). Each probe has a simple data logger interface

and operates on a wide range of supply voltages. They also have the advantage of very little power consumption and simple to service. The tables below give the detailed specifications of these sensors.

Relative humidity measurement

HMP45A and HMP45D	
Measurement range	0.8 ... 100 % RH
Accuracy at +20 °C (+68 °F) field calibration against references:	± 2 % RH (0 ... 90 % RH) ± 3 % RH (90 ... 100 % RH)
Sensor	Vaisala HUMICAP® 180

Temperature measurement

HMP45A	
Measurement range	-39.2 ... +60 °C (-38.6 ... +140 °F)
Accuracy +20 °C (+68 °F)	± 0.2 °C (± 0.36 °F)
Sensor	Pt 1000 IEC 751
HMP45D	
Measurement range	-40 ... +60 °C (-40 ... +140 °F)
Sensor	Pt 100 IEC 751 1/3 Class B

Operating environment

Temperature operation	-40 ... +60 °C (-40 ... +140 °F)
storage	-40 ... +80 °C (-40 ... +176 °F)

Inputs and outputs

Operating voltage	7 ... 35 VDC
Power consumption	< 4 mA
Output load	> 10 kohm (to ground)
Output scale	-40 ... +60 °C (-40 ... +140 °F) equals to 0...1V
Output signal	resistive 4-wire connection

Mechanics

Cable length	3.5 m
Weight	350 g (including package)
Material (housing)	ABS plastic
Housing classification (electronics)	IP65

Figure-AII below shows the diagram of the HMP45A sensor showing it electrical terminals.

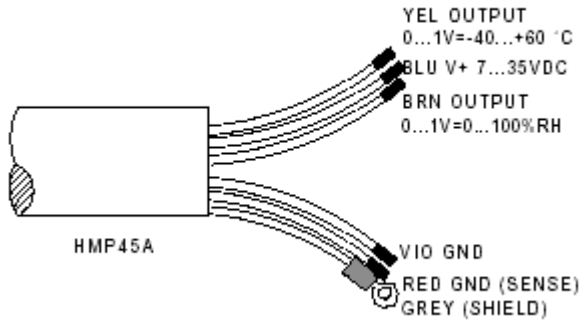

Figure-AII: HMP45A sensor and its 6 terminals

The terminals were connected to the appropriate points of each channel of the DT500 DataTaker in the following order:

1-RED GND: to R

2-YEL output: to –

3-BRN output: to +

4-BLU: to *

5-VIO GND: to –

6-GREY: to Ground

APPENDIX IIb

HMP45A Hygrometer Sensors Recorded by Data taker 500

A DT 500 data taker as shown in Figure II_2 was used for experiments in this research. Red, yellow and brown cables of HMP45A thermo hygrometer were connected to R, – and + junctions of each data taker channel, respectively.

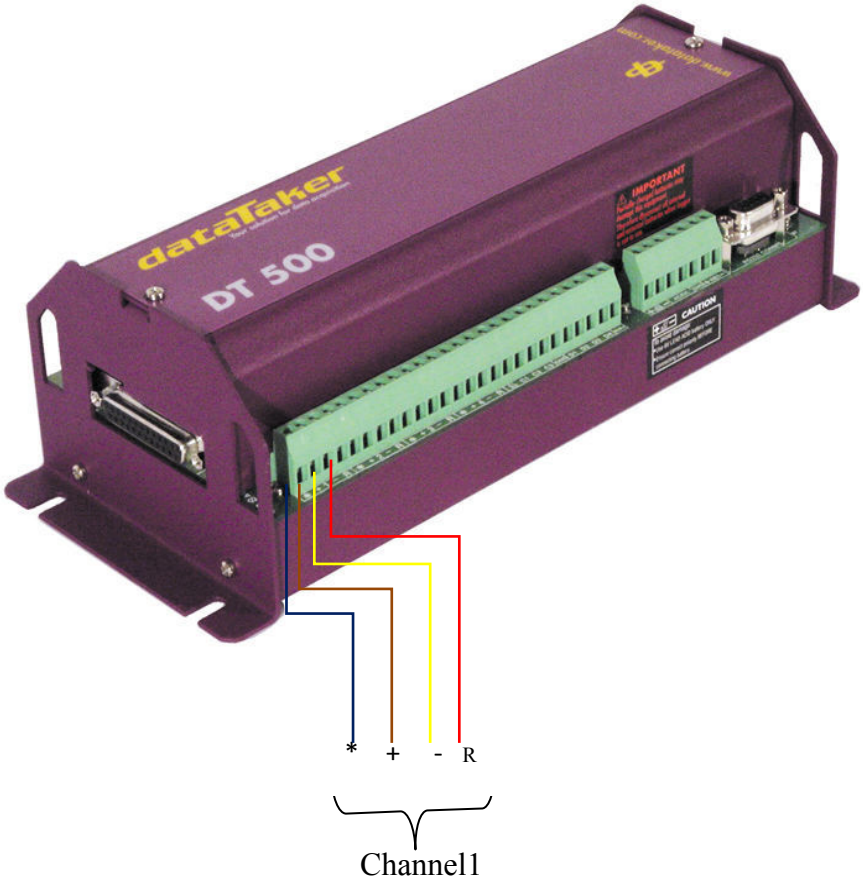

Figure-AIII: DT500 Data taker showing the sensors connection terminals on one of the channels [http://www.datataker.com/products/dt500zoom.html]

Below is the procedure of setting up the data taker programme:

(1) Programme to measure RH(%) and temperature(deg C) with Vaisala HMP45A

First open Delogger software, left-click main menu window and then select prog1.dlp to get the following program builder box. Set the data recording time interval.

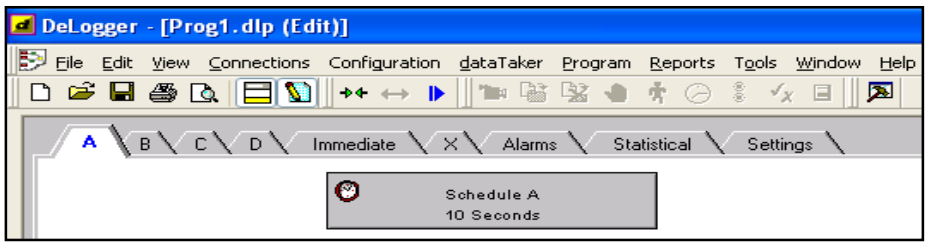

To define span or polynomial:

Either span or polynomial can be used to define to the data taker the calibration required for a particular sensor. Spans can be used to convert sensors with linear calibrations to engineering units while polynomials can be used to convert curvilinear (non-linear) and linear calibrations to engineering units. However, spans were used for this set-up and the settings are as follows:

(i)- Left-click the settings tab of the program builder window to obtain pop-up window as shown below:

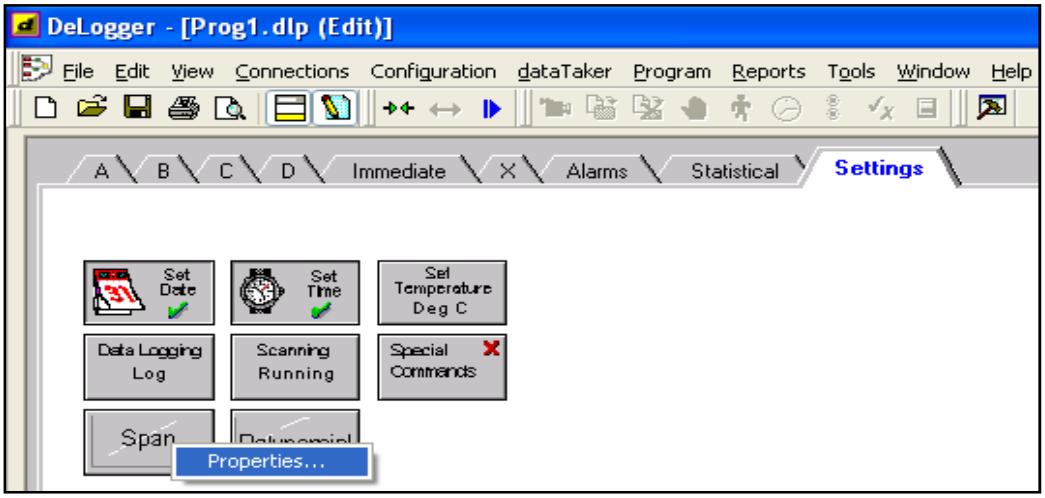

(ii)-Right-click span icon and select properties to open the spans dialogue box shown below.

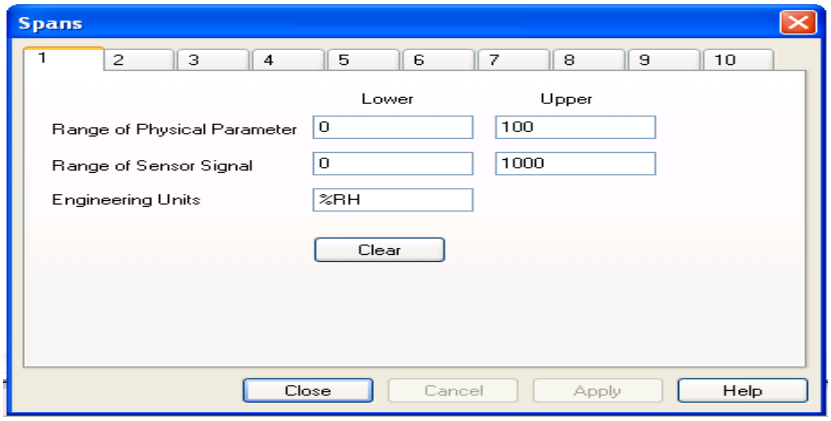

(iii)-On the span box shown above select the **tab** (e.g.1) of the span you want to define and enter the required parameters.

For the relative humidity select number 1 and enter the required parameters in the 5 blank spaces as done in the boxes above. Then click the **close** button**.**

For the **temperature** select number 2 and enter the required parameters in the 5 blank spaces as done in the boxes above. Then click the **close** button**.**

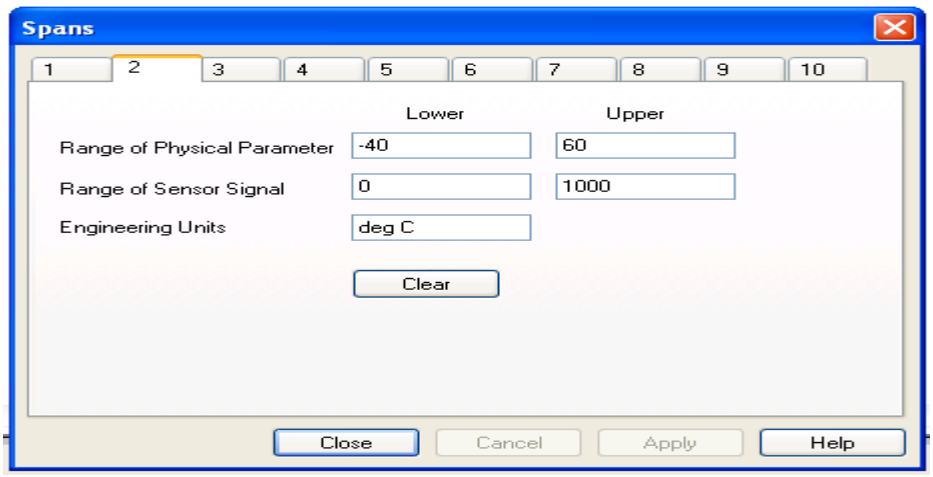

(2) Building the Program

(i)-Select schedule **A** from the programme builder window to obtain the following window.

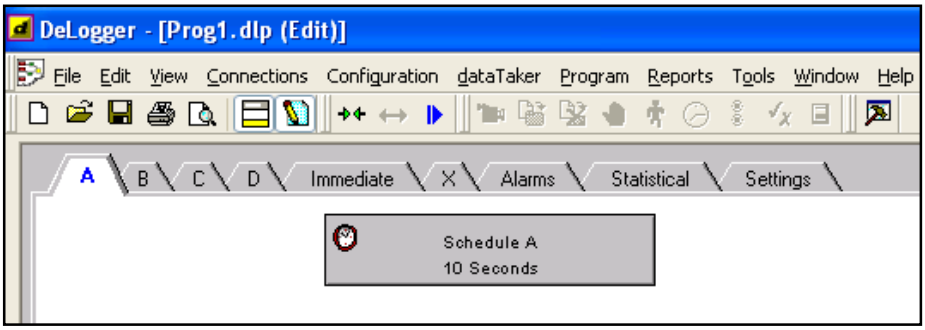

(ii)-Right-click anywhere in the **blank space** of **tab A** to get the following pop-up menu.

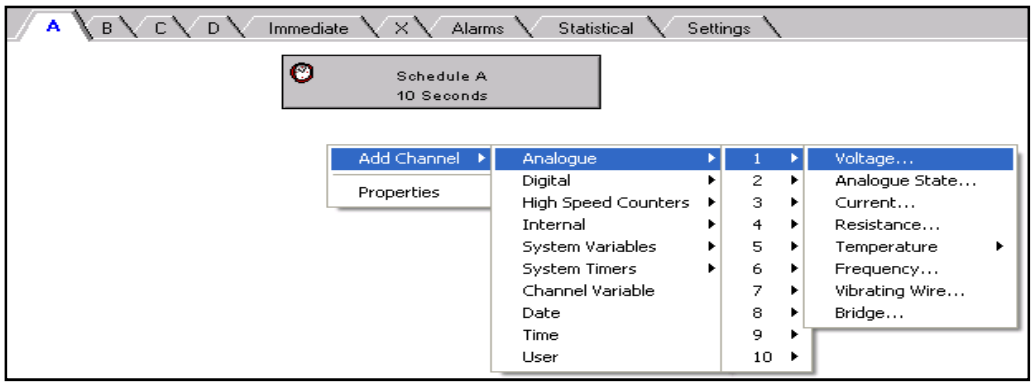

(iii)-To add a channel, select **Add Channel** > **Analogue** > **1** and finally select **Voltage** from the cascade menus that open. The voltage wiring configurations dialog box opens as shown below.

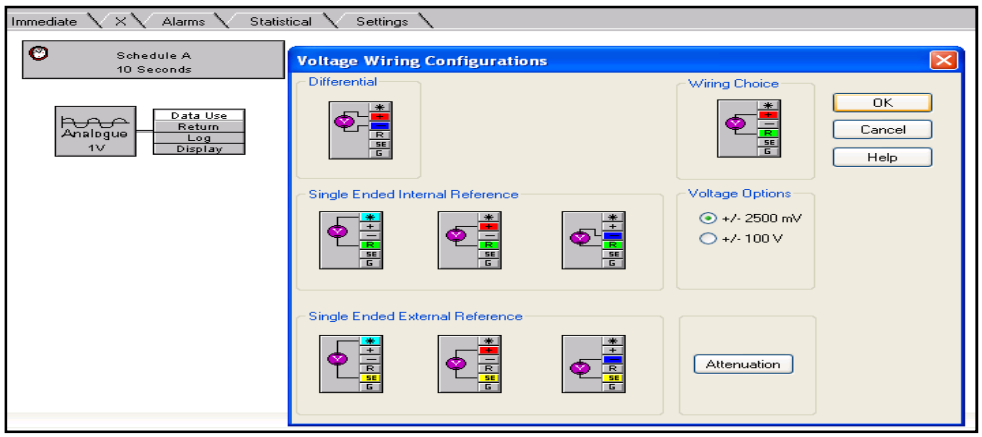

(iv)-On the wiring configuration dialogue box, select Wiring Choice [+ **(v) R**] and then Voltage Option (+/**-2500mV**). Left-click **OK** to close the Voltage Wiring Configurations dialog box.

(v)-Now a voltmeter circulation circuit appears. Right-click the tab Analogue, to open the cascade menus as shown below and then select **1** as number 1 channel for number 1 sensor.

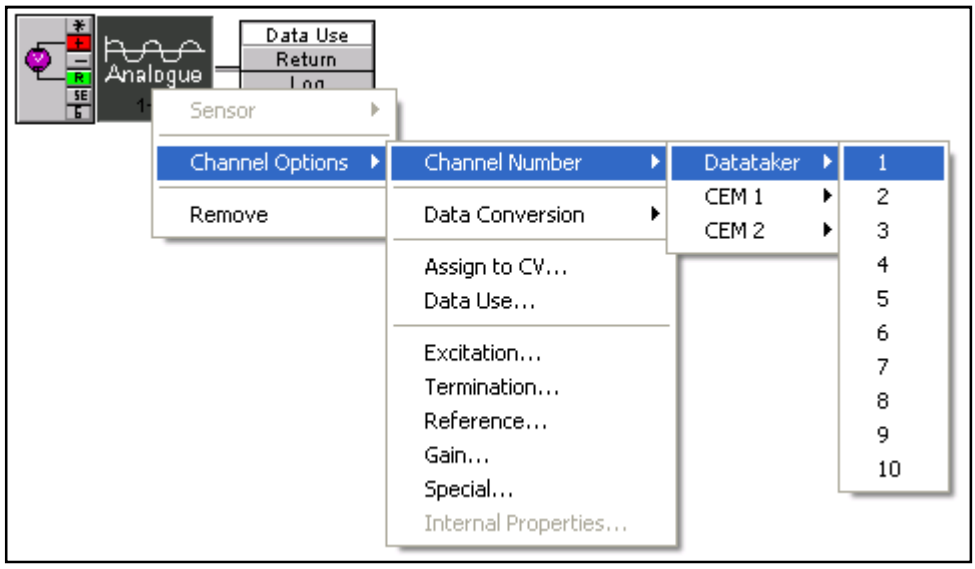

(vi)-In the dialogue box shown below Right-click **Analogue** tab, select **channel options > Data Conversion > Scaling > Span** and finally select %**RH**.

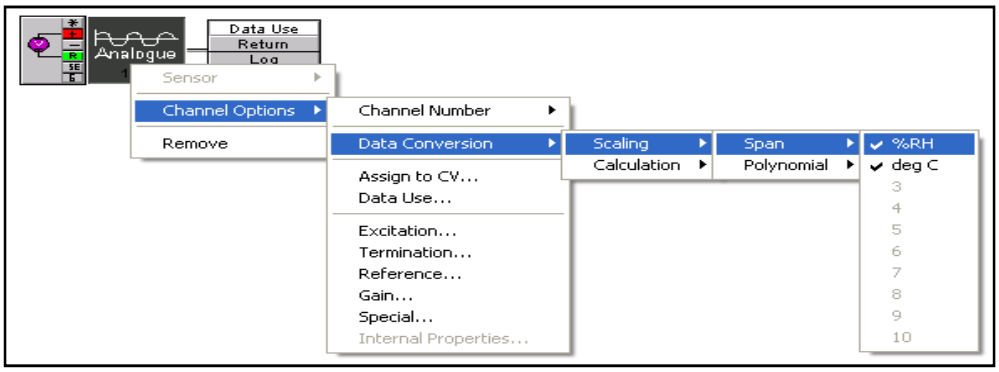

The label can be added by right click on the **Wiring Choice** tab. The following appears after a label, such as “RH1”, is added to this channel for the relative humidity.

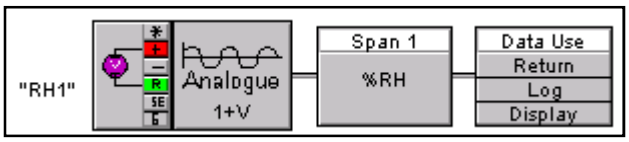

For the temperature setting, step (vi) above is repeated, while the wiring choice in step (iv) - above is changed to [-(v) R] to show the voltage wiring configurations below:

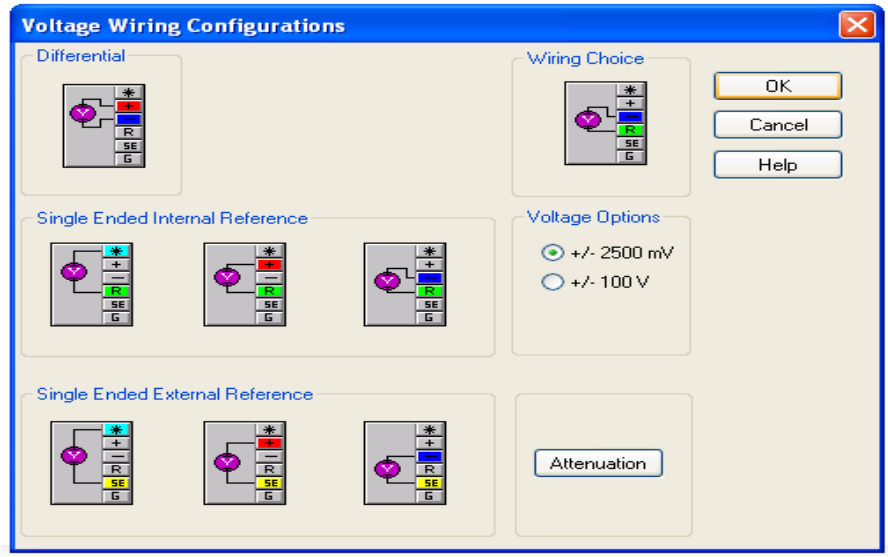

For the temperature repeat steps (iV) and (v) and select deg C to complete the settings for measuring both air temperature and the relative humidity for one Vaisala HMP45A sensor.

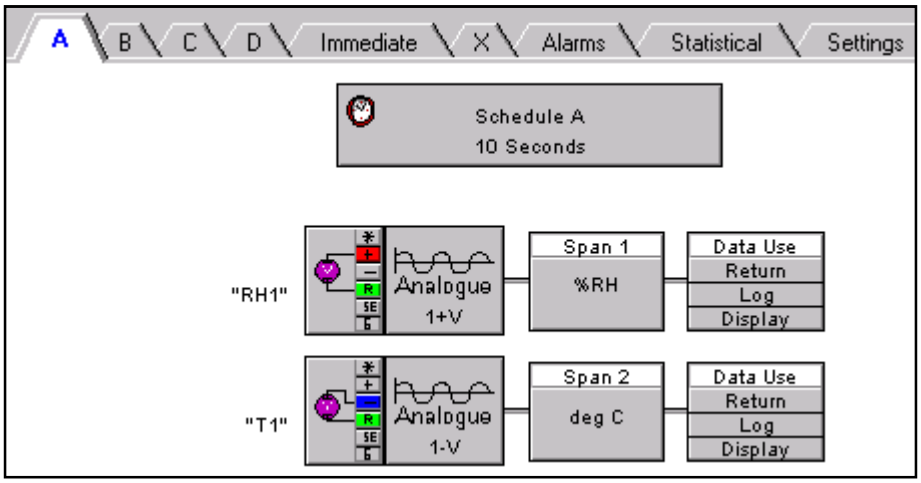

Additional sensors can be added by following the above steps but choosing different channel number for each sensor